INFORMATION TO USERS

This manuscript has been reproduced from the microfilm master. UMI films the text directly from the original or copy submitted. Thus, some thesis and dissertation copies are in typewriter face, while others may be from any type of computer printer.

The quality of this reproduction is dependent upon the quality of the copy submitted. Broken or indistinct print, colored or poor quality illustrations and photographs, print bleedthrough, substandard margins, and improper alignment can adversely affect reproduction.

In the unlikely event that the author did not send UMI a complete manuscript and there are missing pages, these will be noted. Also, if unauthorized copyright material had to be removed, a note will indicate the deletion.

Oversize materials (e.g., maps, drawings, charts) are reproduced by sectioning the original, beginning at the upper left-hand corner and continuing from left to right in equal sections with small overlaps. Each original is also photographed in one exposure and is included in reduced form at the back of the book.

Photographs included in the original manuscript have been reproduced xerographically in this copy. Higher quality 6" x 9" black and white photographic prints are available for any photographs or illustrations appearing in this copy for an additional charge. Contact UMI directly to order.

UMI

A Bell & Howell Information Company
300 North Zeeb Road, Ann Arbor MI 48106-1346 USA
313/761-4700 800/521-0600

CARBONATE DIAGENESIS AND DOLOMITIZATION OF CAMBRO-ORDOVICIAN (SAUK SEQUENCE) PLATFORM STRATA IN CENTRAL NEW YORK

by

SHRUTI SARAH PHILIPS

A dissertation submitted to the Graduate Faculty
in Earth and Environmental Sciences in partial
fulfillment of the requirements for the
degree of Doctor of Philosophy,
The City University of New York

1999

This manual has been read and accepted for the Graduate Faculty in Earth and Environmental Sciences in satisfaction of the dissertation requirements for the degree of Doctor of Philosophy.

2/1/99
Date

Dr. Gerald M. Friedman
Chair of Examining Committee

2/1/99
Date

Dr. Frederick C. Shaw
Executive Officer

Dr. John E. Sanders

Dr. Cherukupalli E. Nehru

Supervisory Committee

THE CITY UNIVERSITY OF NEW YORK

ABSTRACT

CARBONATE DIAGENESIS AND DOLOMITIZATION OF CAMBRO-ORDOVICIAN (SAUK SEQUENCE) PLATFORM STRATA IN CENTRAL NEW YORK

by

Shruti Sarah Philips

Adviser: Professor Gerald M. Friedman

The Cambro-Ordovician platform carbonates exposed on the Saratoga Platform in central New York record a complex diagenetic history ranging from early peritidal dolomitization to late-diagenetic, deep-burial dolomitization. Stratigraphically, this sequence is distinguished here as the Upper Cambrian Little Falls, Galway and Hoyt formations and the Lower Ordovician Gailor and Tribes Hill formations.

Outcrop studies reveal that the bulk of this sequence has been dolomitized. The Little Falls and Galway formations are composed of interbedded dolostones and sandstones that display herringbone cross strata, planar and domal stromatolites, intraclasts, bird's eye structures, and local chert horizons. The Hoyt Formation is extremely fossiliferous; it contains columnar, domal and planar stromatolites and trilobites. The younger Gailor and Tribes Hill formations display planar stromatolites, chert horizons, storm beds, dissolution-collapse breccia, and bird's eye vugs, the strata becoming increasingly

fossiliferous towards the top. The post- Sauk, pre-Tippecanoe surface of unconformity lies atop the Lower Ordovician strata. A peritidal environment of deposition is inferred for the entire sequence.

The facies study of these Sauk Sequence carbonates, shows that an aggrading pattern of multiple meter-scale, upward-shallowing, parasequences developed, during a period of regional transgression.

Transmitted-light and cathodoluminescence petrography have revealed seven different dolomite generations, which differ from one another in terms of their crystal size, luminescence, trace-element content, and stable-isotope compositions. Four stages of dolomitization are recognized in the rocks under study. The first stage is considered to have occurred early in the diagenetic history, when microcrystalline Dolomite (1) and fine-crystalline mosaics of Dolomite (2) formed during and immediately following deposition. The second and main stage was one of massive dolomitization that occurred in the subsurface during progressive burial and involved multiple episodes of textural and geochemical change, resulting in Fe- and Mn-rich, zoned, medium- to coarse-crystalline, planar-e to planar-p Dolomite (3) and nonzoned, xenotopic, medium- to coarse-crystalline mosaics of Dolomite (4). The third stage was one of uplift of the basin, when Fe-poor, meteoric fluids entered the strata producing bright, orange-luminescent Dolomite (5) cements. The fourth and final stage of dolomitization occurred in the deep subsurface, where subsurface brines precipitated Fe-rich Dolomite (6) (saddle dolomite) and Dolomite (7) cements in vugs.

Compared to the early-diagenetic dolomites, the late-diagenetic dolomites are: (1) more stoichiometric; (2) coarser; (3) more depleted in $\delta^{18}O$ and Sr^{2+};(4) more enriched in Fe^{2+} and Mn^{2+}. These geochemical differences imply that early dolomite generations formed from modified seawater in the depositional environment and soon after, whereas later-formed generations of dolomite formed by:(1) recrystallization or neomorphism of early formed dolomite; (2) replacement of limestone at elevated temperatures; and (3) cementation in fractures and secondary pores.

The dolomite fabrics are intimately associated with products of other diagenetic events, such as silicification, dedolomitization, stylolitization, and cementation by burial calcite. The diagenetic sequence, that I have reconstructed in the platform strata is remarkably similar to that worked out by Guo (1994) and by Guo, Sanders and Friedman (1996) in the coeval rocks of the Appalachian fold-thrust belt exposed in eastern New York. This implies that the burial histories of the Sauk Sequence from these contrasting tectonic provinces, Saratoga Platform on the west and the Appalachian fold-thrust belt on the east were comparable.

ACKNOWLEDGMENTS

I am most grateful to my advisor Prof. G.M. Friedman for his guidance and support and for the opportunity to work on this project. My gratitude also goes to Prof. D. Habib and Prof. F.C. Shaw for their encouragement and support over the years I've been in the Ph.D. program at the CUNY Graduate Center. Critical reviews of the manuscript by the members of my advisory committee, Professors G.M. Friedman, J.E. Sanders, F.C. Shaw, and C.E. Nehru are gratefully acknowledged.

I sincerely thank Prof. C.E. Nehru for the use of his microscope at Brooklyn College. I also thank the Northeastern Science Foundation for the use of facilities and equipment. My gratitude also goes to Dr. Martin Prinz for the use of the CL apparatus at the Museum of Natural History, New York. Thanks are also due to Mike Weisberg for his help with the Luminoscope.

Gratitude is extended to Dr. D.W. Fisher for his generous advice and guidance in locating outcrops for this study. I am also grateful to Mrs. Sue Friedman for her help and hospitality during the days I spent at Troy. Thanks are also extended to my faculty and staff at the CUNY Graduate Center and at Brooklyn College for their help and assistance in this effort.

I wish to thank my friend and fellow student Dr. Mossbah Kolkas for his generous help with the microprobe analysis and for his constructive review of the manuscript. Thanks are also extended to Dr. Baiying Guo, Dr. Ali Kaya, Dr. Rajesh Sharma and Laura Whitaker for many fruitful discussions.

I extend special gratitude to my husband, Joseph Philips, to whom I owe much, in particular for his assistance with sample collection and the use of computer graphics, that helped improve the overall presentation of the manuscript. I am most grateful to my mother Mrs. Renu Varghese and my mother-in-law Mrs. Soma Philips for the countless hours of babysitting they provided, without which this achievement would not have been possible. I also wish to thank my father Col. Paul Varghese for his generous support. I thank my sons, Joshua and Paul for patiently putting up with the many hours I spent away from them, working on my dissertation. Lastly, I thank my family and friends for their love and encouragement throughout this endeavor and especially my father-in-law Mr. G.K.O. Philips, who started me on this journey.

This study was supported by graduate assistantships from the Graduate School of the City University of New York, Herbert H. Lehman College and Brooklyn College.

TABLE OF CONTENTS

LIST OF TABLES AND FIGURES
(Page numbers are in italics)

PART I

INTRODUCTION & BACKGROUND

CHAPTER 1 - INTRODUCTION

1.1 Objectives

The diagenesis of carbonate sediments and rocks has been the focus of many investigations for two centuries, yet many aspects of carbonate diagenesis and dolomitization are not fully understood. The origin of massive ancient dolostones has been addressed by numerous authors (e.g. Friedman and Sanders, 1967; Zenger, 1972; Zenger et.al., 1980; Land, 1983, 1985; Morrow, 1990a, 1990b; Machel and Mountjoy, 1986; Gunatilaka, 1987; Hardie,1987; Shukla and Baker,1988; Braithwaite, 1991; Mazzullo, 1992; Guo, 1994; Guo et. al., 1996; Purser et. al., 1994), and dolomite has been interpreted to have formed in different diagenetic environments by different fluids such as evaporative marine brines (e.g. Adams and Rhodes,1960; Lu and Meyers, 1998), mixtures of seawater and freshwater (e.g. Badiozamani, 1973), normal seawater (e.g. Saller, 1984) and subsurface fluids (e.g. Mattes and Mountjoy,1980; Morrow, 1997; Wendte et.al., 1998). However, the problem remains that the fabrics and geochemical relationships of ancient dolomites differ significantly from those of the modern dolomites that are used as analogs to explain the origin of massive ancient dolostones. Petrographic and geochemical studies of ancient dolostones have shown that, during their diagenesis, they have undergone multiple stages of recrystallization and stabilization which has significantly modified the fabrics and chemical signatures that were present in

the initial carbonate sediments (e.g. Land, 1980, 1985; Zenger, 1981, 1983; Harris and Meyers, 1987; Banner et. al.,1988; Montanez and Read, 1988; Zenger and Dunham, 1988; Qing and Mountjoy, 1989; Amthor and Friedman, 1991, 1992; Gao and Land, 1991; Gao et. al., 1992; Kupecz et. al., 1992; Kupecz and Land, 1991, 1994; Dorobek et. al., 1993; Guo, 1994; Qinjun and Demicco, 1997). These studies have demonstrated that the key to explaining the origin of these massive dolostones lies in understanding their diagenetic history.

The regionally extensive Cambro-Ordovician platform strata exposed in central New York (Figure 1.1), which are composed entirely of limestones and dolostones, form an ideal setting for the study of ancient dolomitization. This study describes the origin and diagenetic evolution of these platform dolostones of the Sauk Sequence (Sloss, 1963; Guo, Sanders and Friedman, 1990) from surface outcrops in central-eastern New York.

The purpose of this study is:

1) To provide detailed petrographic descriptions of dolomite rock textures of the Sauk Sequence dolostones in central-eastern New York.
2) To discuss the paragenetic relationships among the dolomite generations and implications for timing, processes, and stages of dolomitization.

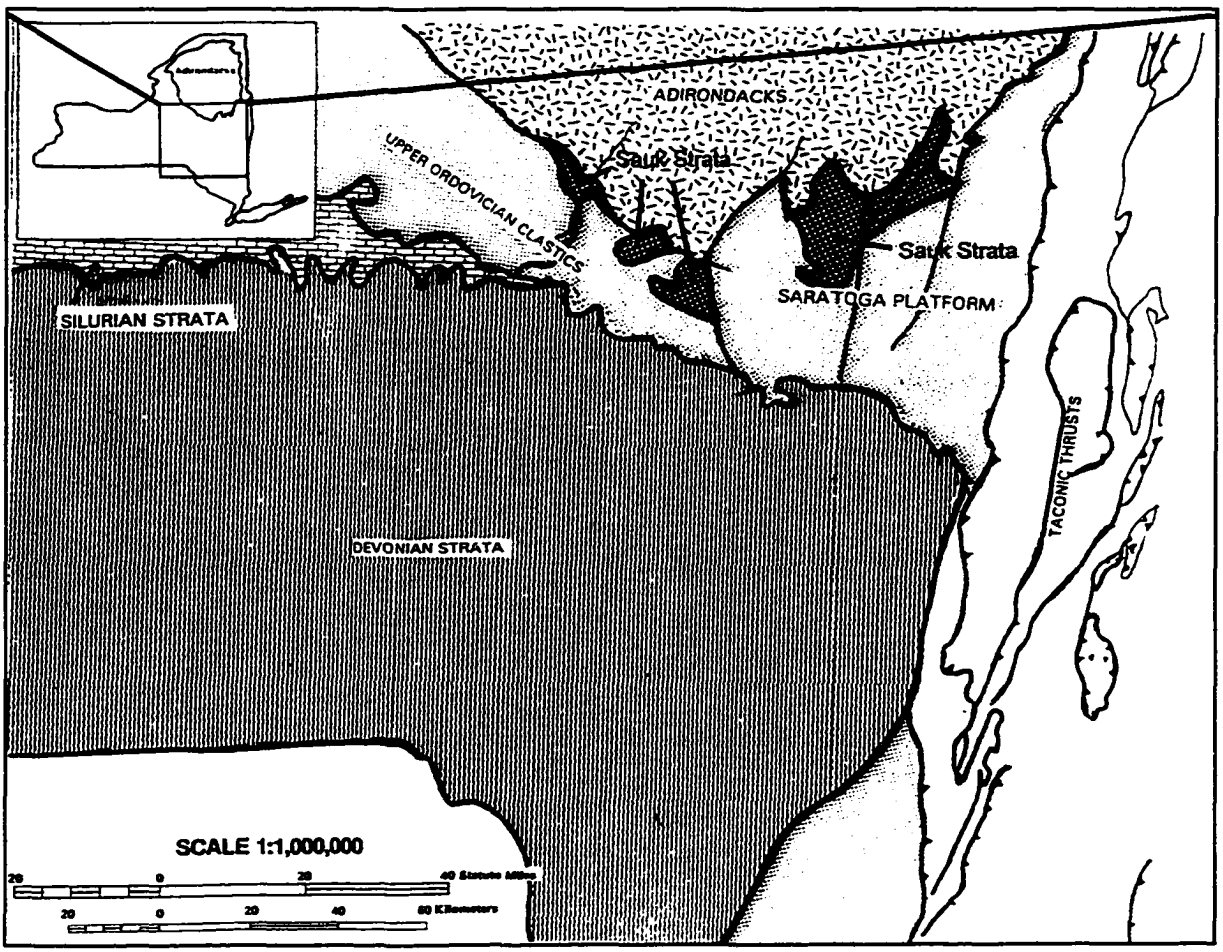

Figure 1.1. Map of Study Area Showing Location of Sauk Strata on the Saratoga Platform in Central New York (Modified from Rogers et. al, 1990).

1.2 Research Methods

1.2.1 Field Work:

Surface outcrops of the Galway, Hoyt, Little Falls, Gailor and Tribes Hill formations, which make up the Cambro-Ordovician carbonate platform sequence in the study area, were examined at 18 locations in the vicinity of Saratoga Springs and in the lower Mohawk valley (Figure 1.2). Table 1 shows the stratigraphic relationships of the Cambro-Ordovician strata in the study area.

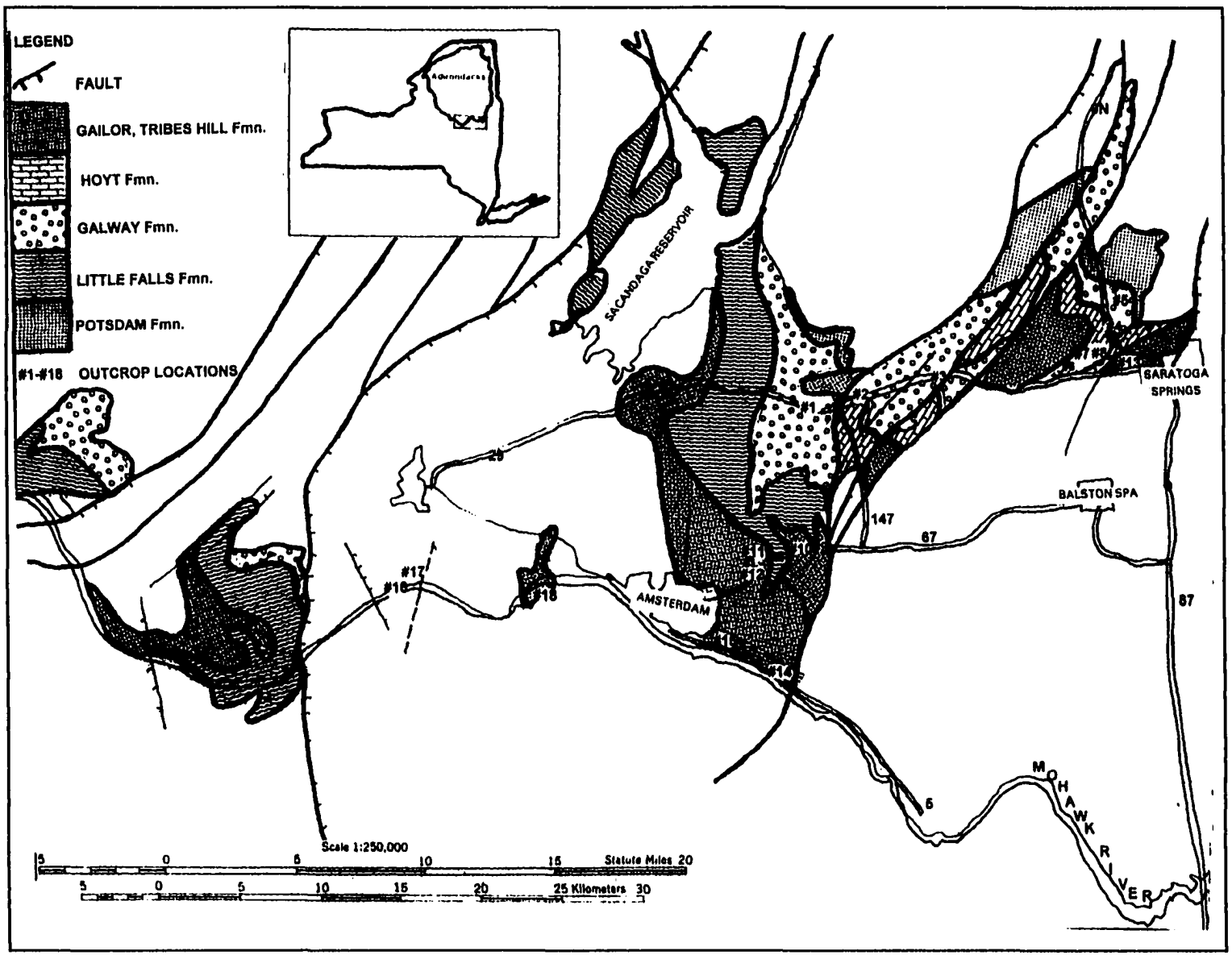

Figure 1.2. Geological Map of Study area Showing Outcrop Locations (Modified from Fisher et. al, 1970).

TABLE 1: STRATIGRAPHY OF THE SAUK STRATA IN CENTRAL NEW YORK

(Modified from Fisher, 1977; Use of Sauk and Tippecanoe after Guo, Sanders and Friedman, 1990; Absolute dates from Gradstein and Ogg, 1996)

PERIOD	AGE (Ma)	SERIES	STAGE	SEQUENCE	FORMATION MOHAWK VALLEY	FORMATION SARATOGA SPRINGS
Middle Ordovician		TIPPECANOE SEQUENCE				
	458		POST-SAUK UNCONFORMITY			
Lower Ordovician		CANADIAN	GASCONADIAN	SAUK	TRIBES HILL: Chuctanunda Creek Dolostone	GAILOR
					TRIBES HILL: Fonda Limestone	
					TRIBES HILL: Wolf Hollow	
					TRIBES HILL: Palatine Bridge	
					TRIBES HILL: Fort Johnson	
	495					
Upper Cambrian		CROIXIAN	TREMPEALEAUAN			HOYT
			FRANCONIAN		LITTLE FALLS	GALWAY
			DRESBACHIAN			POTSDAM
		ACADIAN	POTSDAM UNCONFORMITY			
	545	TACONIAN				
Precambrian						

Hiatus, absence of rock record

The outcrops were measured and sampled, during the summer/fall of 1992. Representative rock samples were collected from points of interest and lithologic change. Dilute hydrochloric acid was used to distinguish dolomite from calcite in the field. Sedimentary structures and megascopic textural variations were recorded. Lithofacies variations in conjunction with depositional structures and textures were used to recognize vertical meter-scale cycles of deposition in some of the outcrops.

Columnar sections of the outcrops, showing lithological descriptions, parasequences and sample locations can be found in the Appendix. Dunham's classification and nomenclature (Dunham, 1962) were used for the descriptions of the collected samples and recognition of lithofacies.

1.2.2 Laboratory Work:

1.2.2.1 Staining:

A total of 158 standard and polished thin sections were prepared by Spectrum Petrographics for the petrographic study. Two kinds of stains were used to distinguish between calcite and dolomite and between ferroan and non-ferroan calcites and dolomites.

Alizarin Red-'S' added into 1.5 % HCl was used to distinguish between calcite and dolomite (Friedman, 1959). Potassium Ferricyanide $K_3(Fe\ CN_6)$ stain

was used to identify ferroan calcite and dolomites (Friedman, 1959; Dickson, 1966).

1.2.2.2 Plane-Light and Cathodoluminescence Petrography:

The thin sections were examined under the petrographic microscope and luminoscope to determine the distribution and textural relationships among the main components dolomite, calcite, and quartz. Petrographic examination of the thin sections was carried out at Brooklyn College and the Northeastern Science Foundation (Rennssalear Center of Applied Geology), affiliated with Brooklyn College.

Cathodoluminescence (CL) was used to identify the different kinds of dolomite fabrics and to examine the cement "stratigraphy". Compositional zoning in the dolomites that are revealed by variations in CL colors, reflect the geochemical evolution of the diagenetic solutions. In carbonate minerals, Mn^{2+} is the most important activator found in bright luminescent zones and Fe^{2+} is the most important quencher found in non-luminescent zones (Machel and Burton, 1991; Machel et.al, 1991).

For CL petrography a Nuclide luminoscope was used and operated under 12-15 Kv beam voltage and 0.6 to 0.8 mA beam current, with a beam diameter of 5mm. The cathodoluminescence study was conducted at the Museum of Natural History in New York. 102 polished thin sections were studied under CL to recognize diagenetic features that are not visible under the standard

petrographic microscope. Under CL, dolomite luminesces in shades of red and calcite luminesces bright or dull yellow. Detrital feldspar luminesces blue, whereas authigenic feldspar is non-luminescent. Quartz is either navy blue or non-luminescent under CL.

The dolomite textures were classified based on the terminology of Friedman (1965) and Sibley and Gregg (1987).

1.2.2.3 Microprobe Analysis:

Selected polished thin sections were carbon-coated and used for microprobe-spot analysis to determine the Ca, Mg, Fe, Mn and Sr contents and stoichiometry of the various dolomite types. The microprobe analysis was carried out at The Rensselaer Polytechnic Institute in Troy, New York. Tables containing the microprobe data for the samples of this study can be found in the Appendix.

1.2.2.4 Stable-Isotope-Ratio Analysis:

42 selected samples were examined for their $\delta^{18}O$ and $\delta^{13}C$ and expressed in $^{0}/_{00}$ relative to the PDB standard. The analysis was conducted at Geochron Laboratories, a division of Krueger Enterprises, Inc., in Cambridge, Massachusetts.

This study is organized into two parts. Part I deals with the geological setting, stratigraphy and facies analysis of the Sauk-Sequence strata in the study

area. Part II deals with the important diagenetic events and concludes with the paragenesis and a discussion of the overall evolution of the carbonate platform. Lists containing the sample numbers, sample locations, outcrop descriptions, geochemical data, and figure numbers are in the Appendix.

CHAPTER 2 - BACKGROUND

2.1 Geological history of the area

This study focuses on an area that was part of the extensive carbonate platform that developed along eastern North America during the Early Paleozoic.

Near the close of the Proterozoic, proto-North America was part of the Grenville Supercontinent which began to split apart in a worldwide rifting event. About 660 million years ago, a large divergent margin developed along the southern coast of proto-North America, approximately along the earlier Grenville Suture Zone. Continued rifting widened the basin and the Iapetus ocean formed (Isachsen et. al., 1991).

Early in the Cambrian Period, seas transgressed progressively north-westward, from the east and south-east, over the North American craton and by the end of the period, the siliciclastics along the southern continental margin had given way to carbonate deposits producing an immense carbonate platform that extended across most of

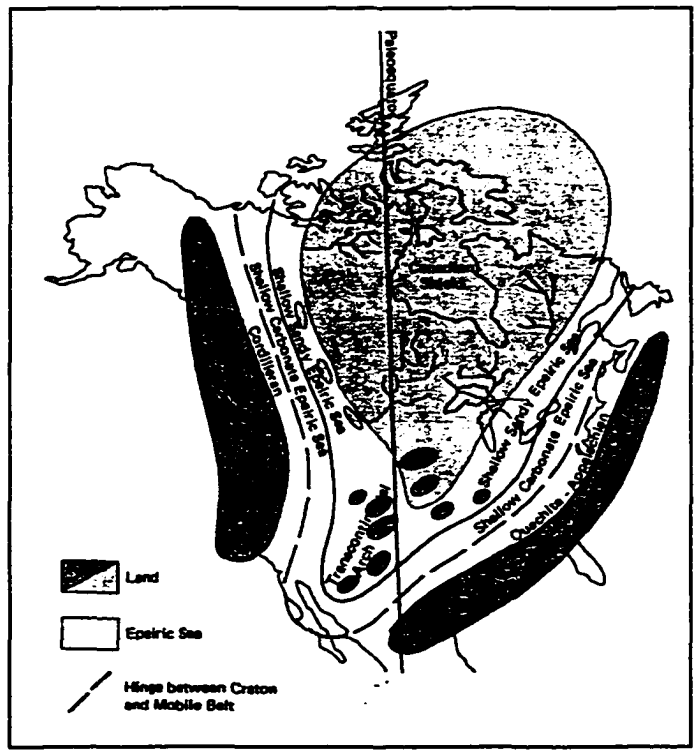

Figure 2.1: Paleogeography of North America during the Cambrian Period (modified from Wicander and Monroe, 1989).

North America (Figure 2.1). These carbonates were deposited in a roughly east-west belt at approximately 20° S latitude (Scotese et. al., 1979,1990; Bambach et. al., 1980), which meant that the carbonate platform developed in a warm, tropical setting. Thus, a shallow epeiric sea covered a large part of the craton during the latter part of the Cambrian.

This was a period of tectonic quiescence. Global sea level was in a process of prolonged rise, which resulted in gradual flooding of the cratons. This second-order eustatic sea-level oscillation (Vail and others, 1977) is observed on most cratonic areas world-wide as deposits of the Sauk Sequence (Sloss, 1963) (Figure 2.2). In central-eastern New York, the Sauk Sequence occurs as generally flat-lying strata forming the Saratoga Platform. Quartz sand and dolomite were deposited in varying intermixed quantities (Potsdam, Galway and Little Falls formations) with localized stromatolite reefs (Hoyt Limestone) fringing the southern shore of the exposed craton (Figure 2.3 A, B, and C).

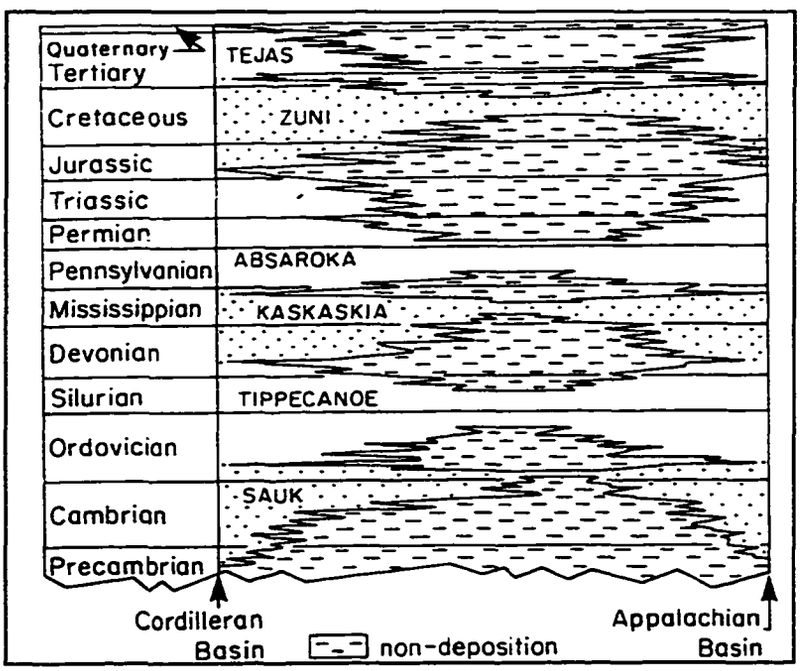

Figure 2.2: The Six Sequences of Sloss (1963).

FIGURE 2.3: Paleogeographic Maps of New York State for the Cambro-Ordovician Period (Modified from Fisher, 1977)

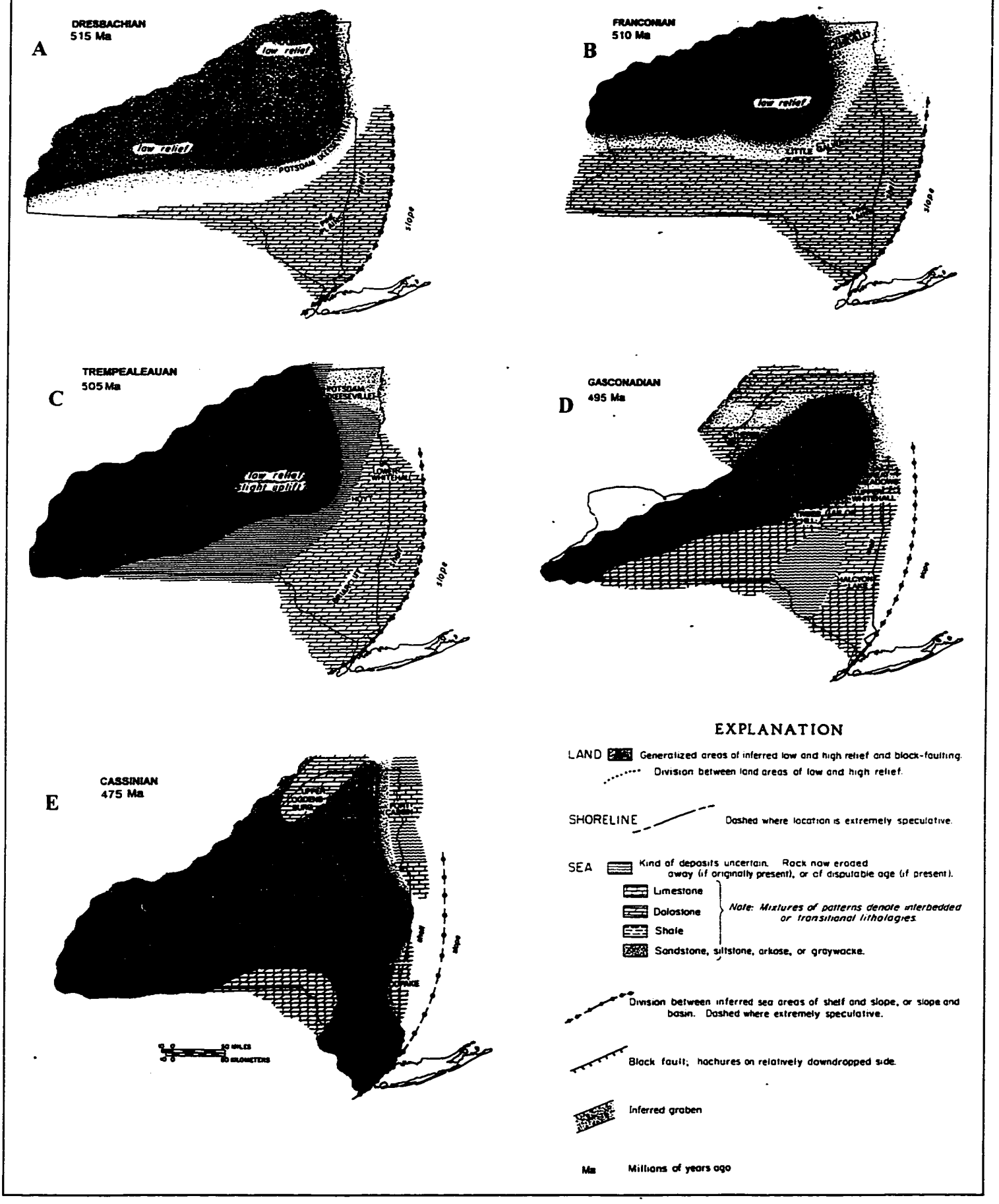

Early Ordovician (500-470 Ma) saw extensive carbonate deposition in a widespread shallow continental-shelf environment. Limestones and dolostones (Tribes Hill and Gailor formations) were laid down on the shallow platform under tectonically stable conditions (Figure 2.3 D). The Tribes Hill Formation was deposited along the then-southern edge of the craton about 35 miles north of the shelf edge and adjacent to the Proterozoic metamorphics of the Adirondacks (Curl, Zagorski and Friedman, 1984). To the south of the platform, deep-water shales and carbonate-clast conglomerates accumulated on the continental slope and rise (Keith and Friedman, 1977) and formed what is known as the Taconic Sequence (Sanders, 1995).

Following the Early Ordovician carbonate deposition, the continental shelf was uplifted and exposed (Figure 2.3 E). This elevation ended the Sauk episode and is recorded as the post-Sauk pre-Tippecanoe surface of unconformity (Isachsen et. al., 1991). By Middle Ordovician time, subsidence of the platform allowed deposition of basal limestones of the Tippecanoe Sequence. This carbonate deposition ceased when the Taconic orogeny was initiated by the collision of North America with an Island Arc that developed within the Iapetus Ocean (Bird and Dewey, 1970). Subduction began and the Iapetus Ocean began to close. The Island Arc overrode the shelf, depressing the carbonate platform and forming a chain of mountains along its margin. The downward flexure of the continental crust produced a foreland basin adjacent to the Taconic mountains and black muds accumulated on a vast scale, where the carbonate bank once stood. Following the accumulation of a thick succession of black siltstones, came

the Taconic thrust sheets that advanced from the south as the Taconic orogeny progressed (Sanders, 1995).

The post-Taconic tensional forces were perhaps responsible for the high-angle normal faults that are prominent structural features observed in the Mohawk Valley today (Figure 1.2). The Cambrian and Ordovician strata in the area form a rim around the Adirondacks today. However, it is believed that they extended across the Adirondacks during the Early Paleozoic time (Rickard, 1973; Isachsen, 1985, 1992; Isachsen et. al., 1991; Sarwar and Friedman, 1994).

The Silurian Period was an interval of renewed quiescence. Erosion leveled the mountains that formed during the Taconic Orogeny and seas again flooded the foreland basin. The remainder of the Paleozoic Era in New York saw two additional orogenic events, namely the Acadian Orogeny in the Devonian and finally the Alleghanian Orogeny in the Carboniferous Period. The effect of the last two orogenies on the strata in the Saratoga-Mohawk Valley area is not known.

There is no record of sedimentation in this area during the Late Paleozoic and Mesozoic eras. However, paleotemperature studies (Urschel and Friedman, 1984; Sarwar, 1992; Sarwar and Friedman, 1994) of the Paleozoic strata, situated around the Adirondacks, including the rocks of the study area, indicate the former presence of thick Devonian and post-Devonian strata along the eastern and southeastern margin of the Adirondacks and possibly across the Adirondacks. Regional uplift and erosion is interpreted to have begun toward the

end of the Permian (Sarwar and Friedman, 1994) and followed into the Tertiary. The uplift of the Adirondacks region, at the end of the Permian, was responsible for the removal of up to at least 7.5 km of the Paleozoic strata in the area (Sarwar and Friedman, 1994). According to Isachsen, (1985), the Adirondacks started rising independently in the Tertiary and continue to rise today at the rate of 3.7mm / yr. Glacial erosion in the Pleistocene was followed by drainage of the area by the Mohawk and Hudson rivers which continues today.

2.2 Previous studies

Geological investigations of the Cambro-Ordovician rocks of the Mohawk Valley began way back in the 1800's, when Amos Eaton, 'the pioneer geologist', surveyed the region for the construction of the historic Erie Canal (Eaton, 1824). Eaton authored several books on the geology of the Erie Canal route and the geology of Albany and Rensselaer counties. In 1842, Lardner Vanuxem wrote the earliest descriptive work on the Tribes Hill Formation. James Hall, who was Amos Eaton's student, in 1847 described and illustrated several fossils from these strata. J. M. Clarke and Schuchert (1899) gave the name Beekmantown to the Lower Ordovician rocks of the Mohawk Valley. Ulrich and Cushing (1910) examined the stratigraphy of the Little Falls and named the Tribes Hill and Hoyt formations. Much of the early work on these strata involved establishing the stratigraphy, which was based largely on paleontology. Fisher's exhaustive work on the detailed stratigraphy of the Canadian strata of the Mohawk Valley dealt

with the Tribes Hill and Cranesville formations (Fisher, 1954). Landing et. al. (1996) presented a revised stratigraphy of the Tribes Hill Formation.

In the Saratoga Springs area, the early investigations included Walcott's study of the Hoyt fauna in 1879 and that of Clarke, who named the Galway formation (Fisher and Hanson, 1951). A map of the Saratoga Quadrangle was published by Cushing and Ruedemann (1914) which was later modified by Fisher and Hanson (1951). Fisher and Hanson (1951) revised the stratigraphy of the Saratoga Springs region and described the lithology and stratigraphic relations of the Potsdam, Galway, Hoyt and Gailor formations in the region.

Once the stratigraphy of the Mohawk Valley and Saratoga Springs had been reasonably established, the stage was set for further studies on facies analysis and diagenesis. This task was undertaken by G.M. Friedman and several generations of his students. Depositional facies of the Tribes Hill Formation were thoroughly examined by several studies (Braun and Friedman, 1969; Curl, Zagorski and Friedman (1984); Friedman, 1996a, 1997). These studies established that the Tribes Hill strata were deposited in a peritidal environment within a broad, shallow epicontinental sea. A detailed facies stratigraphy was established for the different members of the Tribes Hill Formation which was followed by sequence-stratigraphic studies that recognized parasequences in these strata (Friedman and Braun, 1975; Friedman, 1977, 1994 a, b, 1995; Friedman, Sanders and Martini, 1982). Patterns of sedimentation in the Mohawk Valley and correlative units in eastern New York were examined by several studies (Mazzullo and Friedman (1975, 1977); Buyce

and Friedman (1975); Rubin and Friedman (1977, 1981); Mazzullo (1978); Harris and Friedman (1982); Dolfi and Friedman (1983); Guo, Sanders and Friedman, 1990).

Zenger (1976, 1981) worked out the detailed stratigraphy and facies analysis of the Little Falls Formation. Mazzullo and others (1978) revised the stratigraphy of the Saratoga Springs area and examined depositional facies in the Galway and Gailor formations. Conway and Friedman (1984) studied the depositional conditions of the subsurface Gailor Formation. Sedimentation patterns of the algal products of the Hoyt Formation were examined by Owen and Friedman (1984) and Friedman (1988).

Urschel and Friedman (1984) and Sarwar and Friedman (1994, 1995) investigated the paleodepth of burial of the Beekmantown carbonates. Guo, Sanders and Friedman (1990) studied a subsurface, vertical section from the Finnegan boring (located 20 km south of Saratoga Lake) which penetrated the Taconic overthrust, the Tippecanoe Sequence, the entire thickness of the autochthonous Cambro-Ordovician shelf carbonates (Sauk Sequence) and entered in-situ Precambrian basement. This study (Guo et. al., 1990) also introduced the sequence terms for the Cambro-Ordovician strata in the area. Because a complete section of the Sauk Sequence is present here, it is significant as a good reference section. Additional work by Guo and others (Guo, 1994; Guo, et. al., 1992, 1996; Friedman, 1996, 1997) shed light on the comparison between the Sauk strata on the Saratoga Platform and the correlative units on the Eastern Shelf below the Taconic thrusts.

Continuing the investigation of this Cambro-Ordovician sequence, this study examines the complex diagenesis to which these rocks have been subjected, emphasizing the stages and types of dolomitization involved (Philips and Friedman, 1995). This study focuses on the diagenetic history of the Upper Cambrian Galway and Hoyt formations and the Lower Ordovician Gailor Formation which are exposed in the vicinity of Saratoga Springs, New York. However, some outcrops of the correlative Upper Cambrian Little Falls Formation and Lower Ordovician Tribes Hill Formation that are exposed in the adjacent Lower Mohawk Valley area to the west, were also sampled and are included in this study.

2.3 Stratigraphy

The Cambro-Ordovician strata, which are the focus of this study, are exposed in the Saratoga-Lower Mohawk Valley region of central-eastern New York. Previous studies by D.W. Fisher and coworkers (Fisher and Hanson, 1951; Fisher, 1954; Fisher et. al.1961; Fisher et. al. 1970; Fisher, 1977; Mazzullo et. al., 1978), include the Cambro-Ordovician sequence in this area within the 'Beekmantown Group'. I shall use the term 'Sauk Sequence' for the Cambro-Ordovicioan strata in the study area, following the adoption of the term by Guo et. al. (1990). The post-Sauk pre-Tippecanoe surface of unconformity, also known as the "Knox" unconformity, marks the top of the Sauk strata.

The Potsdam Formation, Little Falls Formation, Galway Formation and Hoyt Formation are Upper Cambrian (Croixian), whereas the Gailor Formation and Tribes Hill Formation are Lower Ordovician (Canadian) in age. In the current area of study, two regions can be recognized namely, the vicinity of Saratoga Springs and the Lower Mohawk Valley. The Saratoga Springs area lies on the southeastern edge of the Adirondacks and the Mohawk Valley lies in the south and southwestern edge of the Adirondacks.

The sequence of Cambro-Ordovician strata observed in the Saratoga area includes the Cambrian Potsdam, Galway and Hoyt formations succeeded by the Lower Ordovician Gailor Formation. In the Mohawk Valley region, the Upper Cambrian Little Falls Formation is overlain by the Lower Ordovician Tribes Hill Formation. The Post-Sauk, pre-Tippecanoe surface of unconformity occurs at the top of the Gailor and Tribes Hill formations.

In the Saratoga area the **Potsdam Sandstone** is the oldest unit of Cambrian age and rests on the irregular Precambrian surface. The Potsdam Formation is composed of mainly orthoquartzite and dolomitic sandstone and grades into the overlying Galway Formation.

The Galway Formation has been assigned a Late Cambrian age (Fisher and Hanson, 1951) due to the presence of Franconian-age trilobite fragments found in several of the units. In the Saratoga Springs region, the Galway dolostones are overlain by the Hoyt Limestone. Sandy dolostones, dolomitic sandstones and calcareous sandstones are characteristic of the Galway

Formation. In general, the beds are nonfossiliferous and cherty. Subsurface studies of the Galway (Mazzullo et. al. 1978; Guo et. al. 1990) indicate that the sand content decreases to the top of the formation. Vugs, filled with sparry calcite or dolomite are common near the top. The dolostones range in color from olive gray through medium gray to brownish gray and are medium- to coarse-textured. Intraclasts, relict ooids, desiccation cracks, cryptmicrobial laminites and stromatolites are found in several subunits. Mazzullo et. al. (1978) have observed a sandstone bed "Mosherville sandstone" below the Hoyt Formation and include it in the upper part of the Galway Formation.

The Hoyt Formation which overlies the Galway, consists primarily of medium-bedded, dark-gray, fine- to coarse-textured limestone and subordinate dolostone. Columnar and domal stromatolites, cryptmicrobial laminates and oolites are abundant in these strata. Fisher and Hanson (1951) observed certain Trempealeauan fauna in the Hoyt. Thus, compared to the other units discussed, the Hoyt is exceedingly fossiliferous. The areal extent of the Hoyt Formation is restricted; it is observed only in the Saratoga Springs area.

The Gailor Formation, which overlies the Galway and Hoyt formations in the Saratoga Springs area is considered to be of Early Ordovician age. It is composed of somewhat cherty and quartzose, coarsely crystalline, massive-bedded dolostone units. The Gailor is in general more fossiliferous than the Galway. Two limestone members have been observed in the Gailor, namely the Ritchie member and the Slade Creek member (Mazzullo et. al., 1978). The

Ritchie limestone is composed of dark-gray oolitic limestone and dolostone. The Slade Creek member is generally dark-gray limestone. Local dissolution-collapse structures have been observed in the upper part of the Gailor Formation. Fisher and Hanson (1951), Zenger (1981) and Fisher & Mazzullo (1976) agree that the Gailor Formation is Canadian in age and believe that the Cambro-Ordovician contact lies within the lower few feet of the Gailor.

In the Mohawk Valley, the Little Falls Formation and overlying Tribes Hill Formation make up the Sauk Sequence and are correlative equivalents of the Potsdam, Galway, Hoyt and Gailor formations that occur in the Saratoga area. The **Little Falls Dolostone** occurs in non-conformable contact over Proterozoic gneiss in the Mohawk Valley. At the type section it is about 400' thick. The formation thins eastward towards Saratoga Springs where it is represented by the uppermost Potsdam, Galway and Hoyt formations (Zenger, 1981). The main lithologies in the formation are dolostone and sandstone. Pure dolostone, mixed dolostone-sandstone and orthoquartzite are also present. Limestones and shales are absent whereas chert and glauconite are common in the upper half of the Little Falls Formation. Vugs, hosting dolomite, calcite, anthraxolite and the 'Herkimer Diamonds', are ubiquitous. The only fossils observed in the formation are stromatolites and cryptmicrobial laminites.

The **Tribes Hill Formation** rests on the Little Falls and can be traced throughout the Mohawk Valley. Compared to the Little Falls, the Tribes Hill Formation is non-cherty, contains more calcite and far less quartz. Based on

their faunal assemblages, these strata have been assigned a Canadian age. The Tribes Hill Formation is divisible into five members: The Fort Johnson, Palatine Bridge, Wolf Hollow, Fonda and the Chuctanunda Creek (Fisher, 1954).

The basal Fort Johnson member is a dark-gray dolomitic limestone grading into calcitic dolostone and feldspathic dolostone.. This member is considered to be a facies equivalent of the Gailor Formation that occurs in the Saratoga Springs area. The Palatine Bridge member is composed of interbedded shale and thinly-bedded quartzitic limestone with pyrite, glauconite, trilobite fragments, storm beds, and distinct mottling. The Palatine Bridge member is overlain by the Wolf Hollow member. This member is distinguished by massive, dark-gray dolomitic limestone, and mottled dolostone. Compared to the older members, the Fonda is highly fossiliferous. The main lithologies observed here are coarse limestones, flat-pebble conglomerates, dolostones, oolitic and skeletal grainstones, and packstones. The fauna include Ribeirids, gastropods, trilobites, cephalopods, brachiopods, and conodonts (Fisher, 1954). At the top of the Tribes Hill Formation are a sequence of medium-to thick-bedded, medium-textured dolostones of Early Canadian age named the **Chuctanunda Creek** dolostone.

A revision of the internal stratigraphy of the Tribes Hill Formation has been proposed by Landing et. al. (1996), where they introduce new names for the members of the Tribes Hill strata. According to their study, the Fort Johnson member and most of the Palatine Bridge member form the new "Sparkers"

member, which includes thin- to medium-bedded dolostone and limestone with intraclasts, fossil hash, and burrows in places. This is overlain by the new "Van Wie " member, which is the top of the earlier Palatine Bridge member and is composed of dark-grey shale and intraclast-trilobite-echinoderm-bearing limestone. The "Van Wie" member is succeeded upwards by the revised "Wolf Hollow " member which is composed of medium- to thick-bedded, burrowed, intraclast-bearing massive limestone and dolostone, with biostromal thrombolites at the top of the member. Fisher's (1954) "Fonda " and "Chuctanunda Creek " members have been combined together and called the "Canyon Road" member, which composes the upper Tribes Hill Formation and includes thin- to thick-bedded, fossiliferous, glauconitic, sandy limestone, and burrow-mottled dolostones.

For the purpose of this study I shall use the stratigraphy established by Fisher and supported by other subsequent studies on the Tribes Hill Formation (Braun and Friedman, 1969; Curl, Zagorski and Friedman (1984); Friedman, 1996a, 1997) as my field observations of outcrops of the Fort Johnson and Palatine Bridge members do not fit that described as the "Sparkers" member proposed by Landing et. al. (1996). Their description of the "Sparkers" member is similar to that of Fisher's "Palatine Bridge" member and does not really include the feldspathic dolostones of the Fort Johnson member observed at the Fort Hunter quarry.

2.4 Structural Features in the Area:

The Sauk Sequence strata in the study area are confined to the Saratoga Platform (Figure 1.1). They are generally, flat-lying beds of sandstone, dolostone and limestone, that strike east-west and dip south-west 1.5^0. The thicknesses of the beds typically vary from about 20 to 90 cm and the beds are defined by stylolites, by contacts between contrasting depositional textures, and by shaly partings. The beds have been gently folded; the degree and intensity of folding increases eastward. Fisher's study (Fisher, 1954) demonstrated that the folding occurred prior to the deposition of the Lowville limestone, which is the oldest unit overlying the post-Sauk, pre-Tippecanoe surface of unconformity in the area.

The Saratoga Platform has been dissected by several normal faults, striking roughly north-northeast (Figure 1.2). These faults affect the Cambro-Ordovician Sauk Sequence as well as the younger, overlying Tippecanoe Sequence. Fisher pointed out that the major folds in the Cambro-Ordovician strata are associated with the major faults, suggesting that the folding may have been a forerunner to the normal faulting, which he considered to have been initiated in the Late Ordovician time (Fisher, 1954). Studies of coeval rocks of the Beekmantown strata, in the Ottawa Embayment, north of the study area, show that these normal faults were perhaps responsible for providing pathways for continental-derived waters that migrated through the strata causing dissolution and producing intrastratal paleokarst features in the Beekmantown rocks there (Dix et. al., 1998).

To the east of the Saratoga Platform is the Appalachian fold-thrust belt where structural deformation has been more extensive (Figure 1.1). Towards the end of the Ordovician, when the Taconian Orogeny was initiated to the then-south of the platform, in the Iapetus Ocean, the Cambro-Ordovician platform strata were subjected to tectonic forces. These compressive forces were perhaps responsible for the gentle folds in the then-north and more intense folds and thrust faults in the south.

CHAPTER 3 - DEPOSITIONAL ENVIRONMENTS, PARASEQUENCES AND FACIES

This chapter discusses the depositional environments, facies, and depositional cycles that have been inferred from observations in selected outcrops of the Galway, Hoyt, Gailor, Tribes Hill and Little Falls formations. For the purpose of this study, the outcrops in the Saratoga area are emphasized, with fewer outcrops studied in the western part of the Mohawk Valley. This is because much of the previous work (see section 2.2) that has been carried out on the Cambro-Ordovician rocks of the Saratoga Platform, has focused on outcrops in the western part of the Mohawk Valley.

The rocks of the Sauk Sequence that are exposed in the study area are part of a transgressive sequence which developed as a result of a large-scale submergence of the North American craton starting in the Late Cambrian and culminating in the Middle Ordovician (Figure 2.1). Within this transgressive sequence, in the studied outcrops, several meter-scale depositional cycles or 'parasequences' (Van Wagoner, et. al., 1988; Friedman, Sanders, and Kopaska-Merkel, 1992) are observed, which reflect the lateral progradation of peritidal facies. These parasequences are upward-shallowing cycles that are composed typically of a transgressive, high-energy subtidal deposit that rests on a basal erosive surface. The subtidal facies is overlain by intertidal and finally capped by supratidal facies. The terms ' subtidal', 'intertidal' and 'supratidal' refer to varying

degrees of exposure that shallow, platform-margin sediments were subjected to. Subtidal sediments were continuously submerged, whereas intertidal sediments were irregularly submerged. At the end of the spectrum, supratidal sediments were only occasionally wetted.

In a shallow, tropical, platform-margin setting, as the carbonate material builds up, the shoreline shifts seaward or progrades, causing a previously subtidal facies to be placed in a shallower sub-environment, where then intertidal facies develop. With progressive build-up and shallowing of the depositional area, finally a supratidal flat develops. This results in emergence of a formerly submergent area. Once emergent, carbonate production ceases and a period of nondeposition ensues. If this period is long enough, diagenetic features related to emergence, such as desiccation cracks, evaporites, intraclasts, silcrete, terra rossa, dedolomite, dissolution features, etc. are likely to develop (Friedman and Radke, 1979; Friedman, 1994 a, b, 1995).

Gradual subsidence of the emergent flats will cause them to be flooded once again and carbonate production will resume, producing another cycle of deposition containing subtidal, intertidal and supratidal deposits superimposed over one another in that order. This process repeatedly occurs, ultimately producing meter-scale, upward-shallowing parasequences. Each individual parasequence is bounded by a 'marine flooding surface' (Friedman, Sanders and Kopaska-Merkel, 1992) that marks the initial submergence or drowning of the platform. Thus, the depositional cycles appear to prograde simultaneously with the regional transgressive migration of the shoreline across the platform.

The development of parasequences may therefore be related to the carbonate production, in which case they may be considered autocyclic (Goldhammer et.al., 1990). However, low-amplitude, high-frequency sea-level fluctuations may also be an important causal factor. During the Late-Cambrian to Middle-Ordovician time, global green-house conditions (Wright, 1992) existed. Under these climatic conditions, sea-level changes were not as dramatic as during ice-house conditions (Wright, 1992) when the accumulation and melting of continental ice sheets caused high-amplitude sea-level fluctuations. These large sea-level fluctuations are considered to be Milankovitch's 100 k.y. rhythms caused by changes in the eccentricity of the earth's orbit. During greenhouse times, however, in the absence of high-amplitude sea-level fluctuations, the smaller-scale, low-amplitude (<10m), high-frequency fluctuations caused by Milankovitch's 20 k.y. precession and 40 k.y. obliquity rhythms were more dominant (Wright, 1992; Read and Horbury, 1993). From sequence-stratigraphic analysis of parasequences of the Tribes Hill Formation, Friedman (1994 a, b;1996 a;1997) concluded that the stacking patterns of the parasequences were generated by fifth-order sea-level changes (50 to 100 k.y. duration), which may also be related to cyclic ('yo-yo'), vertical, tectonic, crustal movements. Therefore, the parasequences observed in the Sauk strata on the Saratoga Platform may have resulted from an interplay of several factors, including high carbonate productivity, subsidence, and rapid, low-amplitude sea-level fluctuations caused by extra-terrestrial rhythms and/or tectonic movements.

3.1 Criteria for Recognition of Depositional Facies:

The recognition of subtidal, intertidal, and supratidal sub-environments of deposition, has been based on the type and proportion of mineralogical and lithological components and primary depositional structures observed in outcrops, hand specimens and thin sections of the rocks that were examined. These characteristics shed light on the water depth and energy conditions that were prevalent at the time of deposition of each facies.

3.1.1 Mineralogical and Lithological Components:

The main lithological and mineral components that are present in the strata under consideration are dolomite, primary calcite particles, intraclasts, quartz and feldspar sands, chert, and dedolomite.

The dominant rock type that is observed in these strata is **dolostone.** Fine-textured dolomudstones are commonly observed towards the top of parasequences, where they display fenestral fabrics and / or cryptmicrobial laminae. The dolomicrite is considered to be a syndepositional replacement of lime mud that formed in low-energy intertidal- or supratidal-flat environments. The coarse-textured dolostones are diagenetic modifications of early formed dolomite or have resulted from dolomitization of sand-sized carbonate particles. The high proportion of dolomite in these rocks also attests to the former presence of arid or semi-arid, evaporitic environmental conditions of deposition (Friedman, 1980).

The primary calcite particles that have been observed are pellets, peloids, ooids, and skeletal particles. **Pellets** and **peloids** are products of a low-energy subtidal environment of only moderate water circulation. The **ooidal / skeletal** grainstones are considered to be products of a high-energy, subtidal or lower-intertidal zone.

Intraclasts, when found at the base of a parasequence, directly overlying an erosional surface or 'maximum flooding surface' is considered a transgressive lag deposit, marking the onset of a new depositional cycle. In such cases, the intraclasts are rip-up clasts of desiccated supratidal dolomudstones. Accumulations of intraclasts, forming edgewise breccias, and chaotic, flat-pebble or round-pebble conglomerates are possibly high-energy, storm-generated deposits or tempestites (Sepkoski,1982 ; Chuanmao et. al.,1993; Friedman,1994a).

Siliciclastic components that are common in these rocks are quartz sands and silt-sized particles of quartz and feldspar. The sandstones are composed of well-rounded, clean sands with virtually no mud component indicating deposition in a high-energy subtidal-intertidal setting. Silt-sized particles of quartz and feldspar are widespread in distribution among the Sauk deposits and are especially found associated with cryptmicrobial laminae, where they may represent continent-derived, wind-blown particles that were trapped by the microbial mats on the intertidal flats.

Chert occurs in dolostones as fillings of inter-crystalline voids, fractures and of spherical vugs, and as discontinuous bedded chert. The association of chert with dolomitized units suggests silicification related to subaerial exposure and deposition in an arid-or semi-arid environment (Rubin and Friedman, 1981; Friedman, 1994 b). Bedded chert is considered to indicate a former silcrete bed formed at or near the surface from evaporation of silica-rich, meteoric solutions. Hence, the presence of chert is indicative of emergent conditions perhaps at the termination of a parasequence or from prolonged exposure during an unconformity.

Dedolomite is a product of replacement of dolomite by calcite which is brought about by circulating meteoric water at low temperatures and hence considered to be a near-surface phenomenon (DeGroot, 1967; Evamy, 1967; Friedman, 1994b; Guo, 1994; Guo et. al., 1996). Therefore, the presence of dedolomite is indicative of subaerial exposure at the termination of a parasequence or at a surface of unconformity.

3.1.2 Depositional Structures:

The major depositional structures observed in the rocks under consideration are fenestrae, mudcracks, cryptmicrobial laminites, stromatolites, herringbone cross strata, channels, burrow-mottles, and dissolution-collapse breccia. These structures have been used in environmental interpretation.

Fenestrae also known as 'bird's eye' structures are open and filled vugs containing sparry calcite, saddle dolomite, or euhedral quartz. They are found to be abundant in dolomudstones and are interpreted as indicative of either dissolved-out former evaporite nodules (Selleck, 1987) or of former gas bubbles within cyanobacterial mats. This feature may therefore indicate deposition in intertidal or supratidal areas.

Mudcracks are formed in supratidal flats where desiccation of dolomicrites form polygonal cracks in an arid or semi-arid climate.

Cryptmicrobial laminites are crinkled or wavy laminae of low relief, believed to have formed by colonization of intertidal and supratidal flats by cyanobacterial mats. The microbial mats develop in the low-energy environments of the intertidal and supratidal flats.

Stromatolites are high-relief, domal or columnar structures made up of crinkly and wavy laminae, which are also products of cyanobacterial colonization. The stromatolites however, are products of a high-energy subtidal or lower-intertidal channel environment.

Herringbone cross strata are common in the sandstones and are perhaps indicative of a tidally influenced high-energy zone. These cross strata are interpreted as products of bidirectional tidal currents in tidal channels. In some of the outcrops trough-shaped channels are observed, which are believed to be cross sections of tidal creeks or channels.

Burrow mottles are observed in some of the outcrops. Both vertically and horizontally burrowed strata have been found in the studied outcrops. These bioturbated units are interpreted as indicative of a shallow subtidal to intertidal environment of deposition.

In some outcrops **dissolution-collapse breccias** are observed which indicate emergence of the strata and subsequent collapse of the beds due to dissolution, by circulating meteoric water, of evaporites from underlying beds.

Taking together the field-, hand-specimen, and petrographic characteristics of the rocks of the entire Sauk Sequence examined, three peritidal sub-environments of deposition are recognized, namely (A) Shallow Subtidal; (B) Intertidal and (C) Supratidal. On the outcrop scale it is commonly noted that the subtidal deposits are massive or thick bedded, whereas the intertidal or supratidal deposits are commonly thin bedded or exhibit layering. A total of eleven lithofacies has been recognized in these sub-environments. Some of the lithofacies may be found in more than one adjacent sub-environment.

- Within the **shallow subtidal facies**, the following lithofacies are recognized:

  Lithofacies 1: Ooid /Peloid/ Skeletal Dolomitic Grainstone/Packstone;

  Lithofacies 2: Burrow-Mottled Dolostone / Limestone;

  Lithofacies 3. Intraclast Dolostone / Limestone;

Lithofacies 4: Stromatolitic Boundstone;

Lithofacies 5: Sandstones (Herringbone cross strata in places);

Lithofacies 6: Shale;

- **Intertidal facies** can be recognized by the following lithofacies:

  Lithofacies 4: Stromatolitic Boundstone;

  Lithofacies 7: Dolomudstone (Fenestral Dolostone);

  Lithofacies 8: Cryptmicrobial-laminated Boundstone;

- The **supratidal facies** contain the following lithofacies:

  Lithofacies 7: Dolomudstone (Fenestral /Mud-cracked);

  Lithofacies 8: Cryptmicrobial-laminated Boundstone;

  Lithofacies 9: Silty Quartzo-Feldspathic Dolostone;

  Lithofacies 10: Chert;

  Lithofacies 11: Dissolution-collapse Breccia;

In the different outcrops that were examined, subtidal, intertidal and supratidal facies are stacked in order from bottom to top forming individual parasequences. However, not all facies are present in all the parasequences. At some places, the products of a supratidal zone are missing, whereas in other cycles, the subtidal facies is not present. In the following sections, depositional facies and parasequences observed in the different formations will be discussed.

3.2 Facies Analysis Of The Galway Formation:

Six outcrops of the Galway Formation were studied (Figure 3.1). Outcrop sections #1 and #2 are located on Route 29, west and east of Junction 147. Outcrop section #3 is located on Route 29 in East Galway. Outcrop section #4 is a roadcut on Route 9N and Section #5 is a railroad cut, close to Route 9N, stratigraphically above section #4. The lower part of the Hoyt section (outcrop #6) in Petrified Gardens Park, is also part of the Upper Galway. Figure 1.2 shows these outcrop locations.

3.2.1 Lithofacies in the Galway Formation:

In general, the Galway strata consist of dolomitic sandstones, sandy dolostones and dolostones with virtually no limestones. The dolostones are fine- to medium-crystalline and in places cherty. These outcrop sections are of limited vertical extent and range from 16' to 29'. However, in all the outcrops examined, two or more upward-shallowing, depositional cycles have been observed, with facies changing from subtidal to intertidal to upper-intertidal or supratidal.

Figure 3.1. Outcrops of the Galway Formation (Figure 1.2 is map showing location of sections)

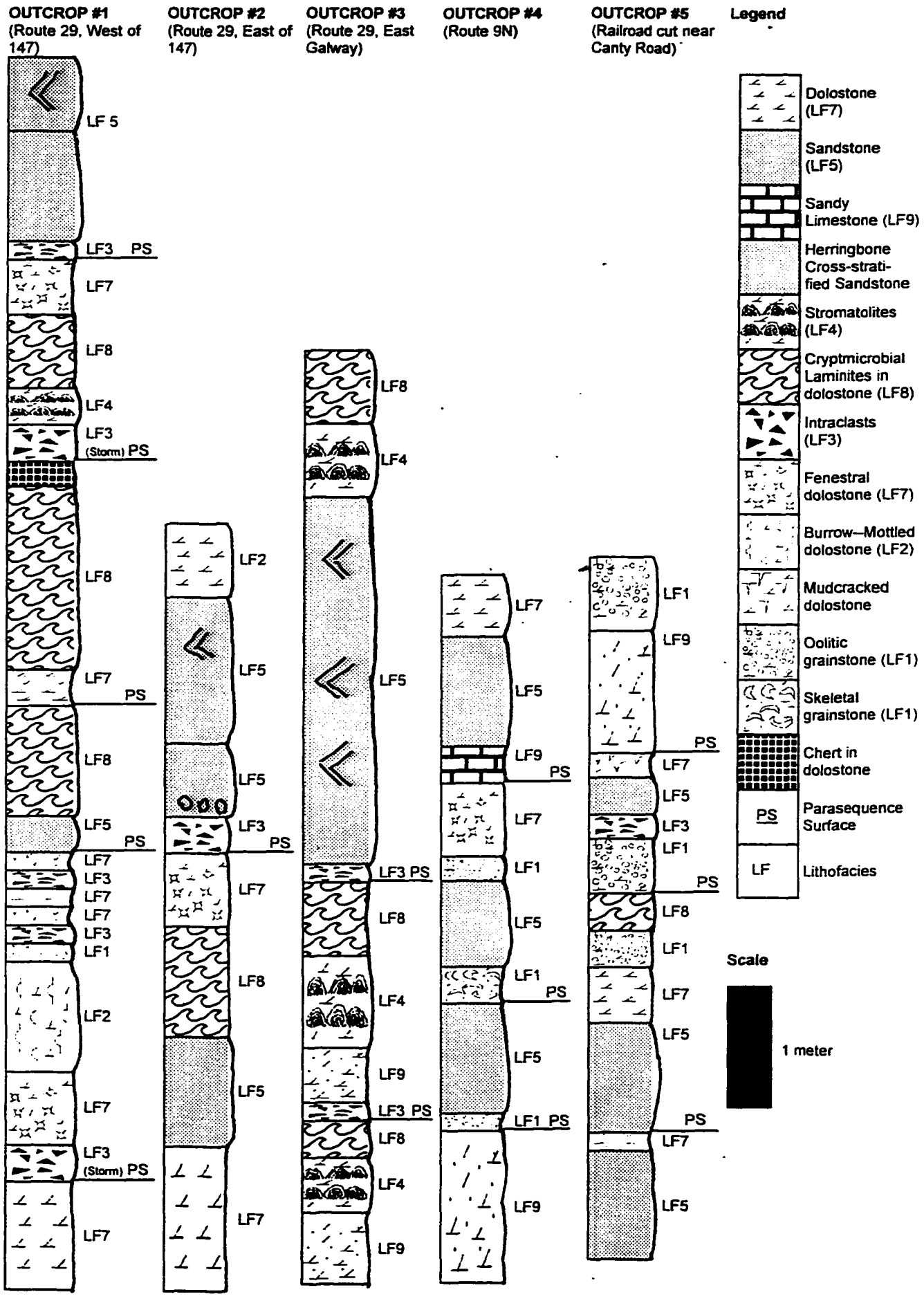

Petrographically, the dolostones are in general, pervasively dolomitized with some dolostones revealing ghosts of former allochems. However, on the outcrop scale, some sedimentary structures can be recognized. The dolomitic sandstones are interbedded with the dolostones and commonly show herringbone cross strata. Several horizons of intraclasts forming flat-pebble conglomerates are observed directly above erosional surfaces. Fine-textured dolostone horizons with mudcracks have also been noted in places. Vugs or fenestrae, either open or filled with sparry calcite and or saddle dolomite are common. Burrow mottles are locally present in some of the beds.

The only notable fossils observed to be present in these strata are domal stromatolites, cryptmicrobial laminites, and minor amounts of trilobite fragments. Fisher (1951) reported trilobites *Elvinia ruedemanni, Berkia saratogensis,* and *Camaraspis* from the sandy limestone units in outcrop section #4 and trilobites *Lingula acuminata* and *Plethometopus* from section #5.

The following lithofacies are observed in the Galway units:

Lithofacies 1: Ooid /Peloid/ Skeletal Dolostone

Lithofacies 2: Burrow-Mottled Dolostone

Lithofacies 3: Intraclast Dolostone

Lithofacies 4: Stromatolitic Boundstone

Lithofacies 5: Herring-bone cross-stratified Sandstone

Lithofacies 7: Dolomudstone (Fenestral / Mud-cracked)

Lithofacies 8: Cryptmicrobial-laminated Boundstone

Lithofacies 10: Chert

Lithofacies 1:Ooid /Peloid/Skeletal Grainstone:

This lithofacies type occurs as light to dark gray dolostones with a fine- to medium-crystalline texture. Although they have been completely dolomitized, relict textures reveal that they were originally oolitic, peloidal, or fossiliferous grainstones or packstones. Petrographically, the allochems and matrix are composed of different types of dolomite. The ooids are concentric (Figure 3.2), but no further detail of their internal structure is observed. The ooids are composed of microcrystalline dolomite, suggesting early syndepositional dolomitization, whereas the matrix is composed of coarser euhedral zoned dolomite which formed during later diagenesis. Other rocks of this lithofacies are composed of peloids and unrecognizable skeletal particles as their internal structures are completely obliterated by repeated episodes of dolomitization. Their outlines are the only hints of their presence, preserved as micrite envelopes (Figure 3.3).

This lithofacies is interpreted as a subtidal or intertidal channel deposit as the presence of ooids and other allochems, perhaps skeletal particles, suggest a high-energy environment of deposition. The ooids may represent shoals within or proximal to tidal channels. This lithofacies is observed in outcrop sections #1, #4 and #5.

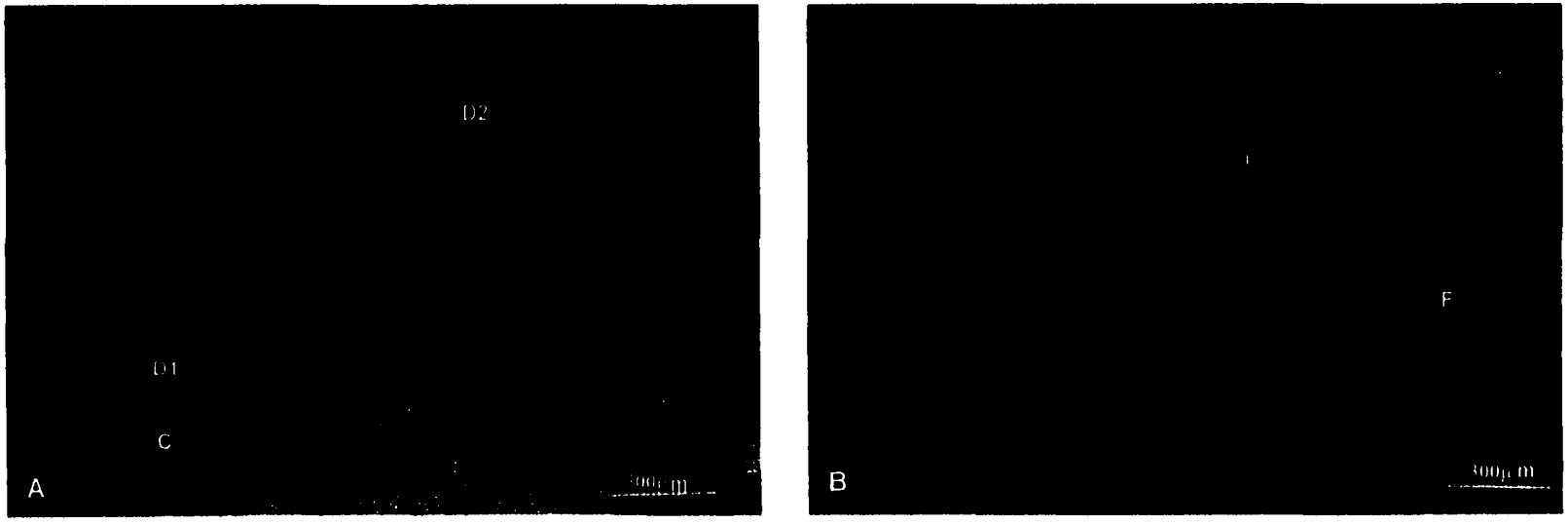

Figure 3.2 : Oolitic dolostone (Sample # GB-10, Lithofacies 1, Galway Formation, outcrop section # 1). The ooids are composed of dolomicrite (D1) that has replaced concentric micritic laminae, which envelope coarser, unzoned dolomite (D2) within the ooids. The inter-particle cement (C) is zoned late-stage dolomite, which grew around the ooids and detrital quartz grains (Q). (A) is seen in plane-polarized light and (B) is the same view under cathodoluminescence, where dolomite luminesces orange-red, quartz luminesces navy blue and feldspar (F) luminesces bright blue.

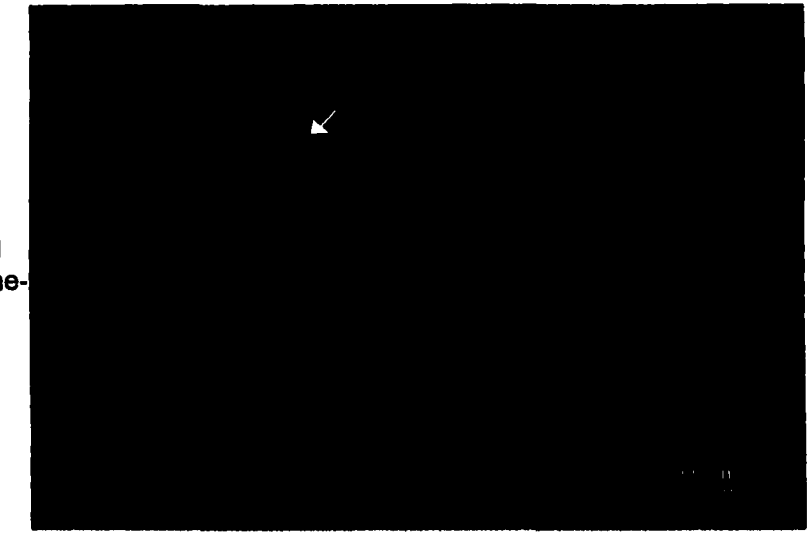

Figure 3.3: Lithofacies 1 in the Galway Formation, located in outcrop section #1, showing micrite envelopes (arrow) around allochems (Sample# GB-1). Thin section is viewed under plane-polarized light.

Sandy skeletal limestones are observed only in outcrop #4 and occur as thin fissile beds of limited vertical extent. They are fossiliferous and composed of silt- and sand-sized detrital quartz and feldspar particles. The skeletal debris in these strata are mainly composed of trilobite fragments.

This lithofacies occurs at a couple of horizons in outcrop section #4 and at each place overlies low-energy intertidal dolomudstones of Lithofacies 7 and underlies high-energy, subtidal sandstones of Lithofacies 5. This implies that Lithofacies 1 formed as a subtidal lag deposit, deposited in a high-energy regime, during a rapid submergence at the onset of a new parasequence.

Lithofacies 2: Mottled Dolostone:

This lithofacies is rare in the Galway and occurs only in one massively bedded unit in outcrop section #1. Both horizontal and vertical burrows are observed in this lithofacies. The rock is composed of pervasive mosaics of medium-crystalline dolomite. Under the luminoscope, these dolomites are nonzoned, high in Mn, and low in Fe. The burrows, however are composed of zoned dolomite with a more porous texture (Figure 3.4). No other depositional texture is observed in this lithofacies, but the bed composed of this lithofacies is overlain by units containing ooids and peloids.

The mottled structure in these rocks is recognized better in the outcrop (Figure 3.5) and in hand specimen. As the mottling is inferred to have resulted from burrowing, this lithofacies probably represents a depositional setting where bioturbation was prevalent. In addition, the massive nature of this bed is

Figure 3.4: Thin section of burrow-mottled dolostone (Lithofacies 2) in the Galway Formation, located in outcrop #1 (Sample # GB-11). Under the microscope, the burrows (B) appear as porous patches within the replacement dolomite mosaic, where late-diagenetic dolomite cement (C) has formed, partially occluding the porosity. Thin section is viewed under plane-polarized light.

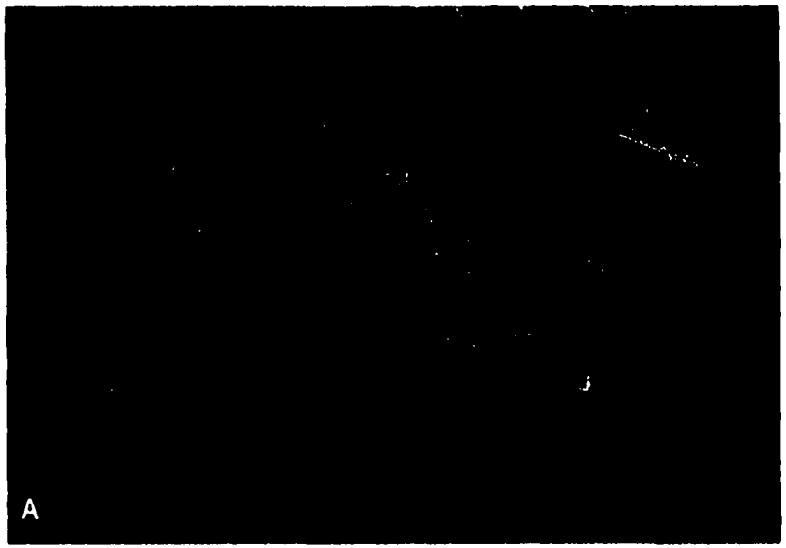

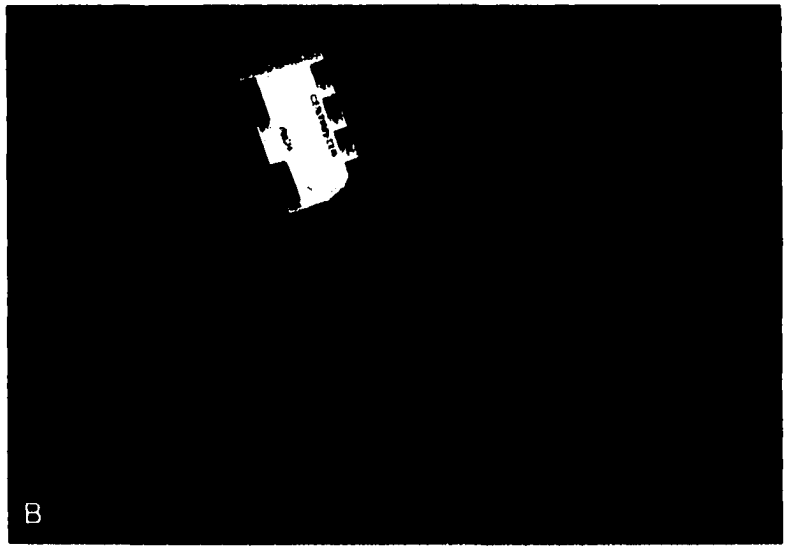

Figure 3.5A & B: Outcrop view of mottled dolostone (Lithofacies 2), in the Galway Formation, located in outcrop #1. Arrows point to mottles. Hammer is for scale in (A).

suggestive of a low-energy subtidal setting where organisms burrowed into the subtidal muds. The lack of burrow mottles in any of the associated intertidal and supratidal beds of the Galway dolostones is probably due to the hypersaline conditions that may have been prevalent there. The porous nature of the burrows suggest that they may have served as conduits for dolomitizing fluids during diagenesis.

Lithofacies 3: Intraclast Dolostone:

This lithofacies is observed at several places in the outcrop sections #1 and #4. The intraclasts are composed of very fine-crystalline or microcrystalline dolomite and are surrounded by a coarser-crystalline dolomite with detrital sand particles and ghosts of peloids. The dolomite within the intraclasts has a high Sr content and is generally low in other trace-elements.

This lithofacies is inferred to represent the rapid submergence that occurs at the onset of an upward-shallowing, depositional cycle. The presence of the intraclasts as flat-pebble conglomerates above an erosional surface (Figure 3.6 A) suggests that a rapid submergence or storm caused mud chips of the mudcracked, supratidal or intertidal flat to be ripped up and incorporated in the basal lag of the ensuing subtidal facies. The chaotic nature of some intraclast beds in the Galway (Figure 3.6 B), imply rapid, high-energy conditions. Such accumulations of intraclasts may therefore indicate deposition resulting from particularly intense storms (Aigner, 1982, 1985; Sepkoski, 1982; Chuanmao et.al., 1993; Friedman, 1994a).

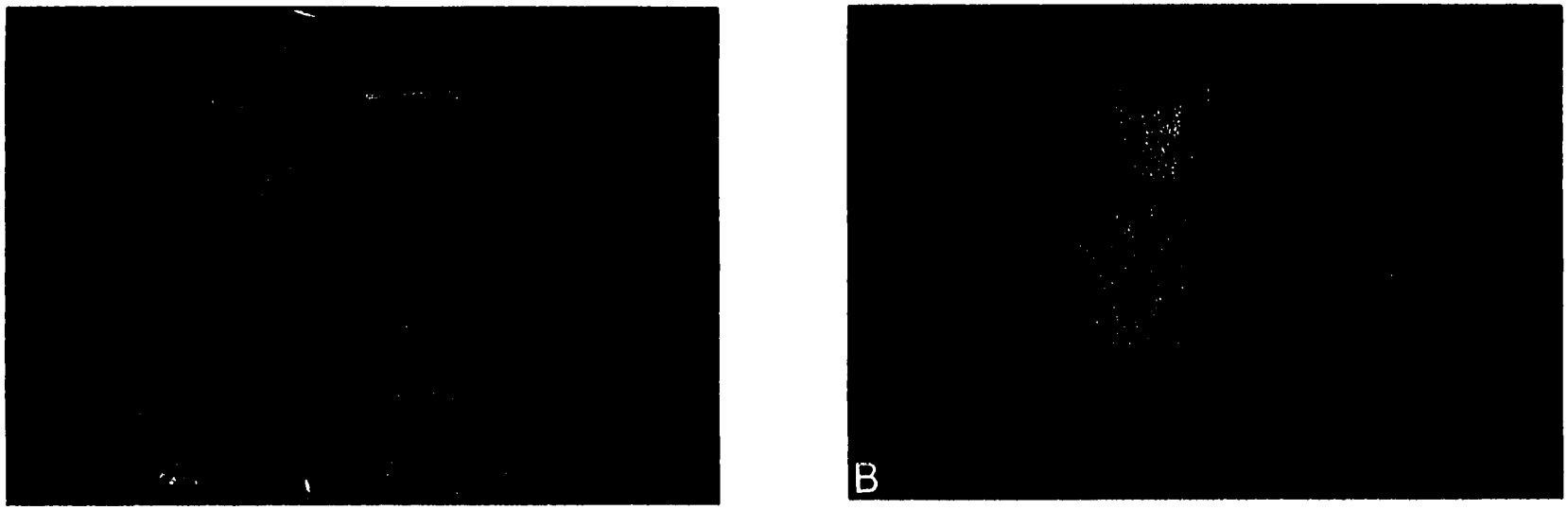

Figure 3.6: Intraclasts (Lithofacies 3) in dolostone bed in the Galway formation located in outcrop # 1. In (A) the intraclast bed overlies an erosional, parasequence surface. (B) is a thicker intraclast bed, possibly a storm deposit. The intraclasts are composed of dolomicrite. Knife and hammer are for scale.

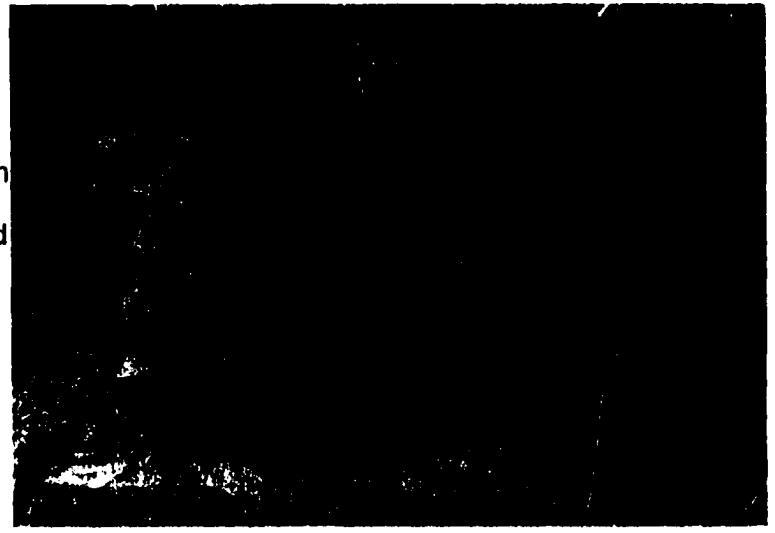

Figure 3.7: Pseudobreccia in the Galway dolostones, located in outcrop # 1 . The mudcracked layer has produced intraclasts that appear to fit back together as they have not been removed from their place of origin. The 'V' shaped disturbance of the layer may indicate a local dissolution-collapse. This is a very common feature in these units. This unit is inferred to be supratidal in origin. Marker used for scale is 16cm. long.

Figure 3.7 shows pseudobreccias that were produced by desiccation cracks on an emergent surface. The intraclasts are parallel to the bedding and fit back together. In this case the collapse may indicate local dissolution-collapse. The fine texture and geochemical relationships of the intraclasts attest to their origin on a desiccated, supratidal flat where syndepositional dolomitization may have occurred due to the elevated salinities produced in an arid, evaporative environment. These intraclast (flat-pebble conglomerate) units, thus serve as markers to recognize storm events and rapid submergence at parasequence surfaces.

Lithofacies 4:Stromatolitic Boundstone:

Domal or hemispheroidal stromatolites are observed in outcrop sections #1 and #3 (Figure 3.8), forming thick beds of high-relief structures. They are composed of fine-crystalline, dolomite laminae interlayered with detrital sand, skeletal particles, and ooids. Laminoid fenestrae are observed between the stromatolitic laminae. The stromatolites are interbedded with herringbone cross-stratified, dolomitic sandstones (Figure 3.9). Almost all of outcrop section #3 is made up of this sequence.

Stromatolites are interpreted as "organo-sedimentary structures, produced by sediment trapping, binding and/or precipitation as a result of the growth and metabolic activity of micro-organisms, principally cyanophytes" (Walter 1976). The voids or fenestrae observed between the laminae may have formed as a result of gases generated by organic decay, which can lift subaqueous or buried

Figure 3.8: Domal stromatolites (Lithofacies 4) in the East Galway section (outcrop # 3) of the Galway Formation. Hammer is for scale.

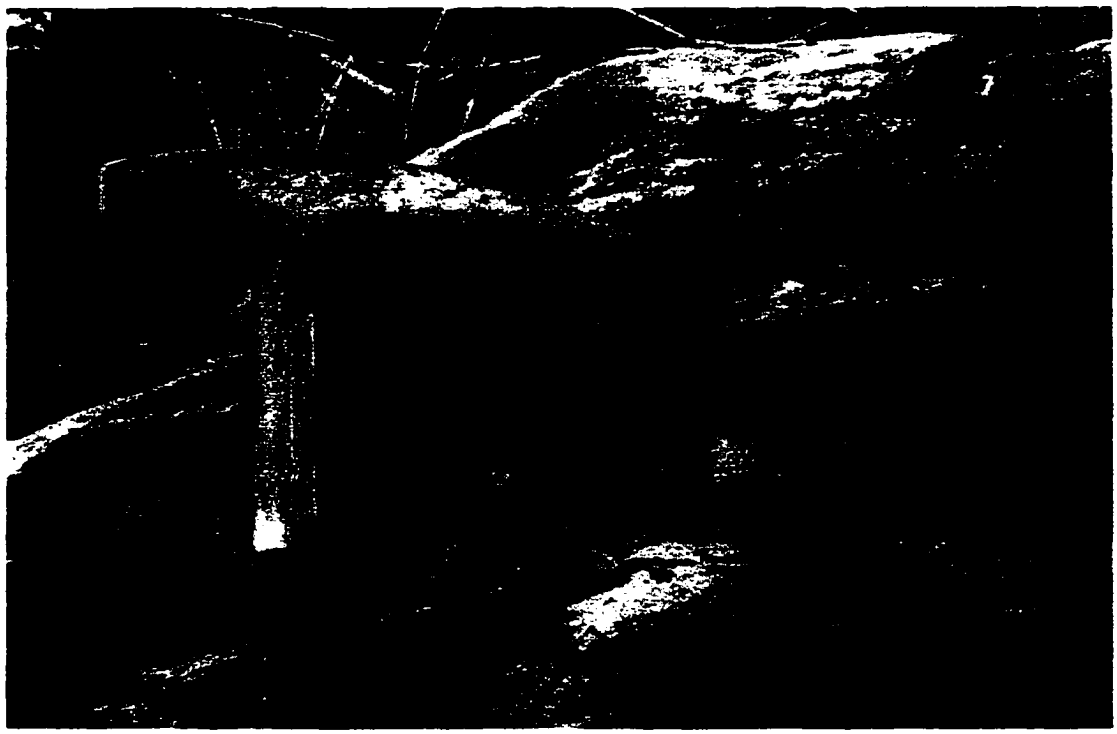

Figure 3.9: Herringbone cross strata in the sandstones (Lithofacies 5) of the Galway Formation (outcrop #1). These tidal-current deposited sandstones are in places interbedded with domal stromatolites. Hammer is for scale.

mats. They may also form by drying out of the mats causing them to wrinkle lift and separate. This may happen when the stromatolites are subaerially exposed (Demicco and Hardie, 1994).

The morphology and association of the stromatolites with cross-stratified sandstones and the presence of skeletal and detrital debris suggest a high-energy subtidal to lower intertidal channel depositional environment for this lithofacies. The presence of well-developed stromatolites also indicate fair-weather conditions, when biochemical deposition is favored.

Lithofacies 5: Herringbone Cross-stratified Sandstone:

This lithofacies is very common and observed in all the outcrops of the Galway Formation. The dolomitic sandstones are coarse- to medium-textured and light gray in color and form thick massive beds of about 0.5 to 1m thick. In outcrop #2 they are very coarse and conglomeratic at the base. The sandstones contain well-rounded and moderately-sorted detrital quartz and feldspar particles. These detrital particles show authigenic overgrowths and have scattered rhombs of zoned dolomite in their interstitial spaces. On the outcrop scale, these dolomitic sandstones display beautifully preserved herringbone cross strata (Figure 3.9). The feldspathic dolostones are composed entirely of nonzoned, xenotopic, fine- to medium-crystalline mosaic dolomite with silt-sized detrital feldspar and quartz. The feldspar and quartz particles display authigenic overgrowths in places.

The dolomitic sandstones are interpreted as subtidal and lower-intertidal channel deposits. The herringbone cross strata they preserve are inferred to result from the bidirectionality of tidal currents. The abundance of quartz and feldspar in this lithofacies can be explained by the landmass to the north of the paleo-depositional area (Fisher 1954), i.e the Proterozoic metamorphic rocks of the ancestral Adirondack mountains that were exposed during Cambro-Ordovician time. Mazzullo et. al. (1978) suggest their origin to be from nearby coastal eolianites.

Lithofacies 7: Dolomudstone / Fenestral Dolostone:

The dolostones of this lithofacies are light to dark gray and consist of microcrystalline to fine-crystalline dolomite. They contain irregularly shaped vugs that are partly or completely filled with late-diagenetic quartz, calcite, and saddle dolomite. Some of the microcrystalline dolomite horizons contain lenticular molds completely filled with late calcite. It is not clear if these are in fact evidence of former evaporite crystals. Mudcracks are observed in this lithofacies. Intraclasts are usually composed of this lithofacies type. Fine, plane laminae are seen occasionally in this lithofacies. The dolomudstones are commonly thin bedded (roughly 10-20cm thick) and in places form more massive beds (roughly 1m thick).The more massive dolomudstones may be products of low-energy subtidal conditions, whereas the thin-bedded units are possibly intertidal to supratidal deposits.

Petrographically, these dolomudstones are composed of very fine-crystalline xenotopic to hypidiotopic mosaic dolomite which appears either nonzoned or displays dull, blotchy luminescence.

Where this lithofacies occurs as thin beds associated with intraclasts and mudcracks, it is interpreted as the product of pervasive dolomitization of lime mud in supratidal and upper-intertidal flats on the basis of analogous features observed in most modern and other ancient tidal deposits (Demicco and Hardie,1994). Mudcracks are clear indicators of desiccation on supratidal and intertidal flats where they represent shrinkage of supratidal muds due to subaerial exposure.

The vugs or fenestrae are irregular to subspherical and may be formed by desiccation (Shinn, 1968). They may also result from gas bubbles trapped during deposition or may have been generated by post-depositional decay of organic matter. It is also possible that these fenestrae represent evaporite molds. These are remarkably similar to the voids described by Selleck (1987) in correlative dolostone units of the Theresa and Ogdensburg formations. He has interpreted these voids as having originated as anhydrite nodules that grew displacively in the host sediment. Extensive zones of vugular porosity have been reported in subsurface units of the correlative Theresa Formation in southwest New York. Tests for oil and gas in these porous horizons have suggested that these rocks may, as a result, be economically productive (Linn, 1998).

The fine-crystalline nature of this type of dolostone suggests early syndepositional dolomitization of the intertidal-flat muds. The fine crystal sizes of

the dolomudstones may indicate rapid nucleation of dolomite crystals during replacement of fine-crystalline precursor carbonate. Fine-crystalline precursor lime-mud particles were perhaps more susceptible to rapid dolomitization due to the large surface area that was exposed to dolomitizing fluids (Gregg and Sibley, 1984). The geochemical characteristics also support an early syndepositional origin for these dolomites in an environment low in trace-elements Mn and Fe and high in Sr. The high Sr (663 ppm) content suggests a hypersaline environment of dolomitization.

Lithofacies 8:Cryptmicrobial-laminated Boundstone:

This lithofacies is observed in outcrop sections #1 and #5. On the outcrop scale, this lithofacies is recognized as irregularly laminated dolostones with wavy or crinkled laminae (Figure 3.10). Petrographically it is composed of fine-crystalline dolomite mosaics with ghosts of parallel laminae. The cryptmicrobial laminated dolostones are associated with laminar fenestrae and ghosts of ooids. Also present among the layers are detrital quartz and feldspar.

The wavy, irregular nature of these laminae suggests their biological origin. Pervasive dolomitization and diagenesis have obliterated all original microbial material and their former presence is only suggested by the traces of organic matter seen as dark laminae. The well-preserved cryptmicrobial laminites are interpreted as having resulted from microbial mats on the upper intertidal and supratidal flats, where the high salinity protected them from being destroyed by

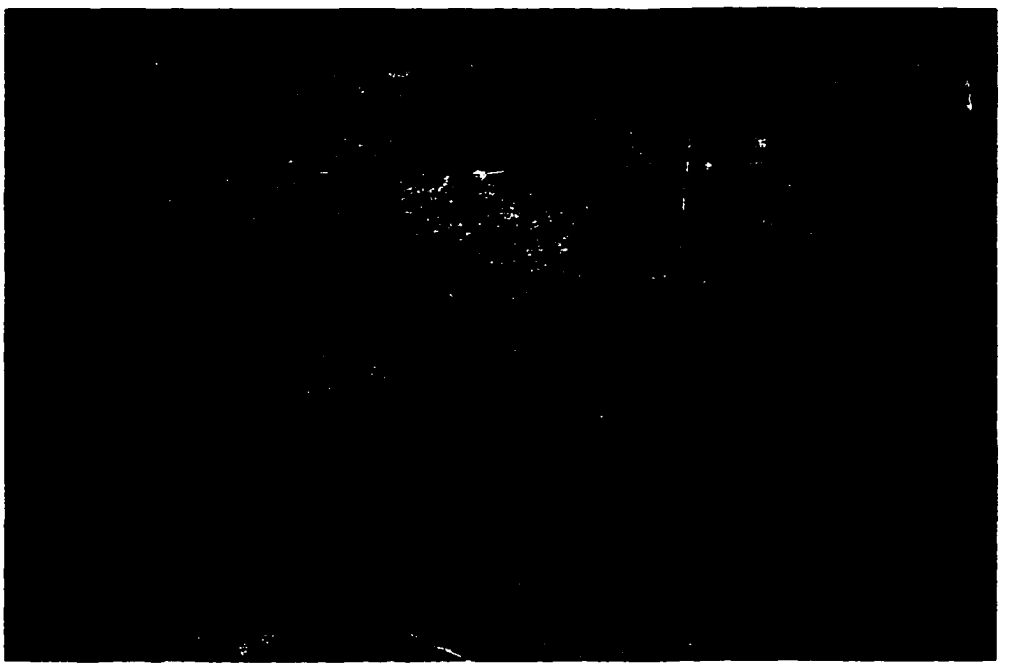

Figure 3.10: Cryptmicrobial laminites in the Galway dolostones (Lithofacies 8), located at outcrop #1. The laminae appear wavy and crinkled and are in places overlain by intraclast dolostones. This unit is inferred to be an upper-intertidal unit. The overlying intraclasts mark a change to a high-energy depositional regime possibly due to storm tides. Knife is for scale.

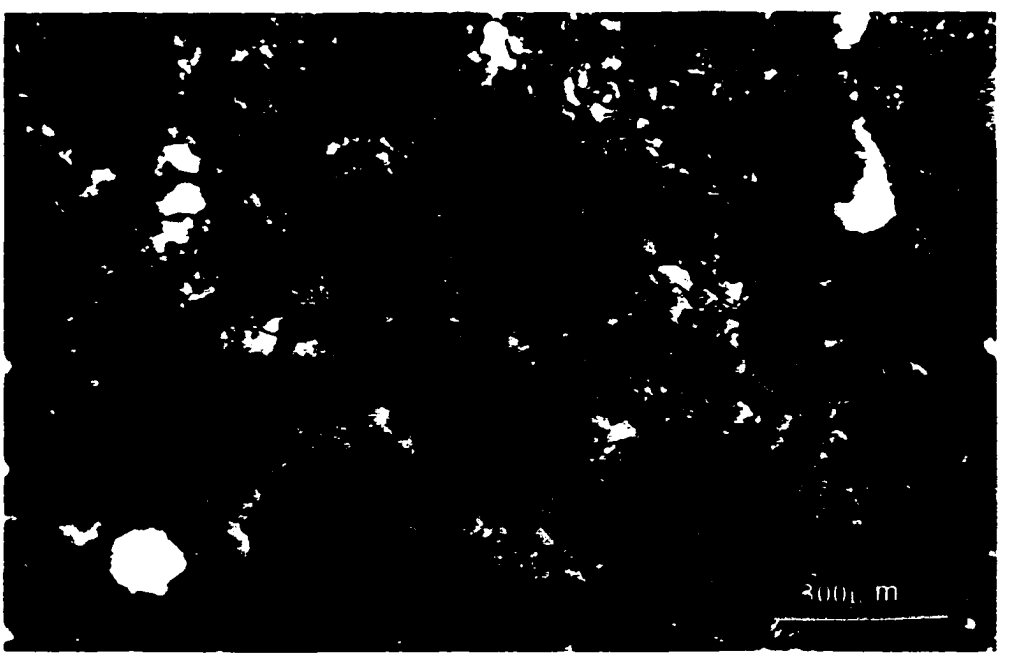

Figure 3.11: Thin-section photomicrograph of silicified ooids in the Galway strata that occur stratigraphically below the Hoyt formation, in outcrop # 6. Thin section is viewed in plane-polarized light.

grazing organisms. These microbial mats trap between their layers wind-blown sands and ooids washed over from the adjacent lower intertidal channels.

Thus, this lithofacies is interpreted as representing upper-intertidal to supratidal sub-environments of low-energy tidal flats.

Lithofacies 10: Silicified Ooid/ Skeletal grainstone, Dolomitic Chert:

Microcrystalline quartz and megaquartz occurs as patches in oolitic dolostone in outcrop #1. In outcrop #6, which is interpreted as uppermost Galway and stratigraphically below the Hoyt, a horizon of silicified ooids and some skeletal particles is recognized. The ooids are replaced by microcrystalline quartz and the matrix and fossil fragments are replaced by megaquartz (Figure 3.11).

In the first example, the petrographic relationships indicate that the chert postdated dolomitization and predated burial-diagenetic cements. It is interpreted as a replacement or silicification related to uplift of the basin where meteoric, acidic waters precipitated silica. If so, then this chert is therefore a product of shallow diagenesis. In the case of the completely silicified ooids, silicification may have occurred when oolite shoals were subaerially exposed or emergent allowing meteoric waters rich in silica to circulate through them, which may imply early, post-depositional diagenesis. The oolitic dolostones and completely silicified oolites are inferred to represent deposition in a subtidal environment of moderate turbulence.

3.2.2 Parasequences in the Galway Formation

In outcrops sections 1 to 5, which are surface exposures of the Galway Formation several parasequences were observed. In general the parasequences range in thickness from about 1 to 5 m. In outcrop section #1, three to four parasequences are observed. Each of these cycles displays a change from high-energy to low-energy conditions or from a deeper to shallower realm of deposition. At the base of some of the parasequences a lag deposit composed of intraclasts, quartz sand, or ooids can be seen above an erosive parasequence surface denoted as 'PS' in the figures.

The lower parts of the individual parasequences are commonly composed of high-energy lithofacies, such as clean quartz-arenite sandstones, ooid-peloid-intraclast grainstones, and domal stromatolites or subtidal low-energy facies such as burrow-mottled dolostones, and dolomomudstones. Towards the top of the parasequences these subtidal facies are overlain by low-energy shallow-water intertidal and supratidal facies denoted by the development of Lithofacies 7 (fenestral dolomudstone) and Lithofacies 8 (cryptmicrobial laminites). At the termination of the individual parasequences, some features related to emergence of the strata, such as desiccation-cracks, dedolomite, and chert are noted.

Outcrop section #2 is comparatively limited in thickness and hence only two parasequences are observed here. In this outcrop, the cycles are composed of a lower high-energy facies containing coarse, conglomeratic sandstones

(Lithofacies 5) that are in places herring-bone cross stratified, overlain by intertidal dolomudstones of Lithofacies 7. A lag deposit of intraclasts, skeletal fragments and ooids is observed at the parasequence surface denoting a rapid flooding event that suddenly inundated a microbial laminated intertidal-supratidal flat.

In outcrop section #3, three parasequences are observed, each composed of a succession of lithofacies starting with cross-stratified dolomitic sandstones (Lithofacies 5) or sandy dolostones (Lithofacies 9) at the base followed by domal stromatolites (Lithofacies 4) and finally topped by thinly-laminated planar stromatolites or cryptmicrobial laminites (Lithofacies 8). Intraclasts are observed interspersed among the cryptmicrobial laminae near the top of the parasequences indicating emergent horizons.

The three parasequences observed in outcrop #4 are composed of a basal lag deposit of intraclasts, and skeletal fragments overlain by high-energy subtidal, oolites and cross-stratified sandstones which are topped by intertidal fenestral dolomudstones.

Similar successions are seen in outcrop #5 as well, where the parasequences are composed of subtidal high-energy facies, such as cross-stratified dolomitic sandstones, sandy dolostones, and oolitic grainstones that are topped by cryptmicrobial laminated dolostones, dolomudstones, or mud-cracked sandstones.

3.2.3 Summary of Depositional Facies in the Galway Formation:

The Galway outcrops can be characterized as mixed carbonate-siliciclastic units, composed of dolomite, silty, sandy dolomite, and sandstones. The siliciclastics are probably formed by reworking of eolian sand by tidally influenced water movements.

The stacking of lithofacies in the outcrops of the Galway Formation shows at least two or more upward-shallowing cycles or parasequences (Figure 3.1). Each cycle has lithofacies ranging from subtidal to intertidal to supratidal sub-facies.

The intraclast breccias overlying erosional surfaces indicate a rapid submergence occurring on a previously supratidal flat formed as a result of a storm event or a sea-level fluctuation. The products of the ensuing subtidal sub-environment are characterized by ooidal / peloid / skeletal dolostones, mottled dolostones, stromatolites, or cross-stratified dolomitic sandstones (Lithofacies 1, 2, 4, & 5). The upper-intertidal and supratidal flat facies are low-energy zones, where features related to desiccation are common. Here the lithofacies observed are cryptmicrobial laminites, and mudcracked- and fenestral dolomudstones (Lithofacies 8 & 7). Chert and dedolomite are also observed in places and are inferred to mark episodic emergence of the strata.

The paucity of fauna and high Sr values for the supratidal dolomite suggest an arid depositional setting where high evaporation rates may have created a hypersaline environment conducive for early dolomitization. The

repeated stacking of upward-shallowing cycles indicates high carbonate production in a shallow marine, transgressive, peritidal setting.

3.3 Facies Analysis of The Hoyt Formation:

Three outcrops (#6, 7 & 8) of the Hoyt Formation were examined, all located in the vicinity of Saratoga Springs. The two main sections that were sampled were outcrop section #6 in the Petrified Gardens and outcrop sections #7 located in Lester Park Quarry. Outcrop #8, a roadcut on Petrified Gardens road and a section in Skidmore Quarry was also examined. Columnar sections of outcrops 6, 7, and 8 are sketched in Figure 3.12.

3.3.1 Lithofacies in the Hoyt Formation:

The Hoyt limestone has been thoroughly studied by generations of geologists starting in the 1800s and continuing up to the present. The depositional environments in the Hoyt Formation were examined and worked out by Owen and Friedman (1984) and Friedman (1988). They concluded that the Hoyt strata represent a sequence of oolite shoals separated from the peritidal shoreline by a lagoon, and inferred a "high-energy shoreline" depositional environment.

The Hoyt strata are composed mostly of dolomitic limestones and calcareous dolostones. Of the Sauk carbonate units in the Saratoga Springs area, the Hoyt Formation is the most calcareous and the most fossiliferous. The

Figure 3.12 Outcrops of the Hoyt Formation
(Figure 1.2 is map showing location of sections)

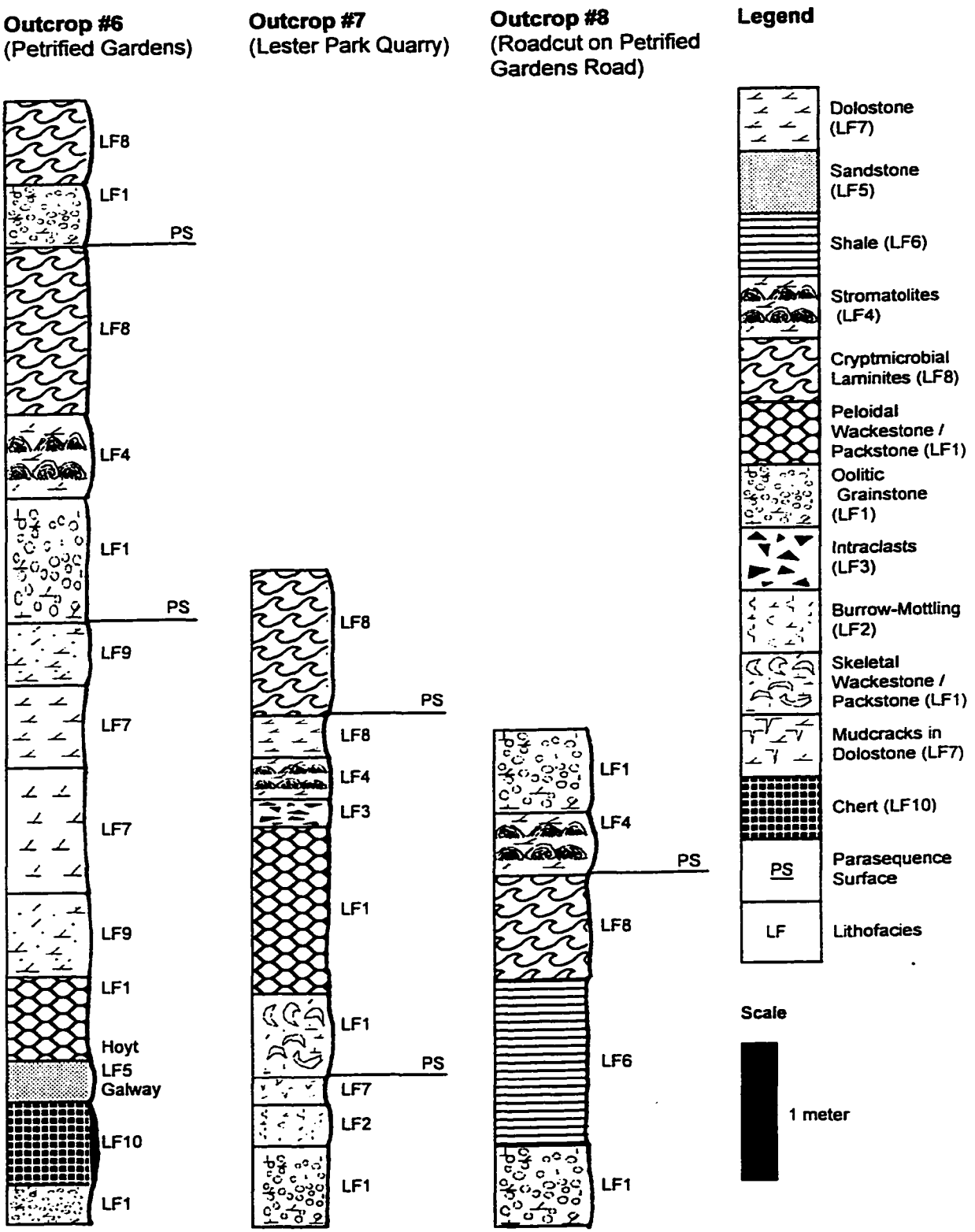

faunal assemblage reported from the Hoyt includes columnar and domal stromatolites, cryptmicrobial laminites (*Cryptozoon proliferum, C. ruedemanni, C.* cf. *undulatum)* and several genera of trilobites namely *Keithiella speciosa, Saratogia calcifera, Plethopeltis saratogensis*, *Prosaukia eboracensis* (Fisher and Hanson, 1951).

The depositional structures observed in these units are spectacular columnar and domal stromatolites, abundant cryptmicrobial laminites, mudcracks, burrow mottles, and 'bird's eye' structures or fenestrae, that are open or filled with calcite and saddle dolomite. Seven lithofacies are observed in the Hoyt outcrops which reveal an interfingering complex of the products of peritidal sub-environments. The vertical successions of lithofacies show several upward-shallowing parasequences, indicating the lateral shift of depositional facies over time. The following lithofacies are observed in the Hoyt strata:

Lithofacies 1: Ooid /Peloid/ Skeletal Packstone (displaying varying degrees of dolomitization); (Lithofacies 1 of Owen and Friedman, 1984)

Lithofacies 2: Burrow-Mottled Dolostone;

Lithofacies 3: Intraclast Dolostone; (Lithofacies 1 of Owen and Friedman, 1984)

Lithofacies 4: Stromatolitic Boundstone; (Lithofacies 4 of Owen and Friedman, 1984)

Lithofacies 6: Shale; (Lithofacies 3 of Owen and Friedman, 1984)

Lithofacies 7: Dolomudstone / Fenestral Vuggy Dolostone;(Lithofacies 5 of Owen and Friedman, 1984)

Lithofacies 8: Cryptmicrobial laminated Boundstone; (Lithofacies 2 of Owen and Friedman, 1984)

Lithofacies 1:Ooid /Peloid/Skeletal Packstone:

This lithofacies is the most common in the Hoyt and is observed in all the outcrops. Included in this lithofacies are pelletal limestones, oolitic limestones, and fossiliferous limestones. In the case of the oollitic packstones or grainstones, the ooids are either not dolomitized or partially to completely replaced by medium-crystalline planar-s or planar-e dolomite (Figure 3.13). Internal structures in these ooids are conspicuously absent, indicating that dolomitization has completely obliterated any trace of them. Where the ooids have been replaced by dolomite, only ghost outlines attest to their former presence. As the internal structures of these particles are not clear, it is possible that they were pellets instead of ooids. In case of skeletal packstones and grainstones, the fossil fragments have been leached and only their micrite envelopes remain with dolomite and late calcite filling the biomolds (Figure 3.14). The pelletal and peloidal limestones have also been partially replaced by dolomite. However, these peloidal limestones contain much less dolomite. Some nondolomitized grapestone horizons are also present (Figure 3.15). Towards the top of outcrop #8, at one place, a small channel-like feature is observed in the oolitic-grainstone facies (Figure 3.16).

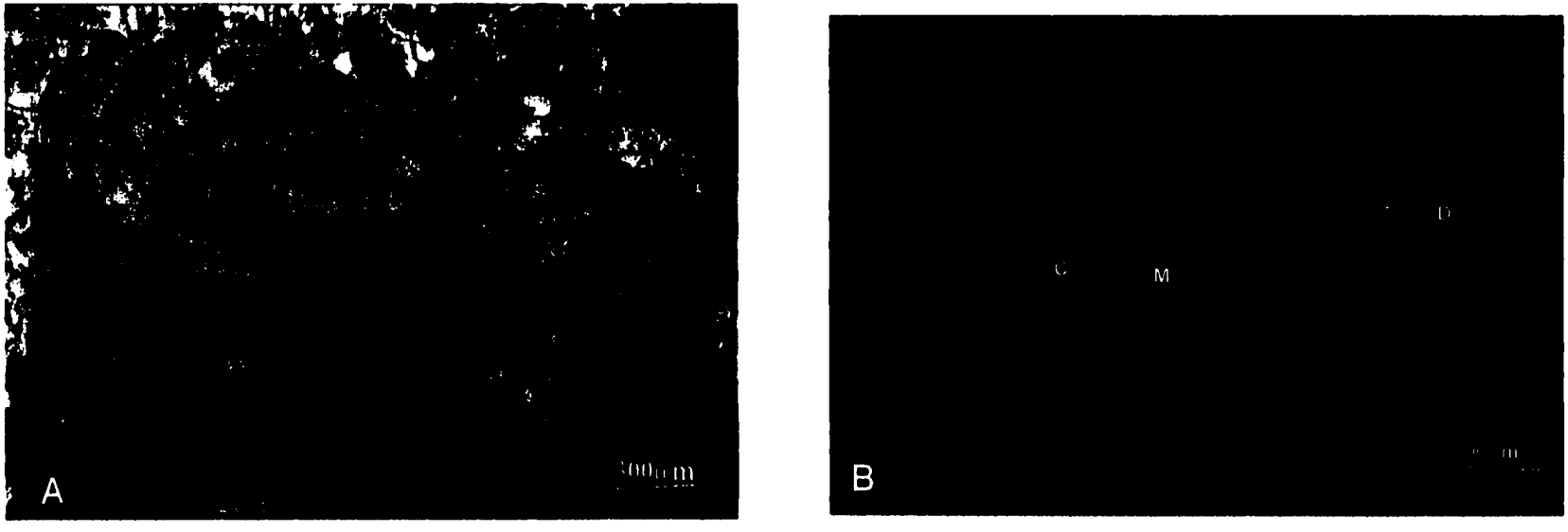

Figure 3.13: Partially dolomitized (D) ooids (Lithofacies 1, Hoyt Formation, outcrop # 6) composed of micrite (M). The interparticle cements (C) are composed of early-diagenetic calcite cement . (A) is viewed in plane-polarized light and (B) is the same view under Cathode light. Calcite is stained red with Alizarin in (A) and ferroan dolomite is stained blue with Potassium Ferricyanide. In (B) dolomite luminesces red, calcite dull-yellow and detrital feldspar luminesces blue.

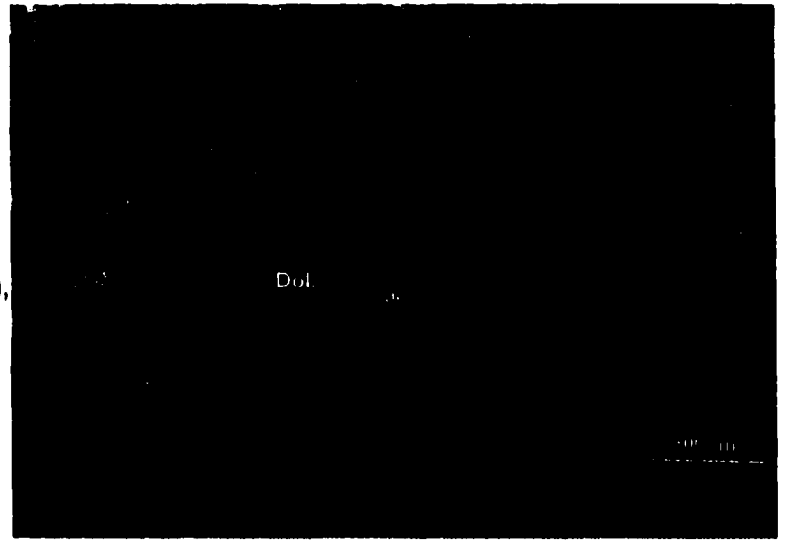

Figure 3.14: Lithofacies 1, (skeletal / peloidal packstone) composed of partially dolomitized allochems with micrite envelopes is observed in the Hoyt Formation (Sample # SQ-1), located at Skidmore Quarry.

Figure 3.15: Unreplaced cluster of ooids forming composite grains or grapestones in Hoyt limestone, observed in outcrop #6. Thin section is viewed in plane-polarized light.

Figure 3.16: Outcrop photograph of a tidal channel observed at the top of section section of Hoyt strata on Petrified Gardens road (outcrop # 8). The channel feature is observed in beds composed of oolitic grainstones (Lithiofacies 1).

This lithofacies contains products of both the high-energy and low-energy subtidal sub-environment. The oolitic and skeletal grainstones are interpreted as representing oolite shoals in a high-energy, subtidal setting adjacent to and in lower-intertidal channels (Lithofacies 1 of Owen and Friedman, 1984). The quiet-water facies of grapestones, pellets, and fossil fragments occurring as packstones are inferred to represent a subtidal lagoonal setting (corresponding to Lithology 3 in Owen and Friedman, 1984).

Lithofacies 2: Mottled Dolostone :

This lithofacies is observed at the base of outcrop section #7 associated with Lithofacies 1. On the outcrop-scale burrow mottles are observed, but petrographically, all depositional textures have been obliterated by dolomite. The dolomite is medium-crystalline and nonzoned or displays blotchy luminescence suggesting repeated episodes of recrystallization during diagenesis.

This lithofacies is interpreted as a product of the subtidal sub-environment. A close association with rocks of Lithofacies 1 also suggests a subtidal setting, where burrowing organisms were present.

Lithofacies 3: Intraclast Dolomitic Limestone:

This lithofacies is observed in the Lester Park Quarry section. The intraclasts are irregular in shape and composed of peloids and ooids and are either not dolomitized or partially dolomitized. Sparry, fine-textured calcite occurs between the intraclasts along with scattered pellets and peloids.

This lithofacies is interpreted as being the product of a low-energy, subtidal setting, perhaps in the lee of oolite shoals. The occurrence of peloids and pellets between the intraclasts suggests a subtidal setting. The oolitic intraclasts perhaps originated from oolite shoals, where ooids were bound together by microbial mats. Destruction and subsequent transport of these oolitic clasts during storms can explain their deposition in a quiet-water, subtidal setting in the lee of a shoal (Owen and Friedman, 1984). This lithofacies is similar to Lithology 1 recognized by Owen and Friedman.

Lithofacies 4: Stromatolitic Boundstone:

The most spectacular features of the Hoyt strata are the well-preserved columnar (SH-V structures of Logan et. al 1964) and domal stromatolites. They form a ledge in Petrified Gardens (outcrop #6) (Figure 3.17) and on the side of Petrified Gardens road. These stromatolites occur associated with Lithofacies-1. The domal stromatolites are described as laterally linked hemispheroids (LLH) following the terminology of Logan et. al.(1964) and are also observed in the Lester Park section. The stromatolites are composed of alternating layers of zoned, euhedral dolomite and micrite with no trace of carbonate particles (Figure 3.18). In the columnar stromatolites, detrital silt and rounded sand-sized quartz particles are observed.

The stromatolites are interpreted as having grown by the process of trapping detrital material by mats of cyanobacteria. The carbonate laminae are interpreted as having resulted from calcium-carbonate precipitation by

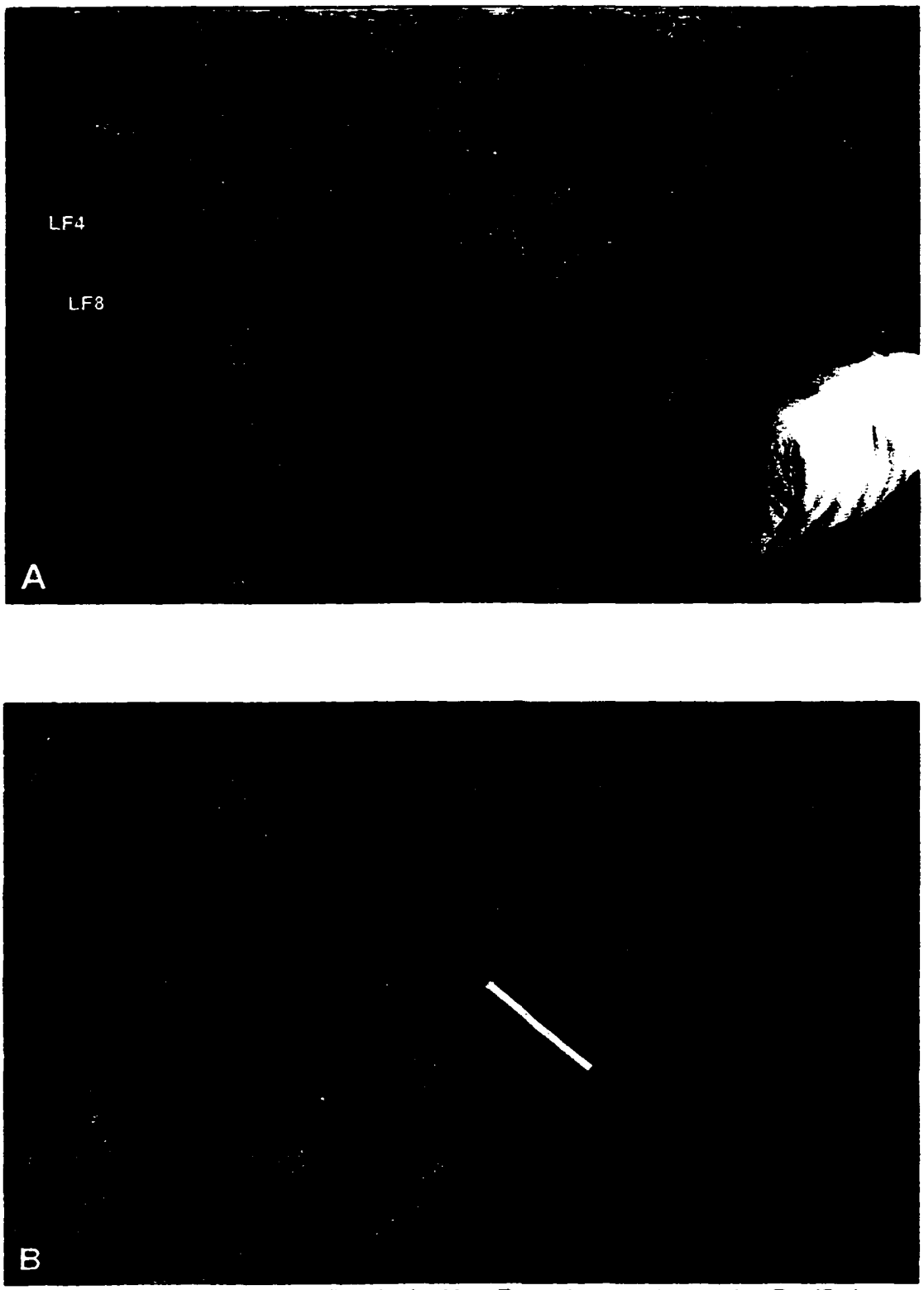

Figure 3.17: Columnar stromatolites in the Hoyt Formation are observed at Petrified Gardens (outcrop #6). (A) is a cross-sectional view, of stromalolites (Lithofacies 4) overlying cryptmicrobial laminites (Lithofacies 8). Person for scale. (B) shows top view of the stromatolite reef at same location. Pen for scale.

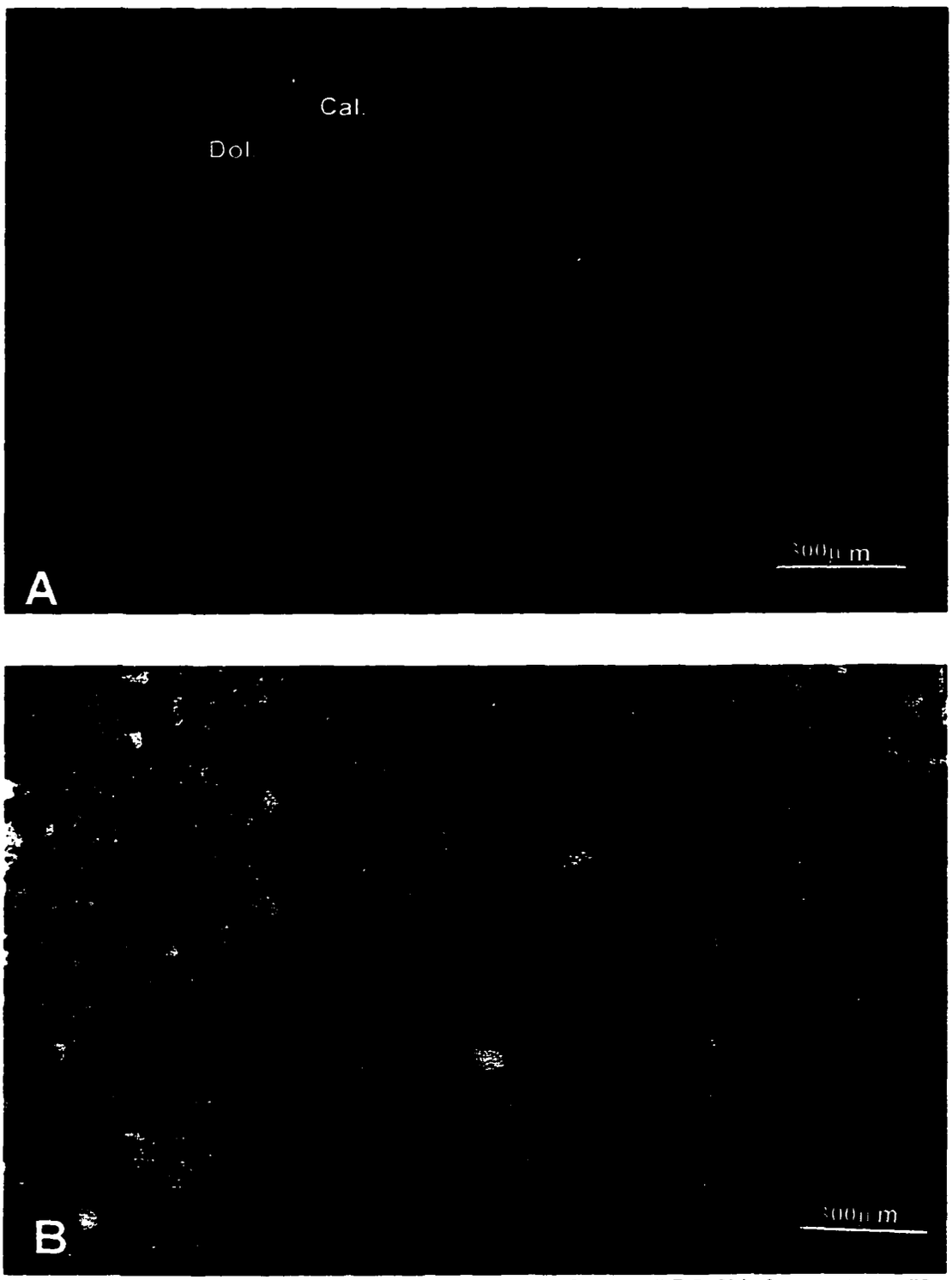

Figure: 3.18: Thin section view of Hoyt stromatolites (Sample # PG-6b), from outcrop #6, showing alternating dolomite and micrite (calcite) laminae. In (A), observed under cathodoluminescence, the zoned dolomites luminesce red and the micrite dull yellow. Feldspar luminesces blue. Same view in (B), shows that micrite is stained red with Alizarine and the dolomite is colorless. Ferroan dolomite appears stained blue with Potassium Ferricyanide.

cyanobacteria. The dolomite laminae may have resulted from formation of high-Mg calcite laminae and subsequent diagenesis to dolomite (Owen and Friedman, 1984; Friedman, 1988). The high-relief structures are interpreted to develop in areas of high-energy whereas the low-relief structures, in areas of low energy. From their characteristic features and facies associations, it is inferred that the columnar stromatolites developed adjacent to the oolite shoals and the domal stromatolites formed in the subtidal to lower-intertidal setting in tidal channels.

Lithofacies 6:Dolomitic Shale:

This lithofacies occurs as dark, fissile units in outcrop section #8. The rock is composed of fine silt, pyrite, coated carbonate particles and some dolomite.

A quiet-water, subtidal lagoonal environment of deposition is inferred for the rocks of this lithofacies. The pyrite present in these beds may have formed diagenetically as a byproduct of bacterial sulfate reduction during organic-matter diagenesis under anoxic conditions. Such a reducing environment may have existed in a lagoonal setting, where deeper parts were anoxic or in the shallow subsurface where pore waters were anoxic.

Lithofacies 7: Dolomudstone / Fenestral, Vuggy Dolostone:

This lithofacies is observed in outcrop sections #6, #7 and #8. The rocks have been pervasively dolomitized and composed of very fine-crystalline, planar-s dolomite mosaics. Fenestrae are common in this lithofacies, and occur filled with coarse-crystalline, zoned dolomite and late-diagenetic calcite. Scattered silt-

sized detrital quartz and feldspar are also present. The mosaic dolomite here displays a relatively high Sr content (214 ppm) compared to the total absence of Sr in all other lithofacies of the Hoyt.

This lithofacies is inferred to represent an upper-intertidal to supratidal flat sub-environment, where fine lime mud was syndepositionally replaced by fine-crystalline dolomite. The Sr content reflects dolomitization in the depositional environment. However the Sr content is less than 550 ppm and therefore not high enough to indicate hypersalinity (Tucker and Wright, 1990, p. 379). The presence of fenestrae suggests desiccation prevalent on intertidal and supratidal flats. Thus, these dolomites may be products of dolomitization in a normal marine, upper-intertidal and supratidal flat sub-environment.

Lithofacies 8: Cryptmicrobial-laminated Boundstone:

Cryptmicrobial laminites are abundant in the Hoyt strata and occur in outcrop sections #6, #7and #8. The rocks of this lithofacies are composed of laminae made up of alternating coarse and fine texture. The coarse laminae contain detrital quartz and feldspar sands and ooids, whereas, the fine laminae contain silt-sized detrital quartz and feldspar. Dolomite occurs as zoned euhedral rhombs and occurs sporadically. In some units, dolomite occurs as bands alternating with microcrystalline calcite where no depositional texture is seen. The second type of cryptmicrobial laminite is associated with the domal stromatolites. On the outcrop scale, the wavy, crinkled nature of the laminae is

very apparent (Figure 3.17A). Laminoid fenestrae with sand, sparry calcite or dolomite are present.

The rocks of this lithofacies are interpreted to have formed in an area of quiet- water deposition bordering the lagoonal area (Owen and Friedman, 1984). The coarse material is probably derived from the adjacent oolite shoals and high-energy subtidal areas. These microbial laminites are believed to have been deposited by the trapping of detrital material by microbial mats on the shallow subtidal and intertidal flats. The decay of microbial mats may also have aided in the dolomitization. The laminoid fenestrae are interpreted to have formed possibly as a result of gases generated by organic decay, which can lift subaqueous or buried mats. They may also form by drying out of the mats causing them to wrinkle, lift, and separate. This may have happened when they were subaerially exposed (Demicco and Hardie, 1994). This lithofacies is similar to Lithology 2 and 5 described by Owen and Friedman.

3.3.2 Parasequences in the Hoyt Formation:

In all three outcrops, one or more parasequences were identified. In each of the individual parasequences, the basal portion is composed of oolitic grainstones, peloidal wackestones with interspersed skeletal fragments and silt-sized quartz and feldspar. Overlying these subtidal lithofacies are moderate- to high-relief domal stromatolites which are also products of a high-energy subtidal environment. At the top of the parasequences, thinly laminated, intertidal to

supratidal beds composed of cryptmicrobial laminites are present. Thus, in the Hoyt outcrops each parasequence displays a change from subtidal to intertidal deposition. The parasequences depict the lateral shifting of adjacent environments such as oolite shoals, shallow subtidal lagoon, and intertidal flats.

3.3.3 Summary of Depositional Facies in the Hoyt Formation:

The vertical distribution of the lithofacies in the outcrop sections (Figure 3.12), reveals the changing of sub-environments from oolite shoals to lee of shoal to lagoon to intertidal and supratidal flats. The oolitic grainstones make up the oolite shoals lithofacies (Lithofacies 1), whereas intraclasts (Lithofacies 3) and columnar stromatolites formed in the sub-environment, lee of the shoal. The dolomitic shale (Lithofacies 6), pelletal packstones and mottled dolostone (Lithofacies 2) indicate deposition in the lagoonal sub-environment. The domal stromatolites (Lithofacies 4) mark the shallow subtidal to lower intertidal zone. Cryptmicrobial laminites (Lithofacies 8) represent the intertidal flats and the fenestral dolomudstones (Lithofacies 7) are representative of the upper-intertidal and supratidal flats. Tidal-channel deposits include Lithofacies 1,3 and 4 and occur in the shallow subtidal to lower-intertidal zone.

3.4 Facies Analysis of the Gailor Formation

The Gailor Formation was examined at outcrop sections #9, #10, #11 and #12, all located on Route 67 in the vicinity of Saratoga Springs, West of Ballston

Spa and the junction with Route 147 (Figure 3.19). The section of Upper Gailor, exposed in the Pallette Quarry (outcrop #13) was also examined (Figure 3.20).

3.4.1 Lithofacies in the Gailor Formation:

In general the Gailor strata are composed of light to dark gray dolostones. Mazzullo et. al. (1978) noted two limestone members in the subsurface, which are not exposed at these outcrops. Notable features commonly observed in these strata include stromatolites, cryptmicrobial laminites, current laminae, intraclast breccias, dissolution-collapse breccias, burrow-mottles, fenestrae, and chert. Fossils are rare in these rocks, although Fisher and Hanson (1951) have recognized Lower Canadian fossils namely *Ophileta, Helicotoma uniangulata, and Ectenoceras* in some dolostones of the Gailor Formation.

The following lithofacies are observed in the Gailor strata:

Lithofacies 1: Skeletal Grainstone;

Lithofacies 2. Burrow-Mottled Dolostone / Limestone ;

Lithofacies 3. Intraclast Dolostone;

Lithofacies 4. Stromatolitic Boundstone;

Lithofacies 7. Dolomudstone / Fenestral Dolostone;

Lithofacies 8. Cryptmicrobial-laminated Boundstone;

Lithofacies 9. Quartzo-Feldspathic Dolostone;

Lithofacies 10. Dolomitic Chert;

Lithofacies 11. Dissolution-collapse Breccia;

Figure 3.19 Outcrops of the Gailor Formation

(Figure 1.2 is map showing location of sections)

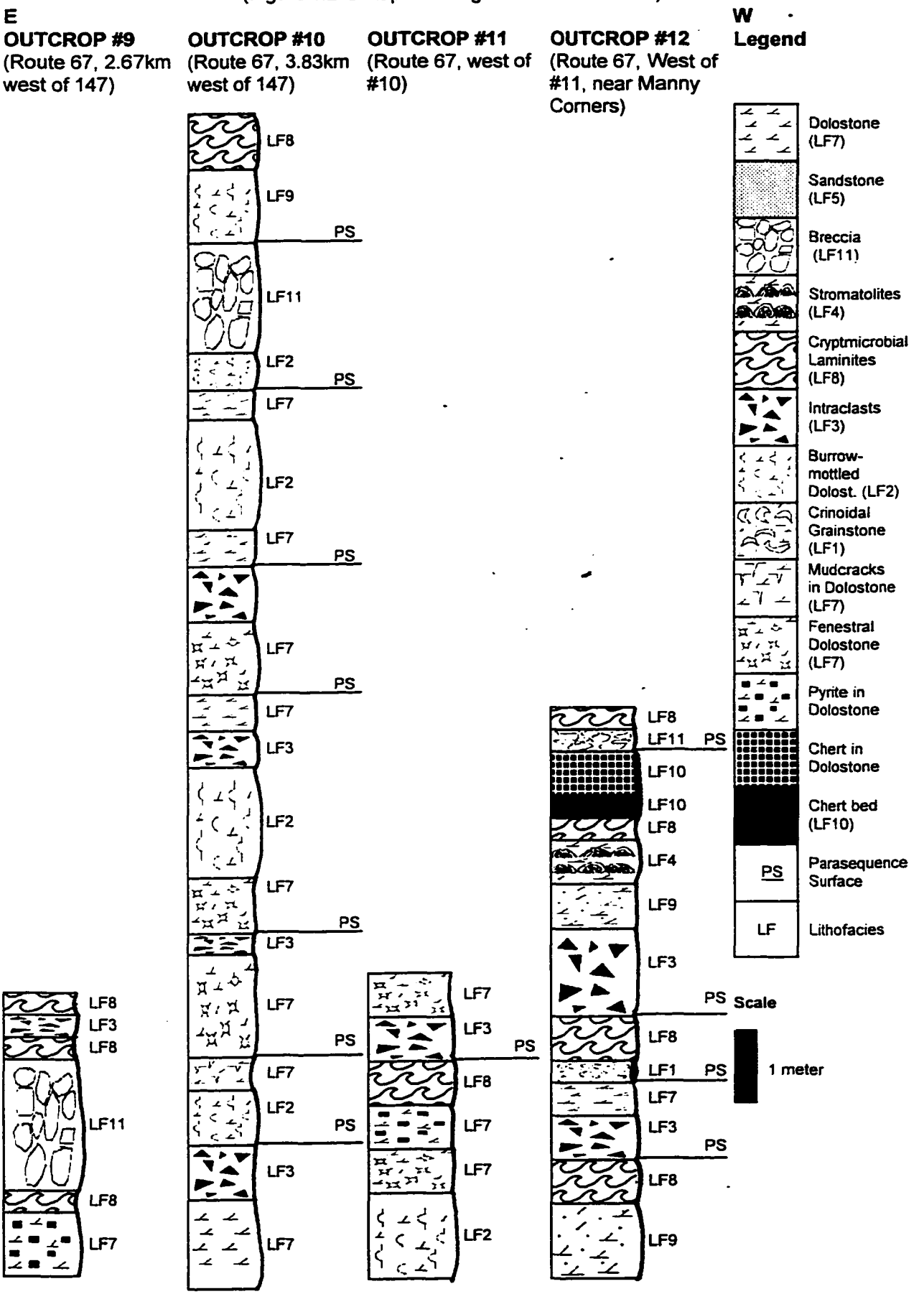

Figure 3.20. Columnar Section of the Upper Gailor Formation in the Pallette Quarry 1-8R, Route 29W, Saratoga Springs

(modified from columnar section prepared by J. Lange for the Pallette Stone Corporation)

OUTCROP #13 (Figure 1.2 is map showing location of sections)

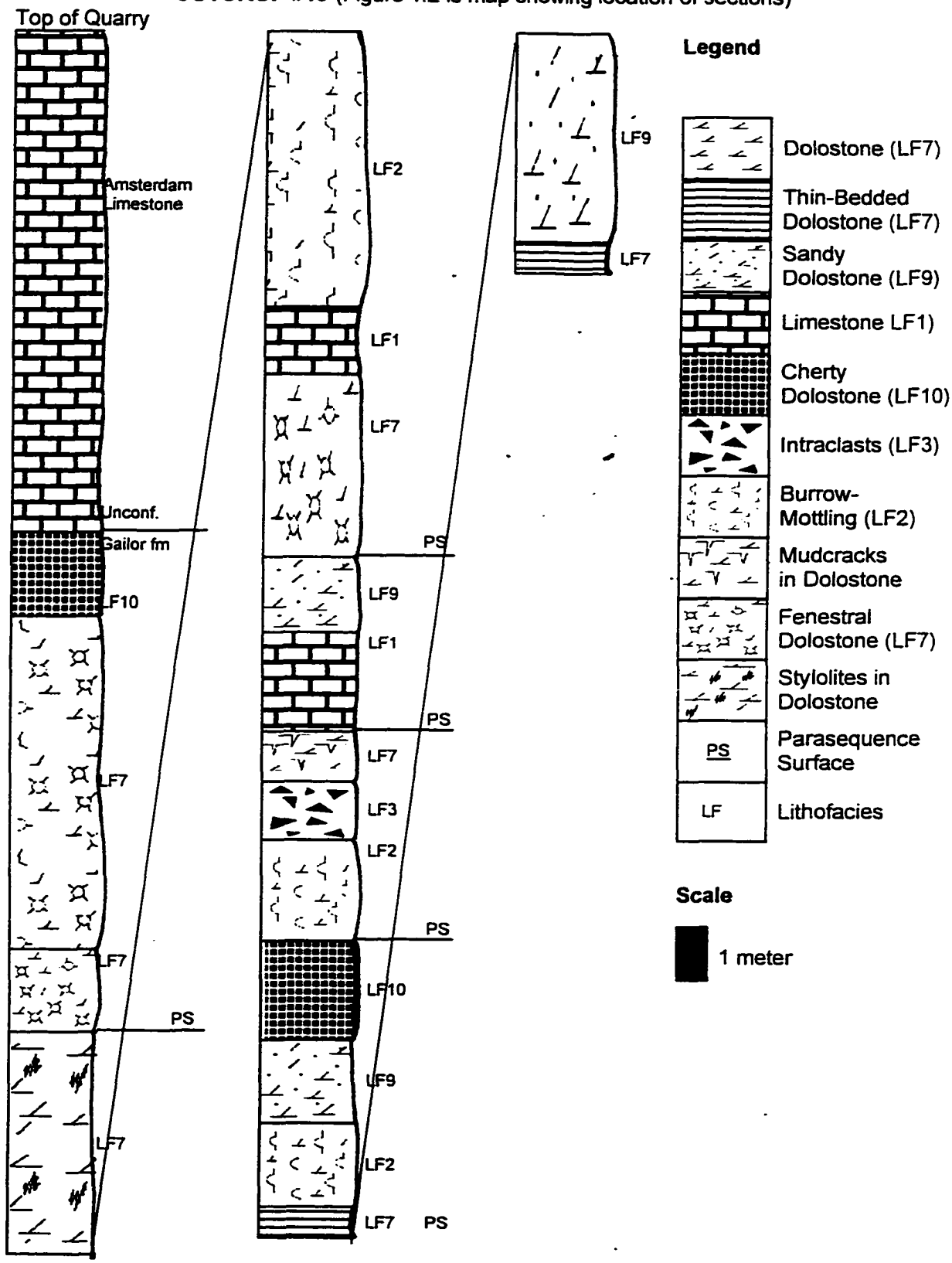

Lithofacies 1: Skeletal Grainstone:

This lithofacies is not common in the outcrops of the Gailor Formation that were examined. However, one unit of dolostone containing crinoid fragments is observed in outcrop #12. The crinoid fragments are composed of dull-luminescent precursor calcite that is in places partially dolomitized (Figure 3.21). This lithofacies is inferred to represent a high-energy subtidal deposit.

Lithofacies 2: Mottled Dolostone / Limestone:

This lithofacies is observed in outcrop sections #10, #11 and in the Pallette Quarry. Alternating mottles of light gray dolomicrite and dark-gray limestone are observed (Figure 3.22) in some beds. Burrow mottles are also observed in rocks that are completely dolomitized. Several such mottled layers are common in outcrop #10, where massive beds of coarse-textured, burrow-mottled, dolostones occur interbedded with fine-textured dolomudstones. A bedding-plane surface exposure of worm burrows that showed a network of horizontal burrows was observed in the Pallette Quarry (Figure 3.23).

This lithofacies is interpreted to represent the results of partial bioturbation. Modern, shallow-subtidal sediments, where burrowing organisms disrupt the physical layering, commonly show bioturbation structures (Demicco and Hardie, 1994). In the dolomitic limestone the tubular burrows are selectively composed of dolomicrite. Thus, by analogy, the burrow-mottled dolomitic limestones and dolostones in the Gailor outcrops are inferred to represent a shallow-subtidal depositional setting.

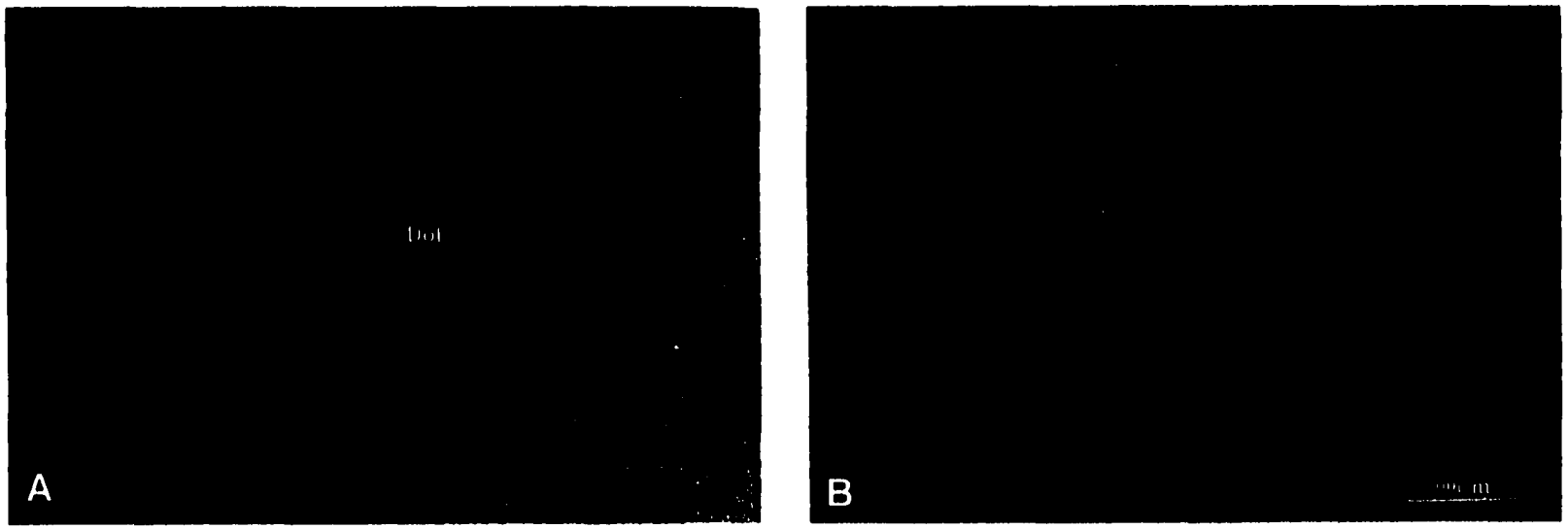

Figure 3.21: Photomicrograph of crinoidal dolostone (Lithofacies 1, Gailor Formation, sample # GL-16, outcrop # 12). The crinoid particles are dull-luminescent when viewed under cathodoluminescence, appearing dirty yellowish-brown. Red-luminescent euhedral dolomite partially replaces the crinoid particles. (A) is viewed in plane-polarized light and B under cathodoluminescence.

Figure 3.22: Mottled dolostone in the Gailor Formation, observed in the Pallette Quarry (outcrop # 13). Pen for scale is 13.6cm long.

Figure 3.23: A bedding-plane surface showing a network of horizontal burrows in a mottled dolostone, of the Gailor Formation observed in the Pallette Quarry (outcrop #13). Knife is for scale.

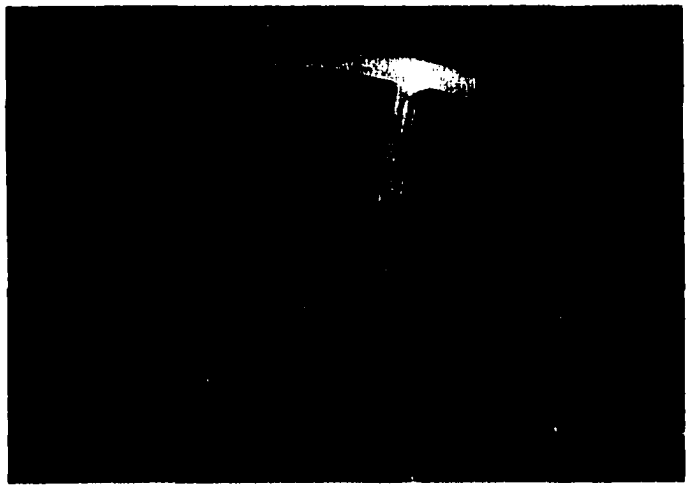

Figure 3.25: Edgewise breccia in Gailor dolostone seen at outcrop # 12, composed of flat chips packed parallel to each other. Hammer is for scale.

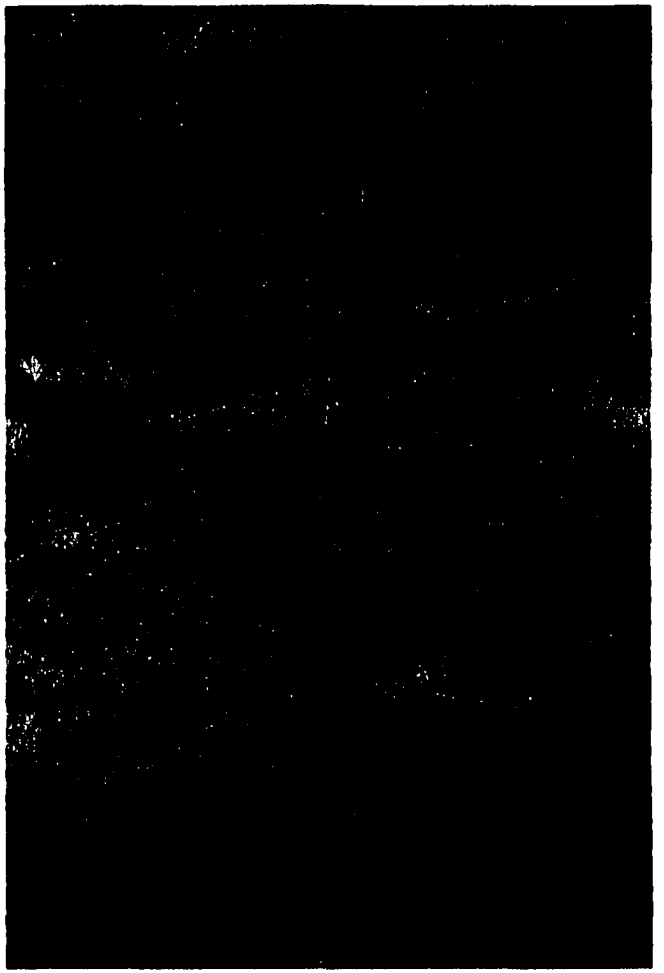

Figure 3.24: Thick bed of intraclasts in Gailor dolostones in roadcut on Route 67 (outcrop # 11). The chaotic nature of this bed of flat-pebble conglomerate is inferred to be a storm deposit. Knife is for scale.

Lithofacies 3: Intraclast Dolostone:

Beds of intraclast dolostone are observed in all of the outcrops. Figure 3.24 shows a thick bed of intraclasts displaying a chaotic arrangement of randomly oriented clasts, indicating that deposition took place in a turbulent, high-energy medium. This unit is therefore possibly a tempestite or storm deposit. In other outcrops, intraclasts occur as flat-pebble conglomerates (Figure 3.25) and as round-pebble conglomerates. The intraclasts themselves are invariably made up of fine-crystalline, tight dolomite mosaic compared to the matrix which is usually coarser and more porous. In one horizon, intraclasts of zoned fine- to medium-crystalline dolomite, are found in a microcrystalline chert matrix with scattered dolomite rhombs. In places, coarse, authigenic pyrite is associated with the dolomite.

The intraclasts are interpreted to have originated on the upper-intertidal and supratidal flats by desiccation of lime mud. Mud-cracks that formed due to desiccation caused the formation of mud chips which were ripped up and transported to adjacent sub-environments by storms or waves and were possibly, reworked into subtidal or intertidal channel sediments (Aigner, 1982, 1985; Sepkoski, 1982;Chuanmao et.al., 1993). The intraclasts may not have travelled far from their source, especially if they are preserved as flat, angular chips. The presence of silica in the matrix of some of the intraclast breccias is inferred to be diagenetic. Where the matrix is silicified and dolomitized, it is hard to interpret the depositional environment, as all original depositional textures have been obliterated.

Lithofacies 4: Stromatolitic Boundstones:

Stromatolites are not very common in the Gailor strata. Only one bed of small hemispheroidal, domal stromatolites was observed in outcrop section #12 (Figure 3.19). The stromatolites are interpreted to be high-relief structures that form by the trapping and binding of carbonate mud and detritus by cyanobacterial mats in a high-energy setting. Hence, this lithofacies is inferred to represent a shallow-subtidal or lower-intertidal channel setting.

Lithofacies 7:Dolomudstone / Fenestral,Vuggy Dolostone

The dolomudstones are very common in the Gailor and occur as light- to dark-gray dolostones. This lithofacies is composed of microcrystalline to very fine- crystalline, zoned dolomite with low trace-element content (Fe and Mn) and a Sr content between 250 and 1400 ppm. Some iron-rich zones are observed in the fine-crystalline dolomites. Sparry calcite, saddle dolomite, and quartz-filled vugs are common in this lithofacies (Figure 3.26). In outcrop #11 (Figure 3.26B), the vugs appear to be concentrated in narrow horizontal zones oriented subparallel to bedding.

The dolomudstones are interpreted to have formed originally as lime mud on upper-intertidal and supratidal flats, where they were syndepositionally dolomitized. The relatively high strontium content signifies salinities ranging towards hypersalinity. This would signify an arid, evaporative environment where interstitial waters may have elevated salinities. Such a scenario would aid in the dolomitization of fine-textured lime muds on intermittently exposed tidal flats. The

vuggy nature (Figure 3.26) of this lithofacies may be indicative of the former presence of evaporite nodules, which were subsequently leached away by meteoric dissolution. Similar voids have been inferred to have originated as anhydrite nodules in correlative units of the Theresa and Ogdensburg formations (Selleck, 1987). The horizontal layers of vugs indicate that dissolution was related to surface water rather than formation water. In addition, their position at the top of a parasequence implies subaerial exposure and infiltration of the strata by meteoric water following deposition of the upward-shallowing cycle.

Lithofacies 8: Cryptmicrobial laminated Dolostone:

This lithofacies occurs in outcrop sections #9, #11 and #12. The beds of dolostone belonging to this lithofacies are recognized in the outcrop as having irregular, wavy or crinkled laminae. Petrographically, they are composed of layers of tight, dull-red luminescent, fine-crystalline dolomite alternating with more porous, medium-crystalline dolomite with bright-luminescent younger zones. Silt-sized, detrital feldspar is present within and among the dolomite. Spherical fenestrae filled with saddle dolomite are common in this lithofacies.

This lithofacies is interpreted as having formed by the binding and trapping of carbonate mud and detrital particles by microbial mats on the intertidal and supratidal flats. The high strontium values of the dolomite (ranging from 309 to 781ppm) suggest an environment where evaporation, possibly due to subaerial exposure, caused elevated salinities in the interstitial pores of the lime muds aiding in their early dolomitization. Therefore, it is possible that the

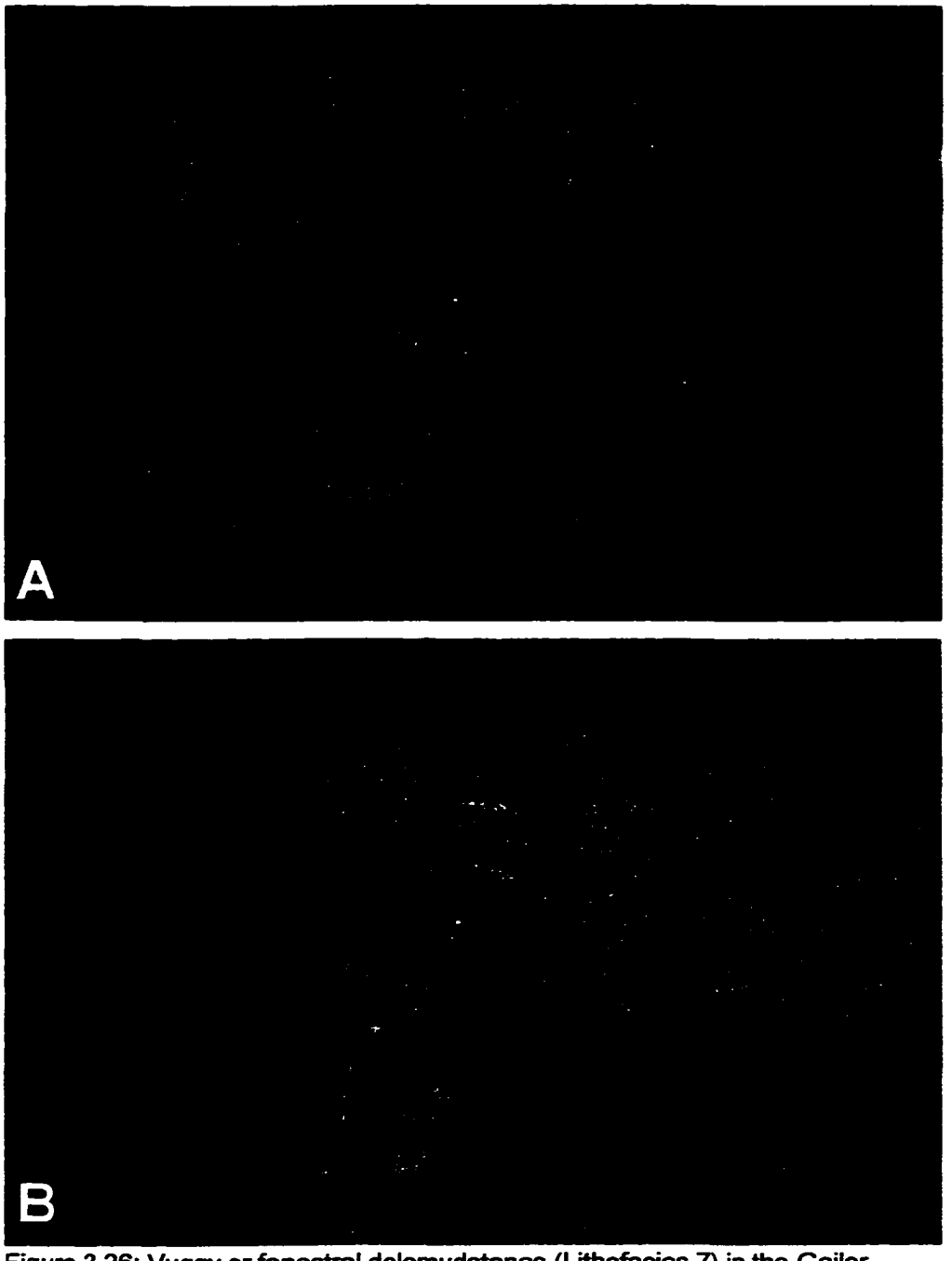

Figure 3.26: Vuggy or fenestral dolomudstones (Lithofacies 7) in the Gailor Formation. (A) is from outcrop # 12 and (B) is from outcrop # 11. The vugs are either open or filled with saddle dolomite or calcite. Knife for scale.

spherical fenestrae, observed in this lithofacies are perhaps remnant molds of former evaporite nodules. From the fine textures and the low-relief morphology of the cryptmicrobial laminae, and their geochemical characteristics, it is inferred that this lithofacies represents an upper-intertidal to supratidal flat environment of deposition, where salinity was high.

Lithofacies 9: Quartzo-Feldspathic Dolostone:

This lithofacies consists of light to dark gray, medium- to coarse-textured sandy dolostones. Silt- to sand-sized quartz and feldspar particles occur and rounded to sub-rounded quartz particles are scattered among the dolomite. These sandy dolostones are associated with chert and in some strata with burrow mottles and shaly partings.

Mottled feldspathic dolostones occur towards the the top of outcrop #10. The weathered outcrop displays a mottled appearance but microscopically these dolostones are composed of clusters and patches of abundant authigenic alkali feldspar occurring interspersed with silt-sized detrital feldspars and as authigenic overgrowths around the detrital feldspars (Figures 3.27 & 3.28). These dolostones do not reveal any depositional textures as all carbonate material has been pervasively dolomitized. However, the feldspathic dolostones in outcrop #10 are succeeded by cryptmicrobial laminated dolostones and therefore are inferred to have been associated with intertidal deposits.

The abundant authigenic alkali feldspar in these dolostones may have formed early in the diagenetic history of these dolostones under near-surface

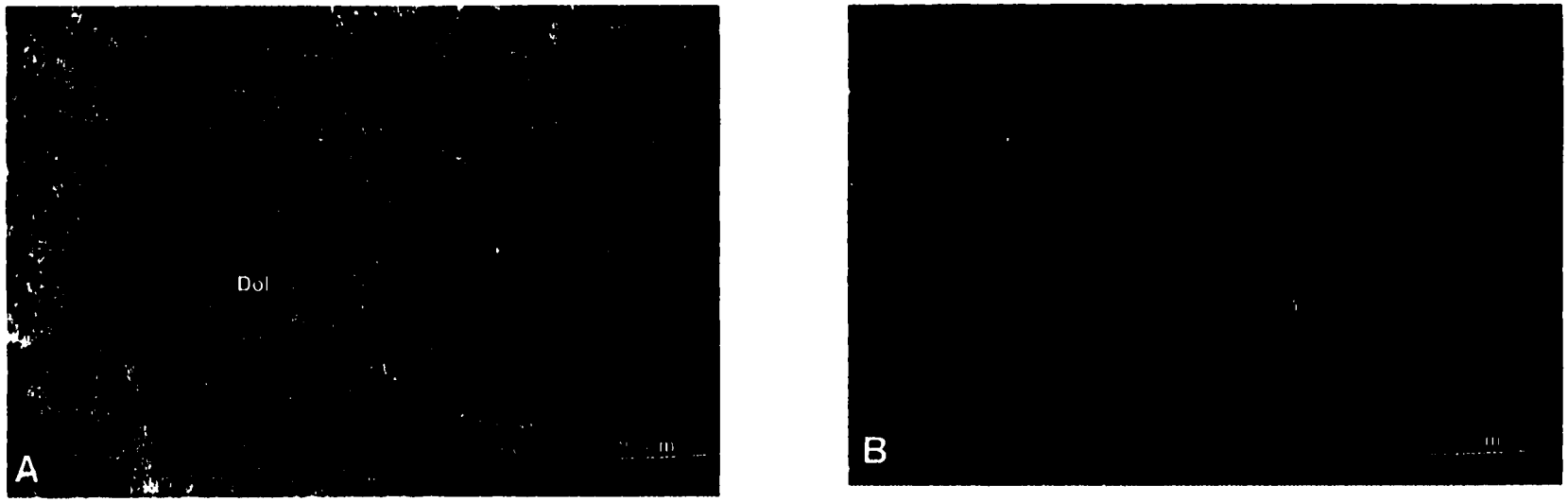

Figure 3.27: Thin-section photomicrograph of feldspathic dolostone (Lithofacies 9) from the Gailor Formation (outcrop #10, sample #GL-10). (A) is viewed in plane-polarized light and (B) under cathodoluminescence. Detrital feldspar (F) luminescences bright blue and authigenic feldspar is non-luminescent.

Figure 3.28:Thin-section photomicrograph of mottled feldspathic dolostone from the Gailor Formation (sample # GL-10, outcrop #10), containing clusters of authigenic feldspar within the dolomite mosaic. Thin section is viewed under crossed nicols.

conditions of low temperatures, high alkalinity, and high salinity (Buyce and Friedman, 1975). Similar feldspathic beds have been reported in correlative beds of the Fort Johnson member of the Tribes Hill Formation (Braun and Friedman,1969) (discussed in section 3.6.1). The alkali feldspar in the Tribes Hill beds are reported to have been derived from the dissolution of detrital feldspars and also perhaps from the diagenetic alteration of wind-blown tephra that was trapped by the intertidal-flat sediments (Friedman and Braun, 1975; Buyce and Friedman, 1975 ; Friedman, 1990; Friedman, Sanders and Kopaska-Merkel, 1992, p.276). By analogy, the feldspathic dolostones of the Gailor Formation are also perhaps of similar origin.

Lithofacies 10: Dolomitic Chert:

Light to dark gray chert is observed in outcrop sections #9, #10, #12 and #13. Bedded chert occurs in the upper part of outcrop #12 and in outcrop #13. The chert occurs as microcrystalline silica with scattered dolomite rhombs, patches of fibrous spherulites of chalcedony and linear patches of void filling length-slow chalcedony. Chert also occurs as large 2" to 4" pods in karst breccia. Megaquartz clusters occur in dolostones within otherwise pervasively dolomitized rocks. Megaquartz is also seen lining subspherical vugs in predominantly cherty rocks.

This lithofacies is interpreted as indicative of either emergence of the strata early in the diagenetic history or during uplift of the basin associated with the post-Sauk, pre-Tippecanoe surface of unconformity. Uplift of the basin,

would have brought the strata into the realm of meteoric diagenesis, where continent-derived, meteoric waters supersaturated in silica were able to circulate through these sediments. The bedded chert may represent a former silcrete bed formed by silica precipitation at or near the Earth's surface, by evaporation of upwardly-moving silica-rich pore-fluids in an arid climate (Friedman, 1994a,b; Friedman and Radke, 1979; Guo, 1994; Guo et.al., 1996).

Where chert is observed in dolostones, silicification appears to have interrupted early dolomitization. In some cases silicification is limited and appears to be incomplete. However in other examples chert seems to have replaced all nondolomitized carbonate material. Void-lining megaquartz, spherulites and length-slow chalcedony may represent vanished evaporites (Folk and Pitman, 1971; Milliken, 1979). In outcrops #10 and #12, chert is found located near the top of parasequences, further supporting an association with emergence of the strata.

Lithofacies 11: Dissolution-collapse Breccia:

This lithofacies is observed in outcrop sections #9, #10, and #12, towards the top of the upper Gailor Formation. Clasts of fine-crystalline dolomite along with pods of dolomitic chert, calcite, and saddle dolomite are found scattered in a coarse-crystalline sandy dolostone (Figure 3.29). Above and below the breccia are bedded units of fine-crystalline dolomite or cryptmicrobial laminated dolostone. The breccia in outcrop section #12 is associated with bedded chert below it.

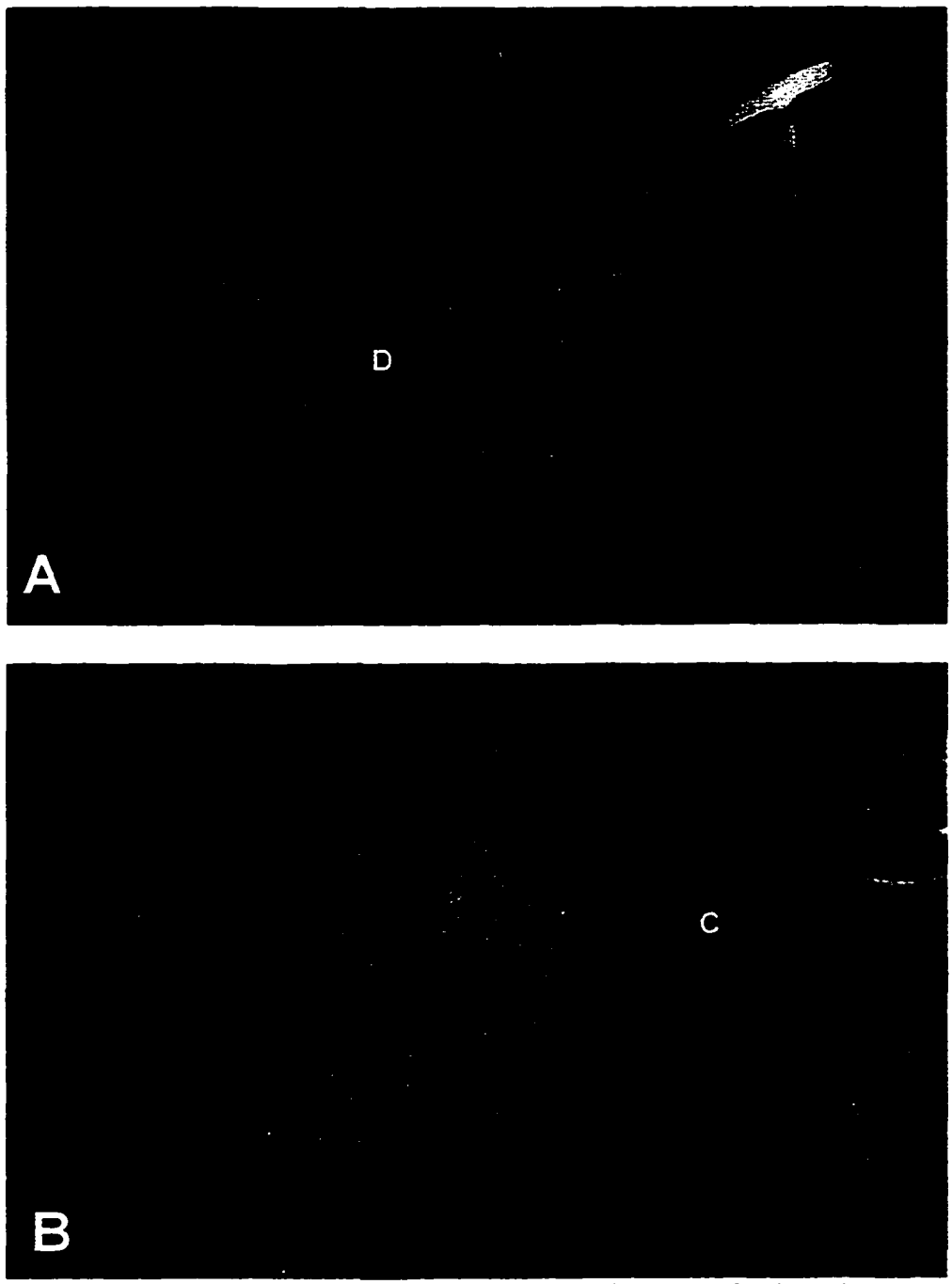

Figure 3.29 A & B: Angular clasts of fine-crystalline dolostone, laminated dolostones (D) and intraclastic dolostone, pods of calcite and chert (C) in the karst breccia is observed in the Gailor Formation, at outcrop # 9. Hammer is for scale.

This lithofacies is interpreted as dissolution-collapse breccia. Evaporite horizons in supratidal dolostones undergo dissolution, when the strata are exposed to meteoric fresh water. As a result, the overlying strata would collapse, causing brecciation. In this lithofacies, the breccia is interpreted to result from dissolution collapse, because of the fact that it is overlain and underlain by bedded units. The clasts are made up of supratidal dolomicrite and the associated chert contains patches of length-slow chalcedony which is inferred to represent evaporite replacement. The occurrence of this lithofacies may thus suggest the emergence of the strata in this basin, where the strata were introduced into the realm of meteoric diagenesis. This event may be related to the widespread post-Sauk, pre-Tippecanoe surface of unconformity, which occurs at the top of the Gailor in this area.

3.4.2 Parasequences in the Gailor Formation:

Among the outcrops of the Gailor Formation that were examined, well developed parasequences were recognized in outcrop sections 10, 11, and 12. The individual parasequences show an upward-shallowing trend similar to that observed in the Galway and Hoyt formations. The common association of lithofacies in the Gailor outcrops are high-energy storm deposits composed of intraclasts and in places crinoid fragments alternating with fenestral dolomudstones and, or cryptmicrobial laminated dolostones of the low-energy intertidal zone.

In outcrop #10, roughly six parasequences are recognized. Within these depositional cycles, a change from subtidal to intertidal-supratidal facies is observed. The basal part of the cycles commonly displays coarse-textured, mottled, dolostones or storm beds composed of intraclasts. The upper part of the cycles are composed of either fenestral dolomudstones or plane-laminated dolostones, with mudcracks and horizontal intraclasts that appear to be *in situ*. A similar succession is observed in outcrop #11, where subtidal mottled dolostones are overlain by vuggy dolomudstones or cryptmicrobial laminated dolostones. In this outcrop, the tops of parasequences are made up of dolomudstones having horizontal zones of vuggy porosity that is considered evidence of subaerial exposure. A thick, storm bed overlies the parasequence surface indicating the onset of a high-energy deposition.

Storm-influenced deposition appears to be an important factor in the sequence observed in outcrop #12 as well. At this outcrop, the basal part of most of the parasequences is composed of coarse-textured dolostones made up of flat-pebble, or round-pebble conglomerates or crinoid fragments. These are indicative of deposition in a high-energy setting. The upper part of the parasequences represent deposition in quiet-water conditions where the development of microbial mats on the intertidal and supratidal flats was favored. The fine-textured dolomudstones, common in the upper part of the parasequences, may indicate deposition of fine carbonate material from suspension, in the aftermath of a storm.

At the top of some parasequences, especially in the upper part of outcrop #12, dedolomite and chert are present, indicating emergence or near-surface conditions. Near the top of outcrop section #12, a chert bed is noted which may represent a former silcrete bed that formed during emergence of the strata and termination of a parasequence (Friedman, 1994a,b; Friedman and Radke, 1979;Guo, 1994; Guo et.al., 1996).

3.4.3 Summary of the Depositional Facies in the Gailor Formation:

From the above discussion it is apparant that the Gailor Formation is primarily composed of dolostones and displays lithofacies similar to those noted in the Galway and Hoyt formations. However, compared to the Galway Formation, the parasequences in the Gailor outcrops contain virtually no subtidal sandstones (Lithofacies 5). In addition domal stromatolites (Lithofacies 4) are not nearly as abundant as in the Galway and Hoyt formations. The depositional facies in the Gailor outcrops indicate that, on the Saratoga Platform during Early Ordovician time, shallow-water carbonate production was high. The fact that many of the parasequences appear to be storm generated, indicate that storms may have been common during this time.

Although no evaporite minerals are observed in the Gailor strata, hypersalinity, at least associated with the supratidal flats, can be inferred from the high strontium values of the dolomudstones, the length-slow chalcedony in the cherts, and the presence of dissolution-collapse breccia. The presence of

detrital quartz and feldspar in these units are believed to be derived from weathering of the ancestral Adirondack mountains that were exposed to the north of the Saratoga-Mohawk area during Cambro-Ordovician time (Fisher, 1954). According to Mazzullo and Friedman (1975), the Adirondacks were locally exposed during this Period, as a series of low-relief peninsulas and islands.

The depositional structures and lithofacies that are observed in the Gailor units imply a peritidal depositional environment. The succession of upward-shallowing cycles observed in the Gailor outcrops are perhaps indicative of the lateral shifting of peritidal environments in response to the interplay of a variety of local and external factors including subsidence, carbonate production, sea-level fluctuations, and/or tectonics.

3.5 Facies Analysis of the Little Falls Dolostone:

The Little Falls Formation was examined at a roadcut on Route 5 E (outcrop section #14) (Figure 3.30). Conformably overlying the Little Falls strata are younger beds of the Tribes Hill formation which are exposed as a cliff face along Route 5W.

3.5.1 Lithofacies in the Little Falls Formation:

The beds of Little Falls Formation along Route 5E are composed almost entirely of gray dolostones, with two sandstone horizons. They are in general

Figure 3.30 Outcrop #14 of the Little Falls Formation (Route 5 East)
(Figure 1.2 is map showing location of sections)

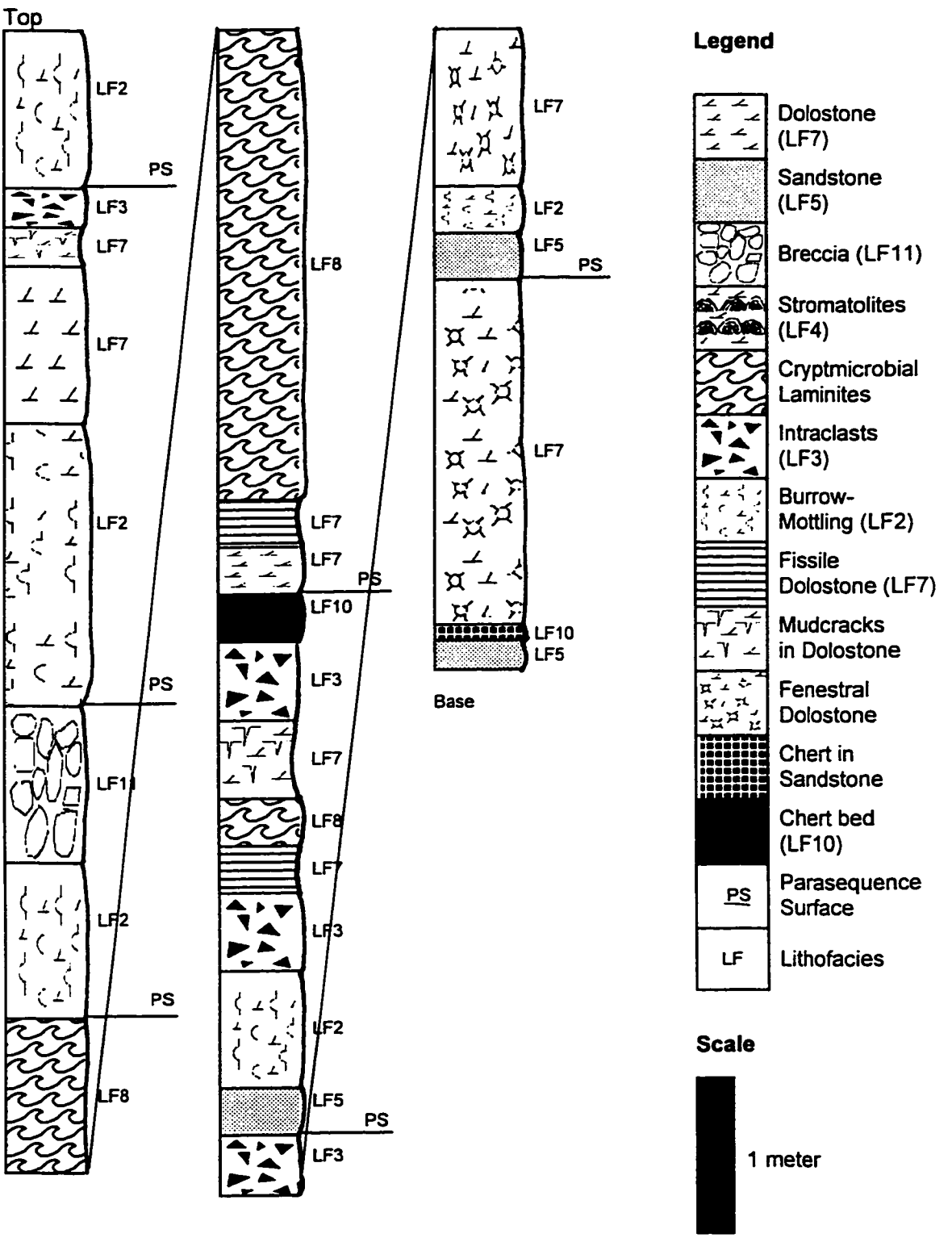

made up of gently folded horizontal beds with some fractures. The dolostones are not entirely devoid of original depositional structures although they have been pervasively dolomitized. In some units detrital sands are observed.

Two horizons of chert occur towards the base and middle of the section. One of these cherty beds contains silicified ooids. Intraclasts and cryptmicrobial laminites, with small hemispheroids of stromatolites in places, are also present in this section. Mottles are observed in the coarser dolostones which overlie sandstones. Vugs or fenestrae, filled with late calcite, saddle dolomite, and quartz are common in the fine dolostones and absent in the mottled dolostones.

The following lithofacies are observed in the Little Falls Formation:

Lithofacies 2. Mottled Dolostone;

Lithofacies 3. Intraclast Dolostone;

Lithofacies 4. Stromatolitic Boundstone;

Lithofacies 5:Dolomitic Sandstone ;

Lithofacies 7.Dolomudstone / Fenestral Dolostone;

Lithofacies 8. Cryptmicrobial laminated Boundstone;

Lithofacies 10. Silicified Ooid Grainstone/ Chert/ Dolomitic Chert;

Lithofacies 11. Dissolution-collapse Breccia;

Lithofacies 2: Mottled Dolostone:

This lithofacies is seen at five horizons in this outcrop section (Figure 3.30) and composed of a mottled texture. The mottled dolostones are entirely made up of medium-crystalline, zoned dolomite. Petrographically, the mottles are

not clearly defined. However patches of porous dolomite with silty material in the interstices are observed, which may be responsible for the mottles. This lithofacies occurs commonly in the lower part of the depositional cycles.

The mottles may represent the result of burrowing activity, but the paucity of fossils in the strata and lack of distinct burrows prevents such an interpretation. Therefore, the depositional environment of this lithofacies is not clear. However, its coarser texture and the fact that they are, in places, underlain by high-energy sandstones and overlain by fine-textured low-energy vuggy dolostones, suggests that these mottled dolostones may represent a transitional environment of deposition such as a shallow subtidal setting.

Lithofacies 3: Intraclast Dolostone:

This lithofacies is commonly associated with Lithofacies 7 and interlayered with it in this outcrop. Intraclasts of very fine-crystalline tight mosaic dolomite occur in a matrix of medium- to coarse-crystalline dull red, zoned dolomite with abundant silt-sized feldspar.

In at least four of the parasequences in outcrop #14, beds of intraclasts are observed. In the lower part of the sectrion, a couple of horizons of intraclast-bearing beds are observed, where randomly oriented intraclasts alternate with fine-textured dolomudstone layers. The intraclasts themselves are inferred to have originated as a result of desiccation of the upper-intertidal- and supratidal-flat muds. Rapid submergence of the supratidal flat during storm events, causes partially lithified carbonate clasts from the the intertidal and supratidal zones to

be dislodged and redeposited as a flat-pebble conglomerate (Aigner, 1982, 1985; Sepkoski, 1982;Chuanmao et.al., 1993). The alternating fine micrite layers probably represent fine muds in suspension that settled from the water column during the aftermath of the storm, when low-energy conditions returned to the site of deposition. This lithofacies is therefore inferred to be the product of a high-energy setting resulting from a storm, marking perhaps the onset of a new cycle of deposition.

In some intraclast beds, the intraclasts appear not to have been moved much from their original positions. In this unit, alternating layers of cryptmicrobial laminae and intraclastic laminae are observed. The parallel layers of flat-lying intraclasts in this example represent the mud-cracked surface of the upper-intertidal and supratidal flats, where desiccation in an arid climate caused polygonal cracks to develop on the exposed tidal flat muds, generating intraclasts (Figure 3.31). Intermittent wetting of the exposed tidal flat sediments allowed the development of microbial mats, which ultimately generated a succession of inter-layered intraclasts and cryptmicrobial laminae.

Lithofacies 4: Stromatolites:

High-relief stromatolites are not observed in this outcrop, however, they have been reported from other outcrops of the Little Falls Formation (Zenger, 1981). In this outcrop small hemispheroids are associated with the cryptmicrobial laminites.

Figure 3.31: Vertical mud-cracks (arrow) appear to have cut through thin layers of dolomudstone, observed near the top of outcrop # 14 in the Little Falls Formation (divisions on scale are in cm).

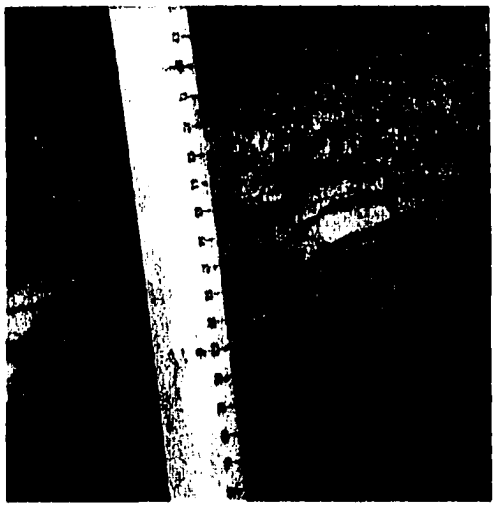

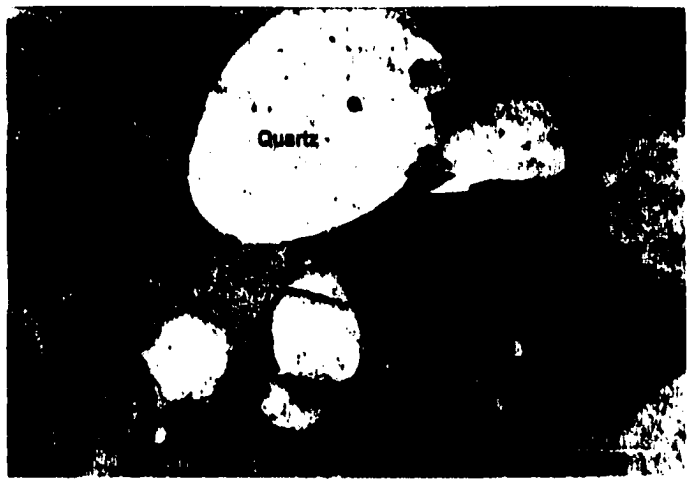

Figure 3.32: Rounded quartz grains in dolomitic sandstone unit of Little Falls at outcrop #14. Dedolomite appears stained red with alizarine.

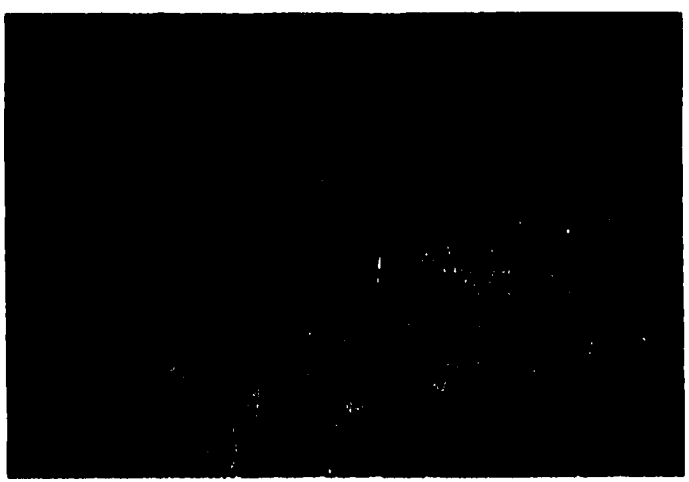

Figure: 3.33: Cryptmicrobial laminites (Lithofacies 8) in the Little Falls dolostones (outcrop # 14). Hammer is for scale.

Figure 3.34: Outcrop photograph of the Little Falls dolostone (outcrop #14), showing a discontinuous layer of bedded black chert. Person's hand is for scale.

The stromatolites are interpreted as structures built by cyanobacteria trapping detrital particles and precipitating calcium carbonate between their mucilagenous mats. These biogenic structures can develop in waters of normal and elevated salinity. However, they tend to be preserved in areas of elevated salinities, where they are protected from grazing organisms that cannot tolerate hypersalinity. Compared to cryptmicrobial laminites, stomatolites exhibit high-relief structures which form in high-energy environments, such as shallow subtidal to lower-intertidal channels. The presence of stromatolites is also indicative of high-energy, fair-weather conditions of deposition.

Lithofacies 5: Dolomitic Sandstones:

Dolomitic and calcareous sandstones are common in outcrop section #16. These sandstones are composed of rounded coarse particles of quartz and contain some scattered dolomite in their intergranular spaces (Figure 3.32). Herringbone cross strata, although not observed in this section, has been reported by Zenger (1981) in other outcrops of the Little Falls Formation.

These sandstones are inferred to represent a high-energy subtidal to lower- intertidal channel facies. The cross strata may have resulted from the bimodal flood and ebb tides (Demicco and Hardie, 1994). It is also likely that the bidirectional cross strata resulted from seasonal wind reversal. The high sand content in these units is interpreted as having been derived from the ancestral Adirondack Mountains to the north, where the Proterozoic metamorphics were exposed during Cambro-Ordovician times. The well-rounded nature of the sands

suggest eolian transport as well as reworking in the high-energy subtidal zone. The detrital grains in the dolostones are however sub-angular and silt-sized and perhaps derived from the coarser sands (Zenger, 1981).

Lithofacies 7: Dolomudstone / Fenestral Vuggy Dolostone:

This lithofacies is common in this section and is composed of light gray, microcrystalline to very fine-crystalline dolomite with fenestrae filled with late-diagenetic, void-filling calcite and dolomite. The dolomites occur as pervasive mosaics and are in general low in trace elements (Mn and Fe) and display relatively high Sr values ranging from 167 to 777ppm.

The very fine-crystalline nature of the dolomite and the presence of subspherical vugs in them indicate early syndepositional dolomitization of intertidal and supratidal lime muds. The low trace-element content supports early diagenesis in the depositional environment. The high Sr content suggests that dolomitizing fluids were marine derived and bordering on the hypersaline. These textural and geochemical characteristics imply a supratidal flat sub-environment of deposition, where excessive evaporation can result in hypersalinity of interstitial fluids. The dominance of vugs in this lithofacies may hint at the former presence of evaporite nodules that could have been leached during meteoric diagenesis leaving their remnant molds as voids to be filled with cements. Thus, this lithofacies is interpreted as representing an upper-intertidal to supratidal sub-environment of deposition.

Lithofacies 8: Cryptmicrobial laminated Dolostone:

On the outcrop scale this lithofacies appears as flat-lying, wavy, commonly crinkled laminae in a gray dolostone. Fenestrae, with late-diagenetic saddle dolomite and or calcite are also present. The presence of wavy, crinkled laminae and the very fine texture of the dolomite suggests that these are cryptmicrobial laminites (Figure 3.33). They are interpreted as representing an upper-intertidal to supratidal flat setting where microbial mats trapped and bound carbonate mud. The flat low-relief structures suggest a low-energy environment of quiet water, which is achieved on the upper-intertidal and supratidal flats. The hypersaline environment discouraged grazing organisms and thus helped preserve these microbial mats. Syndepositional dolomitization may have occurred in a hypersaline setting, perhaps aided by the decay of the organic matter in these microbial mats.

Lithofacies 10:Silicified Ooid Grainstone/ Chert/ Dolomitic Chert:

Chert occurs in the form of silicified ooids, microcrystalline silica, and megaquartz. The ooids show concentric laminae and radial structures. A partly discontinuous bed of chert occurs in outcrop #14, positioned at a parasequence boundary (Figure 3.34). This chert bed is composed of silicified ooids. Underlying the chert bed is a thin-bedded unit of cryptmicrobial laminites.

Microcrystalline chert and megaquartz are also observed in some calcareous and dolomitic sandstones, where the dolomitization of the carbonate material between quartz particles appears to have been interrupted by

silicification (discussed more in chapter 5). In this example, silicification is not pervasive and seems to have been local and restricted, as some carbonate material is still nondolomitized and nonsilicified.

The ooids and sands were probably deposited in a shallow, subtidal zone of moderate turbulence. The silicification is a diagenetic phenomenon associated with perhaps emergence of the strata periodically during deposition or related to uplift of the basin in the Ordovician. The chert bed in outcrop #14 is located at a parasequence boundary indicating that silicification may be associated with emergence at a parasequence surface. During arid climatic conditions, evaporation of silica-rich meteoric fluids can precipitate silica and cause silicification among near-surface sediments (Friedman, 1994a,b; Friedman and Radke, 1979;Guo, 1994; Guo et.al., 1996). Thus, the presence of chert in these units may be indicative of intermittent emergence of the strata at the termination of depositional cycles.

3.5.2 Parasequences in the Little Falls Formation:

At least five parasequences are observed in the outcrop #14. The individual parasequences at this exposure of the Little Falls Formation, are composed of a basal high-energy subtidal facies overlain by a low-energy intertidal-supratidal facies. The basal subtidal units are composed of dolomitic shale, dolomitic sandstones, oolitic grainstones or coarse-textured mottled

dolostones. The low-energy units that form the upper part of the parasequences are either fenestral dolomudstones or cryptmicrobial laminated dolostones.

A storm-dominated parasequence occurs in the lower part of the section, where intraclasts and fenestral dolomudstones form alternating layers. The intraclast layers indicate deposition during storms and the fine-textured dolomudstones represent deposition of fines from suspension during fair-weather conditions in the aftermath of the storm.

Some features that indicate emergence of the strata at the parasequence boundaries are observed at this outcrop. Among them the most significant are the mudcracks (Figure 3.31), chert (Figure 3.34), and dedolomite (Figure 3.32).

3.5.3 Summary of the Depositional Facies in the Little Falls Formation:

The lithofacies and depositional features discussed above suggest periodic emergence and submergence related to tidal influence. The presence of fine-textured dolomite, intraclasts and cryptmicrobial laminites and geochemical evidence of hypersalinity suggest the presence of intertidal and supratidal flats, where intermittent drying and evaporative processes were prevalent.

The oolitic grainstones, cross-stratified dolomitic sandstones, mottled dolostones, and the presence of hemispheroidal stromatolites suggest shallow, subtidal conditions of deposition. Several small-scale upward-shallowing cycles of deposition are noted in this outcrop section. The basal three cycles are composed of subtidal sandstones overlain by coarse, mottled dolostones and

fine-textured vuggy dolomudstones topped by intraclasts. The top three cycles are composed of subtidal shale, oolitic chert, or mottled dolostones overlain by cryptmicrobial laminated and stromatolitic fine-textured dolostones with local mudcracks and intraclasts. Thus, the Little Falls strata are inferred to be products of an aggradational peritidal depositional sequence.

3.6 Facies Analysis of the Tribes Hill Formation

Outcrops of the Tribes Hill Formation (Figure 3.35) were examined at roadcuts and abandoned quarries. Outcrop section #15 is a roadcut on Route 5, east of Amsterdam and contains exposures of the Palatine Bridge and Wolf Hollow members of the Tribes Hill Formation. Outcrop section #16 is a section of the Palatine Bridge and Wolf Hollow members exposed in the Van Wie creek. The roadcut on Borden road (#17) is stratigraphically above the section in the Van Wie creek and contains the Fonda member topped by a surface of disconformity above which are younger rocks of the Tippecanoe sequence (Lowville and Larabee limestones of the Trenton Group). The Fort Johnson member of the Tribes Hill Formation is exposed in the Fort Hunter quarry (outcrop section #18). The Chuctanunda Creek dolostone and the Cranesville Dolostone were not examined in this study.

Figure 3.35 Outcrops of the Tribes Hill Formation (Figure 1.2 is section location map)

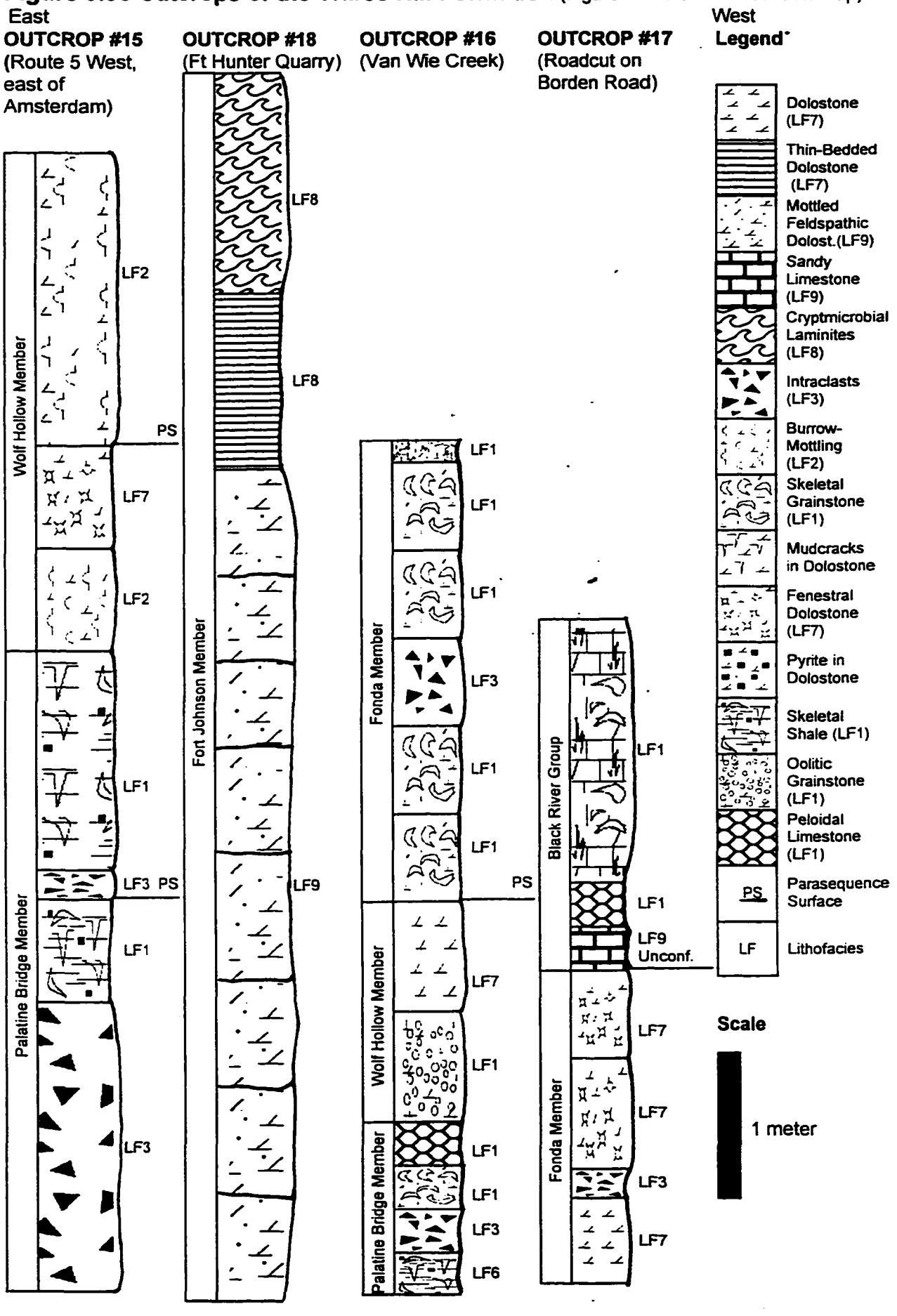

3.6.1 Lithofacies in the Tribes Hill Formation:

The Fort Johnson member is the oldest unit in the Tribes Hill Formation. The rocks of the Fort Johnson member are generally composed of feldspathic dolostones that are exposed at the Fort Hunter Quarry (Braun and Friedman, 1969; Friedman and Braun, 1975, Friedman, 1985, 1990). The outcrop section in the Fort Hunter Quarry is described in detail by Braun and Friedman (1969). The lower part of the section is composed of mottled, feldspathic dolostones, overlain by cryptmicrobial laminated dolostones, containing feldspar-rich laminae alternating with dolomite. At the top of the section are sandy limestones, composed of thin beds of pellets, intraclasts, fossil fragments, and pebbles of micrite.

The rocks of the Palatine Bridge member, which are exposed at outcrop sections #15 and #16, are composed of bedded units similar to the limestones at the top of the Fort Johnson. The limestones have been partially dolomitized and fossil fragments, pellets, ooids, intraclasts and burrow mottles are common. Fossil tracks and trails (Figure 3.36) are also commonly observed in this member. Wavy beds with fine laminae and cross laminae are noted as well. Some scour-and-fill channel features are observed with coarse debris of intraclasts, fossils, and pellets as channel lags.

Comparatively, the overlying Wolf Hollow member is composed mostly of dolostones and dolomitic limestones. In this member, burrow mottles are more common, with isolated horizons of intraclasts and mudcracks. Friedman (1996a)

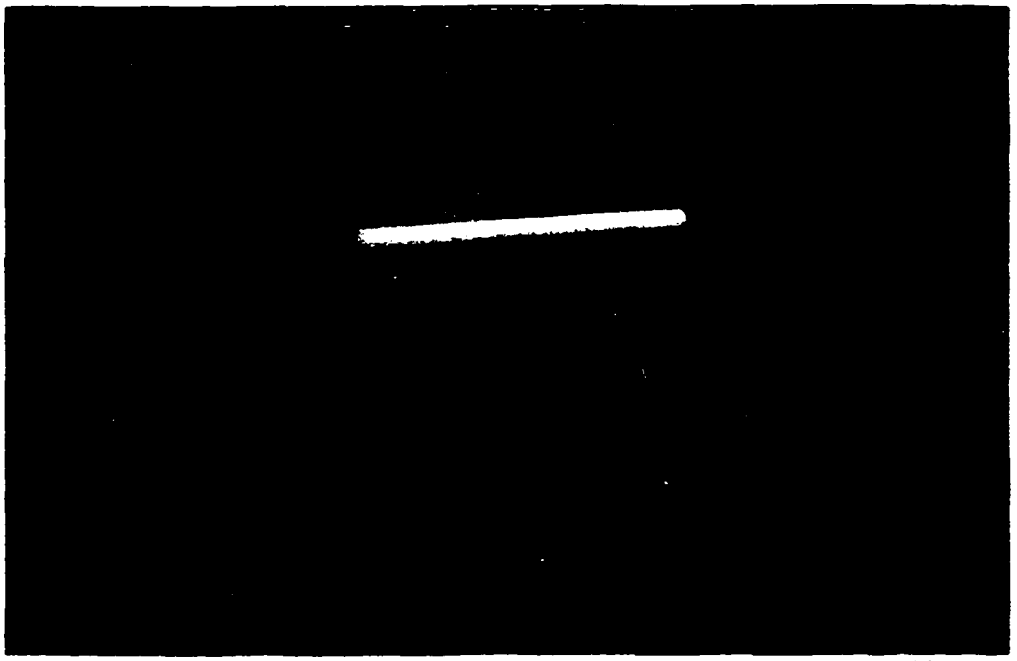

Figure 3.36: Outcrop photograph showing fossil tracks and trails observed in rocks of the Tribes Hill Formation (Palatine Bridge member) at outcrop # 15.

Figure 3.37: Outcrop photograph of storm-deposited intraclast bed found at base of outcrop # 15 (Palatine Bridge member of Tribes Hill Formation) (divisions of scale are in cm.)

reported microbial reef mounds in the Wolf Hollow member that are inferred to represent a high-energy facies.

The youngest member is the Fonda member which is exposed at outcrop sections #16 and #17. The units of the Fonda member are composed of fossiliferous dolomitic sandy limestones and calcitic dolostones. Fossils, such as the arthropod *Ribeira* are noted by Fisher (1954) in addition to trilobites *Clelandia, Hystricurus* and *Symphysurus.* Fisher also recognized many species of snails (*Ophileta, Ecculiomphalus, Gasconadia*), brachiopods (*Finkelnburgia, Tetralobula*) and nautiloids (*Ellsmereoceras, Ectenoceras, Clarkoceras).*

The following lithofacies are recognized in the Tribes Hill Formation:

LITHOFACIES (This Study)	LITHOFACIES (Braun and Friedman, 1969)
Lithofacies 1: Ooid /Peloid/ Skeletal Packstone (With varying degrees of dolomitization);	Lithofacies 10: Biointramicrite and biomicrite; Lithofacies 9: Oobiosparite and biointraoosparite;
Lithofacies 2. Mottled Dolostone / Limestone ;	Lithofacies 7: Mottled dolomitic micrite and biomicrite;
Lithofacies 3. Intraclast Dolostone/ Limestone;	Lithofacies 8: Intrasparite and biointrasparite; Lithofacies 4: Pebble conglomerate;
Lithofacies 8. Cryptmicrobial-laminated Dolostone;	Lithofacies 2: Laminated Feldspathic dolomite;
Lithofacies 9: Feldspathic dolostone;	Lithofacies 1: Mottled Feldspathic dolomite;

Lithofacies 1:Ooid /Peloid/ Skeletal Grainstone/Packstone / Wackestone:

This lithofacies is observed in all the members of the Tribes Hill Formation. Skeletal fragments and or peloids occur in a calcitic micrite matrix which is dull-luminescent, low in trace elements Fe and Mn and high in strontium (1200-1400ppm). In most of the occurrences, fine-crystalline, zoned dolomite

has replaced part of the micrite matrix. In places, dolomite appears to be associated with stylolites. This lithofacies is similar to Lithofacies 9 (oobiosparite and biointraoosparite and Lithofacies 10 (biointramicrite and biomicrite) of Braun and Friedman (1969).

These skeletal limestones are interpreted to represent a subtidal setting. In horizons where the amount of micrite is less and the skeletal particles display a packstone or grainstone texture, they are inferred to be products of a high-energy subtidal environment or perhaps a lower-intertidal channel facies. The peloidal limestones and the skeletal wackestones are inferred to represent a low-energy subtidal setting.

Lithofacies 2: Mottled Dolostone / Limestone :

This lithofacies is observed mostly in the Wolf Hollow member, and less commonly in the other three. The mottled appearance is due to the light and dark gray patches of dolomite and limestone. The burrows are filled with light gray, fine-crystalline dolomite and may be horizontal or vertical. In some cases, horizontal worm burrows are also observed. The mottled rocks may be composed of dolomitic micrite and skeletal limestone.

A subtidal setting is implied by the horizontally burrowed strata, whereas the vertically burrowed strata are inferred to be intertidal deposits (Braun and Friedman, 1969). This corresponds to Lithofacies 7 (mottled dolomitic micrite and biomicrite) of Braun and Friedman which they interpret to be of intertidal origin.

Lithofacies 3: Intraclast Dolostone/ Limestone:

Intraclasts are common in dolostones of the Wolf Hollow and in limestones of the Palatine Bridge member. In outcrop #15, a thick unit composed of intermixed intraclasts and skeletal fragments alternating with fine-textured dolomitic limestone is observed at the base of the exposure (Figure 3.37). The intraclasts are composed entirely of micrite or dolomicrite, and usually occur as flat- or round-pebble conglomerate in a sandy, coarse matrix of skeletal fragments.

This lithofacies is interpreted to represent a high-energy intertidal, subtidal or storm deposit. Tidal currents or storm-generated waves and currents, could have ripped up and redeposited micrite chips from the supratidal and intertidal flats producing a chaotic mixture of sketetal debris and partially lithified lithoclasts (Aigner, 1982, 1985; Sepkoski, 1982; Chuanmao et.al., 1993). The interlayered fine-textured dolomitic limestones possibly represent deposition of fines from suspension during fair-weather conditions in the aftermath of the storm. This lithofacies corresponds to Lithofacies 4 (pebble conglomerate) and Lithofacies 8 (intrasparite and biointrasparite) of Braun and Friedman (1969).

Lithofacies 8: Cryptmicrobial-laminated Dolostone:

This lithofacies is observed only in the Fort Johnson member. It occurs as thinly bedded dolostones, which display characteristic irregular, crinked laminae.

These laminated beds are interbedded with shaly dolomite, which appear as recessed beds in outcrop.

The fine, irregular laminae in these rocks are interpreted as cryptmicrobial laminites, which are structures formed by the trapping and binding of carbonate mud on the upper-intertidal or supratidal flats by microbial mats. Pervasive dolomitization of this lithofacies is interpreted to be the product of penecontemporaneous dolomitization by hypersaline interstitial fluids. The open and filled fenestrae, abundant in this lithofacies are interpreted as being due to desiccation of the microbial mats or indicating the former presence of evaporite nodules. The flat, low-relief morphology of these cryptmicrobial laminites supports their formation in a low-energy tidal flat setting.

Mineralogically, this lithofacies is composed of fine dolomite with alternating feldspar-rich zones (Figure 3.38). The dolomite is fine to medium textured. The feldspar rich laminae are composed of authigenic potassium feldspar. Friedman and Braun (1969) have described these beds as 'laminated feldspathic dolostone' (Lithofacies 2 of Braun and Friedman,1969). They explain the origin of the feldspar in this lithofacies as having either been derived from the dissolution of detrital feldspar or from the decomposition of wind-transported tephra. Detrital quartz and feldspar are common in the shallow-water carbonates of the Saratoga Platform and are possibly derived from the weathering of the adjacent nonvegetated craton (Buyce and Friedman, 1975). Wind-blown tephra (volcanic ash) may have been trapped by the microbial mats that colonized the intertidal and supratidal flats. The authigenic feldspar in these beds are perhaps

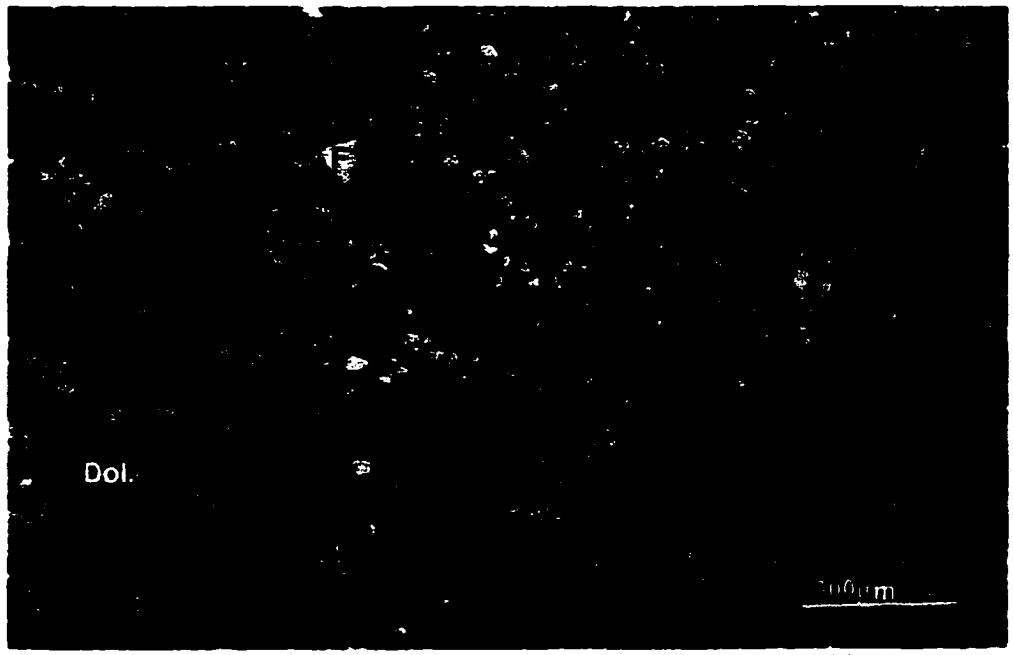

Figure 3.38 : Photomicrograph of cryptmicrobial laminated feldspathic dolostone (Lithofacies 8) in the Fort Johnson member of the Tribes Hill Formation (Sample # FJ-12; outcrop # 18). Alternating laminae of authigenic feldspar (F) and mosaic dolomite are seen in this thin section. Thin section is viewed under crossed nicols.

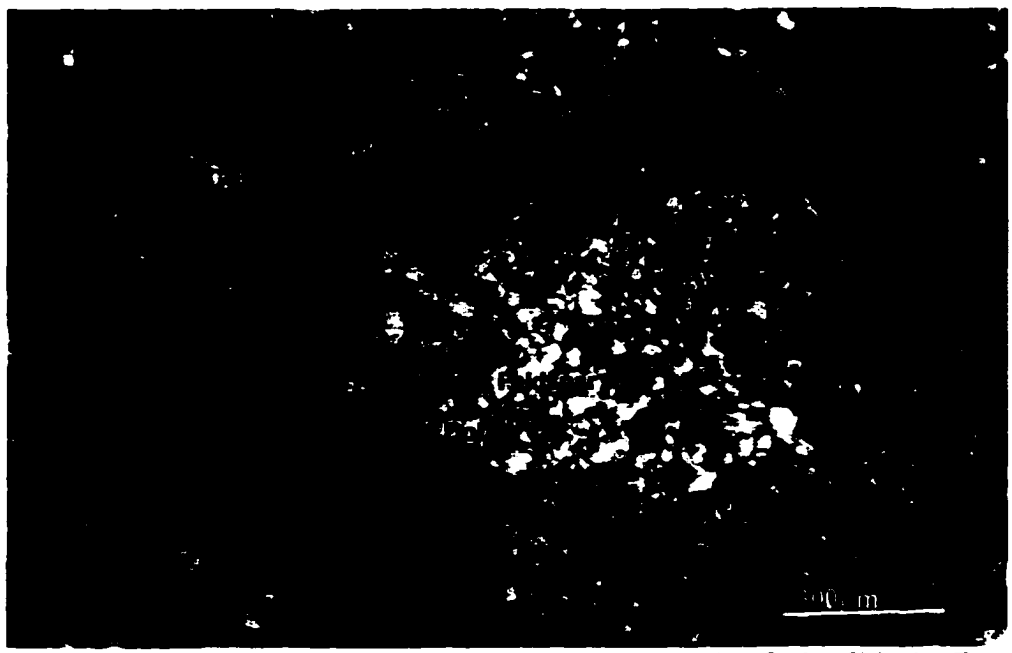

Figure 3.39: Photomicrograph of Feldspathic dolostone (Lithofacies 9) in the Fort Johnson member of the Tribes Hill Formation (Sample # FJ-13; outcrop #18). Seen here are patches of authigenic feldspar within the dolomite mosaic that give the rock a mottled appearance on the outcrop scale. Thin section is viewed under crossed nicols.

end products of the diagenetic alteration of zeolites that formed by the alteration of volcanic glass (Friedman and Braun, 1975; Buyce and Friedman, 1975; Friedman, 1990; Friedman, Sanders and Kopaska-Merkel, 1992, p.276).

Lithofacies 9: Feldspathic Dolostone

Rocks of this lithofacies are common in the Fort Johnson member and are composed of fine crystalline, planar-s mosaic dolomite with abundant authigenic feldspar. Skeletal particles are absent in this lithofacies. Mineralogically, the only difference between this lithofacies and Lithofacies 8 is that the authigenic feldspar does not occur as horizontal laminae, but instead as patches (Figure 3.39). These patches give the rock a mottled appearance in the outcrop. This lithofacies is the same as Lithofacies 2 (mottled feldspathic dolostone) described by Braun and Friedman (1969). According to Braun and Friedman (1969), microcline is the abundant feldspar in this lithofacies.

Formation of alkali feldspar in these rocks may indicate a highly alkaline (pore waters rich in K^{+}, Al^{3+} and Si^{4+}) and hypersaline environment (Buyce and Friedman, 1975). Strong alkalinity may have resulted from dissolution of detrital feldspar, which is common in most of the Cambro-Ordovician strata. The authigenic feldspars may also have formed as a result of the diagenetic alteration of wind-transported tephra that deposited among the intertidal-flat sediments (Friedman and Braun, 1975; Buyce and Friedman, 1975 ; Friedman, 1990; Friedman, Sanders, and Kopaska-Merkel, 1992, p.276) during the

deposition of the Fort Johnson strata. Similar feldspathic dolostones are observed in the correlative Gailor dolostones (Figure 3.28).

3.6.2 Parasequences in the Tribes Hill Formation:

In the units of the Tribes Hill Formation that were examined, upward-shallowing depositional cycles or parasequences are observed in some of the outcrops. In outcrop #15, where units of the Palatine Bridge and Wolf Hollow members are exposed, the parasequences are composed of a lower high-energy subtidal facies followed by an upper low-energy, intertidal to supratidal facies. The first parasequence at this outcrop that occurs in the lower part of this section, is composed of a storm deposit . The parasequence starts out as a high-energy storm deposit composed of a chaotic array of intraclasts, skeletal fragments, and silt-sized particles of quartz and feldspar. Interbeds of fine-textured limestone and dolostone alternate with the storm layers indicating intervening periods of fair-weather deposition. The upper part of the parasequence is composed of thin beds of dolomitic shale containing exposure-related features, such as mud cracks. In the overlying parasequences, the subtidal facies are represented by skeletal lags and intraclasts following up into fenestral dolomudstones (that are mottled in places) of the intertidal flats.

The parasequences observed in Van Wie creek are in places composed of a lower high-energy subtidal unit followed by a low-energy subtidal unit, and lacking any intertidal or supratidal facies. The high-energy subtidal facies are

composed of oolitic, intraclastic and skeletal grainstones, whereas the low-energy subtidal facies are composed of pelletal or peloidal, skeletal wackestones. In some of the parasequences fine-textured dolostones or dolomitic limestones occur near the top, indicating intertidal deposition.

In outcrop #17, no parasequences are observed, perhaps due to the limited vertical extent of this outcrop. However, a surface of disconformity separates the underlying Tribes Hill strata from the overlying fossiliferous beds of the Tippecanoe sequence. At the disconformity surface a white-weathering unit composed of sandy feldspathic limestone is present.

3.6.3 Summary of the Depositional Facies in the Tribes Hill Formation:

Compared to all the other formations discussed above, the Tribes Hill is observed to contain less dolostones and more limestones. The lithofacies changes indicate more limestones and fossiliferous strata towards the top of the formation, suggesting an overall submergence of the basin towards the top. In the Tribes Hill strata, starting with the Fort Johnson member deposition was in a supratidal to intertidal setting. This was followed by deposition in a lower-intertidal environment, where the lithofacies of the Palatine Bridge member were deposited. This was followed by supratidal and intertidal deposition of the Wolf Hollow member. Finally, a predominantly subtidal to lagoonal lithofacies of both high- and low-energy subtidal environments was recognized in the Fonda member.

3.7 CONCLUSIONS:

In an overall sense, the Sauk sequence carbonate strata in the Saratoga-Mohawk Valley area, appear to have been deposited in a shallow-marine, sea-marginal, peritidal setting, where in places hypersaline environments may have been prevalent, especially within the supratidal sediments, due to evaporative concentration of interstitial sea water. The lithofacies types recognized in the Sauk strata correspond to supratidal, intertidal, and shallow subtidal sub-environments of deposition on the shoreward side separated from oolite shoals on the seaward side by subtidal lagoonal sub-environments. The vertical distribution of these depositional settings suggests an overall transgressive trend for the Cambro-Ordovician strata, composed of small-scale upward-shallowing cycles recognizable in some outcrops.

Table 2 lists the distribution of biogenic, physical and chemical facies characteristics used to interpret the sub-environments of deposition for the Sauk carbonates in this study.

TABLE 2: SEDIMENTARY STRUCTURES AND DIAGENETIC FEATURES OBSERVED IN THE SAUK SEQUENCE CARBONATES IN CENTRAL NEW YORK

Y = OBSERVED
N = NOT OBSERVED

	FEATURES	LITTLE FALLS	GALWAY	HOYT	GAILOR	TRIBES HILL
BIOGENIC FEATURES	Domal Stromatolites	Y	Y	Y	Y	N
	Cryptmicrobial laminites	Y	Y	Y	Y	Y
	Invertebrate Fossils	N	Y	Y	Y	Y
	Distinct Burrows	N	Y	Y	Y	Y
PHYSICAL STRUC-TURES	Mottling	Y	Y	Y	Y	Y
	Intraclasts	Y	Y	N	Y	Y
	Peloids	Y	Y	Y	Y	Y
	Ooids	Y	Y	Y	Y	Y
	Desiccation Cracks	Y	Y	N	N	Y
	Fenestrae	Y	Y	N	Y	Y
	Channels	N	N	Y	Y	Y
	Cross Strata	N	Y	N	Y	N
	V. Fine Crystalline Dolomite	Y	Y	Y	Y	Y
CHEMICAL FEATURES	Dissolution Collapse Breccia	N	Y	N	Y	N
	Chert	Y	Y	N	Y	N
	Dedolomite	Y	Y	Y	Y	Y
	Evaporites	N	N	N	N	N

PART II

DIAGENESIS

CHAPTER 4 - DOLOMITIZATION

4.1 Introduction:

The general observation in the Sauk sequence strata that have been examined for this study, is that the bulk of the strata have either been partially or pervasively dolomitized. The most effective analytical method used for the study of dolomitization in these rocks was cathodoluminescence. Using cathodoluminescence petrography, several types of dolomite with compositionally varied zones were identified. These different dolomite types represent a sequence of diagenetic changes, that these rocks were subjected to, during the course of their evolution from the original carbonate material in the depositional environment to their occurrence as dolostones in surface outcrops today.

Taking together their petrographic and luminescence characteristics, geochemical composition and stable-isotopic compositions of oxygen and carbon, seven dolomite types have been identified in the rocks of the entire Cambro-Ordovician sequence under study (Table 3). These seven fabric types are inferred to represent four main stages of diagenesis:

(1) Early stage of diagenesis (syndepositional dolomitization);

(2) Main stage of diagenesis (subsurface burial dolomitization);

(3) Third stage of diagenesis associated with uplift;

(4) Fourth and final stage of deep-burial dolomite cementation;

TABLE 3: THE DIFFERENT KINDS OF DOLOMITE NOTED IN THE SAUK CARBONATES OF THIS STUDY

DOLOMITE TYPE	DESCRIPTION	CATHODOLUMINESCENCE PATTERN	GEOCHEMISTRY	TIMING	INFERRED DEPTH OF DOLOMITIZATION	FORMATION	LITHOFACIES
DOLOMITE (1)	Microcrystalline (<15μm), replacement mosaic	Unzoned / Finely zoned, red-luminescent	Non-stoichiometric: 51.8-56 mole % $CaCO_3$ Fe: variable (70-2400ppm) Mn: 300-500ppm Sr: 0-214ppm $\delta^{18}O$: -5.39 to -5.88 ‰ $\delta^{13}C$: -1.4 to -2.1 ‰	EARLY-STAGE	NEAR-SURFACE	GALWAY HOYT	LF-I: Ooid/skel Packstone /grainstone; LF-3: Intraclast Dolostone
DOLOMITE (2)	Very Fine-crystalline (20 to 60μm) Planar-s to non-planar, replacement mosaic	Zoned or unzoned, red-luminescent, dull-luminescent, mottled luminescence or non-luminescent	Non-stoichiometric: 53-58 mole % $CaCO_3$ Fe: variable Mn: Most values 259-377ppm (rarely as high as 3022 and as low as 0 ppm) Sr: 0-777ppm $\delta^{18}O$: -5.5 to -6.85 ‰ $\delta^{13}C$: +0.1 to -2.2 ‰	EARLY-STAGE	NEAR-SURFACE	GALWAY HOYT GAILOR LITTLE FALLS TRIBES HILL	LF-I: Ooid/skel Packstone /grainstone; LF-3: Intraclast Dolostone LF-7:Dolomudstone LF-8: Cryptmicrobial-laminated dolostone
DOLOMITE (3a)	Fine to medium-crystalline (60 to 500μm) Planar-e to planar-s replacement mosaics	Distinctly zoned: Bright and dull red luminescence, mottled luminescence in places	Variable stoichiometry: 51-59 mole% $CaCO_3$ Fe : variable Mn: 300-900ppm Sr: usually absent(rarely 100-500ppm) $\delta^{18}O$: -5.1 to - 10.73 ‰ $\delta^{13}C$: -0.4 to -3.2 ‰	MAIN-STAGE	SHALLOW-BURIAL	GALWAY HOYT GAILOR LITTLE FALLS TRIBES HILL	LF-I: Ooid/skel Packstone /grainstone; LF-2: Mottled Dolostone; LF-4: Stromatolitic boundstone; LF-7:Dolomudstone LF-8: Cryptmicrobial-laminated dolostone
DOLOMITE (3b)	Very fine-crystalline (10 to 150μm), Planar-P, porphyrotopic, scattered clusters of replacement crystals in limestone mosaic, associated with stylolites.	Zoned, red-luminescent cores, thick non-luminescent zones and thin orange-luminescent rims.	Non-stoichiometric: 53.7 - 57.5 mole% $CaCO_3$ Fe:1724- 7394 ppm Mn: 0-356 ppm Sr: 0-260 ppm $\delta^{18}O$: -8.11 to - 8.88 ‰ $\delta^{13}C$: -1.4 to -1.9 ‰	MAIN-STAGE (post-compaction)	SHALLOW-BURIAL (Below the depth at which stylolites develop)	TRIBES HILL	LF-I: Ooid/skel Packstone /grainstone;
DOLOMITE (4)	Fine- to medium-crystalline (60 to 500μm) Planar-s to non-planar replacement mosaics	Unzoned, red-luminescent	Nearly stoichiometric (49.7 to 52.6 mole % $CaCO_3$ Fe: variable (300-5000ppm) Mn: 150-900ppm Sr: usually absent(rarely 150-540ppm) $\delta^{18}O$: -6.07 to -9.76 ‰ $\delta^{13}C$: -0.8 to -2.5 ‰	MAIN-STAGE	SHALLOW-BURIAL	GALWAY HOYT GAILOR LITTLE FALLS TRIBES HILL	LF-I: Ooid/skel Packstone /grainstone; LF-2: Mottled Dolostone; LF-3: Intraclast Dolostone;
DOLOMITE (5)	Medium- to coarse-crystalline (250 to 1000 μm) Planar-e void-lining cements (rarely as replacement mosaics)	Bright orange luminescence	Stoichiometry: variable (49.5 to 59.7 mole % $CaCO_3$) Fe: Usuall low ranging from 0 to 658ppm (rarely as high as 17854ppm) Mn: ranges from 69 to 659 ppm (rarely as high as 3579ppm) Sr: variable (0 to 327ppm)	UPLIFT-STAGE	NEAR-SURFACE / SHALLOW-BURIAL	GALWAY HOYT GAILOR LITTLE FALLS TRIBES HILL	LF-3: Intraclast Dolostone LF-7:Dolomudstone LF-8: Cryptmicrobial-laminated dolostone
DOLOMITE (6) (Saddle Dolomite)	Coarse- crystalline (500 to 1000μm) Non-planar-c, milky-white, void-filling cements	Commonly non-luminescent, unzoned (In places zoned with final non-luminescent zone)	Variable stoichiometry (50 to 56 mole % $CaCO_3$) Fe: High (2000 to 20,000 ppm) Mn: Low <100ppm (in nonluminescent cements), 300 or 3000 in bright luminescent cements) Sr: absent $\delta^{18}O$: -9.27 to -10.44 ‰ $\delta^{13}C$: -2.5 to -2.6 ‰	LATE-STAGE	DEEP-BURIAL	GALWAY GAILOR LITTLE FALLS TRIBES HILL	LF-7:Dolomudstone LF-8: Cryptmicrobial-laminated dolostone
DOLOMITE (7)	Planar-e, void-filling cement	Non-luminescent	Non-stoichiometric: (52.4 to 55 mole % $CaCO_3$) Fe: High (8000 to 21000 ppm) Mn: variable (200 to rarely 5000 ppm) Sr: absent	LATE-STAGE	DEEP-BURIAL	GALWAY HOYT GAILOR LITTLE FALLS TRIBES HILL	LF-I: Ooid/skel Packstone /grainstone; LF-2: Mottled Dolostone; LF-7: Dolomudstone

The dolomite fabrics are intimately associated with other diagenetic features, such as chert, dedolomite, stylolites, and cements of burial calcite. These relationships will be explored in the following chapters. In this chapter, the different dolomite fabric types will be described and interpreted and their relationship with one another will be examined, in the context of the diagenetic stages that they are inferred to represent. The dolomite-cement stratigraphy evident in the zoned dolomite fabrics will also be examined.

4.2 Dolomite Texture Types:

Seven dolomite types have been recognized in the strata under study (Table 3). They are numbered 1 to 7. Dolomite (1) and Dolomite (2) are inferred to result from early diagenesis during or soon after deposition. Dolomite (3) and Dolomite (4) occur as zoned or unzoned, recrystallized dolomite mosaics having resulted from dolomitization in the subsurface. Dolomite (5), which occurs as brightly zoned cements associated with fracture- and vug-filling and as replacement of earlier-formed dolomite, represents the uplift stage. The late, deep-burial stage of diagenesis is represented by zoned- and nonzoned, dull- to non-luminescent cements of Dolomite (6) and Dolomite (7).

4.2.1 Dolomite (1):

Description: This dolomite texture occurs as tight mosaics of microcrystalline (<15μm) dolomite. It is observed in the Galway and Hoyt formations.

Petrographically, these dolomites are nonzoned (Galway) or finely zoned (Hoyt), and exhibit red luminescence. The microcrystalline size makes it hard to recognize the crystal shapes. Dolomite (1) is common in intraclasts (Lithofacies 3) and commonly associated with vugs containing Dolomite (5) and Dolomite (7). This texture is usually homogeneous and unimodal in distribution. Rarely, Dolomite (1) contains molds of unrecognizable allochems filled with Dolomite (5), Dolomite (7) and dedolomite (Figure 4.1). In one example, ooids (Lithofacies 1) composed of Dolomite (1), enveloping coarser Dolomite (4) were observed in the Galway Formation (Figure 3.2).

Geochemistry: Dolomite (1) is generally non-stoichiometric with $CaCO_3$ mole% ranging from 53 to 56. The predominant cathodoluminescence color is a dull red, which denotes moderate iron and manganese contents. Microprobe analysis indicates that the iron content is variable ranging from 70 to 2400 ppm. The manganese content is approximately 300 to 500 ppm, and the strontium content ranges from 0 to 214 ppm.

The oxygen-isotope values in these dolomites range from -5.39$^0/_{00}$ to -5.88$^0/_{00}$. Compared to the oxygen-isotope values of least-altered marine invertebrates and marine cements of the Cambrian which is -5.0 $^0/_{00}$ (Allan and Wiggins, 1993, Appendix II), the values are slightly depleted. In addition, compared to other Phanerozoic dolomites, these dolomites exhibit values that fall within the range of overlap between high-temperature and low-temperature dolomite which is between -6.5 to -2.2 $^0/_{00}$ (Allan and Wiggins, 1993, p. 27).

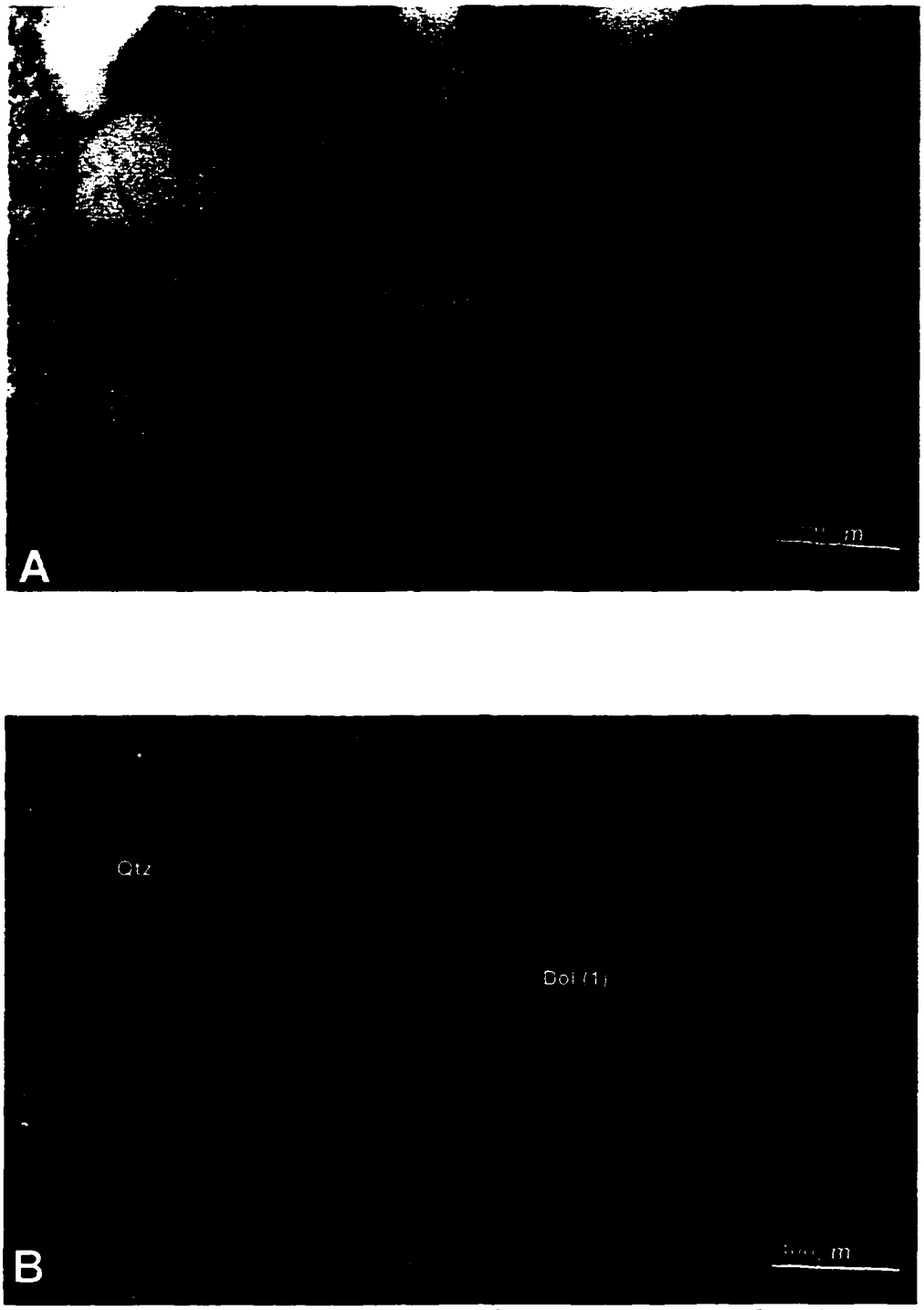

Figure 4.1: Thin-section photomicrograph of intraclastic dolostone from the Galway Formation (sample # GB-8, outcrop #1) where microcrystalline Dolomite(1) forms the matrix in which are present detrital quartz grains and allochem molds, partially filled with zoned replacement dolomite. Moldic porosity is occluded by bright-yellow luminescent dedolomite . Veins filled with dedolomite indicate that late-stage fractures served as conduits for the dedolomitizing solutions . (A) is viewed under plane-polarized light and (B) under cathodoluminescence.

Interpretation: The microcrystalline, relatively homogeneous texture implies that Dolomite (1) formed as an early replacement of lime mud. The extremely fine crystal size suggests high density of nucleation sites (Sibley, 1982) and high supersaturation of the dolomitizing fluid which was possibly modified seawater. The high surface-area-to-volume ratio of lime-mud particles, that occur on tidal flats would provide numerous sites for dolomite-crystal nucleation, resulting in a very fine-textured dolomite as in this example.

In addition, the low trace-element contents (Figure 4.2) also support the idea of early replacement. The strontium content, which is in places >100 ppm, may indicate an evaporitic setting (Veizer and Demovic, 1974). The supratidal-flat sediments were intermittently exposed and wetted as a result of normal peritidal processes. The facies characteristics examined in the previous chapter indicate that the supratidal flats show desiccation features, such as mudcracks, intraclasts, and fenestrae. In such an environment, evaporation of interstitial seawater would result in elevated salinities and supersaturation with respect to dolomite causing syndepositional dolomitization.

Compared with the $\delta^{13}C$ values of least-altered marine calcite cements of the Cambrian (0.7 $^{0}/_{00}$) and Early Ordovician (-1.5 to -0.5 $^{0}/_{00}$) (data from Allan and Wiggins, 1993, Appendix II), the carbon-isotope values of Dolomite (1) range from -1.4 $^{0}/_{00}$ to -2.1$^{0}/_{00}$ indicating the CO_3^{2-} was derived partly from organic-matter diagenesis. The oxygen-isotope values, although depleted, compared to unaltered marine carbonates, are heavier than the values observed in the other dolomite types formed during shallow and deep burial (Figure 4.3).

Figure 4.2: Trace-Element Composition of Sauk Sequence Carbonates.

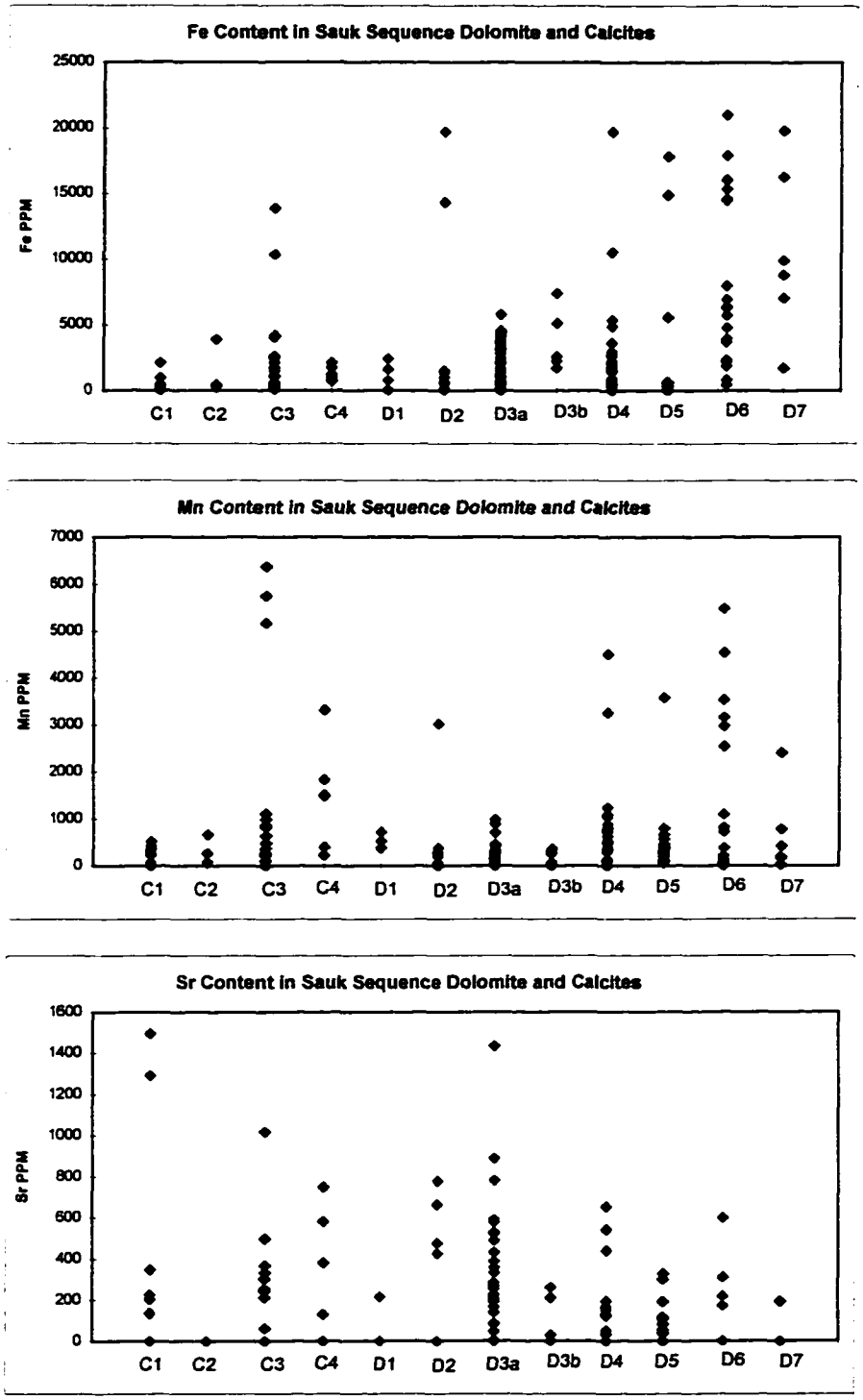

Explanation: Distribution of trace-elements Fe, Mn and Sr in the different kinds of calcites and dolomites recognized in the rocks of this study. C1(micrite) and C2 (sparry calcite) are precursor calcites. C3 is ferroan calcite and C4 is dedolomite. D1, D2, D3a, D3b, D4, D5, D6 and D7 are Dolomite (1), Dolomite (2), Dolomite (3a), Dolomite (3b), Dolomite (4), saddle dolomite and Dolomite (7) respectively.

Figure 4.3: Isotopic Compositions of Sauk Sequence Carbonates

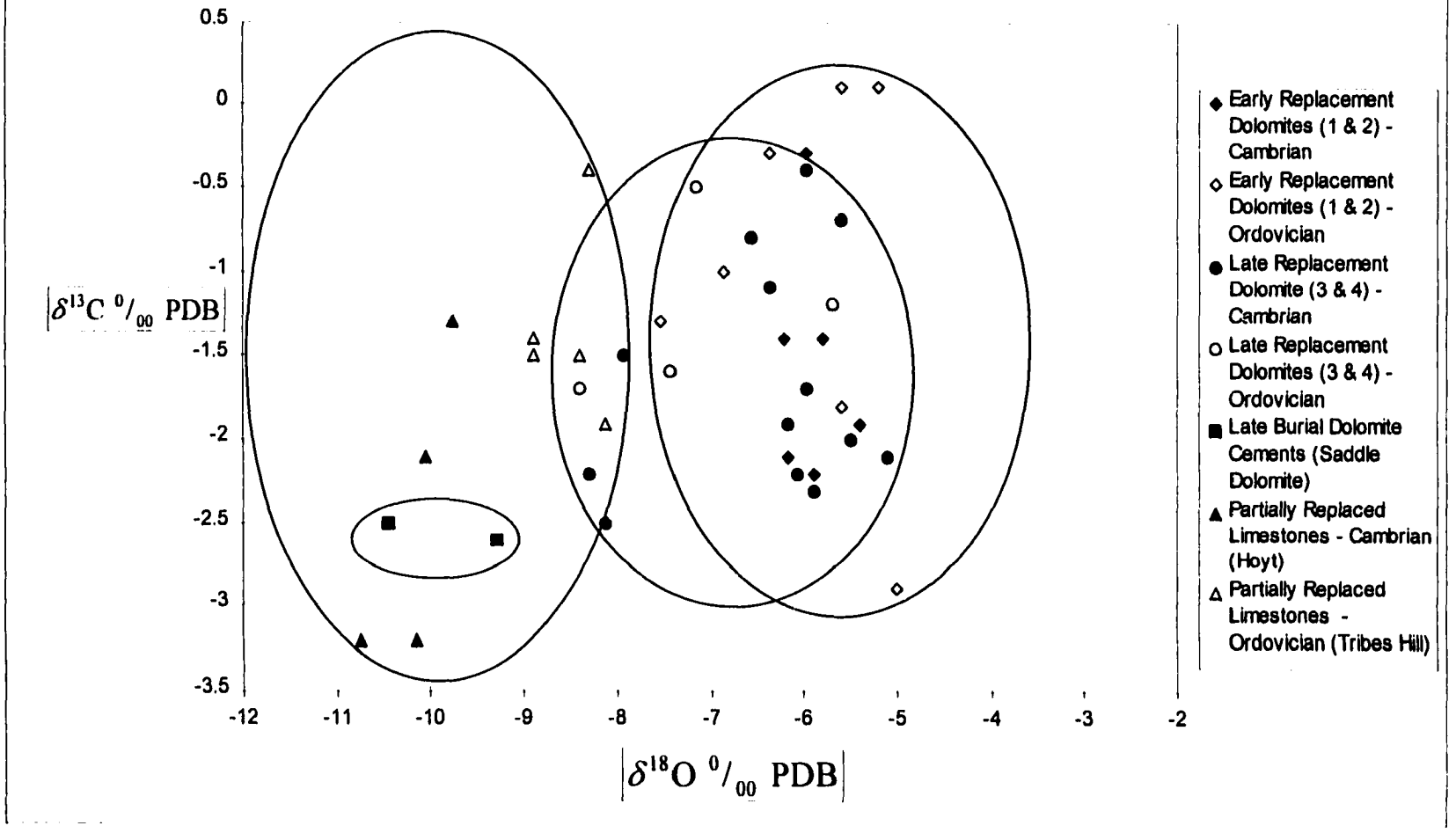

This pattern of oxygen-isotope enrichment in Dolomite (1) compared to Dolomites 3, 4, 5, 6, and 7 supports an early-diagenetic time for the formation of Dolomite (1).

4.2.2 Dolomite (2):

Description: This dolomite type is characterized by tight mosaics of zoned, very fine-crystalline dolomite ranging in size from 20 to 60 μm (Figure 4.4). It is present in all the formations and commonly found in vuggy dolomudstones (Lithofacies 7), intraclasts (Lithofacies 3), cryptmicrobial laminated dolostones (Lithofacies 8) (Figure 4.5), partially dolomitized skeletal packstones (Lithofacies 1) and mottled dolostones (Lithofacies 2).

This dolomite type occurs as:

(a) pervasive fabric-destructive mosaics with a unimodal, planar-s (hypidiotopic) texture or non-planar (xenotopic) texture;

(b) early-diagenetic replacement of micrite envelopes around allochems;

(c) replacement of allochems surrounded by Dolomite (1) that has replaced the micrite matrix.

The zoned mosaics exhibit a series of dull-red to brown zones followed by a non-luminescent zone and finally a dull-orange zone (Figure 4.4). In this example, it can be seen that some of the rhombs may have been replaced by dedolomite. The cores of Dolomite (2) appear to be non-luminescent. In places,

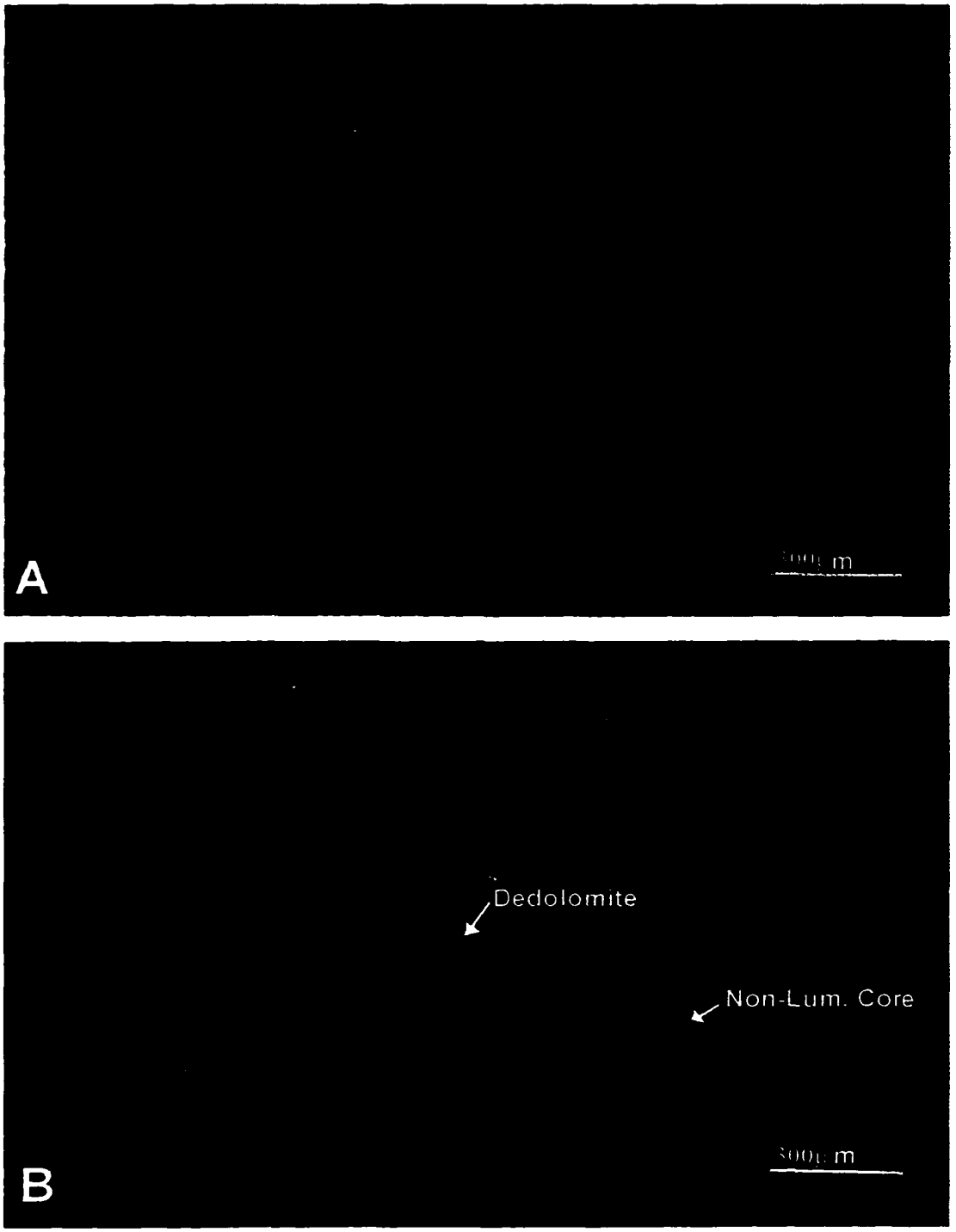

Figure 4.4: Unimodal, hypidiotopic to idiotopic, replacement mosaic composed of Dolomite(2) in breccia clast of dolomudstone is found in the karst facies observed in the Gailor Formation (sample # BS-1, outcrop # 9) . Cores of Dolomite(2) rhombs are nonluminescent, indicating that early nucleation of dolomite occurred in a near-surface, oxygenated setting, where dolomitizing solutions were not rich in divalent Fe and Mn ions. In places, dedolomitization has occurred. Dedolomite appears bright yellow under cathodoluminescence. (A) is viewed under plane-polarized light and (B) under cathodoluminescence.

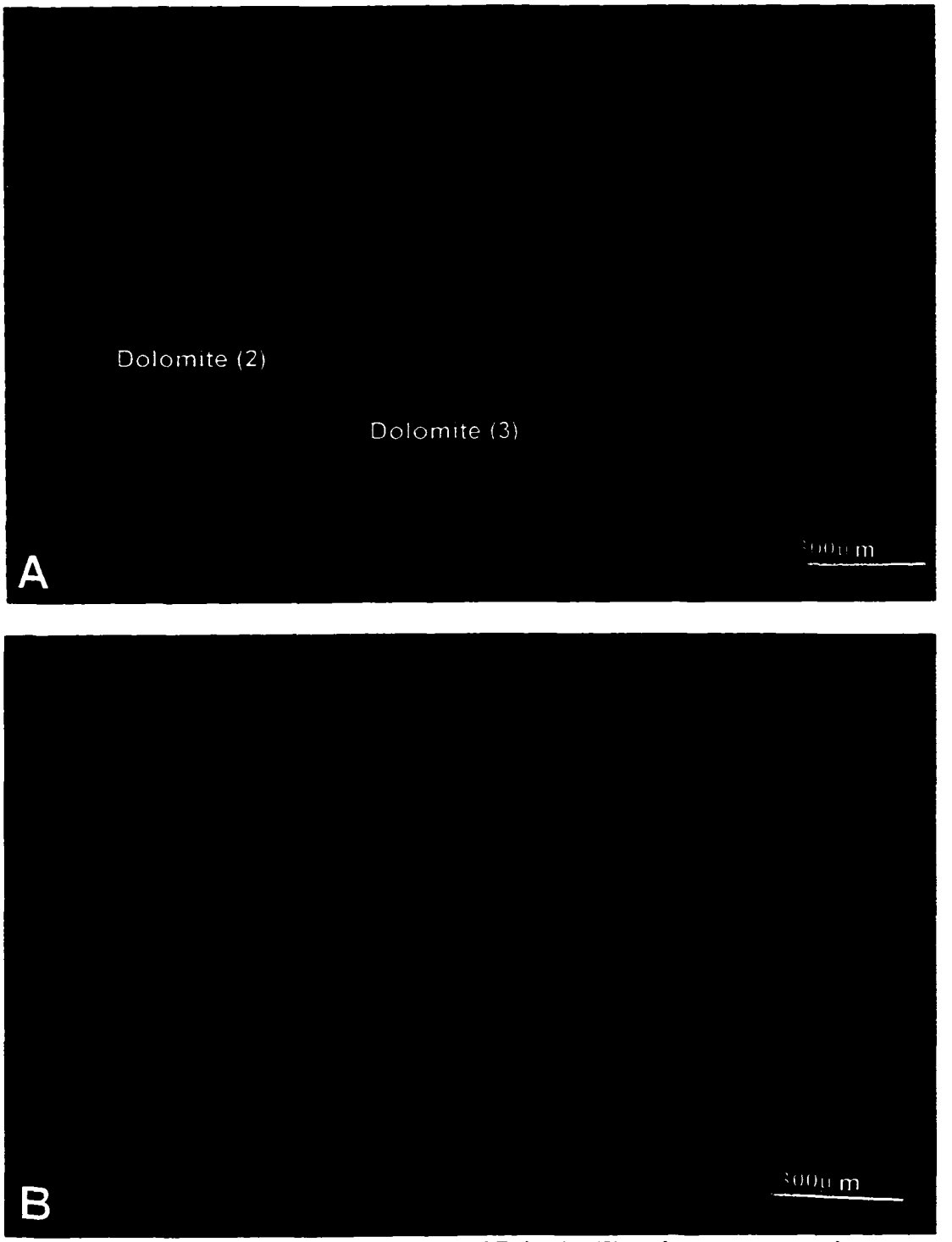

Figure 4.5: Alternating laminae of fine-textured Dolomite (2) and coarse-textured Dolomite (3) are observed in cryptmicrobial laminated dolostone from the Gailor Formation (Sample # BS-6, outcrop #9). Both dolomite types appear cloudy and inclusion-rich, which is indicative of their replacive origin. In the coarser laminae, the dolomite rhombs display clear rims around the cloudy cores. Under cathode light, it can be seen that the clear rims correspond with distinctly zoned, overgrowth cements.(A) is viewed under plane-polarized light and (B) under cathodoluminescence.

unstable cores appear to have suffered some alteration resulting in a mottled luminescence pattern.

Dolomite (2) may also occur as nonzoned and non-luminescent replacement mosaics (Figure 4.6). When associated with fractures, stylolites, and vugs, it is clearly evident that Dolomite (2) predates dolomites 5, 6, 7, Calcite (3) and dedolomite (Figures 4.7, 4.8 and 4.9).

Geochemistry: Dolomite (2) is non-stoichiometric; its $CaCO_3$ values range from 53 to 58 mole %. They exhibit variable iron contents ranging from inner zones in places having no traceable iron to iron-rich, non-luminescent intermediate zones with values as high as 14000 to 19000 ppm. The range in other dull-luminescent zones is from 50 to 1000 ppm. Manganese contents are fairly consistent with average values around 300 ppm and rarely as high as 3000 ppm. The strontium content in this dolomite type is relatively high ranging from 0 to 777 ppm.

The oxygen-isotope values observed in Dolomite (2) are similar to those of Dolomite (1) and range from -5.2 to -6.85 $^{0}/_{00}$ for the Lower Ordovician rocks and from -5.88 to -5.97$^{0}/_{00}$ for the Upper Cambrian rocks. The $\delta\ ^{13}C$ values of Dolomite (2) range from +0.1$^{0}/_{00}$ to -2.2$^{0}/_{00}$.

Interpretation: The very fine-crystalline and unimodal texture of this dolomite type implies an early, syndepositional replacement origin similar to that of Dolomite (1). The main distinction between the two is that Dolomite (2) is slightly coarser

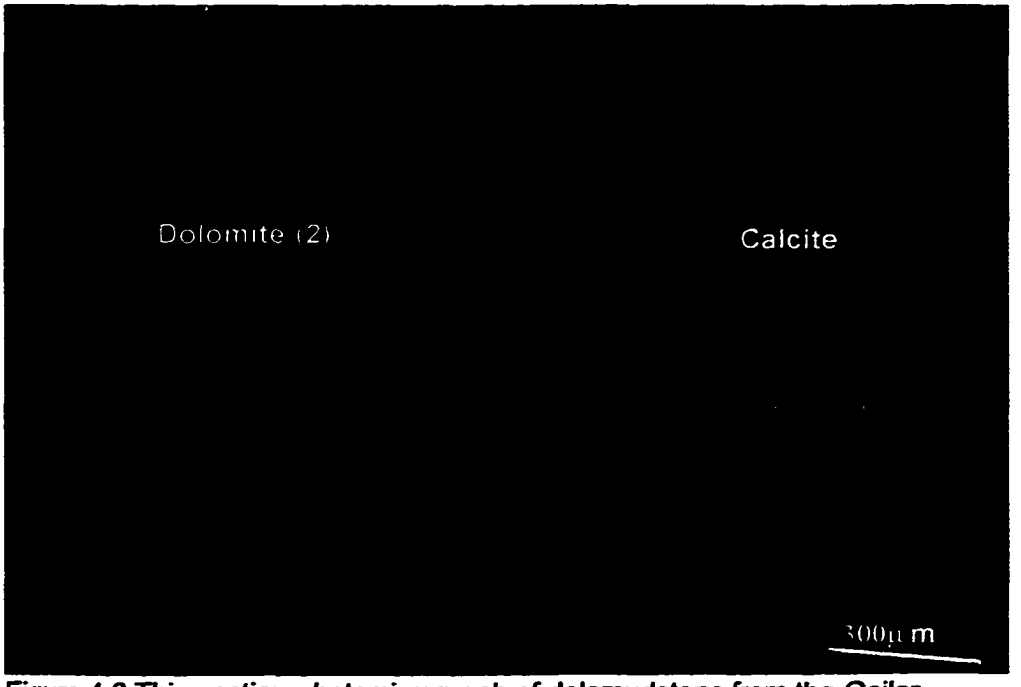

Figure 4.6:Thin-section photomicrograph of dolomudstone from the Gailor Formation (sample # BS-4, outcrop #9) is composed of nonluminescent Dolomite (2), associated with bright-luminescent calcite (yellow) in void. Thin section is viewed under cathodoluminescence.

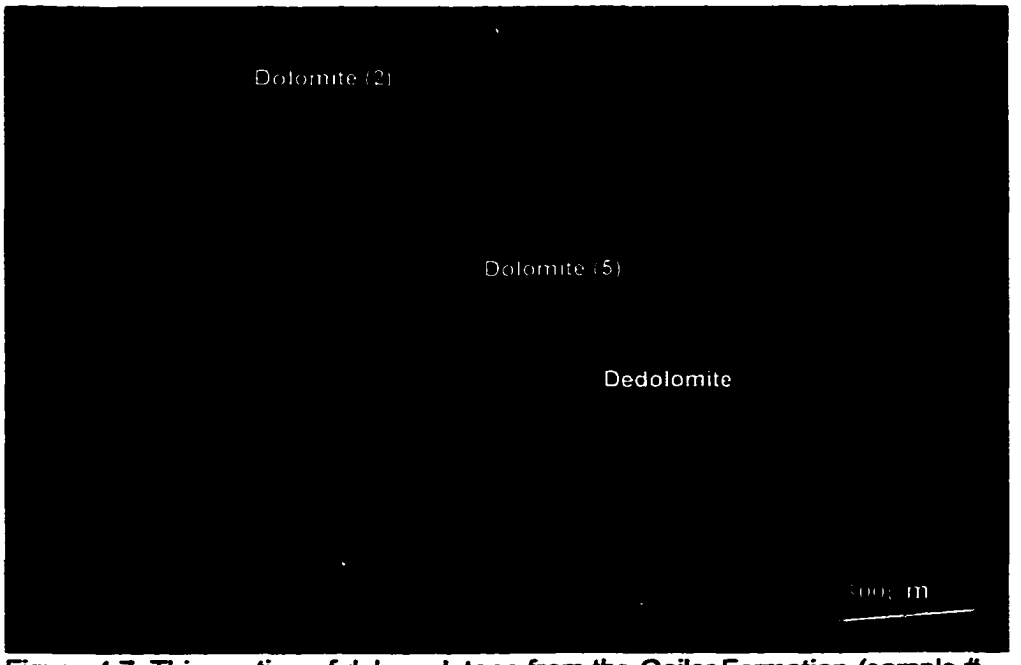

Figure 4.7: Thin section of dolomudstone from the Gailor Formation (sample # GL-9, outcrop #10), viewed under cathodoluminescence, shows hypidiotopic to idiotopic, replacement mosaic composed of Dolomite (2) cross-cut by two sets of fractures filled with Dolomite (5) and dedololmite respectively.

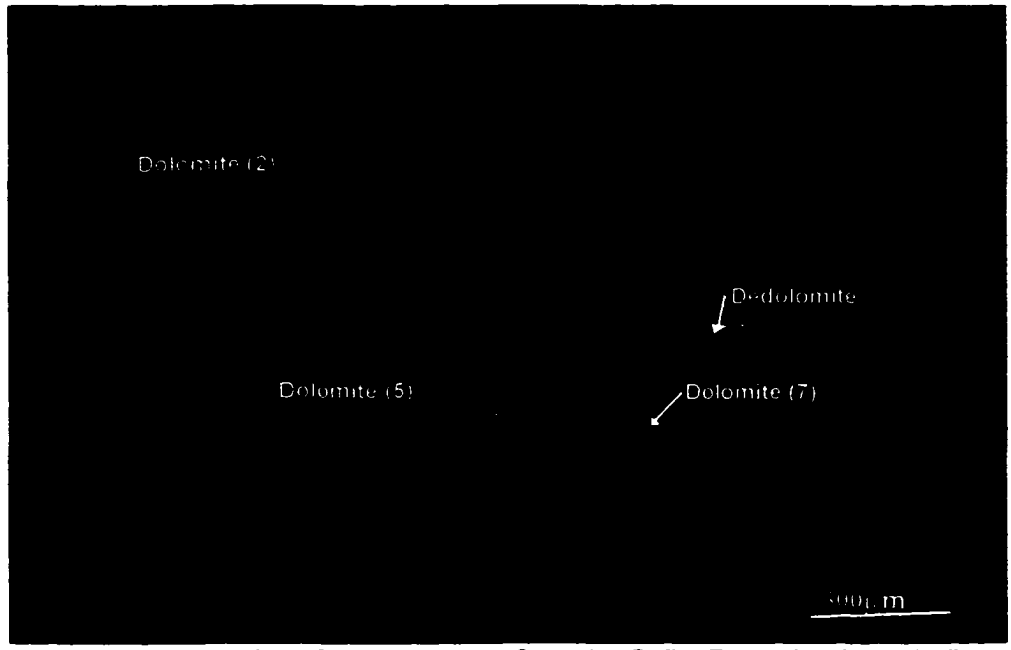

Figure 4.8:Thin section of dolomudstone from the Gailor Formation (sample # BS-6 outcrop #9), viewed under cathodoluminescence has zoned, dull-orange Dolomite (5) in fracture crosscutting Dolomite (2) mosaic. Dolomite (5) is postdated by non-luminescent Dolomite (7) cement, dull-luminescent ferroan calcite and bright luminescent dedolomite.

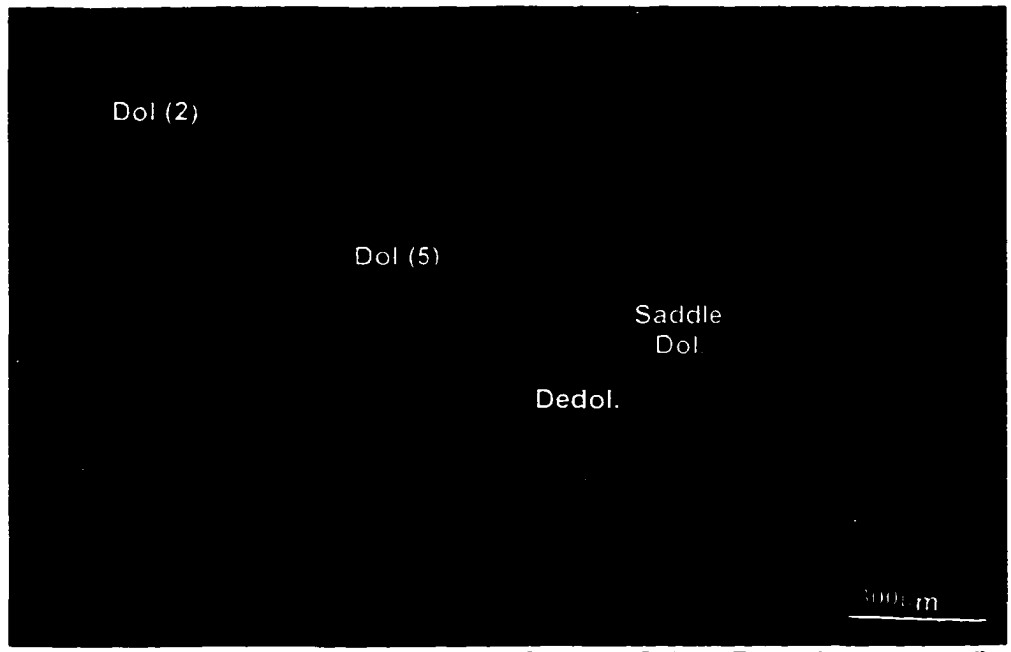

Figure: 4.9:Thin section of dolomudstone from the Galway Formation (sample # GB-8, outcrop #1), viewed under cathodoluminescence. Vug in Dolomite (2) mosaic is lined by Dolomite (5)(orange-red) , non-luminescent saddle dolomite (dark brown) and occluded by bright luminescent dedolomite (yellow).

than Dolomite (1), which may perhaps suggest that the slightly coarser precursor lime muds were intertidal or subtidal in origin compared to the microcrystalline supratidal muds. The unimodal texture suggests a single nucleation event with homogeneously distributed nucleation sites and uniform growth rates (Sibley, 1982; Sibley and Gregg, 1987). The high surface-area-to-volume ratio of fine-textured precursor lime muds provides numerous sites for nucleation of dolomite, assuming geochemical conditions were suitable for replacement to occur.

The high strontium value of Dolomite (2), which is consistently higher than 200 ppm and as high as 777 ppm, suggests that interstitial fluids responsible for dolomitization were evaporitic and may have been even hypersaline. A strontium content of around 550 ppm would suggest precipitation from marine water or a mixture containing >20% seawater (Tucker and Wright, 1992). Holocene 'protodolomites' from evaporitic and marine environments generally exhibit Sr values of about 550 to 700 ppm. If the strontium values are greater than 550 ppm it would mean that strong evaporation and gypsum precipitation have elevated the Sr/Ca ratio producing hypersaline fluids capable of dolomitization. According to Machel and Anderson (1989), ancient dolomites with more than 155 ppm Sr, probably originated in an evaporitic environment. Thus, the comparatively high Sr content of Dolomite (2) implies that the early diagenetic fluids were evaporitic.

The relatively homogeneous nature of the nonzoned, non-luminescent Dolomite (2) mosaics seen in figure 4.6, implies that there was no compositional variation in the dolomitizing fluids. The lack of luminescence in these

replacement mosaics also indicates that dolomitization was carried out in an oxidizing environment. The tight mosaics may also have helped to protect these dolomites from reacting with late-diagenetic fluids. Both Dolomite (1) and the nonzoned Dolomite (2) thus represent early formed dolomites that appear to have survived subsequent diagenesis.

The dull-red luminescent, zoned mosaics are inferred to represent the early diagenetic dolomite. The non-luminescent cores present in the zoned Dolomite (2) mosaics (Figure 4.4), indicate that early dolomite nucleation may have occurred in a near-surface, oxidizing environment, where Fe^{2+} and Mn^{2+} ions (that are responsible for luminescence) were not present in the dolomitizing fluids. The cores are perhaps remnants of the early diagenetic stage. In some examples, these cores appear blotchy due to incomplete replacement of soluble, early dolomite phases by younger, less soluble, more iron-rich dolomitizing fluids (Figures 4.7, 4.8 and 4.9). The blotchy cores are rimmed by distinct overgrowth zones that display a progression of duller and duller luminescence up to a non-luminescent zone and then finally a bright zone. This sequence of overgrowth zones represents the changing composition of dolomitizing fluids as the early formed dolomitic sediments were progressively buried towards more reducing environments. The high iron and manganese contents of the younger Dolomite (2) zones signify the subsidence or burial of the tidal sediments into the subsurface where reducing conditions prevailed. Compared to the nonzoned, non-luminescent Dolomite (2) mosaics, the zoned Dolomite (2) mosaics appear to have been subjected to more alteration.

In Figure 4.10, Dolomite (2) occurs as fine euhedral rhombs that form rims around allochems in an ooidal-peloidal, sandy grainstone (Lithofacies 1) from the Galway Formation. The dolomite appears to have selectively replaced early diagenetic micrite envelopes. The micrite envelopes may have formed around the particles by repeated algal borings followed by the filling of the borings with micrite (Friedman, 1964; Bathurst, 1994). The micritized areas of carbonate particles are more susceptible to dolomitization due to their greater microporosity and greater surface area. Selective dolomitization of the micrite envelopes may also imply that they were composed of high-magnesium calcite (Buchbinder and Friedman, 1980). The allochems in this case appear to have been dissolved subsequent to micritization. Some dolomite may have nucleated in the particle interiors which proceeded to grow into coarser, zoned crystals, after the nondolomitized precursor carbonate allochem had been dissolved. The dolomitization of the micrite envelopes may have been contemporaneous with dissolution of particle interiors (Kaldi and Gidman, 1982). The dolomitized micrite envelopes subsequently served as substrates for Dolomite cement (5) that grew into the interparticle voids.

In Figure 4.11 Dolomite (2) appears to have replaced ooids and unrecognizable skeletal particles in an oolitic-bioclastic grainstone that forms a lag deposit above a parasequence boundary in rocks of the Galway Formation (outcrop #4). Dolomite (2) here is interpreted to have nucleated in the matrix and the allochems simultaneously, but as the allochems are coarser than the matrix, the dolomite nucleii were farther apart and grew into slightly coarser crystals. The

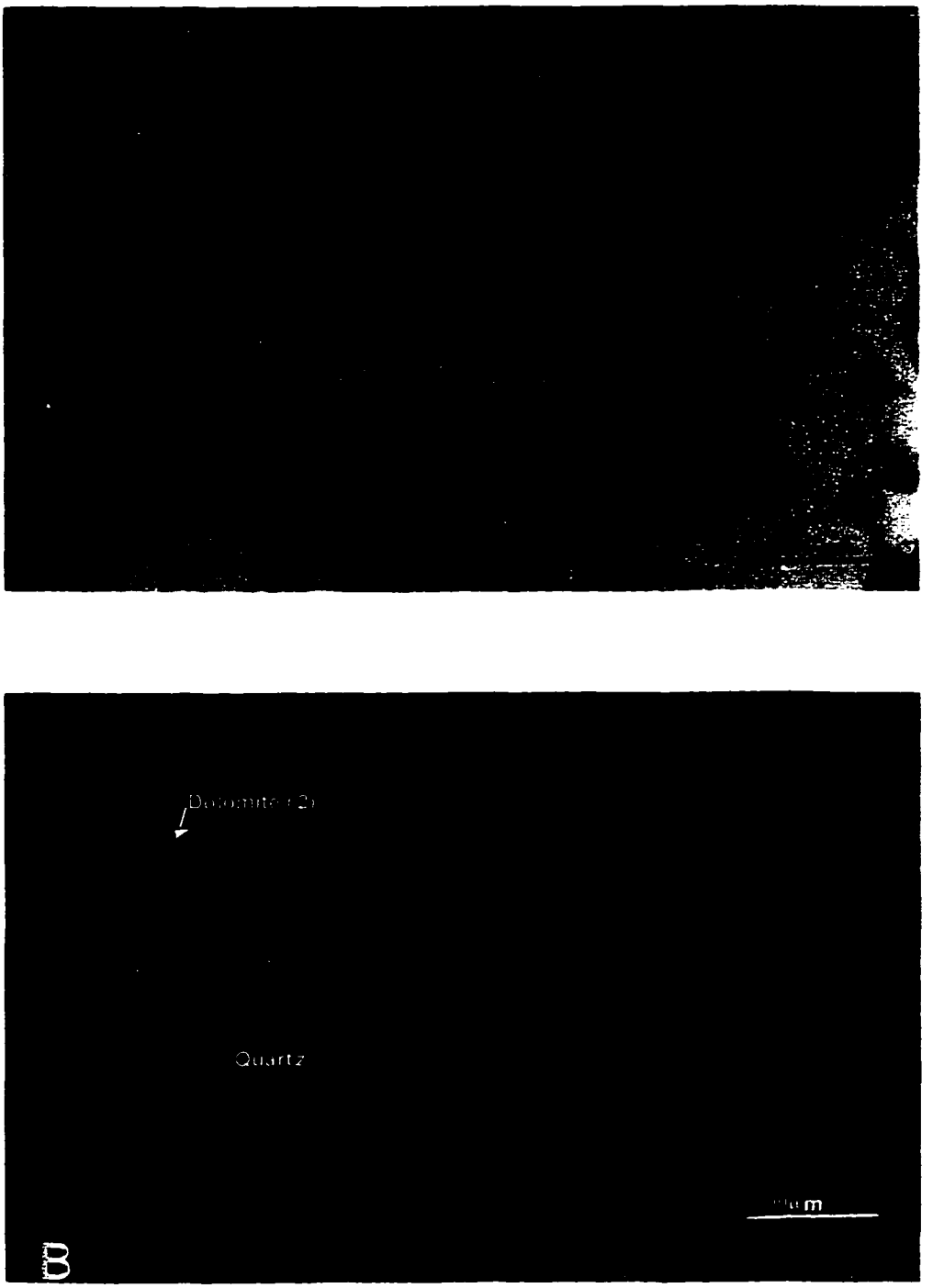

Figure 4.10:Thin-section photomicrograph of ooidal-peloidal, sandy grainstone (Lithofacies-1) from the Galway Formation (sample # GA-2, outcrop #4), where micrite envelopes around allochems, have been selectively replaced, by Dolomite (2). The particle interiors were only partially dolomitized before dissolution of undolomitized precursor carbonate took place. The moldic porosity that resulted allowed the dolomite rhombs to grow into coarser crystals and develop overgrowths of late stage, ferroan dolomite cements (stained blue with potassium ferricyanide in A and nonluminescent in B). (A) is viewed under plane-polarized light and (B) under cathodoluminescence.

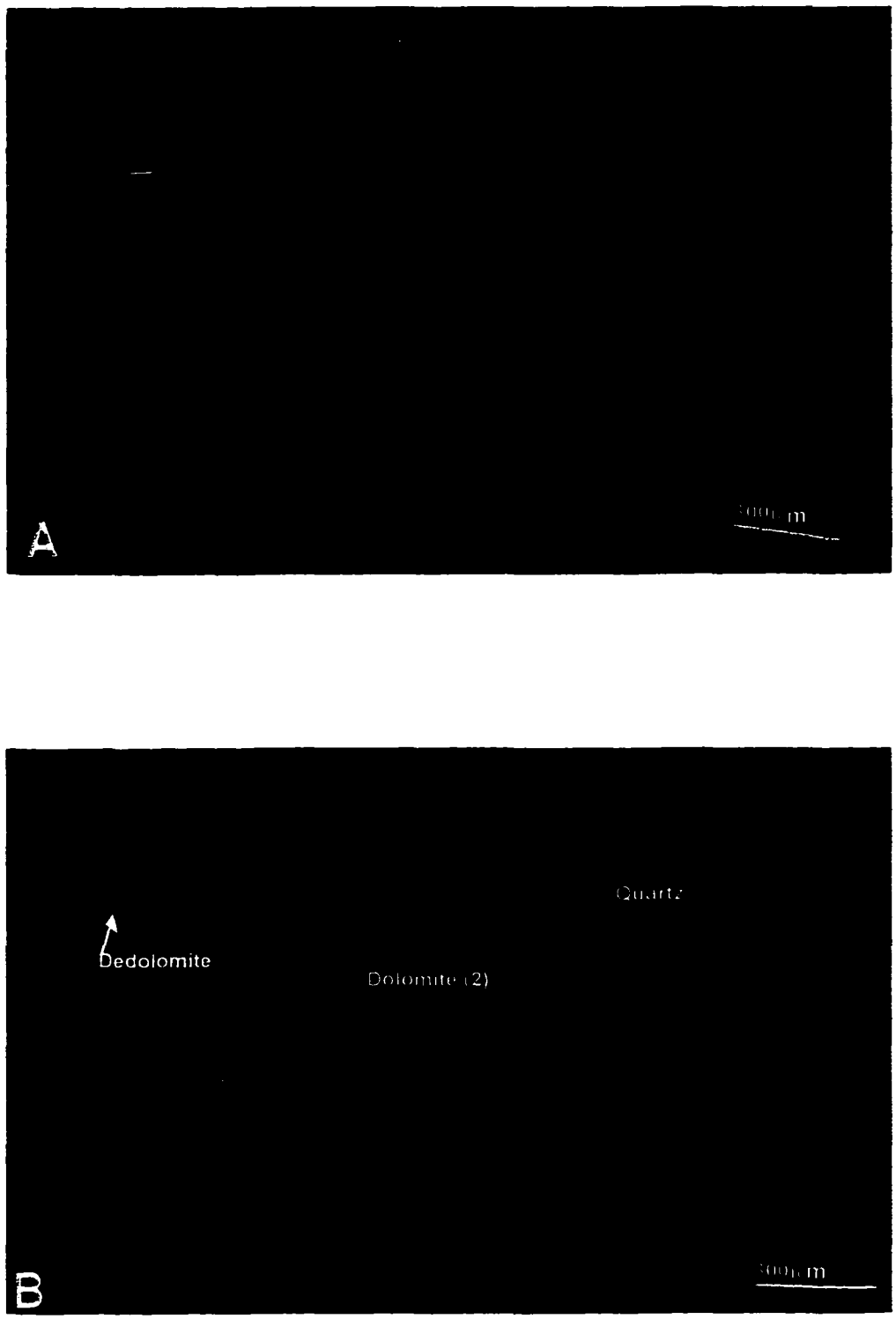

Figure 4.11: Thin-section of oolitic-bioclastic grainstone from the Galway Formation (outcrop # 4, sample # GA-3), that has been replaced by Dolomite (2). Dolomite (2) in the allochems appears to have been subjected to dedolomitization. Under cathodoluminescence , dedolomite appears bright yellow whereas dolomite appears red. (A) is viewed under plane-polarized light and (B) under cathodoluminescence.

matrix was completely dolomitized but the replacement of the allochems was incomplete. During meteoric diagenesis the nondolomitized carbonate in the allochems was dissolved. The Dolomite (2) within the allochems were subjected to dedolomitization at a later stage, perhaps during emergence related to formation of parasequences or uplift of the basin.

Compared with the $\delta^{13}C$ values of least-altered marine calcite cements of the Cambrian (0.7 $^{0}/_{00}$) and the Early Ordovician (-1.5 to -0.5 $^{0}/_{00}$) (data from Allan and Wiggins, 1993, Appendix II), the carbon-isotope values of Dolomite (2) are slightly depleted indicating incorporation of CO_3^{2-} partly from organic-matter diagenesis (Tucker and Wright, 1992). The range of $\delta^{18}O$ values for the least-altered marine invertebrates and marine cements is from -5.0 $^{0}/_{00}$ to -4.7 $^{0}/_{00}$ for the Cambrian and from -4 to -6.6 $^{0}/_{00}$ for the Ordovician (Alan and Wiggins, 1993). Compared to these ranges Dolomite (2) in the Upper Cambrian dolostones has slightly depleted values (Figure 4.3). However these values are heavier than those of the other late-diagenetic dolomites 3, 4, 5, 6, and 7, which indicates that the Cambrian Dolomite (2) mosaics are of a comparatively early diagenetic stage. In case of the Ordovician dolostones of the Gailor Formation, the Dolomite (2) values lie well within the range for least-altered marine invertebrates and cements, thus leaving no doubt as to their early diagenetic origin. Thus, from the above discussion it is clear that the lithofacies, textural, and geochemical characteristics of Dolomite (2) point to its early diagenetic origin in a peritidal, possibly hypersaline depositional environment.

4.2.3 Dolomite (3):

Description: Dolomite (3) occurs as sucrosic, planar-e to planar-s pervasive mosaics in all the formations under study. It also occurs as partial replacements in limestones of the Hoyt and Tribes Hill formations. The crystal size of Dolomite (3) is fine- to medium-crystalline, i.e ranging from 60 to 500 μm. Under cathodoluminescence, this dolomite type exhibits distinct zoning. Typically, the cores of Dolomite (3) are dull-red and /or mottled and rimmed by a series of distinct zones. The zoning varies slightly in the different formations.

Based on their differences in zonation and their distribution, Dolomite (3) may be subdivided into two types namely 3a and 3b. Of these types Dolomite (3a) is the most widespread type occurring as replacive mosaics in the Galway, Hoyt, Little Falls, and Gailor formations. Dolomite (3b) occurs associated with stylolites and is the common replacement type in the Tribes Hill Formation.

In the oolitic dolostones (Lithofacies 1) of the Galway strata (Figure 4.12) Dolomite (3a) has replaced ooids and composite particles that contain remnant micrite envelopes. The Dolomite (3a) rhombs display blotchy or irregularly luminescent thick cores, that are rimmed with overgrowth zones that are alternately dull red, and orange red. The paragenetic relationships here show that after formation of the Dolomite (3a), dissolution of nondolomitized carbonate material occurred followed later by filling of the resultant molds by non-luminescent Dolomite (7). In pervasively dolomitized rocks of the Galway, where the mosaic is composed of Dolomite (3a), the zoning pattern is similar to the

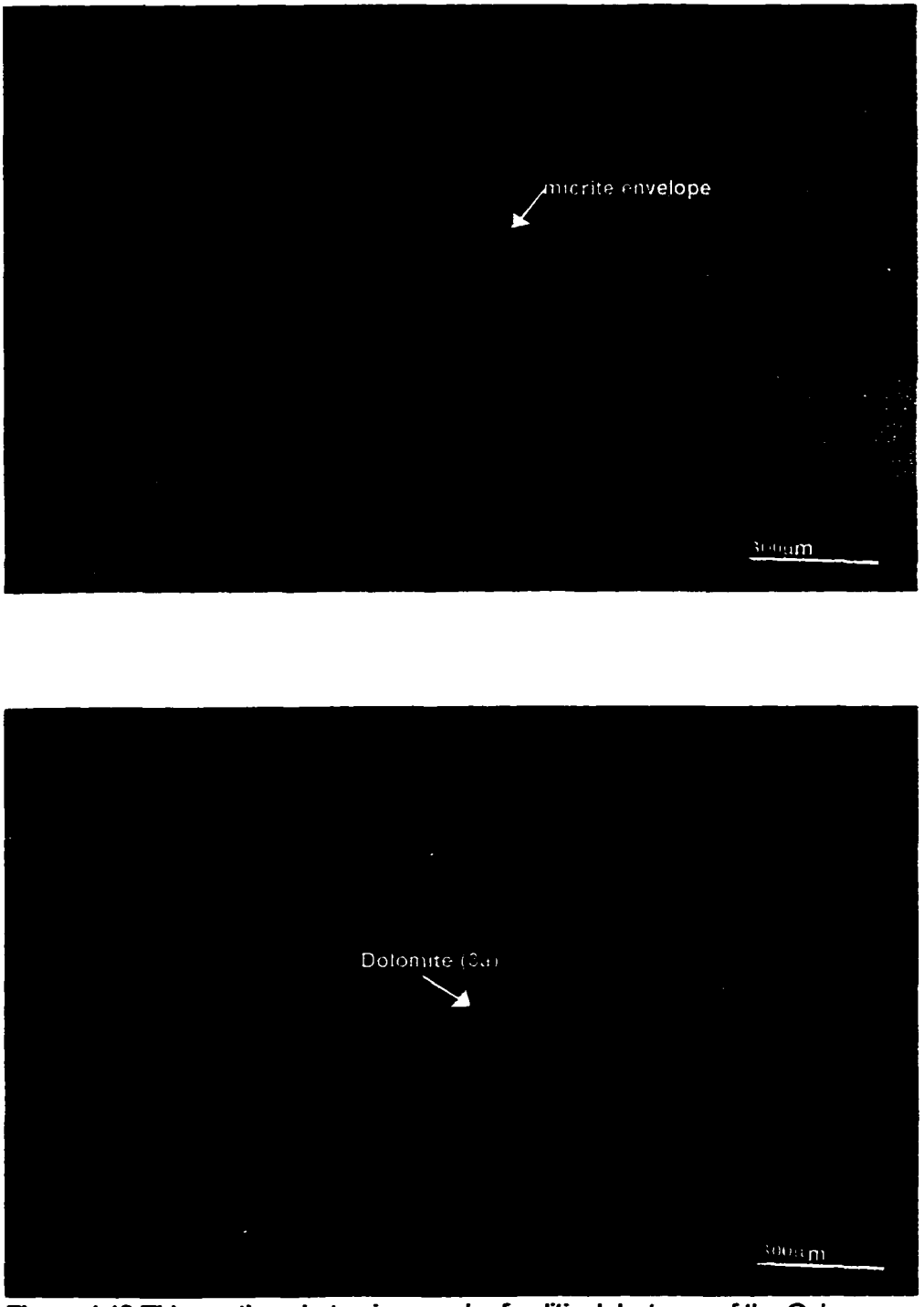

Figure 4.12:Thin-section photomicrograph of oolitic dolostones of the Galway Formation (sample # GA-2, outcrop # 4). Dolomite (3) has replaced ooids and peloids which have preserved their micrite envelopes. Dolomite (3a) rhombs have blotchy, irregularly luminescent, thick cores rimmed by overgrowth zones that are alternately dull red and orange red. Dark brown non-luminescent Dolomite (7) post-dates Dolomite (3) and occurs as void-filling cement. (A) is viewed in plane-polarized light and (B) under cathodoluminescence.

oolitic dolostones, except that the outermost zone is dull-luminescent burial calcite.

In the Hoyt (stromatolitic and oolitic) limestones (Lithofacies 4 & 1), Dolomite (3a) occurs as partial replacements. Alternating layers of Dolomite (3a) and micrite occur in the stromatolites (Figure 3.18). Here Dolomite (3a) displays red cores, that are rimmed by fine, dark red zones, orange zones and finally bright-yellow dedolomite that crosscuts some of the outer zones. Some of the cores have been corroded and replaced by non-luminescent dolomite. The stromatolitic laminae are marked by fine stylolitic horizons which seem to have truncated or even corroded the dolomite rhombs. In the oolitic limestones (Figure 3.13) also, the same pattern of zoning is observed. In the Little Falls, Dolomite (3a) mosaics are characterized by dull-red cores followed by alternating thick non-luminescent zones and thin dull-red zones, followed by a thick outer rim of blotchy dull orange-yellow zone (Figure 4.13). Some cores have been corroded and replaced by bright orange Mn-rich, Fe-poor dolomite. Here, the inner parts are euhedral but the irregular outer part of the Dolomite (3a) crystals create an anhedral mosaic.

In cryptmicrobial laminated dolostones (Lithgofacies 8) of the Gailor Formation, Dolomite (3a) occurs as coarse mosaics that display red-luminescent cores and progressively darker luminescent rims under cathodoluminescence. Laminae of clear, more porous mosaics of Dolomite(3a) alternate with cloudy, fine-textured mosaics of Dolomite (2) (Figure 4.5).

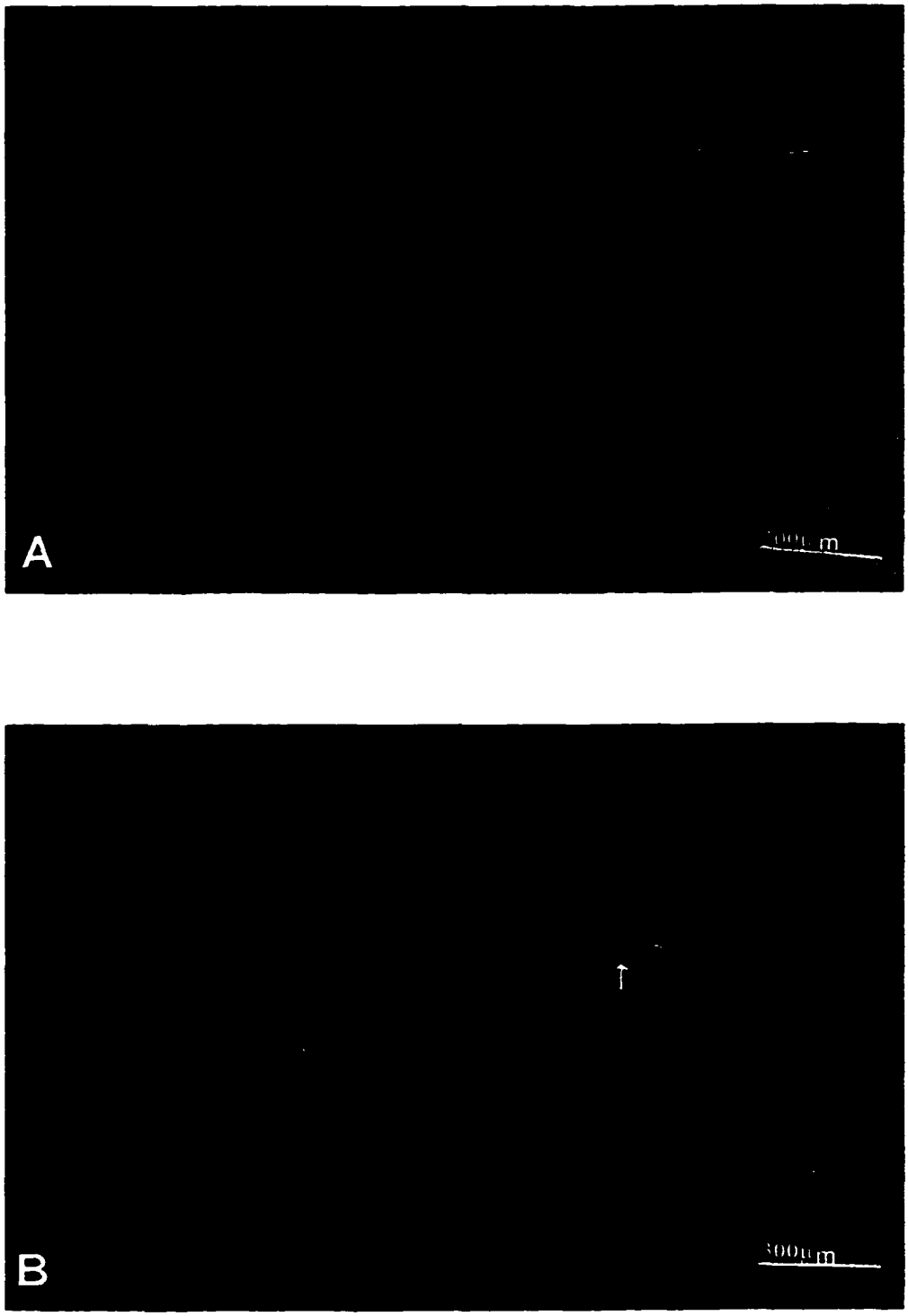

Figure 4.13: Dolomite (3a) forms a pervasive mosaic, in a burrow-mottled dolostone of the Little Falls Formation (sample # H/8, outcrop # 14). In places, cores of Dolomite (3a) are more euhedral than the rims. The euhedral cores are composed of distinct zones of non-luminescent and dull-luminescent dolomite. Some of the cores of Dolomite(3a) have suffered dissolution and appear irregularly luminescent (arrow). (A) is viewed in plane-polarized light and (B) under cathodoluminescence

Bright, orange-luminescent Dolomite (5) occurs as an outer cement zone of Dolomite (3a) in some Gailor dolostones (Lithofacies 7), where the crystalline mosaic is porous, facilitating the passage of Fe-poor, Mn-rich dolomitizing fluids (Figure 4.14).

Dolomite (3a) appears to predate stylolitization in Figure 4.15, where corroded and fragmented dolomite crystals are seen along the wispy stylolites that are confined to fine silty zones in the dolomite mosaic. In this example, Dolomite (3a) occurs within a matrix composed of microcrystalline chert. Dolomitization is interpreted to have been postdated by silicification followed by stylolitization.

In the rocks of the Tribes Hill formation, Dolomite (3a) occurs as medium-crystalline mosaics (Figure 4.16), replacing precursor micrite. In contrast, Dolomite (3b) forms scattered clusters of planar-p, porphyrotopic crystals, associated with stylolites that traverse the skeletal wackestones (Lithofacies 1). The Dolomite (3b) crystals contain red-luminescent cores followed by fairly thick non-luminescent zones and are rimmed by thinner orange-red outer zones (Figure 4.17). Dolomite (3b) is very fine-crystalline ranging in size from 10 to 150 μm. This type appears to selectively replace the micrite matrix and seldom are the skeletal particles replaced (Figure 4.18). At the top of the Fonda member of the Tribes Hill formation where the post-Sauk, pre-Tippecanoe surface of unconformity is observed, the dolostone units (Figure 4.19) are composed of Dolomite (3a) replacive mosaics with parts of the mosaic replaced by Mn-rich Dolomite (5), and in places followed by dedolomite.

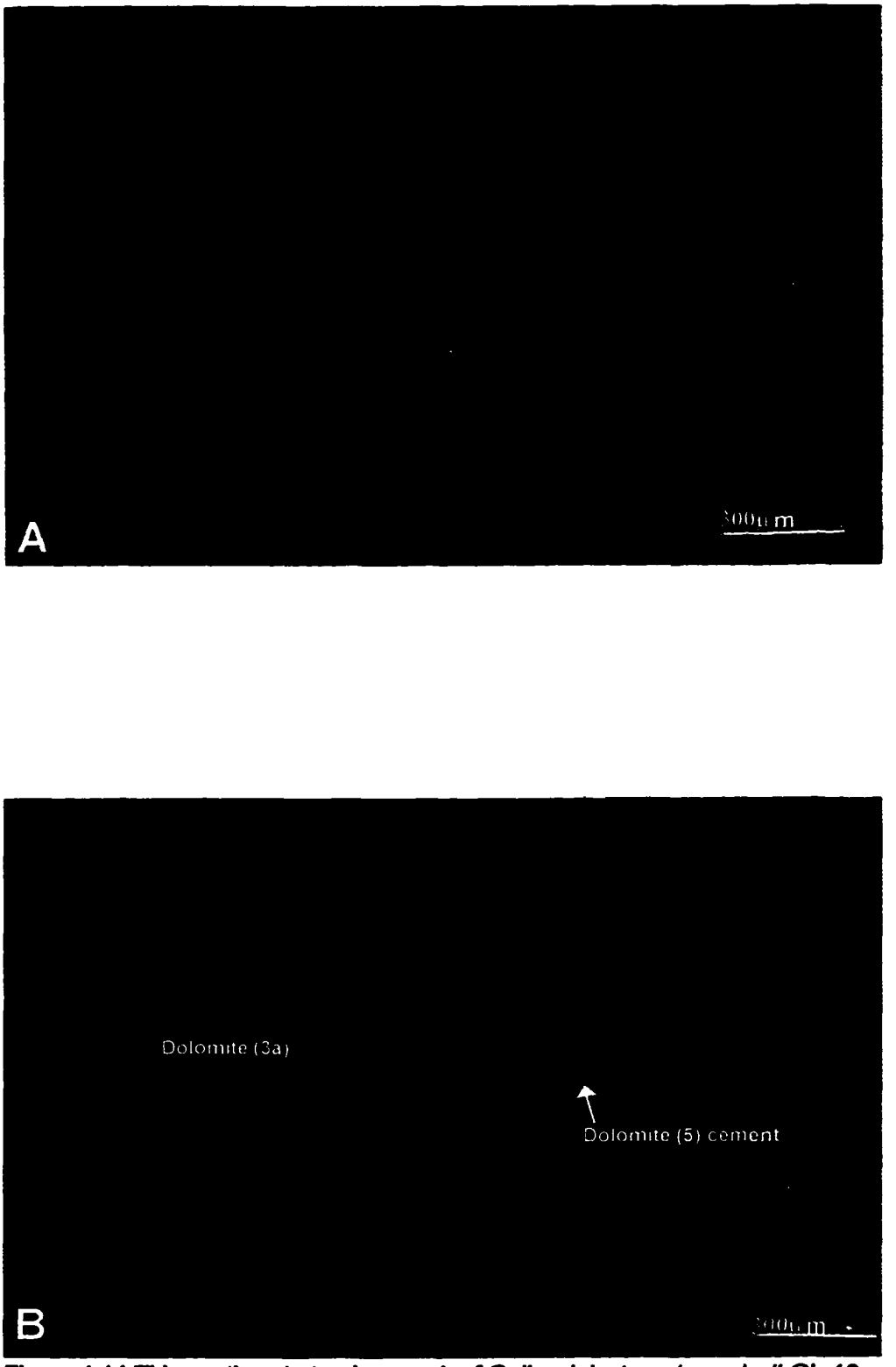

Figure 4.14:Thin-section photomicrograph of Gailor dolostone (sample # GL-16, outcrop # 12) composed of irregularly zoned Dolomite (3a) mosaics. Dolomite (5) forms outer bright, orange-luminescent zone in porous parts of the mosaic. (A) is viewed in plane-polarized light and (B) under cathodoluminescence.

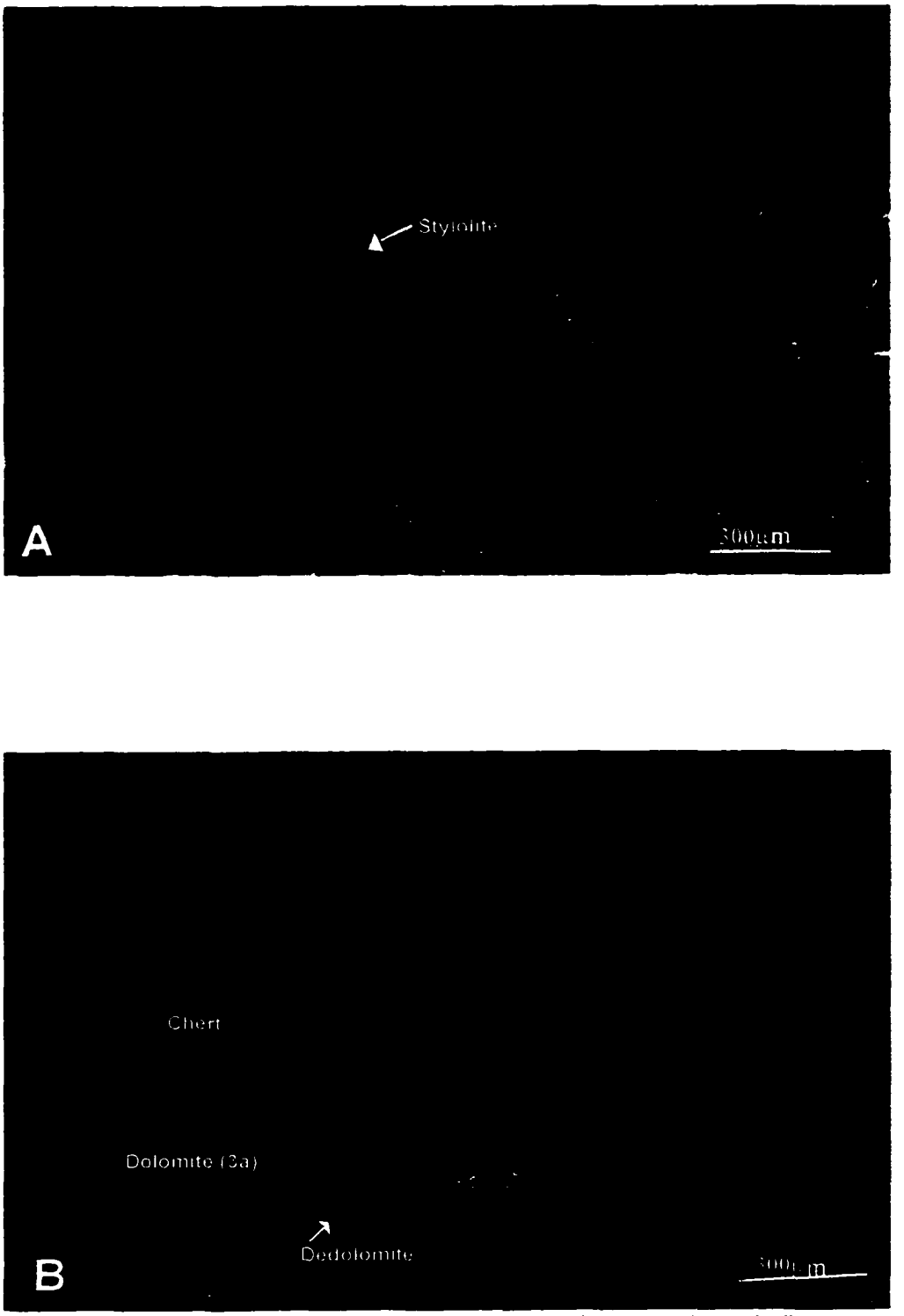

Figure 4.15:Thin-section photomicrograph of Gailor dolostone (sample # GL-18, outcrop # 12), where Dolomite 3a predates chertification and stylolitization. Wispy anastomosing stylolites indicate chemical compaction following dolomitization and chertification. The etched outlines of the dolomites indicate chertification and stylolitization occurred later.(A) is viewed in plane-polarized light and (B) under cathodoluminescence.

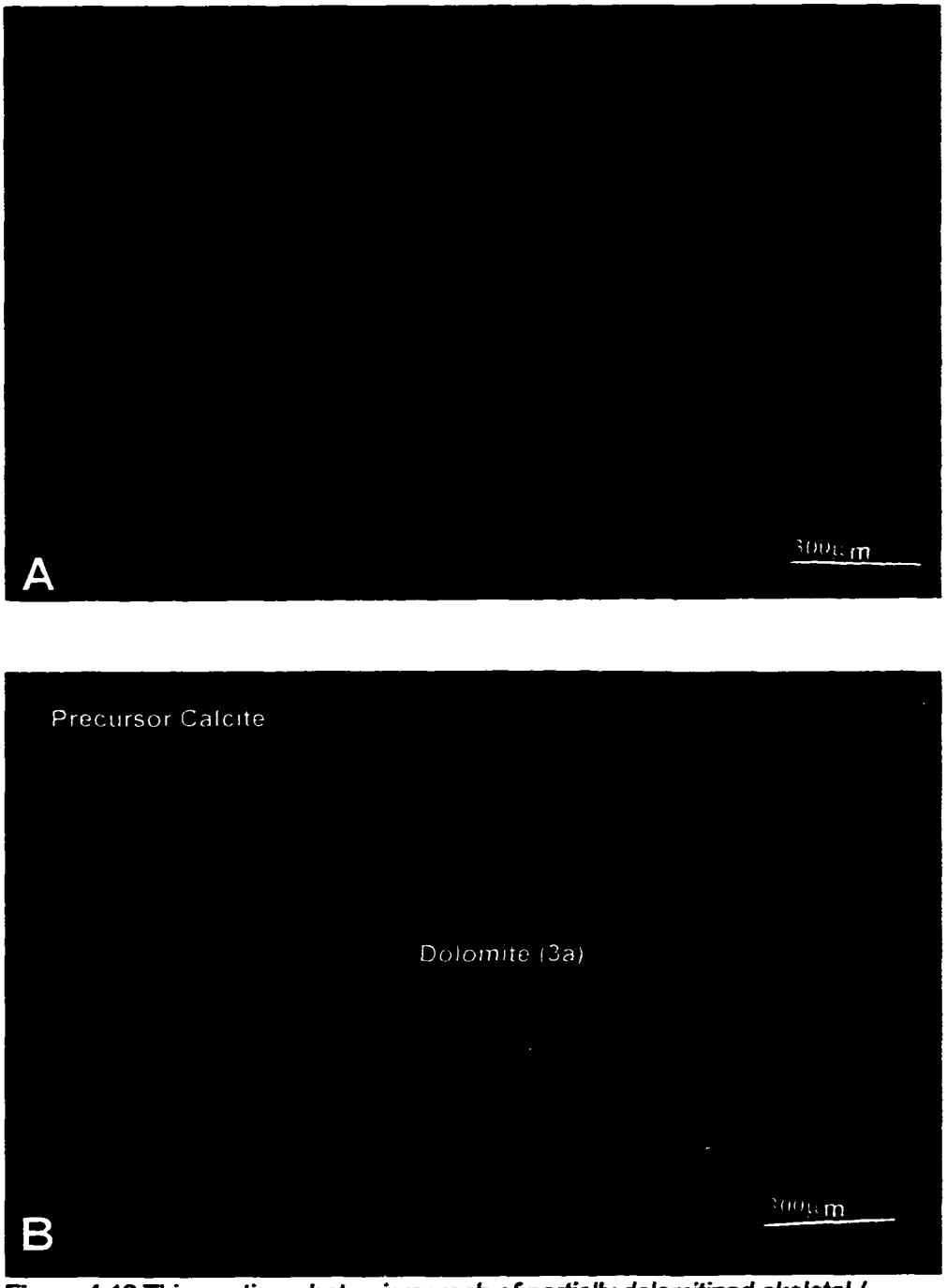

Figure 4.16:Thin-section photomicrograph of partially dolomitized skeletal / intraclastic grainstone (sample # V-9, outcrop # 16) from the Fonda member of the Tribes Hill Formation. Medium-crystalline Dolomite (3a) has replaced precursor calcite. Precursor calcite displays dull yellow luminescence. Dolomite (3a) is distinctly zoned , with red-luminescent cores followed by a thick dark-luminescent zone followed by bright, orange-luminescent rims. (A) is viewed in plane-polarized light and (B) under cathodoluminescence

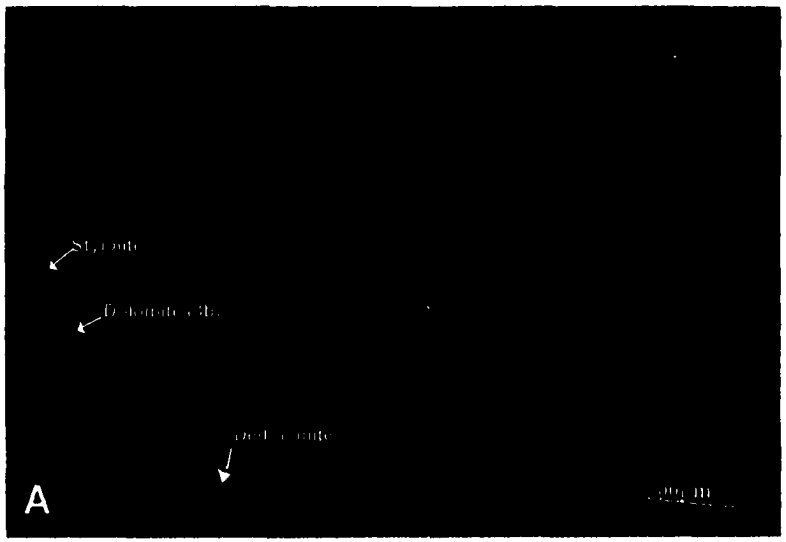

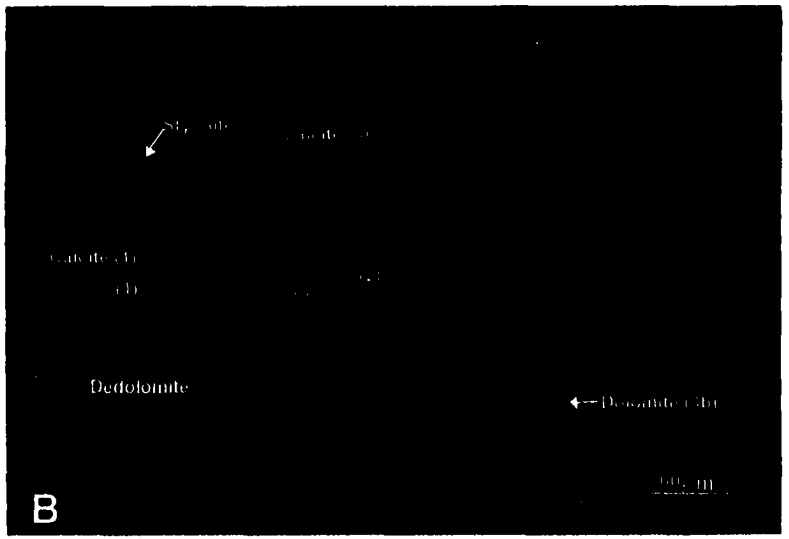

Figure 4.17: Thin-section photomicrographs show stylolite-controlled dolomitization in skeletal limestones of the Fonda member (sample #V-11(A)) and the Wolf Hollow member (sample #V-6(B)) of the Tribes Hill Formation from outcrop #16. Dolomite (3b) appears distinctly zoned with red-luminescent zones. The micritic matrix is composed of precursor calcite (Calcite (1)) that appears dull yellow under cathode light. Non-luminescent burial Calcite (3) occurs in scattered patches. Bright yellow luminescent dedolomite occurs in veins and porosity. (A) and (B) are viewed under cathodoluminescence. The results of microprobe spot analysis of points numbered (1) through (3) in Figure 4.17B are shown in the histogram. Point (1) is in Calcite (1); point (2) is in Calcite (3) and point (3) is in Dolomite (3b).

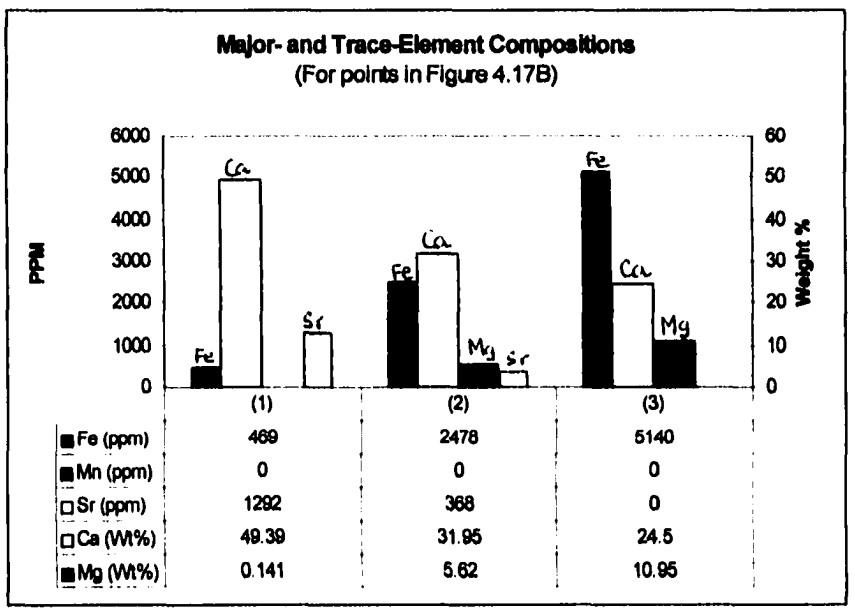

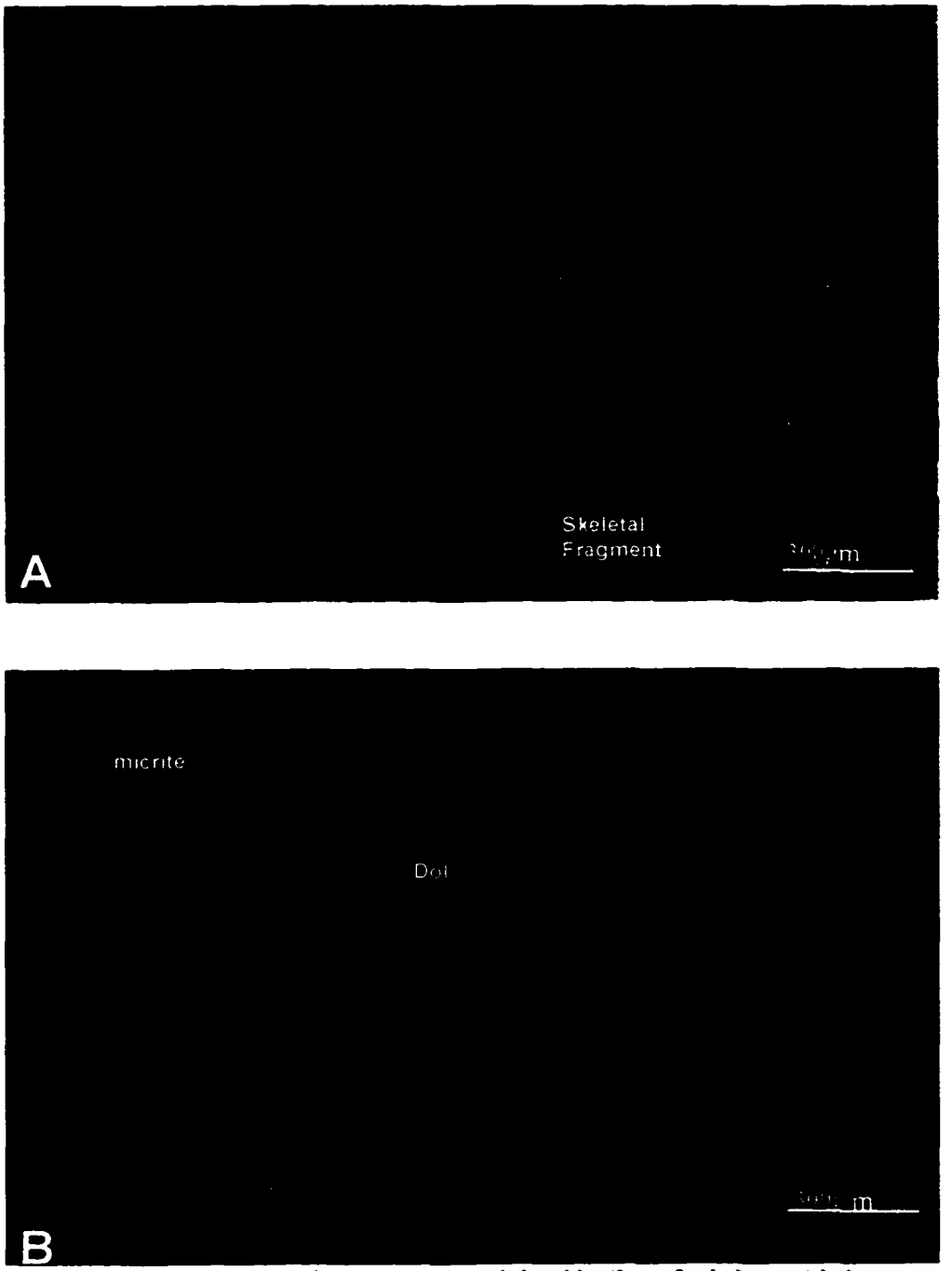

Figure 4.18: Thin section shows selective dolomitization of micrite matrix in a skeletal packstone from the Palatine Bridge member of the Tribes Hill Formation (sample # 16/2, outcrop # 15). (A) is viewed in plane-polarized light and (B) under cathodoluminescence

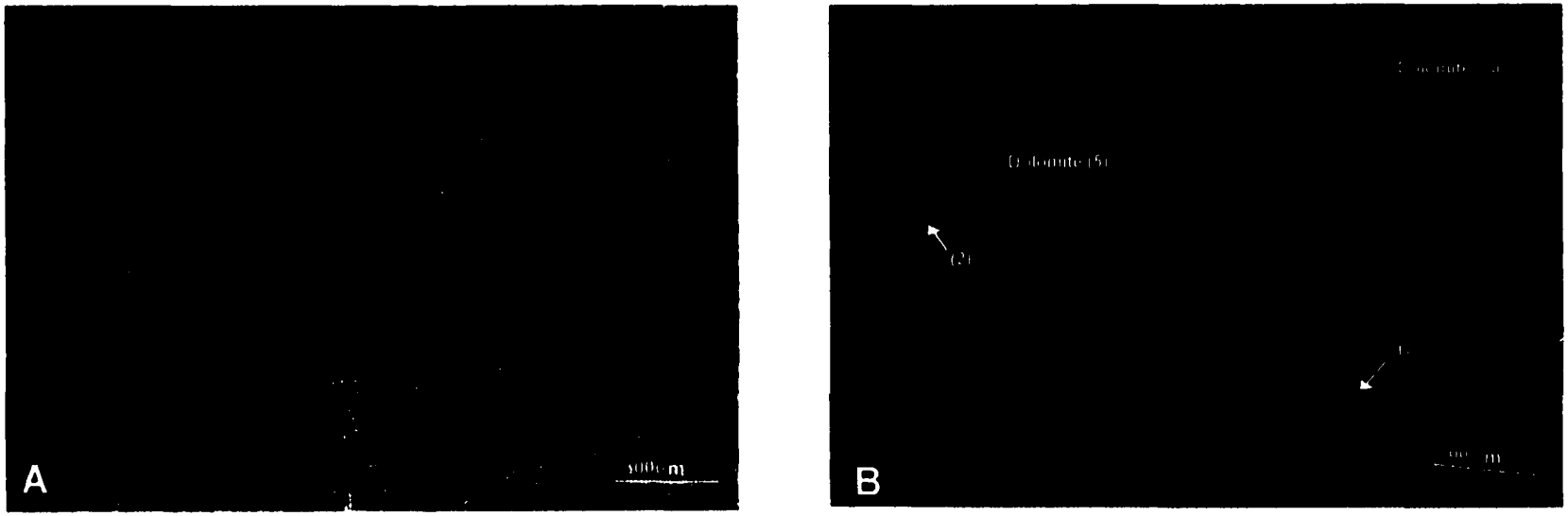

Figure 4.19: Thin-section photomicrograph of dolostone from the Fonda member of the Tribes Hill Formation (sample #TB-1, outcrop #17) shows bright, orange-luminescent, zoned Dolomite(5) that occurs along with dark-luminescent, zoned Dolomite(3a). (A) is viewed in plane-polarized light and (B) under cathodoluminescence.

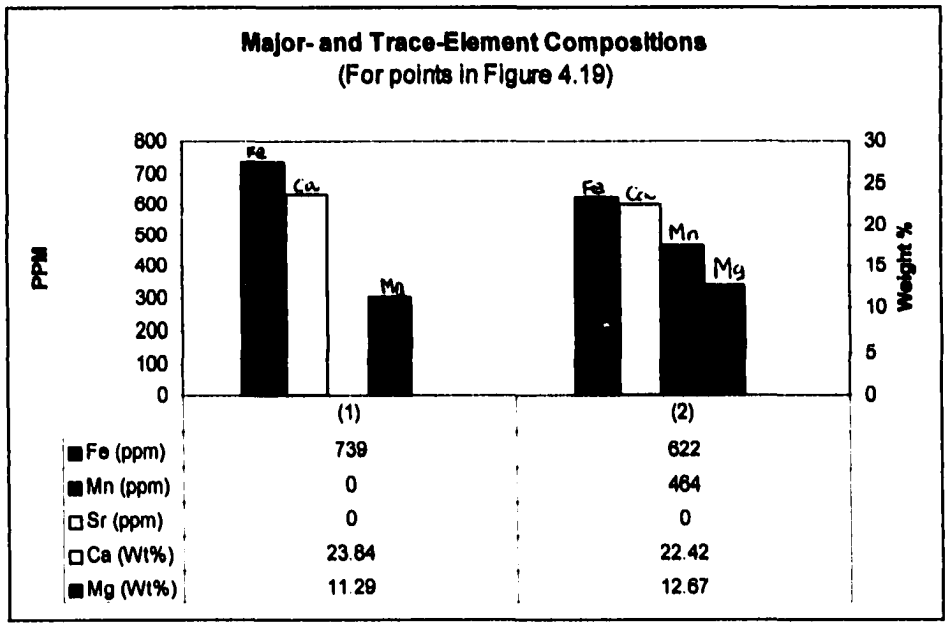

Geochemistry: Dolomite (3) exhibits a range of compositions from 51 to 57 mole % $CaCO_3$, which is due to the compositional zoning present in this dolomite type. The iron-rich zones are dark to non-luminescent and contain around 4000 to 6000 ppm Fe. The Mn content ranges from 300 to 900 ppm. Sr is usually absent but rarely values between 100 and 500 ppm and even as high as 1434 ppm occur.

The $\delta^{18}O$ values of Dolomite (3) in the Cambrian rocks range from -5.1 to -10.73 $^0/_{00}$ and in the Ordovician rocks lie between -5.68 and -8.88$^0/_{00}$. Compared with the $\delta^{18}O$ values of least-altered marine calcite cements of the Cambrian, which is -5.0 $^0/_{00}$ and of the Ordovician, which is between -5.5 and -6.5 $^0/_{00}$, these values are slightly depleted. The $\delta^{13}C$ values in this dolomite type range from -0.4 to -3.2 $^0/_{00}$, the $\delta^{13}C$ values of least-altered marine calcite cements of the Cambrian being -0.7 $^0/_{00}$ and of the Early Ordovician being -1.5 to -0.5 $^0/_{00}$ (data from Allan and Wiggins, 1993, Appendix II).

Interpretation: The coarser texture of Dolomite (3) compared to the very fine texture of the early diagenetic dolomites 1 and 2 suggest that this type resulted from a prolonged period of multiple dolomitizing events. The compositional zoning pattern in this dolomite type indicates the changing composition of the dolomitizing fluids with time and burial. The cores of Dolomite (3a) are usually dull red and may mean that the cores represent the remnants of the earlier formed, near-surface dolomite. The sequence of zones from red to non-luminescent to orange indicate progressive burial. The non-luminescent zone is

perhaps a product of dolomitization by deep-burial brines rich in Fe. The final zones are usually burial calcite followed by dolomite cements 6 and 7 which mark late deep burial.

In the stromatolites of the Hoyt, the preferential occurrence of Dolomite (3a) in certain laminae may indicate their association with organic-rich laminae, which were perhaps high-Mg calcite prior to dolomitization (Friedman et. al, 1973). In the stromatolitic and cryptmicrobial laminated units dolomitization may have resulted from the decomposition of the microbial mats, linked with microbial sulfate reduction (Curtis and Coleman, 1986; Wright, 1997). The resulting removal of sulfate (Baker and Kastner, 1981), increase in alkalinity due to production of HCO_3^- and CO_3^{2-} from the organic matter, and increase in pH probably favored dolomitization. In this case the Mg needed for dolomitization may have been obtained from the organic-rich laminae. Dolomite (3a) in this case, is thus interpreted to have originated in the organic-rich laminae. The zoning observed is, however, an artifact of subsequent diagenesis that occurred with burial. The corrosion of the dolomite rhombs, where adjacent to stylolites, indicates that the formation of Dolomite (3a) predated stylolitization.

The occurrence of Dolomite (3b) replacement clusters along stylolites in the matrix-supported skeletal limestones of the Tribes Hill Formation, suggests that the dolomitization occurred late in the diagenetic history, and was either synchronous with pressure dissolution or was a post-compaction event. If the dolomitiization post-dated stylolitization, it is quite probable that the stylolites served as conduits for the dolomitizing solutions. These dolomites also exhibit

unusually depleted $\delta^{18}O$ values ranging from -6.85 to -8.88 $^{0}/_{00}$ PDB (Figure 4.3). Their thick nonluminescent, Fe-rich zones (Figure 4.17) and depleted $\delta^{18}O$ values suggest a greater burial depth than Dolomite (3a).

The depleted oxygen-isotope values suggest burial dolomitization at elevated temperatures. The span of carbon-isotope values, being slightly depleted or overlapping with the range of least-altered marine calcite cements, suggests that the carbonate was derived partly from precursor carbonate and partly from organic matter diagenesis. This is consistent with the fact that these strata contain abundant stromatolites, cryptmicrobial laminites and skeletal material.

The low strontium content of Dolomite (3) indicates depletion due to recrystallization or dolomitization of stabilized calcite, in any case suggesting that Dolomite (3) is a late-diagenetic phase. Some unusually high Sr values observed are interpreted to represent dolomitization by highly saline basinal brines.

In conclusion, the Dolomite (3) texture, which is distinctly zoned, records progressive dolomitization and recrystallization from early near-surface dolomitization to late shallow burial dolomitization followed by uplift and then subsequent deep burial.

4.2.4 Dolomite (4):

Description: Dolomite (4) occurs as planar-s to nonplanar, tight, mosaics of fine- to medium-crystalline (60 to 500μm) dolomite creating a hypidiotopic to predominantly xenotopic replacive mosaic. Under the luminoscope, these dolomites are nonzoned and luminesce red-orange (Figure 4.20). In places, they partially replace allochems, which may be skeletal fragments (Figures 4.21). In the oolitic dolostones (Lithofacies 1) of the Galway and Hoyt formations, this type of dolomite is seen to have either partially (Figure 4.22) or completely (Figure 4.23) replaced the ooids composed of precursor calcite. In general, Dolomite (4) is fabric-destructive and pervasive, but when original depositional fabric is preserved, replacement is nonmimic. In transmitted light, Dolomite (4) mosaics appear cloudy with dark crystal boundaries. Under cathodoluminescence, the crystal boundaries are not usually recognizable. The crystals appear homogeneous or mottled, with a blotchy luminescence pattern in shades of red. This dolomite type occurs in mottled dolostones (Lithofacies 2), intraclastic dolostones (Lithofacies 3) and skeletal/ peloidal/ oolitic packstones (Lithofacies 1). Where associated with vugs, Dolomite (4) is euhedral and coarser than in the matrix, with a thin, orange-luminescent or dull luminescent rimming zone lining the void space (Figure 4.24). This is the most common replacement type in the Galway Formation. Dolomite (4) is also observed in the Hoyt, Gailor and less commonly in the Tribes Hill Formation.

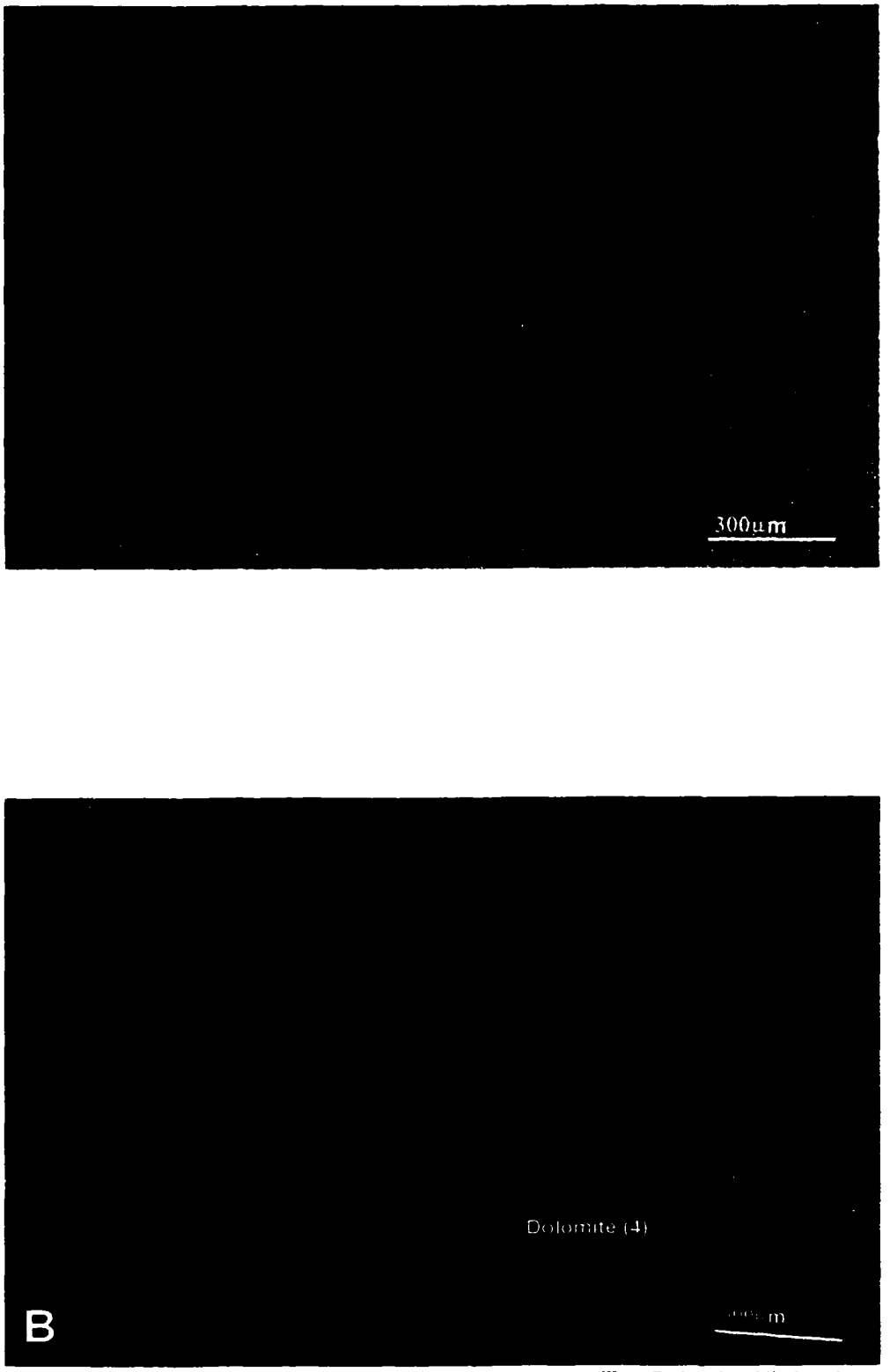

Figure 4.20: Unzoned, red-luminescent, medium-crystalline Dolomite (4) that has formed a fabric-destructive, replacement mosaic in a dolostone from the Galway Formation (sample # GC-2, outcrop #3). (A) is viewed in plane-polarized light and (B) under cathodoluminescence.

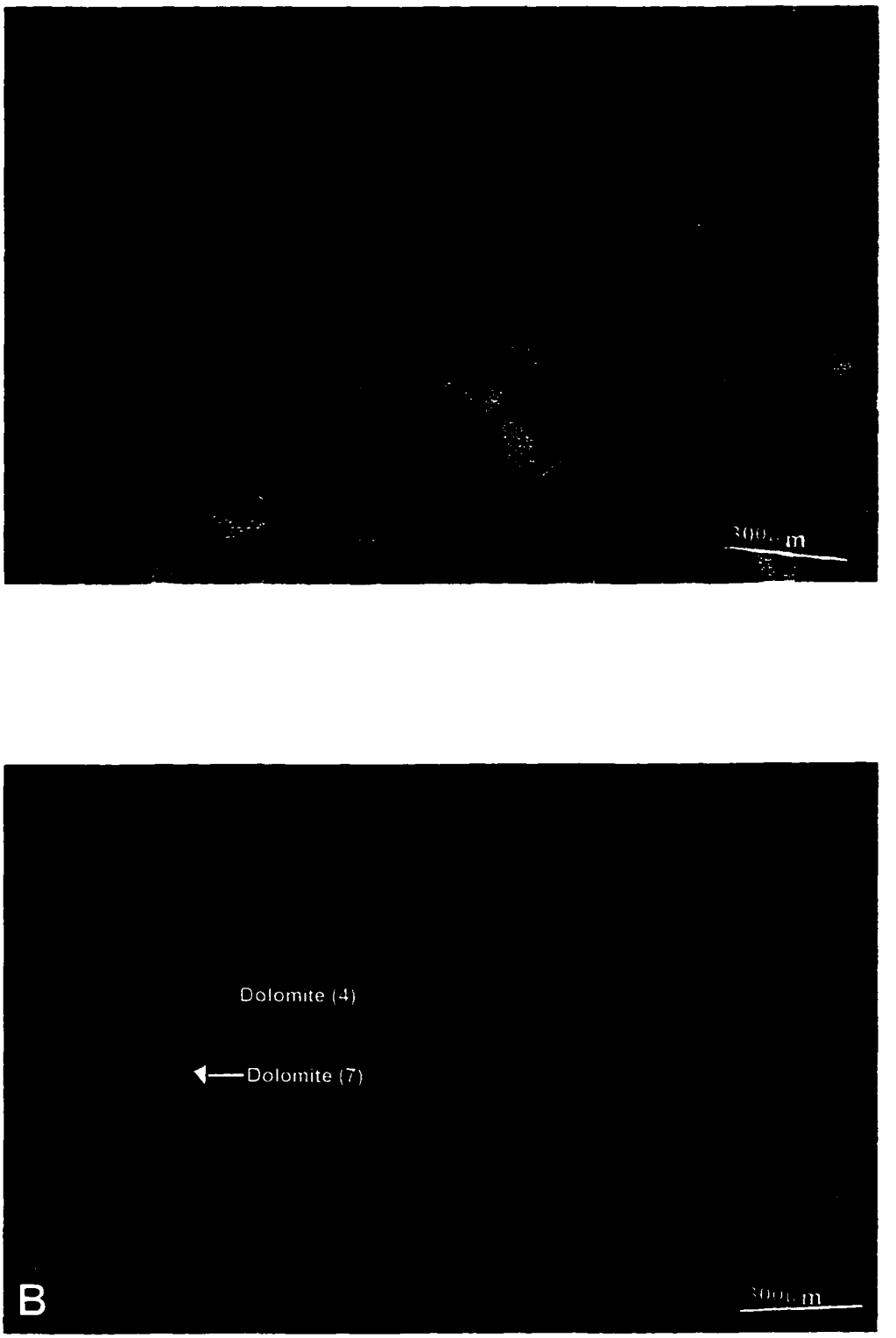

Figure: 4.21: Thin-section photomicrograph shows that unzoned Dolomite (4) has replaced skeletal particles and ooids in a skeletal dolostone from the Galway Formation (sample #R-5, outcrop #5). Dissolution of unreplaced carbonate was followed by non-luminescent Dolomite (7) cement. (A) is viewed in plane-polarized light and (B) under cathodoluminescence.

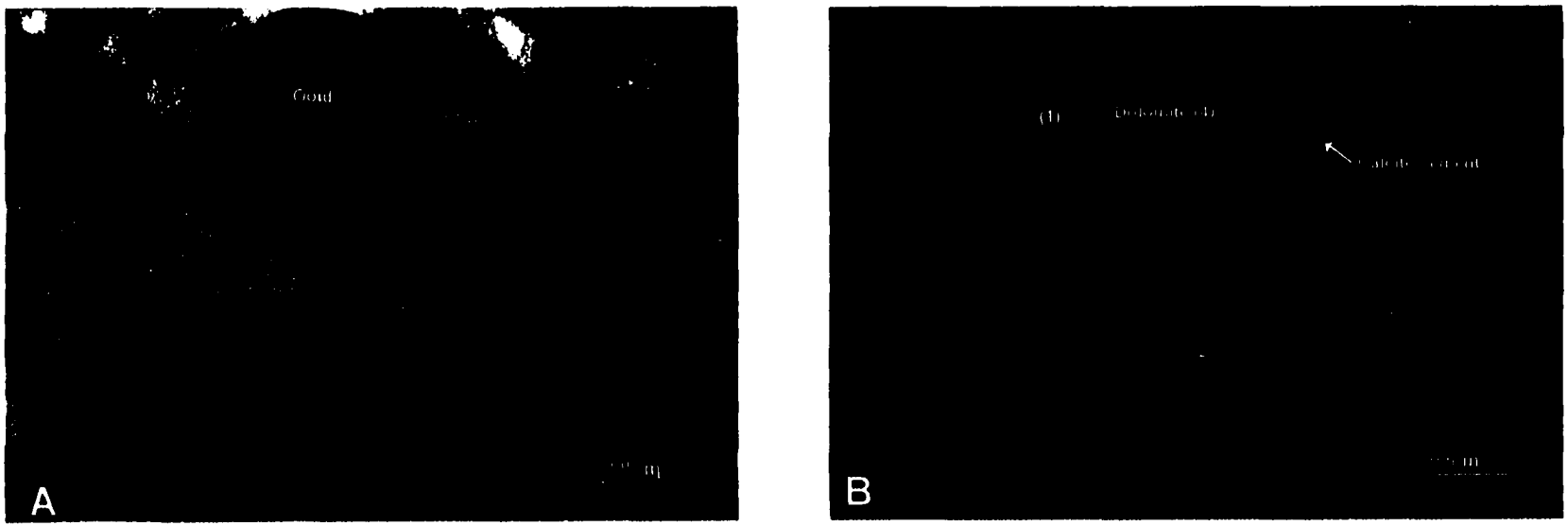

Figure 4.22: Thin-section photomicrograph of oolitic dolostones of the Hoyt Formation (sample #LP-1, outcrop # 7) where Dolomite (4) partially replaced ooids composed of precursor calcite. The interparticle acicular marine calcite cements have not been replaced . The precursor calcite appears dull yellow and replacement dolomite is red luminescent. (A) is viewed in plane-polarized light and (B) under cathodoluminescence. The results of microprobe spot analysis of points numbered (1) through (3) in Figure 4.22B are shown in the histogram below. Point (1) is in precursor Calcite; points (2) and (3) are in Dolomite (4) within the ooids.

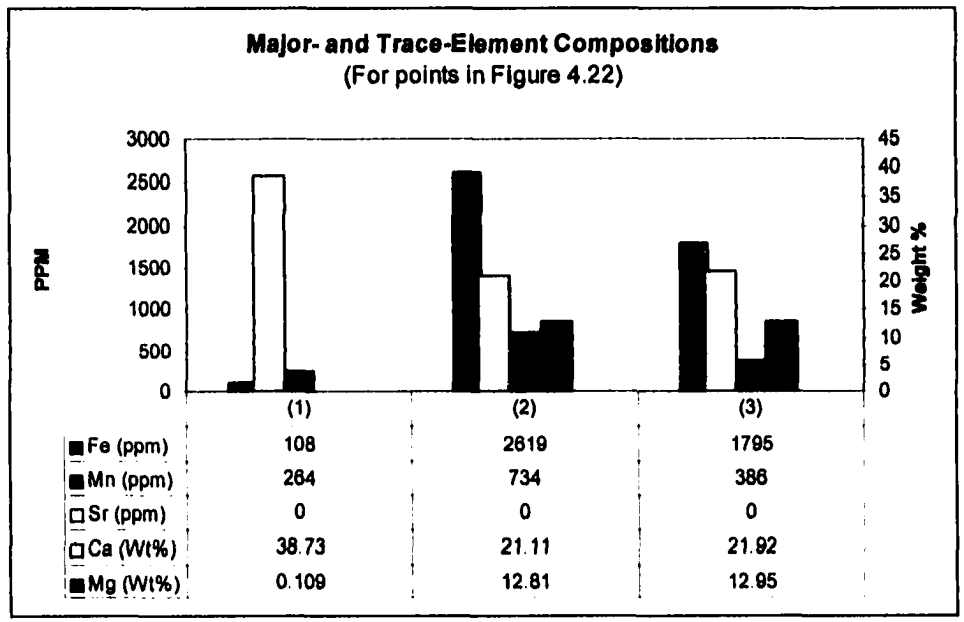

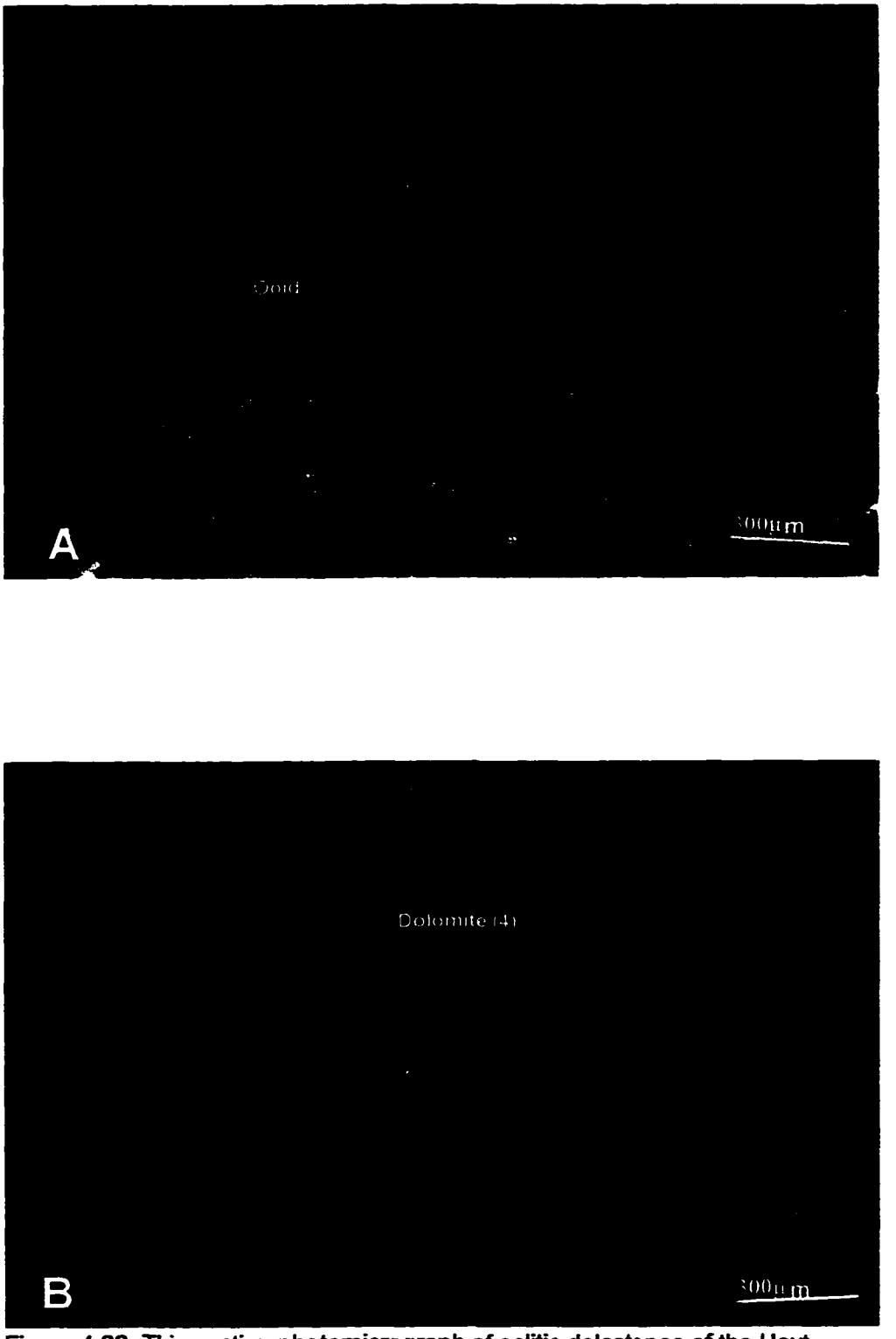

Figure 4.23: Thin-section photomicrograph of oolitic dolostones of the Hoyt Formation (sample #LP-1, outcrop # 7) where Dolomite (4) completely replaced ooids. The precursor calcite appears dull yellow and replacement dolomite is red luminescent. (A) is viewed in plane-polarized light and (B) under cathodoluminescence.

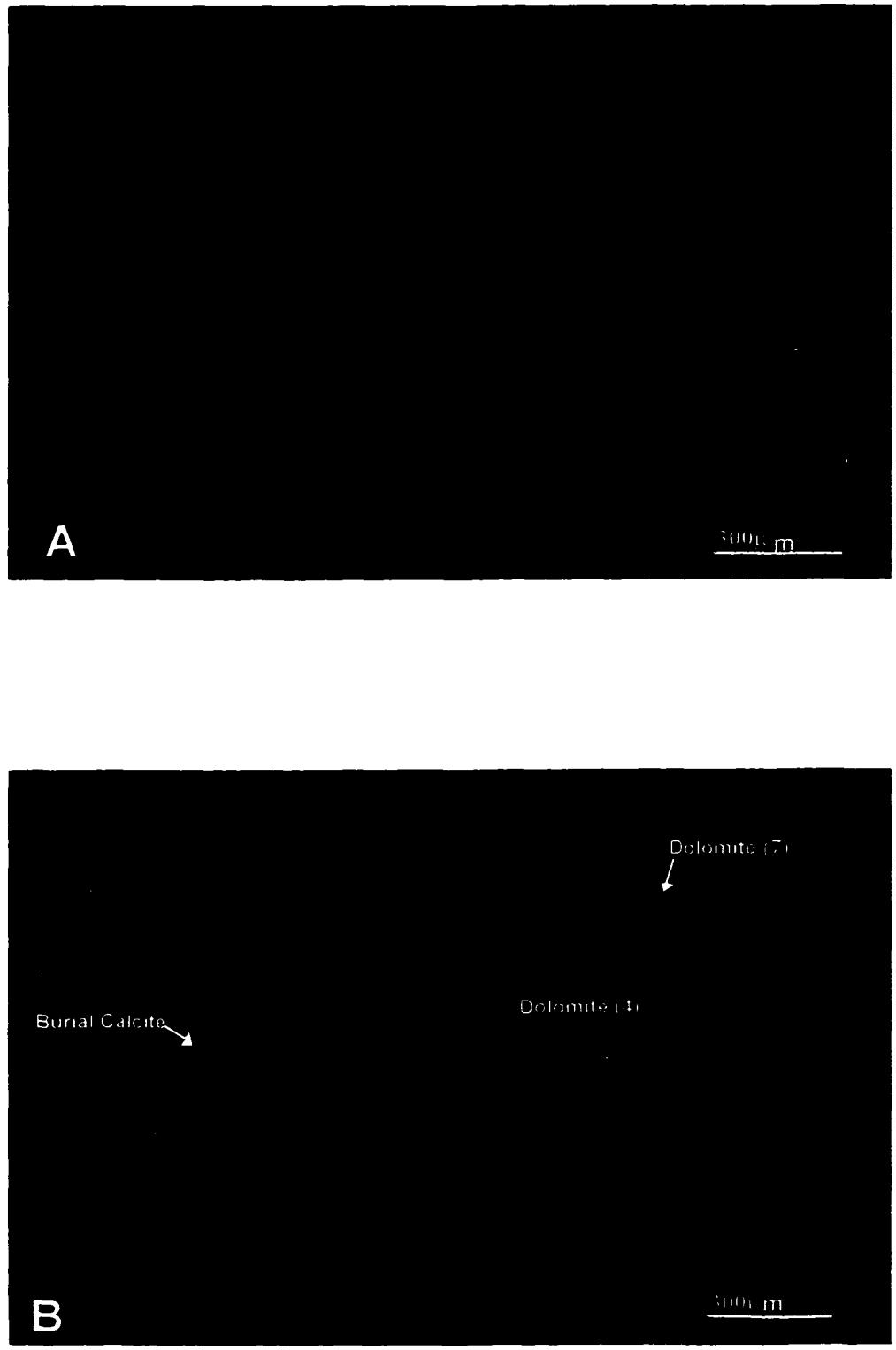

Figure 4.24:Thin-section photomicrograph of vuggy dolostones of the Hoyt Formation (sample # PG-8, outcrop # 6), where vugs in coarse Dolomite (4) mosaic are rimmed with non-luminescent Dolomite (7) and later filled with dull-luminescent burial calcite. (A) is viewed in plane-polarized light and (B) under cathodoluminescence.

Paragenetic associations of Dolomite (4) indicate that it predates silicification (Figure 4.25). Dolomite (4) is in places associated with stylolitization. Dolomite (4) is seen to have replaced Dolomite (3a) in some examples (Figure 4.26), obliterating all the previous zoning in the process. Vuggy or intercrystalline porosity in Dolomite (4) mosaics are lined by brighter luminescent Dolomite (5) indicating that Dolomite (4) definitely predates the cement phase. In Figure 4.27, Dolomite (4) occurs as a coarser and more porous mosaic adjacent to Dolomite (2). In this example, it is possible that Dolomite (4) replaced coarser precursor calcite or early dolomite that nucleated within the coarser precursor carbonate. Any calcite that was not replaced by dolomite was later removed by dissolution allowing Dolomite (4) to grow into a coarser hypidiotopic mosaic. The parent dolomitizing fluid was perhaps compositionally similar as both Dolomite (2) and Dolomite (4) display similar luminescence color. Both dolomite types have been replaced by non-luminescent, Fe-rich Dolomite (7) and later by dedolomite.

Geochemistry: Dolomite (4) is near stoichiometric with values ranging from 49.7 to 52.6 mole % $CaCO_3$ (Figure 4.28). Nonstoichiometry is rare in Dolomite (4). The iron content in the Dolomite (4) mosaics varies from 300 ppm to 5000 ppm. However most of the values lie around 3000 ppm. The manganese content, however is quite consistent and ranges from 150 to 900 ppm. Strontium is usually absent in this dolomite type, but if present may range from 150 to 540 ppm. Dolomite (4) exhibits $\delta^{18}O$ values ranging from -6.07 to -9.76 $^{0}/_{00}$. The $\delta^{13}C$ values however range from -0.8 to -2.5$^{0}/_{00}$.

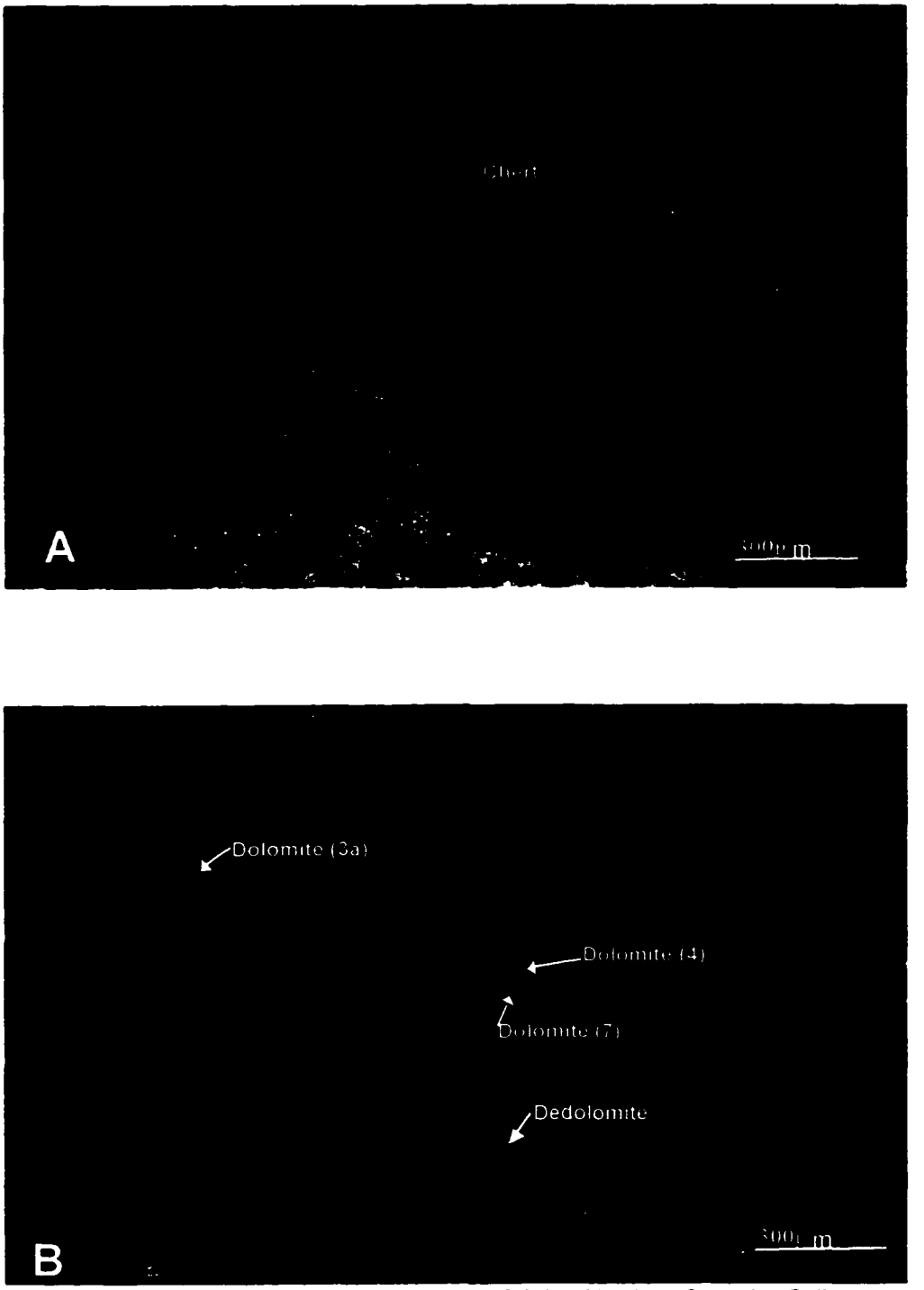

Figure: 4.25:Thin-section photomicrograph of dolomitic chert from the Gailor Formation (sample # GL-20, outcrop # 12). Irregularly luminescent Dolomite (4) with remnant zoning of earlier phases of Dolomite(3a) surrounded by microcrystalline chert. The dolomitization appears to have been followed by silicification and finally dedolomitization. Etched crystal boundaries and subsequent cementation of non-luminescent outer zones (Dolomite (7)) indicates that dolomite was the earlier phase. (A) is viewed in plane-polarized light and (B) under cathodoluminescence.

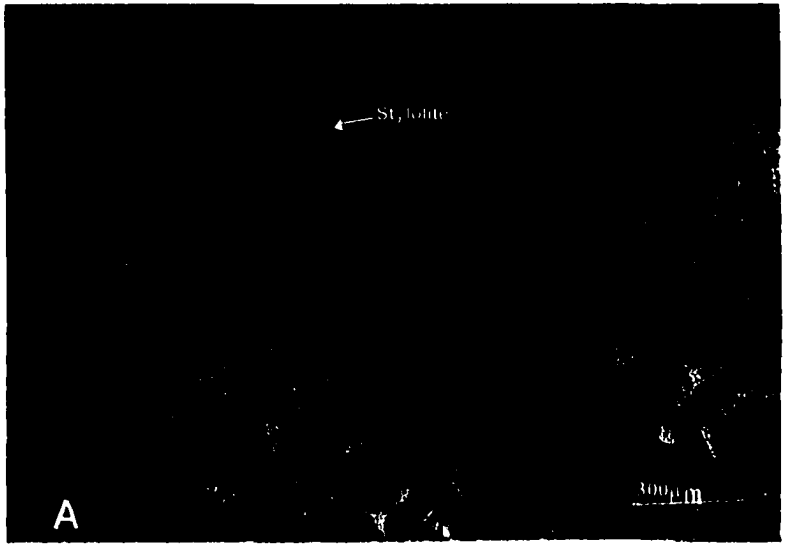

Figure: 4.26:Thin-section photomicrograph of intraclast in a storm layer from the Gailor Formation (sample # GL-14, outcrop # 12). Unzoned, red-luminescent, Dolomite (4) appears to have partially replaced zoned, orange-red luminescent Dolomite (3a). Dolomite (4) is concentrated along the stylolite suggesting that chemical compaction predated the formation of Dolomite (4). (A) is viewed in plane-polarized light and (B) under cathodoluminescence. The results of microprobe spot analysis of points numbered (1) and (2) in Figure 4.26B are shown in the histogram below. Point (1) is in Dolomite (3a) and point (2) is in Dolomite (4).

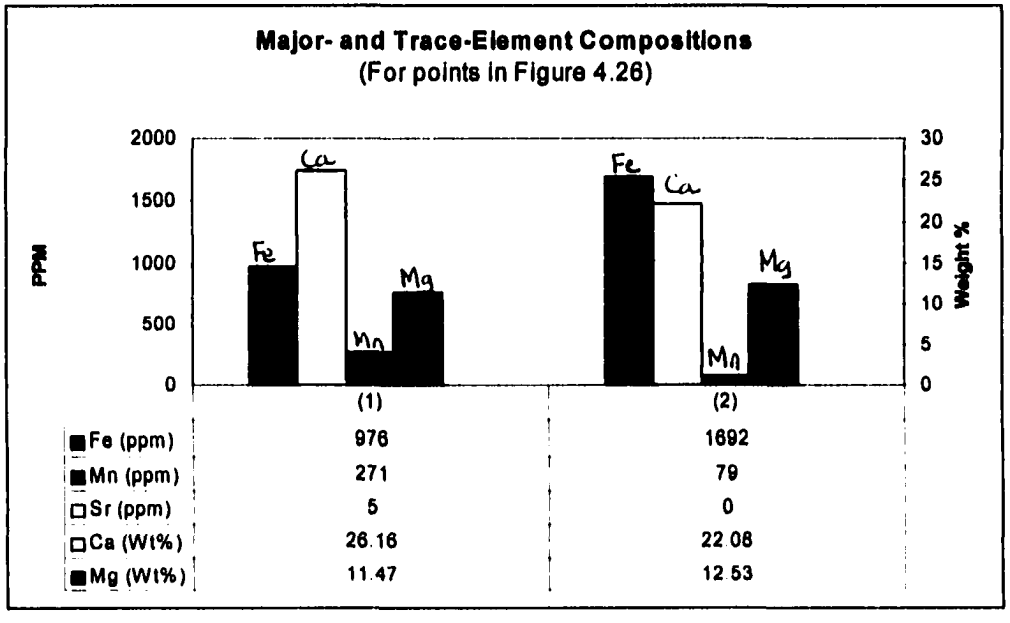

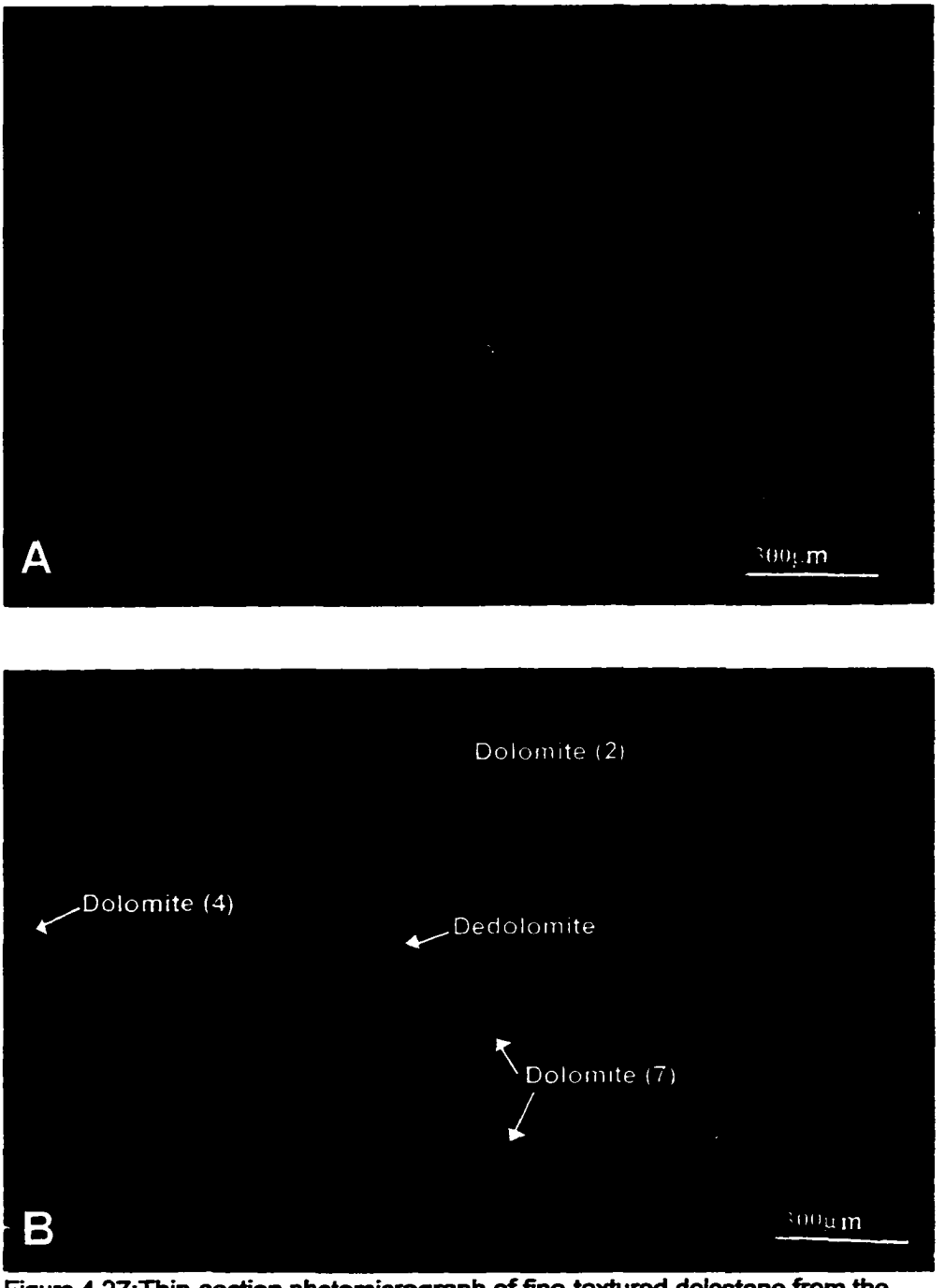

Figure 4.27:Thin-section photomicrograph of fine-textured dolostone from the Galway Formation (sample # GB-12, outcrop # 1). Dolomite (2) occurs as a fine-crystalline, tight mosaic, whereas Dolomite (4) occurs as a porous, relatively coarser mosaic . Both have been irregularly replaced by non-luminescent Dolomite (7) and later by dedolomite. Dedolomite is more prominent in the porous Dolomite (4) mosaic. (A) is viewed in plane-polarized light and (B) under cathodoluminescence.

Interpretation: The coarser texture of Dolomite (4) and its homogeneous luminescence suggests a major, long-lasting dolomitization event. The homogeneous luminescence implies that the dolomitizing fluids were chemically invariant during the formation of this dolomite. Dolomite (4) is more stoichiometric than dolomites 1, 2 and 3. The preservation of depositional textures clearly indicates their replacive origin and suggest that dolomite growth and precursor calcite dissolution took place simultaneously (Dockal, 1988).

Figure 4.28: CaCO3 Mole % in Sauk Sequence Dolomites and Calcites

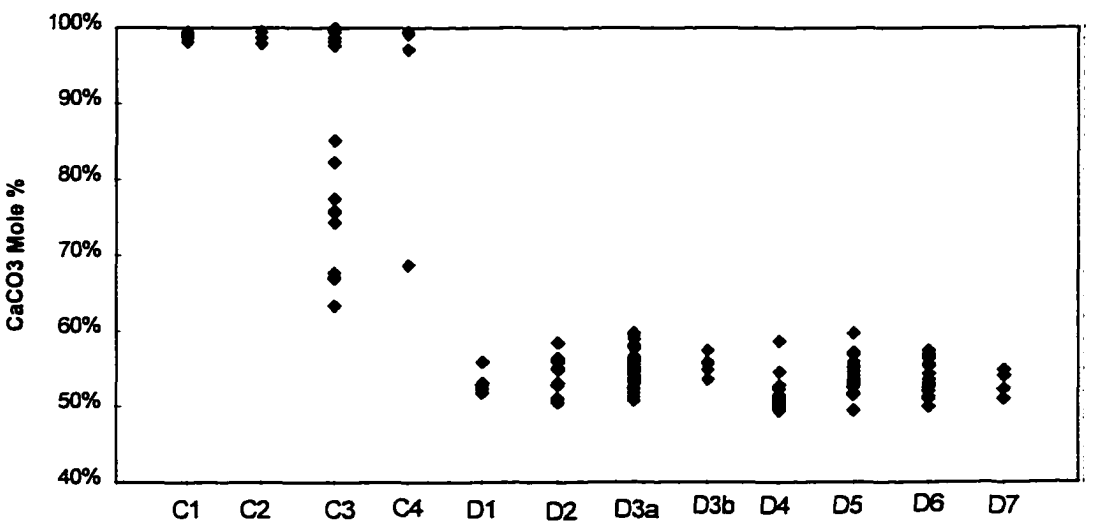

Explanation: Plot of $CaCO_3$ Mole % values in the different types of cacites and dolomites in the rocks of this study. The precursor calcites (C1and C2) and burial calcite (C3) have $CaCO_3$ values close to 100%. However dedolomite (C4) displays a range of values from over 60% to 100%, which may be expected as dedolomite has formed by the replacement of dolomite. The $CaCO_3$ Mole % values for the different dolomites show a wide range from 50 to 60%. The early formed dolomites Dolomite (1) [D1] are less stoichiometric. Dolomite (3b) [D3b] is also less stoichiometric possibly because this dolomite occurs as scattered replacement patches, in limestones where precursor calcite is still preserved. Comparatively, replacement dolomites such as Dolomite (2), Dolomite (3a), Dolomite (4) and Dolomite (5) [D2, D3a, D4 and D5] display a very wide range of $CaCO_3$ Mole % values, ranging from stoichiometric to non-stoichiometric values, due to the fact that they are either zoned dolomites or are products of extensive alteration of earlier dolomites. Saddle dolomite [D6] also displays a wide range of stoichiometry whereas ferroan dolomite cements formed during deep burial [D7] displays more stoichiometric values.

The predominantly xenotopic texture of these dolomites may suggest that they formed at high temperatures above the CRT (critical roughening temperature), which for dolomite is between 50 and 100^{0}C (Gregg and Sibley,1984; Sibley and Gregg, 1987). Therefore, the xenotopic texture of Dolomite (4) may have resulted from burial dolomitization of limestone or burial recrystallization or neomorphism of earlier formed near-surface dolomite. Neomorphism of earlier formed unstable, nonstoichiometric dolomites can occur at elevated temperatures converting them to more stable, stoichiometric forms, usually accompanied by a coarsening of the texture. It is however hard to ascertain if the Dolomite (4) mosaics were the result of neomorphism or replacement, especially where no relict textures are present.

As there are some instances where Dolomite (4) appears to postdate and replace Dolomite (3a), it may be inferred that this phase of dolomitization was so pervasive that it altered the earlier generations of dolomite obliterating all zoning that may have been present before. Both Dolomite (2) and Dolomite (3) are zoned, whereas Dolomite (4) is completely homogeneous or appear mottled indicating irregular replacement of earlier dolomite generations. The major difference between Dolomite (4) and the previous generations of replacive dolomites (2 and 3) is the absence of zoning in the former. This marks a change in the type of alteration. The zoned dolomites have grown by the precipitation of overgrowth cement zones around dull luminescent cores that perhaps represent the initiation of dolomitization in the depositional environment. These cores may also be replaced at a later stage during burial as they are possibly unstable.

Anyhow the following stage of dolomitization in the subsurface was carried out by the growth of cement zones. The later phase of dolomitization marked by Dolomite (4) is different in the sense that, instead of the formation of cement zones, the entire dolomite mosaic is pervasively altered to a homogeneous, nonzoned coarser, more stoichiometric, and generally xenotopic mosaic. This is perhaps characteristic of a long-lasting process of dolomitization at elevated temperatures prevalent in the burial environment.

The moderately high iron and manganese contents (Figures 4.2, 4.22, 4.26) of Dolomite (4) suggests their precipitation from negative Eh pore fluids in which Fe^{2+} and Mn^{2+} were in solution. Such anoxic fluids tend to occur in subsurface environments, a fact which may also point to their burial origin. The low strontium content indicates that dolomitizing fluids were not marine and that the dolomite may have replaced a diagenetic calcite rather than a marine calcite or aragonite (Tucker and Wright, 1992). Thus, the low Sr content may mean that these dolomites resulted from a late-diagenetic event.

The slightly depleted $\delta^{13}C$ values suggest that the carbonate in these dolomites were partly derived from organic-matter diagenesis. The depleted $\delta^{18}O$ values of Dolomite (4) are intermediate between the enriched values of the earlier formed near-surface dolomites (1) and (2) and the extremely depleted values of the deep-burial cements (Dolomite 6 and 7). This is interpreted to indicate dolomitization occurred at intermediate burial depths compared to the deeper burial depths where Dolomite (6) and Dolomite (7) were formed.

Subsidence, sediment loading, or tectonic loading may be responsible for transporting sedimentary strata to burial depths where temperatures are high. Replacement dolomitization is favored at depth, because some of the kinetic barriers to dolomite precipitation are diminished at elevated temperatures. The proportion of hydrated Mg^{2+} ions decreases and the reaction rate of dolomite precipitation increase at high temperatures. In addition, the considerable time that platform strata reside in the subsurface, allows sufficient time for dolomite replacement to proceed to completion (Mattes and Mountjoy, 1980; Hardie, 1987; Morrow, 1990; Tucker and Wright, 1992). Thus, the textural and geochemical characteristics of Dolomite (4) indicates late- diagenetic, replacive dolomitization at elevated temperatures.

4.2.5 Dolomite (5):

Description: Dolomite (5) occurs as clear, medium to coarse crystalline, planar-e crystals that exhibit bright and dull orange zones (Figure 4.29). This dolomite type typically occurs as a cement lining voids, moldic pores, and fractures and in places, filling them (Figure 4.30). These Dolomite (5) cement zones usually truncate the mosaic dolomites 2, 3 and 4 and are postdated by nonluminescent, ferroan Dolomite (7) (Figure 4.31). Fractures or voids in the nonzoned mosaic Dolomite (4) display coarser, euhedral dolomite cement similar to the host dolomite mosaic. The voids or fractures may be filled with late dolomite and or calcite. Dolomite (5) may occur poikilotopically in the late dolomite and calcite

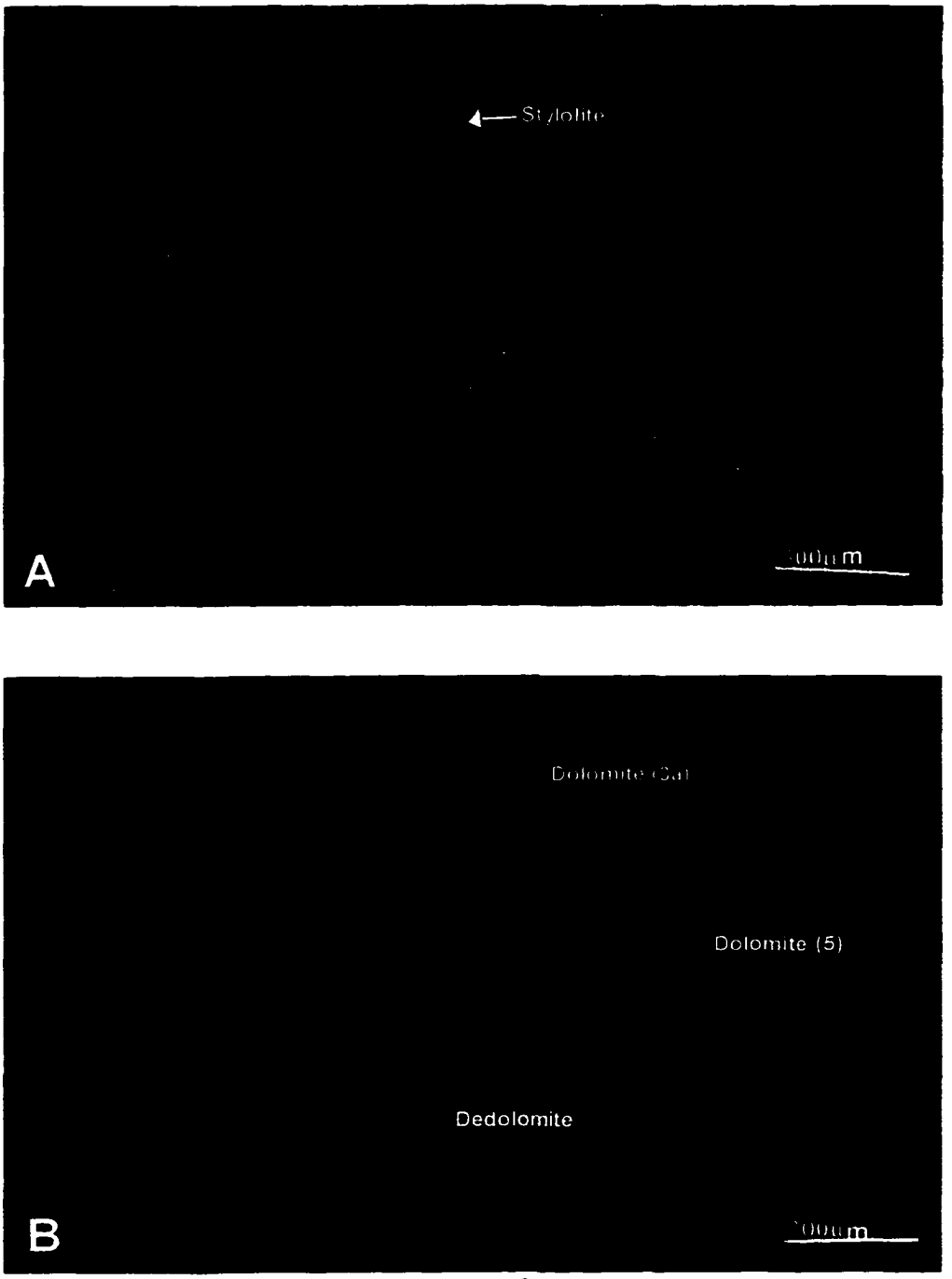

Figure 4.29: Thin-section photomicrograph of a dolostone unit that occurs towards the top of the Tribes Hill Formation (sample #TB-1, outcrop #17). A stylolite cross-cuts zoned Dolomite (3a), postdating the replacement mosaic. Bright orange Dolomite (5) appears to have replaced Dolomite (3a) in porous parts of the mosaic, followed later by dedolomitization (bright yellow luminescence). Both Dolomite (5) and dedolomite, mark alteration of the preexisting, replacement dolomite, by meteoric fluids rich in Mn and relatively poor in Fe. The stylolites may have acted as conduits for the dolomitizing and dedolomitizing fluids. (A) is viewed in plane-polarized light and (B) under cathodoluminescence.

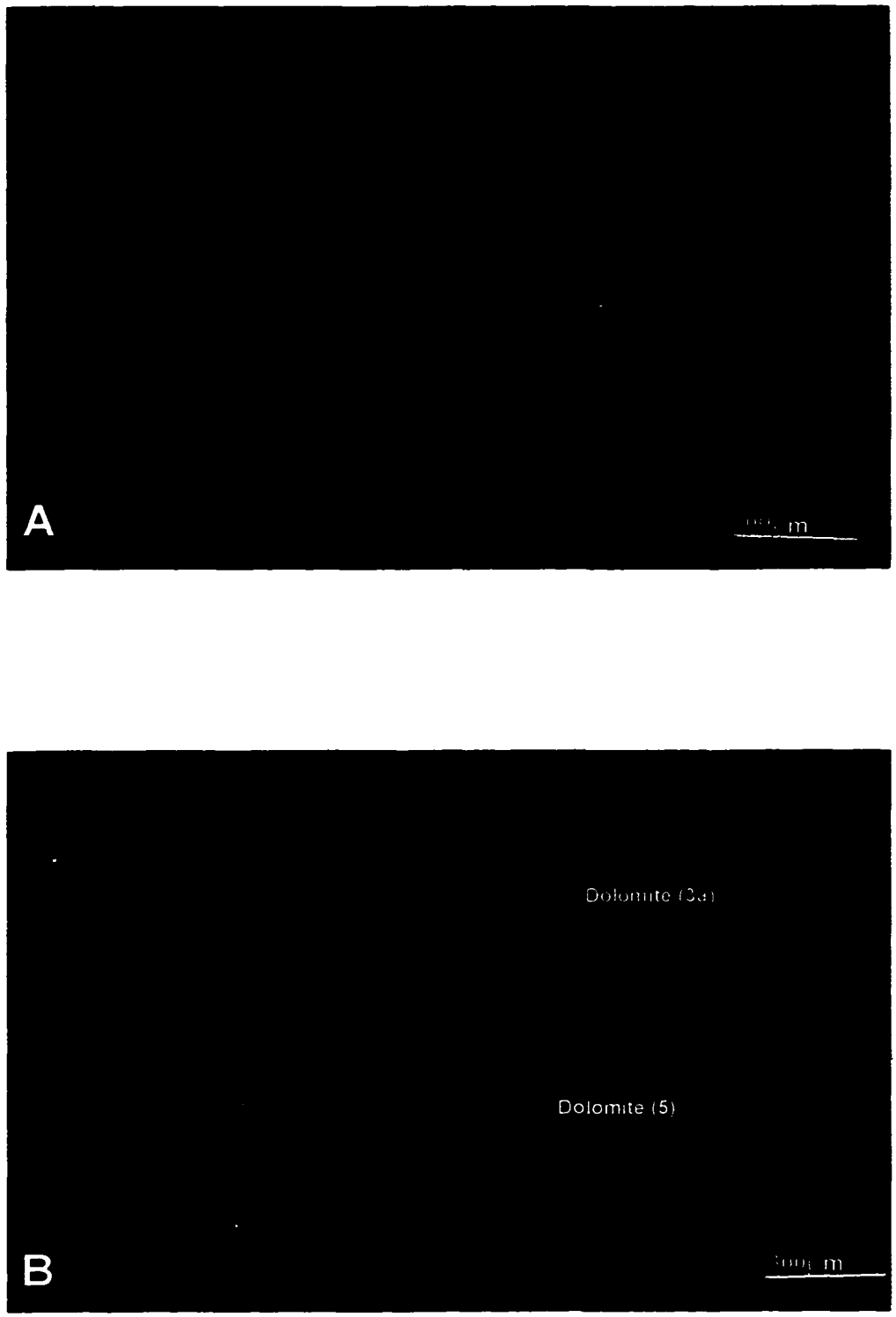

Figure 4.30:Thin-section photomicrograph of a vuggy dolostone from the Gailor Formation (sample # FJ-6, outcrop #11). Zoned, Dolomite (3a) having irregularly luminescent cores and non-luminescent to red-luminescent rims makes up the pervasive mosaic. Bright, orange-luminescent Dolomite (5) occurs as a void-filling within a vug. (A) is viewed in plane-polarized light and (B) under cathodoluminescence.

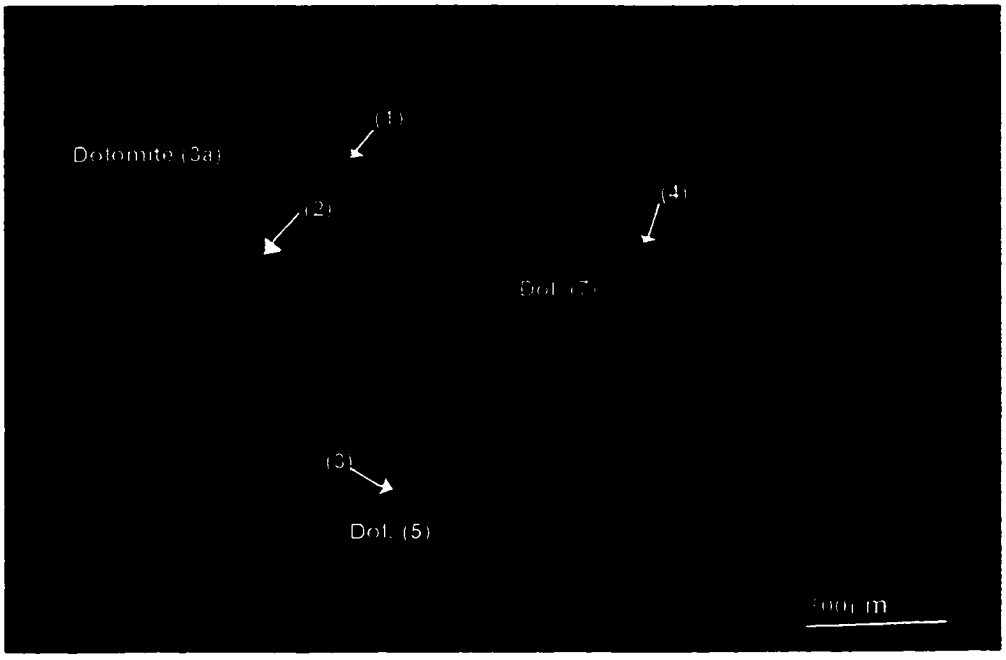

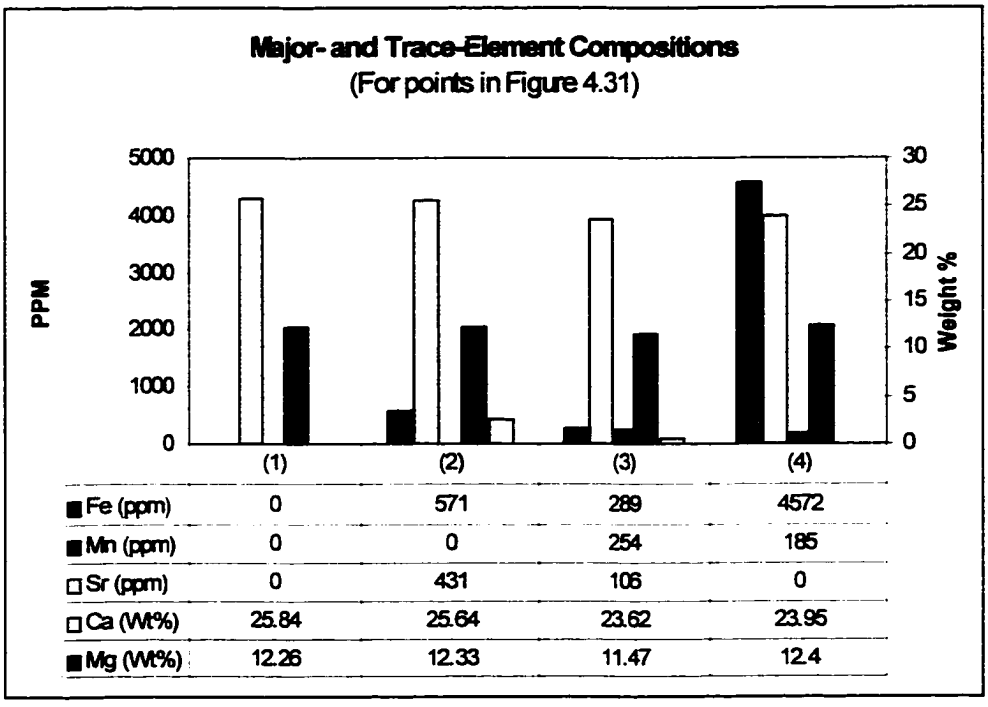

Figure 4.31: Thin-section photomicrograph of a vuggy dolomudstone from the Tribes Hill Formation (sample # 16/7, outcrop #15), where zoned Dolomite (3a) forms a pervasive replacive mosaic and Dolomite (5) occurs as orange-luminescent cement, lining vugs , postdated by non-luminescent Dolomite (7). Thin section is viewed under cathodoluminescence. The results of microprobe spot analysis of points numbered (1) through (4) are shown in the adjacent histogram. Points (1) and (2) are in Dolomite (3a); point (3) is in Dolomite (5) and point (4) is in Dolomite (7).

void-filling cements (Figures 4.31, 4.7). When occurring as bright zoned cements, this dolomite type is usually poor in Fe and Sr and rich in Mn (Figure 4.2). Dolomite (5) also occurs as a replacement of dolomites 3 and 4, where the mosaics are porous (Figure 4.32, 4.19). The luminescence color of Dolomite (5) is bright orange whereas the second-stage dolomites 3, and 4 show shades of red in CL. Dolomite (5) may also occur as thin, orange outer zones lining intercrystalline pores within the second-stage dolomite mosaics.

Interpretation: Dolomite (5) postdates dolomites 1, 2, 3, and 4. It definitely antedates late dolomite cements 6 and 7 and late calcite cements. The main difference between Dolomite (5) and the other dolomites, that is obvious under CL is that Dolomite (5) occurs associated with pore spaces and resulted from the passage of Fe-poor, Mn-rich dolomitizing fluids compared to the host dolomites. This suggests that the parent fluids responsible for the precipitation of Dolomite (5) were not chemically the same as those that were responsible for the second-stage dolomites. Their relative Fe-depletion and Mn-enrichment suggest that they may have been meteoric fluids.

The Dolomite (5) cements occur in voids throughout the Sauk sequence but the presence of replacive Dolomite (5) is restricted to the dissolution-collapse breccia units in the Gailor units and the surface of disconformity atop the Tribes Hill Formation (outcrop #17). Dolomite (5) is therefore interpreted as representative of a phase of uplift of the strata, during which the entire sequence was infiltrated by meteoric fluids. This phase of uplift may have

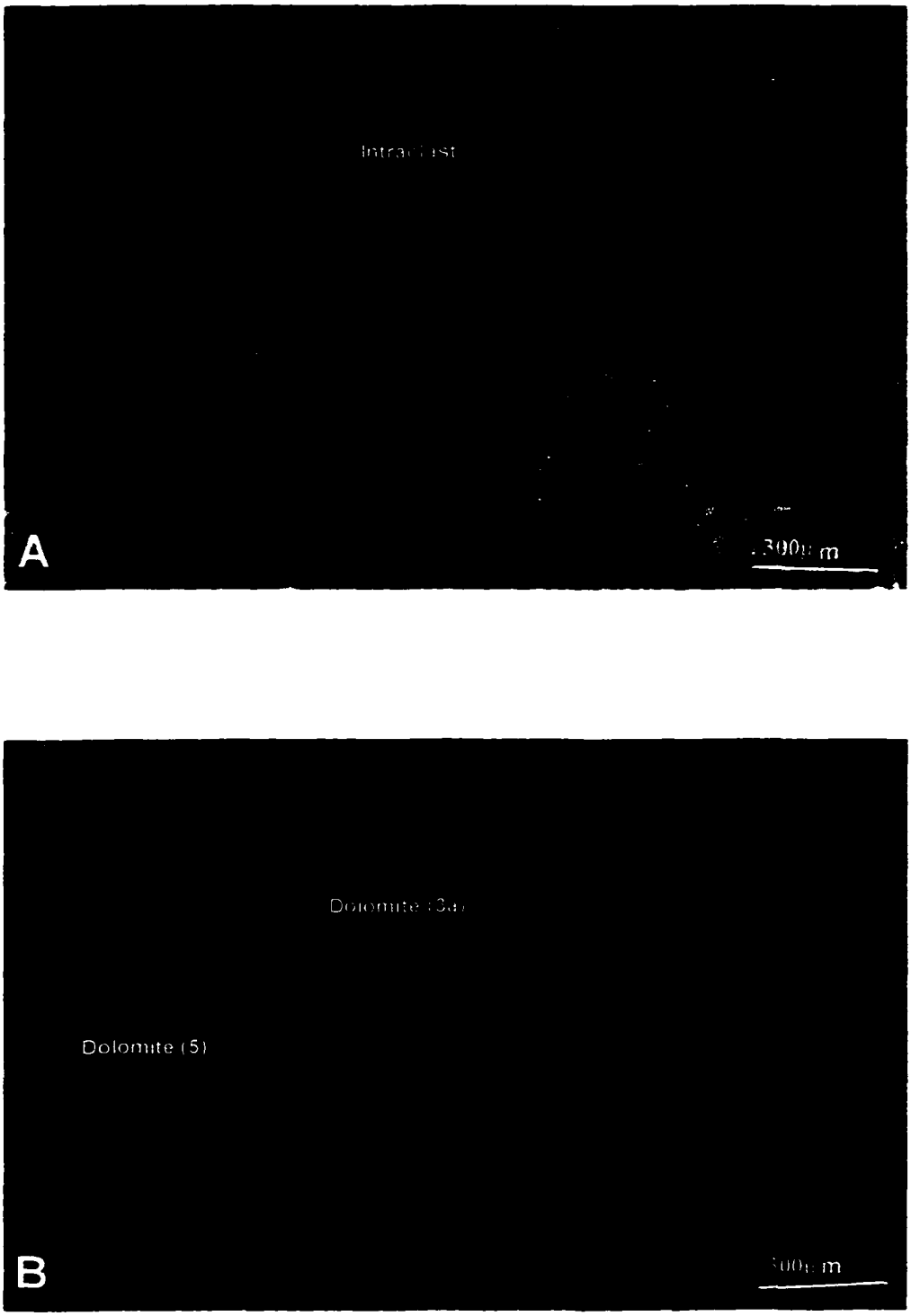

Figure 4.32:Thin-section photomicrograph of a storm bed composed of intraclasts observed in the Gailor Formation (sample # FJ-4, outcrop #11). Zoned, Dolomite (3a) that has irregularly luminescent cores and non-luminescent to red-luminescent rims makes up the pervasively dolomitized intraclasts . Bright, orange-luminescent Dolomite (5) occurs in the porous horizons between the intraclasts. (A) is viewed in plane-polarized light and (B) under cathodoluminescence.

coincided with the development of the post-Sauk, pre-Tippecanoe surface of unconformity.

4.2.6 Saddle Dolomite (6):

Description: Dolomite (6) occurs as coarse, milky-white to clear dolomite cements that fill vugs and fractures. It is recognized microscopically as well as on the outcrop scale. This dolomite type displays curved crystal faces and scalenohedral crystal terminations and is described as having a non-planar-c texture. Under crossed polars Dolomite (6) displays a sweeping extinction (Figure 4.33A). In places Dolomite (6) is associated with stylolites (Figure 4.33B). This cement is, in places, zoned with orange-red luminescent zones followed by a final nonluminescent zone which usually occludes the vug or fracture (Figure 4.34). However, more commonly, Dolomite (6) is non-luminescent (Figures 4.35 and 4.9) and iron rich. Dolomite (6) is associated with most of the dolomite mosaics and commonly predates late void-filling calcite (Figure 4.36). In places, saddle dolomite has been found associated with authigenic quartz (See figures 5.5 and 5.6 in chapter 5).

Geochemistry: Dolomite (6) displays variable stoichiometry with values ranging from 50 to 56 mole% $CaCO_3$. The iron content of Dolomite (6) is typically high with values starting at around 2000 ppm and going as high as 20,000 ppm

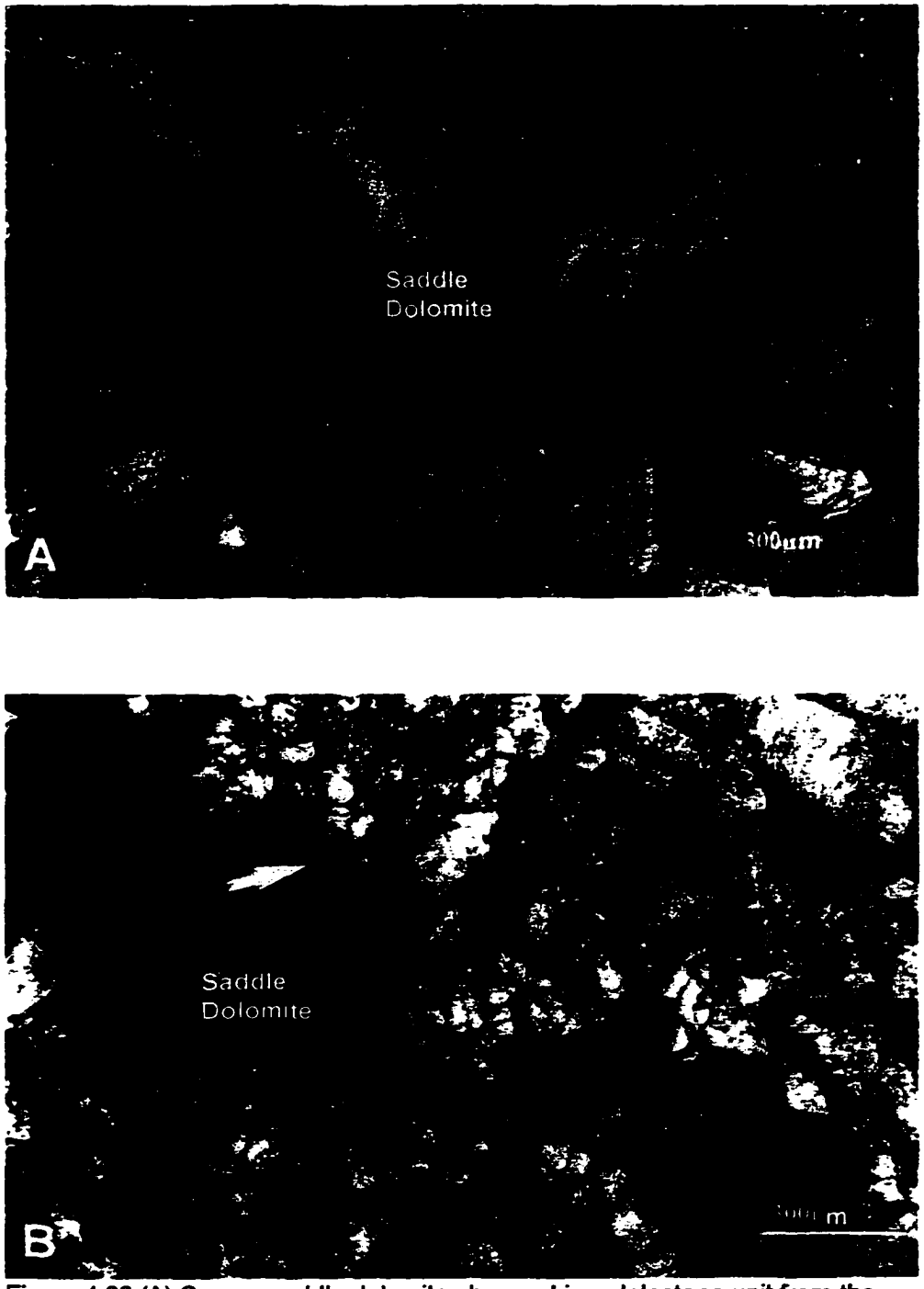

Figure 4.33 (A):Coarse saddle dolomite observed in a dolostone unit from the Gailor Formation (sample # GL-1, outcrop #10), displays sweeping, undulose extinction when viewed under crossed nicols. (B):Coarse saddle dolomite observed in a mottled dolostone unit from the Gailor Formation (sample # GL-3, outcrop #10), is associated with a stylolite (arrow) within a Dolomite (4) mosaic. Thin section is viewed in plane-polarized light.

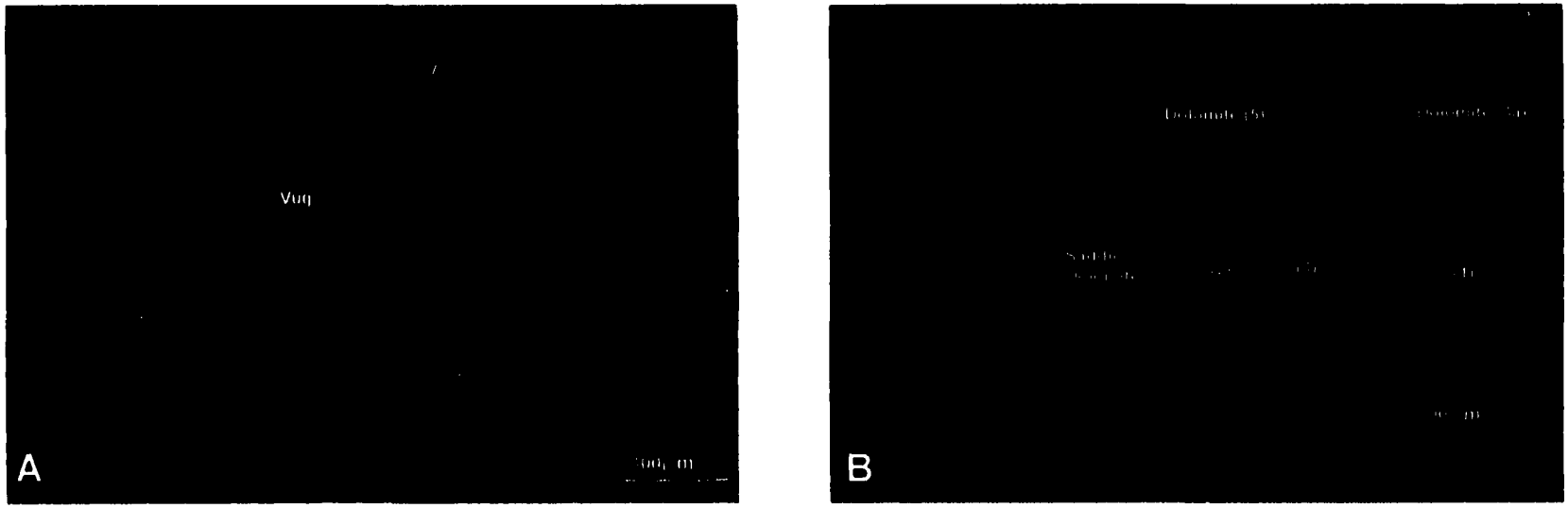

Figure 4.34: Photomicrograph of cryptmicrobial laminated dolostone (Gallor Formation, sample # GL-19, outcrop #12), shows a spherical vug within replacement Dolomite (3a), filled with brightly zoned Dolomite (5) followed by non-luminescent saddle dolomite indicating progressive burial or enrichment in Fe of the dolomitizing fluid. (A) is viewed in plane-polarized light and (B) under cathodoluminescence. The results of microprobe spot analysis of points numbered (1) through (3) are shown in the histogram below. Point (1) is in Dolomite (3a); point (2) is in saddle dolomite and point (3) is in Dolomite (5).

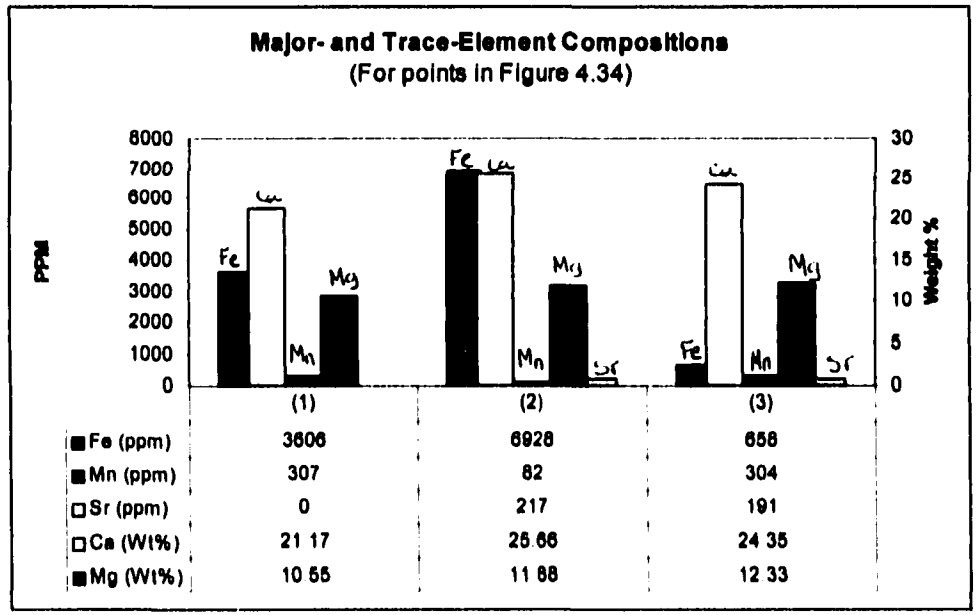

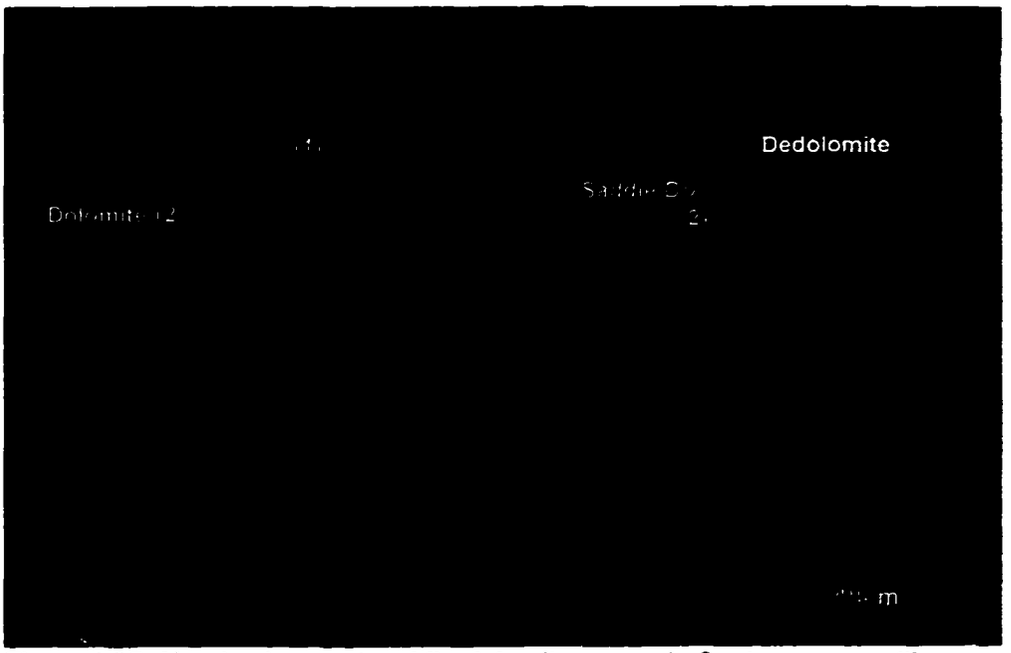

Figure 4.35: Non-luminescent saddle dolomite occurs in fracture crosscutting Dolomite (2) in a dolostone unit from the Galway Formation (sample # GB-12, outcrop # 1). Fe-rich fluids responsible for precipitating saddle dolomite cement has also irregularly replaced the mosaic dolomite. Saddle dolomite is postdated by dedolomitization (bright yellow). Thin section is viewed under cathodoluminescence. The results of microprobe spot analysis of points numbered (1) and (2) are shown in the histogram below. Point (1) is in Dolomite (2) and point (2) is in saddle dolomite.

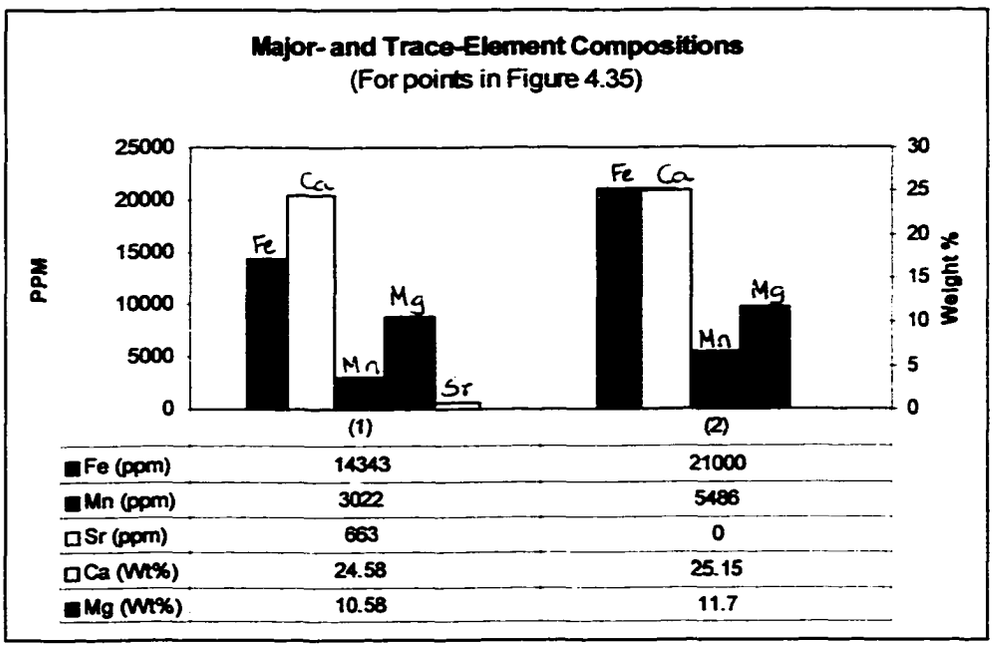

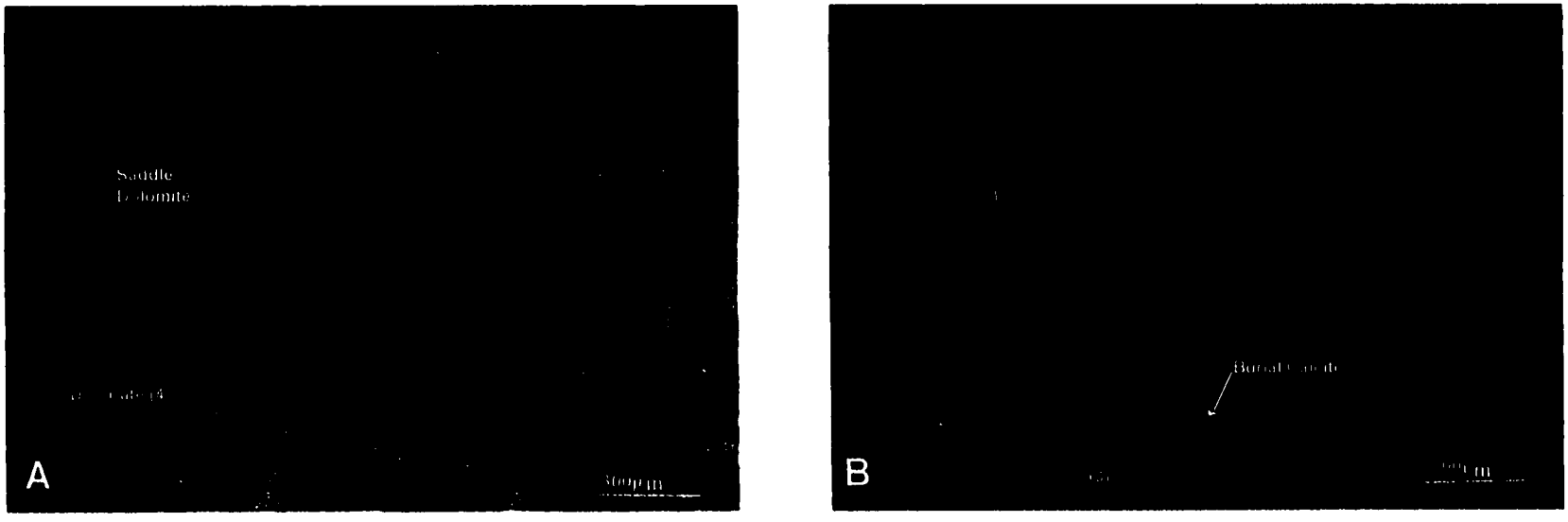

Figure 4.36: Thin-section photomicrograph of a dolostone unit from the Gailor Formation (Sample # GL-14, outcrop #12) where dark red Dolomite (4) has replaced Dolomite (3), obliterating any zoning in the process. Vug is filled with non-luminescent saddle dolomite which is postdated by dull-luminescent burial calcite (dull yellow) and dedolomite (bright yellow). (A) is viewed in plane-polarized light and (B) under cathodoluminescence. The results of microprobe spot analysis of points numbered (1) through (3) are shown in the histogram below. Point (1) is in saddle dolomite; point (2) is in Dolomite (4) and point (3) is in burial calcite void-filling cement.

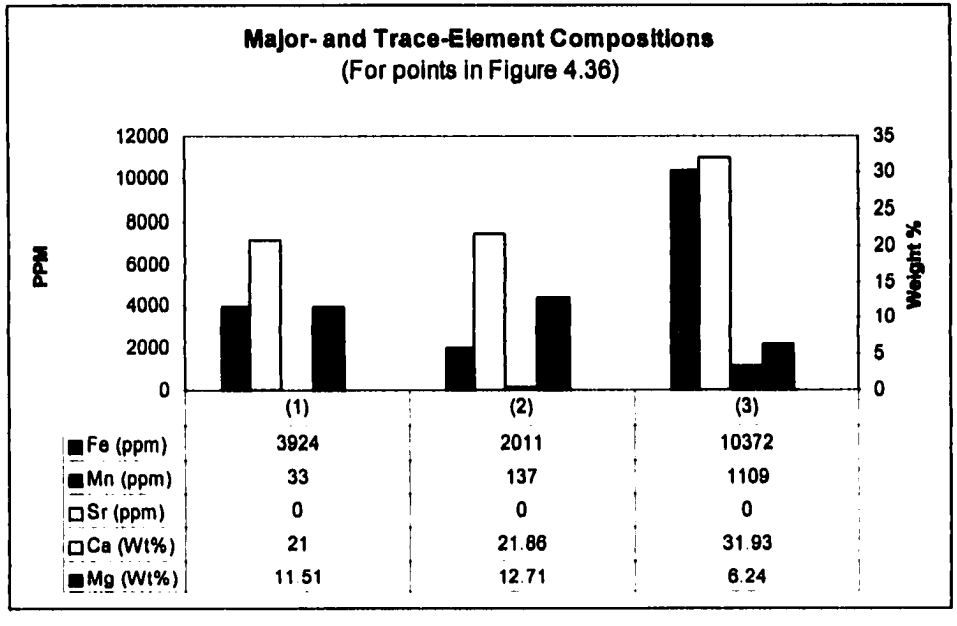

(Figure 4.2).The Mn content is usually low, below 100 ppm in the non-luminescent cements, but may be around 300 ppm and in places as high as 3000 ppm in the bright-luminescent zones of this dolomite type. Sr is usually absent in this dolomite type. The $\delta^{18}O$ content of this dolomite type is considerably depleted with values such as -9.27 and -10.44 $^{0}/_{00}$ (Figure 4.3). The $\delta^{13}C$ values in this dolomite type is about -2.5 o -2.6 $^{0}/_{00}$.

Interpretation: This dolomite type, with its typical coarse, cement nature, undulatory extinction and curved faces has been termed baroque or saddle dolomite. Previous studies of saddle dolomites have interpreted them to have formed as a result of sulfate reduction of organic matter at temperatures between 60 and 150^{0} C (Radke and Mathis,1980). Saddle dolomite is interpreted to have precipitated under extreme supersaturation or where surface-related activation barriers are reduced (Searl, 1989). The depleted $\delta^{18}O$ values in Dolomite (6) point to formation at elevated temperatures. These values are higher than those of the earlier-formed near-surface dolomites 1 and 2 and the mosaic dolomites 3 and 4, which were formed in the main stage of dolomitization during shallow burial. The $\delta^{13}C$ values are slightly depleted, compared to those of Cambro-Ordovician least-altered marine cements (data in Allan and Wiggins, 1993, Appendix II), indicating that the CO_3^{2-} was perhaps partly derived from organic-matter diagenesis.

The paragenetic relationships also show that Dolomite (6) postdates dolomites 1, 2, 3 and 4, and fills tectonic fractures and pore spaces that resulted

from dissolution. Thus comparatively, this dolomite type is interpreted to have formed during deep burial. The nonplanar-c texture, ferroan nature, depleted $\delta^{18}O$, and $\delta^{13}C$ content of Dolomite (6), therefore suggest that they formed at elevated temperatures during deep burial. The spherical vugs that are filled with saddle dolomite may possibly have originated as evaporite nodules in the intertidal-flat dolostones.

4.2.7 Dolomite (7):

Description: Dolomite (7) occurs as a planar-e, void-filling cement that fills vugs, solution-enhanced voids, tectonic fractures, and veins that traverse the dolomite mosaics. Under cathodoluminescence, Dolomite (7) is non-luminescent and forms the outermost zone of void-lining cements. When associated with Dolomite cement (5), it postdates Dolomite (5) (Figure 4.31). Dolomite (7) occurs, in places, associated with poikilotopic calcite (3) that fills voids.

Geochemistry: Dolomite (7) is highly ferroan and displays Fe values as ranging from 8000 to 21000 ppm (Figure 4.2). The Mn values are variable ranging from 200 to rarely 5000 ppm and sometimes even absent. Sr is usually absent in this dolomite type.

Interpretation: Dolomite (7) is interpreted to represent dolomite cement formed by ferroan brines of the deep subsurface. The paragenetic relationships reveal

that Dolomite (7) postdates all the replacement dolomites 1, 2, 3 and 4 and Dolomite (5) and antedates burial calcite (Figures 4.21, 4.24, 4.26, 4.27).

4.3 Dolomitization and Dolomite-Cement Stratigraphy in the Sauk Sequence:

The seven dolomite types identified in the foregoing section differ from one another in terms of their crystal sizes, luminescence, trace-element contents, and stable-isotope compositions (Table 3). In the Sauk sequence strata, four stages of dolomitization are recognized. The first stage is considered to have occurred early in the diagenetic history penecontemporaneously during and immediately following deposition. The $^{87}Sr/^{86}Sr$ ratio of the Galway dolostones is similar to that of Cambrian seawater indicating that dolomitization was initiated early in the diagenetic history of these carbonates, possibly in the depositional environment (Figure 4.37). This implies that the dolomitizing fluid responsible for the initial dolomitization of the Galway dolostones was either Late Cambrian seawater or derived from evaporation of Late Cambrian seawater.

The second stage was one of massive dolomitization that occurred in the shallow subsurface, which involved multiple episodes of textural and geochemical change via neomorphism, dissolution-reprecipitation, and mineral stabilization. Dolomitization in the second stage antedated and postdated burial compaction and stylolitization. The third stage was related to uplift of the basin, when meteoric fluids entered the strata. Dedolomitization and silicification were

associated with this stage of dolomitization. The fourth and final stage of dolomitization occurred in the deep subsurface where subsurface brines precipitated dolomite cements in dissolution vugs, intercrystalline pores, fractures, and veinlets. Table 4 describes some of the dolomite textures observed in the Sauk carbonates of this study.

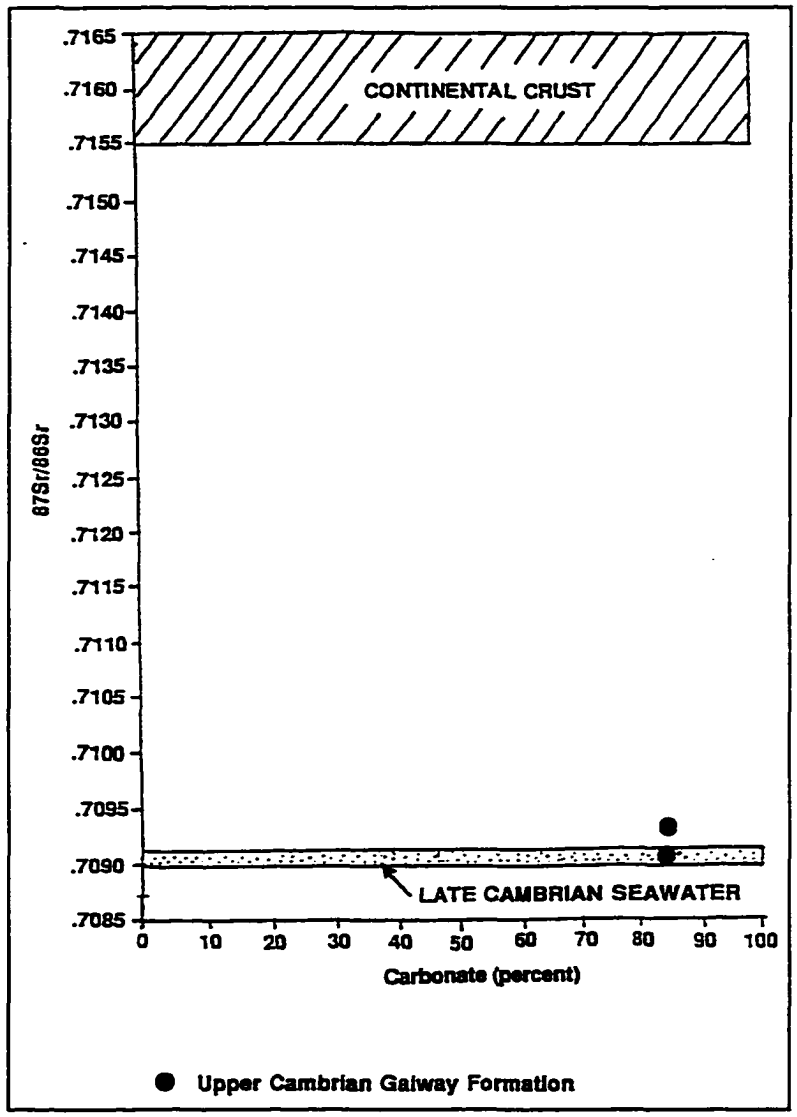

Figure 4.37. Plot of $^{87}Sr/^{86}Sr$ against carbonate concentration for Galway dolostones. The strontium-isotopic ratio of Galway dolostone is consistent with or close to Cambrian seawater. (From Friedman, 1996, p.137)

TABLE 4: DOLOMITE TEXTURES IN THE SAUK CARBONATES OF THIS STUDY	
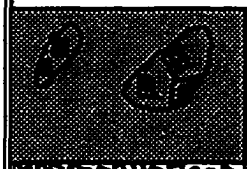	Dolomite (1) forms a microcrystalline matrix surrounding allochems that have been replaced by Dolomite (2). CL: red-luminescent
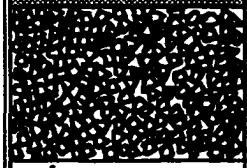	Dolomite (2) occurs as very fine-crystalline, unimodal planar-s to non-planar, pervasive, fabric destructive mosaic. CL: Zoned,/unzoned, red-luminescent zones around non-luminescent cores.
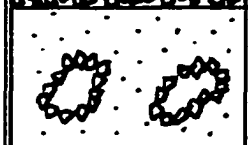	Red luminescent, Dolomite (2) has replaced micrite envelopes around allochems that were partially dolomitized, followed later by dissolution of unreplaced interior.
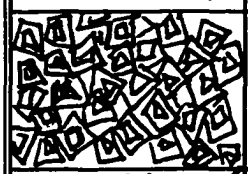	Dolomite (3a) forms a planar-e to planar-s, medium- to coarse-crystalline pervasive mosaic. CL: Zoned, Bright and dull red luminescent zones.
	Dolomite (3b) forms scattered rhombs or clusters of planar-p, porphyrotopic crystals associated with stylolites, partially replacing precursor calcite (micrite). CL: Zoned, red luminescent cores with thick non-luminescent zones.
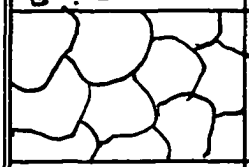	Dolomite (4) forms pervasive, medium- to coarse-crystalline planar-s to non-planar-a mosaics.CL: Unzoned, red luminescent
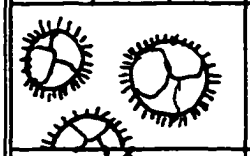	Unzoned, red luminescent Dolomite(4) partially replaces ooids composed of precursor, non-luminescent Calcite (1).
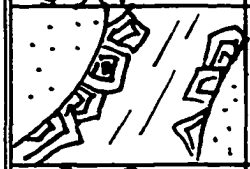	Dolomite (5) forms planar-e, medium- to coarse, clear crystals, lining voids and fractures filled with late dolomite and/ or calcite. CL: Bright Orange red luminescence
	Dolomite (6) forms nonplanar-c, coarse to very coarse crystals with sweeping extinction and curved crystal faces; occurs as void-filling cements (Saddle Dolomite). CL: non-luminescent
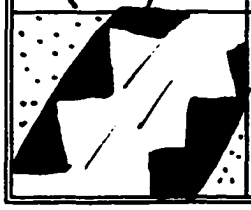	Dolomite (7) forms planar-e void-lining. Fracture-filling cements. CL:Non-luminescent

The extremely fine crystal size (Figure 4.38), low trace-element content (Figure 4.2) and relatively high Sr content of dolomites 1 and 2, as well as their relatively higher $\delta^{18}O$ content (Figure 4.3) suggest that they are products of the early diagenesis of fine crystalline lime mud. These dolomite types occur in the supratidal and upper-intertidal-flat dolomudstones and are associated with intraclasts, fenestrae, mudcracks, and cryptmicrobial laminates which also point to deposition in an arid, evaporative perhaps hypersaline setting. No evaporites are observed associated with these dolomite types. However, the high Sr values

Figure 4.38: Crystal Size Distribution in Sauk Sequence Dolomites

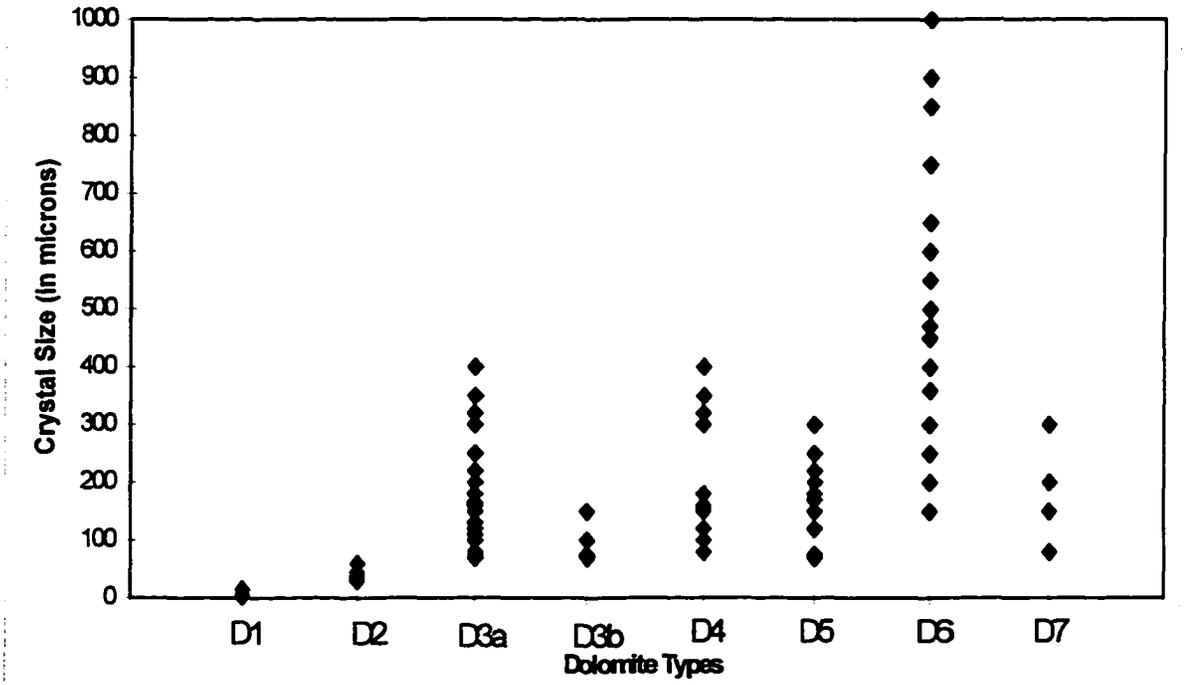

Explanation: Plot showing distribution of crystal-size in the different dolomite types observed in the rocks of this study. The early formed dolomites, Dolomite (1) [D1] and Dolomite (2) [D2] are very fine-crystalline. The main-stage, replacement dolomites, Dolomite (3a) [D3a], Dolomite (3b) [D3b] and Dolomite (4) [D4] form medium- to coarse-crystalline mosaics. Dolomite (5) which represents the uplift stage is commonly medium-crystalline. In contrast, the late-stage, burial dolomites, such as saddle dolomite [D6] and Dolomite (7) [D7] are very coarse-crystalline.

and association with features indicating desiccation (fenestral vugs, intraclasts, mudcracks) and preservation of cryptmicrobial laminites suggest an evaporitic environment. Such a setting where conditions of high salinity, high temperature, and high magnesium-ion concentration exist, is considered ideal for dolomite formation (Friedman and Sanders, 1967).

Dolomites 1 and 2 are therefore interpreted to have formed pene-contemporaneously in the sea-marginal supratidal (Dolomite 1), intertidal, and subtidal (Dolomite 2) sediments where interstitial waters were hypersaline as a result of 'capillary concentration' and or 'seepage refluxion'. During dolomitization by capillary concentration, dolomite is formed at the sediment-air interface where interstitial waters move upwards through porous sea-marginal sediments due to excessive evaporation (Friedman and Sanders, 1967). In the seepage-refluxion model, excessive evaporation causes lagoonal waters to become dense and heavy brines, which infiltrate underlying subtidal lagoonal sediments, dolomitizing them, in the process (Adams and Rhodes, 1960).

Within the stromatolitic and microbial-laminated sediments, the decay and break down of cyanobacterial sheaths and mucilage by sulfate-reducing bacteria, removes sulfate, supplies magnesium, and releases ammonia, thereby increasing the pH and carbonate alkalinity to levels necessary for dolomite formation.

The most common dolomite types, Dolomites (3a) and Dolomite (4), are considerably coarser than dolomites 1 and 2 and are interpreted to represent a

long-lasting episode of subsurface dolomitization. The paragenetic relationships show that Dolomite (3a) may also have been initiated in the near-surface environment, but developed zoned overgrowths with subsequent burial. Cores of Dolomite (3a) are generally homogeneous, dull-red luminescent, and rich in inclusions. The zoned overgrowths are clear and free of inclusions. The contact between the dull cores and the zoned overgrowths is often an irregular dissolution surface. This dolomite type is interpreted to have originated as early formed, near-surface dolomite and subsequently developed zoned overgrowths after dissolution of nondolomitized carbonate and some dissolution of previously formed dolomite. Thus, Dolomite (3a) has been subjected to a long sequence of diagenetic events. The zoned nature of this dolomite type, reveals the multiple stages of dolomitization that took place in these rocks, as the composition of the dolomitizing fluids changed with progressive time and burial.

Dolomite (3b) in the Tribes Hill strata is interpreted to have originated in a deeper-subsurface setting, associated with late-diagenetic stylolitization. The fine compositional zoning in Dolomite (3b) displays orange-red zones, formed in the shallow subsurface, followed by Fe-rich, nonluminescent zones formed in a deeper setting, which was further followed by orange-red luminescent zones, and in places, dedolomite. The dedolomite, being the product of a near-surface process, indicates uplift of the strata. The final stage of dolomitization post-dates the dedolomitization and is represented by burial-dolomite cements (Dolomite 6 & Dolomite 7) and ferroan, calcite cements.

The dolomite textures indicate that Dolomite (4) was a late-replacive stage, that postdated and replaced dolomites (2) and (3). Neomorphism and stabilization with time and burial, may have transformed the early formed dolomites to coarse, xenotopic mosaics of Dolomite (4), in which, as a result, the original oxygen-isotope content, and trace-element compositions were reset.

Dolomite (5), which occurs as void-filling cement and as a replacement, is seen to truncate or replace dolomite types 1, 2, 3, and 4. Compositionally, Dolomite (5) is suggestive of meteoric diagenesis that may be related to uplift of the strata. The dolomite-cement stratigraphy indicates that Dolomite (5) predates dedolomite and deep-burial cements. Dolomites 6 and 7 belong to the final stage of dolomitization, which operated in the deep subsurface where diagenetic fluids that were hypersaline and iron rich passed through the strata through solution vugs and fractures and finally occluded all pores. The paragenetic relationships clearly indicate that saddle dolomite (Dolomite 6) and Dolomite (7) postdate all the other dolomite types (Table 4).

4.4 Geochemistry of the Sauk dolomites:

4.4.1 Stable Isotope Values:

4.4.1.1 Carbon-isotopic compositions:

The isotopic values in this study are reported in $^{0}/_{00}$ PDB (Peedee belemnite). The carbon isotopic composition of dolomite gives information about the source of the carbon in the carbonate, as it reflects the ratio of inorganic

carbon derived from pre-existing limestone and dolomite to organic carbon derived from the microbial and thermal breakdown of organic matter (Allan and Wiggins, 1993).

The organic carbon that is incorporated into the dolomite may come from a number of organic reactions that convert organic matter (CH_2O) to CO_2 or bicarbonate (HCO_3^-). Listed below are specific organic reactions and the approximate range of $\delta^{13}C$ compositions of dolomites precipitated in conjunction with these processes (from Allan and Wiggins, 1993, p.33):

Process	**Reaction**	$\delta^{13}C_{dol}$
Oxidation	$CH_2O + O_2 \longrightarrow CO_2 + H_2O$	-5 to -15
SO_4 reduction	$2CH_2O + SO_4^{-2} \longrightarrow 2HCO_3^- + H_2S$	-5 to -15
Fermentation (methanogenesis)	$2CH_2O \longrightarrow CH_4 + CO_2$	+5 to +20
Methane Oxidation	$CH_4 + 2O_2 \longrightarrow CO_2 + 2H_2$	<-25
Oil degradation	$4CH_2 + 3SO_4^{-2} \longrightarrow 4HCO_3^- + H_2S + HS$	-5 to -15
Thermochemical SO_4 reduction	$CH_4 + SO_4^{-2} \longrightarrow HCO_3^- + HS^- + H_2O$	<-25
Decarboxylation	kerogen $\longrightarrow CO_2$ + kerogen	-5 to -15

Negative values of $\delta^{13}C$ are observed when CO_2 and bicarbonate incorporated into the dolomite result from the aerobic oxidation of organic matter within the sediments. The higher the supply of organic carbon in the pore fluid, the more negative are the resulting $\delta^{13}C$ values. Bacterial sulfate reduction and

fermentation or methanogenesis occur in anoxic pore fluids below the marine sediment-water interface. Sulfate reduction leads to production of ^{13}C depleted carbon, whereas CO_2 produced during methanogenesis displays a distinctly heavy signature, with values of $\delta^{13}C$ ranging from +5 to +20 $^{0}/_{00}$ PDB.

The oxidation of methane, by contrast, produces ^{12}C-enriched carbon, therefore resulting in depleted or negative $\delta^{13}C$ values. Thermochemical sulfate reduction takes place at high temperatures where methane is oxidized using SO_4 and results in generation of H_2S gas, formation of pyrite, native sulfur and late dolomite cement. This process also produces a negative $\delta^{13}C$ signature of <-25 $^{0}/_{00}$ PDB. Thermal decarboxylation or the thermal breakdown of kerogen releases CO_2, which may contribute $\delta^{13}C$ depleted carbon to dolomite cements in fractures and vugs.

The $\delta^{13}C$ values in the Sauk dolomites of this study are plotted in figures 4.39 and 4.40. The $\delta^{13}C$ measurements for the dolomites of the Upper Cambrian Little Falls, Galway and Hoyt formations lie between -0.3 and -3.2 $^{0}/_{00}$ PDB. Listed below are the specific ranges observed in the three formations:

Hoyt Formation:	-1.3 to -3.2 $^{0}/_{00}$
Galway Formation:	-0.7 to -2.6 $^{0}/_{00}$
Little Falls Formation:	-0.3 to -2.5 $^{0}/_{00}$

The marine baseline for the Upper Cambrian, represented by the $\delta^{13}C$ value of least-altered marine carbonates, from other studies of the Cambrian is -0.7 $^{0}/_{00}$ PDB (data from Allan and Wiggins, 1993, Appendix II). The carbon-

isotopic compositions listed above and plotted in figures 4.39A and 4.40 show that most values recorded in this study lie below this value. The $\delta^{13}C$ values that deviate by more than a few per mil from the marine baseline that is contemporaneous with the time of dolomitization signify organic contributions (Allan and Wiggins, 1993). The slightly depleted $\delta^{13}C$ values in the Upper Cambrian dolomites indicate that the carbon in the CO_3^{2-} in these units may have been derived in most part from the precursor carbonate with some contribution from the breakdown of organic matter.

In contrast, the carbon-isotope compositions for the Lower Ordovician rocks of the Gailor and Tribes Hill formations overlap with the values of least-altered marine carbonates of that time with some values that are either slightly enriched or depleted (figures 4.39B and 4.40). The marine baseline for the Early Ordovician is represented by $\delta^{13}C$ values that range from -1.5 to -0.5 $^{0}/_{00}$ PDB (data from Allan and Wiggins, 1993, Appendix II). The specific ranges of $\delta^{13}C$ observed in the Early Ordovician rocks of this study are listed below:

Tribes Hill Formation: -0.3 to -2.9 $^{0}/_{00}$

Gailor Formation: +0.1 to -1.8 $^{0}/_{00}$

The spread of $\delta^{13}C$ values of the Ordovician dolomites, suggests that the carbon in the CO_3^{2-} in these dolomites may have been derived in most part from the pre-existing limestones and dolomites.

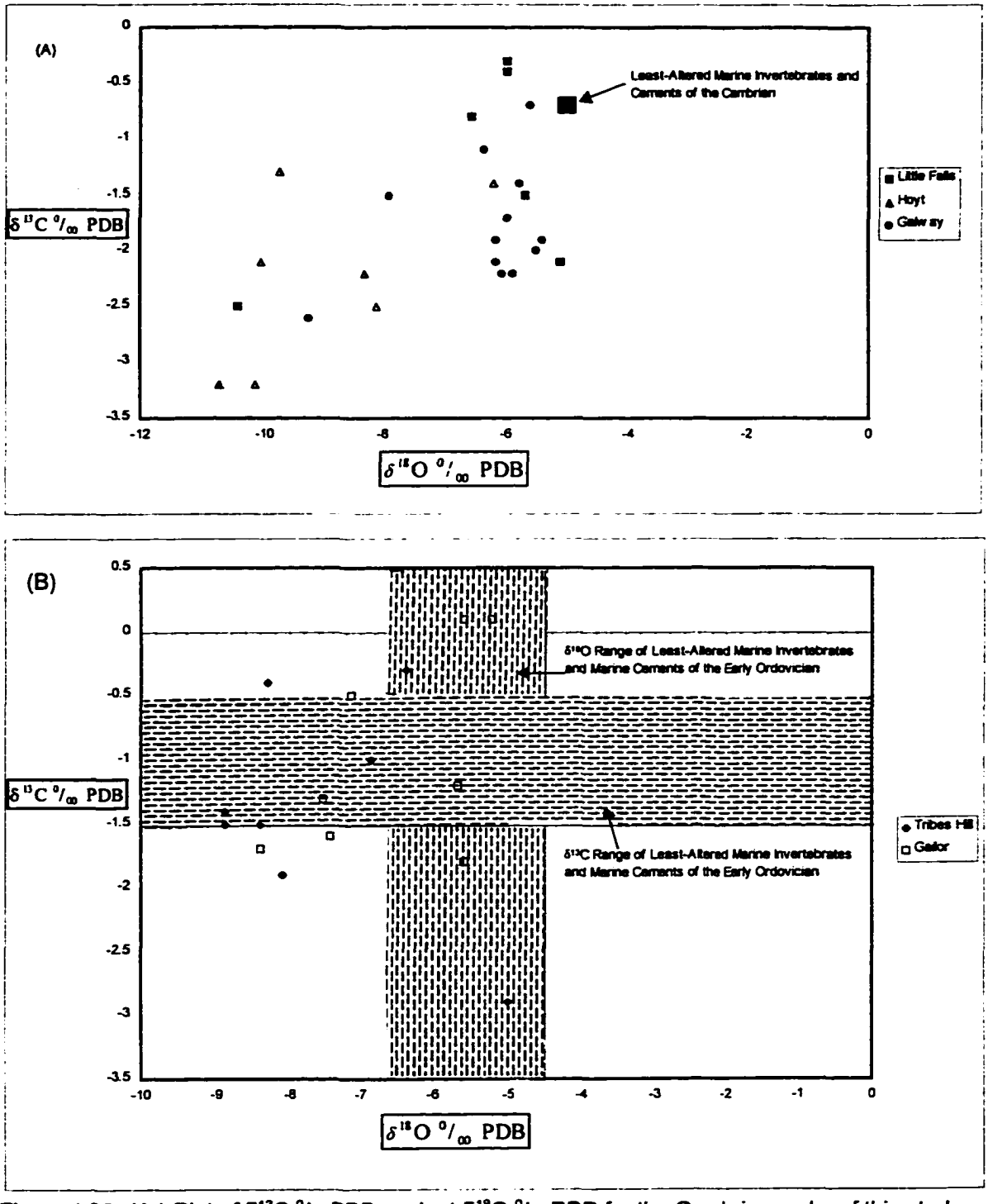

Figure 4.39: (A) Plot of $\delta^{13}C$ °/₀₀ PDB against $\delta^{18}O$ °/₀₀ PDB for the Cambrian rocks of this study. The blue square represents the $\delta^{13}C$ and $\delta^{18}O$ values of least-altered, marine invertebrates and marine cements of the Upper Cambrian (Data taken from Allan and Wiggins, 1993, Appendix II). (B) Plot of $\delta^{13}C$ °/₀₀ PDB against $\delta^{18}O$ °/₀₀ PDB for the Early Ordovician rocks of this study. The shaded areas represent values of $\delta^{13}C$ and $\delta^{18}O$ values of least-altered, marine invertebrates and marine cements of the Early Ordovician (Data taken from Allan and Wiggins, 1993, Appendix II).

Figure 4.40: Stable Isotope Variations in the Sauk Carbonates

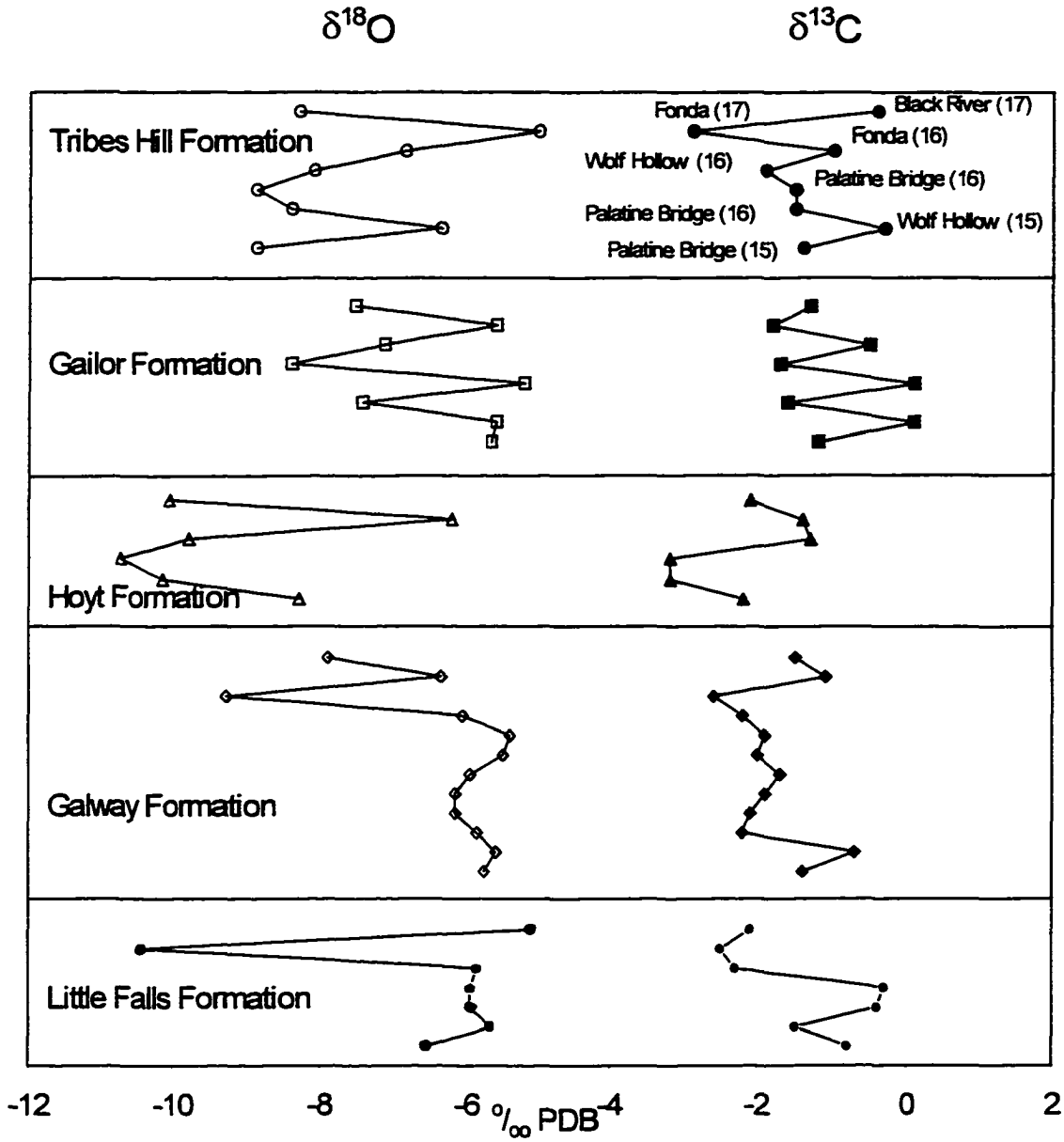

Explanation: The oxygen and carbon isotopic compositions of the Sauk carbonates sampled for this study are plotted vertically in the order they occur in the outcrops. The Upper Cambrian Little Falls, Galway and Hoyt formations are followed upwards by the younger Lower Ordovician Gailor and Tribes Hill formations. For the Tribes Hill formation, the member names with the outcrop numbers in parentheses are noted next to the points. The carbon isotopic values display a slight shift from negative values in the Upper Cambrian towards more positive values in the Lower Ordovician.

The slightly depleted $\delta^{13}C$ values that are observed in the rocks of this study are hard to link to a single carbon source. This is due to the fact that, when the carbon in the mineral is derived from a combination of inorganic and organic sources, the 'organic'-isotope signal is diluted and hence difficult to interpret. However, as extremely positive or extremely negative $\delta^{13}C$ values are not noted in these rocks, the contribution of organic carbon from methanogenesis, methane oxidation, and thermochemical sulfate reduction can be ruled out.

It is likely that some oxidation of organic matter and/or bacterially induced sulfate reduction may have occurred in the organic-rich intertidal-flat sediments of the Sauk strata in this study. Sulfate reduction promotes dolomitization by removing the sulfate ion which is an inhibitor to dolomite precipitation (Baker and Kastner, 1981) and increasing the carbonate alkalinity. In the upper part of the Sauk, especially in the Tribes Hill and Gailor formations, disseminated pyrite is common, which is a byproduct of sulfate reduction. In the sulfate-reduction zone, where conditions are anoxic, the H_2S produced by the oxidation of organic matter by sulfate-reducing bacteria reacts with reduced iron to form metastable monosulfides that later transform to pyrite (Berner, 1970; Compton, 1988; Hesse, 1990 b).

Carbon-isotopic compositions of marine limestones and dolostones have also been used by several workers for correlation of global paleoenvironmental changes (Friedman, et. al., 1996; Friedman and Chakraborty, 1997; Bowring et. al., 1998; Brasier and Sukhov, 1998; Saltzman et.al, 1998). These studies have

demonstrated that marked temporal oscillations in $\delta^{13}C$ and in particular, positive or negative excursions in the isotope profile may reflect climatic extremes and pronounced changes in sealevel, tectonics, and the biosphere.

A negative excursion in the $\delta^{13}C$ at the Permian-Triassic boundary has been related to the mass extinction at the end of the Permian (Bowring et.al., 1998). A large positive $\delta^{13}C$ excursion in the Late Cambrian known as the SPICE excursion has been globally correlated and has been linked to a worldwide extinction event as well (Saltzman et. al., 1998). A similar positive $\delta^{13}C$ excursion has been reported at the Precambrian-Cambrian boundary, which has been related to climatic change from icehouse to greenhouse conditions that was associated with global extensional tectonics, which in turn may have affected organic-matter production, oxidation, and burial resulting in the positive shift of $\delta^{13}C$ values (Friedman et. al., 1996, 1997).

A positive $\delta^{13}C$ excursion can result from (1) increased rate of preservation of organic matter in the ocean and (2) increased rate of photosynthetic organic carbon production in the ocean and therefore increased biomass (Friedman et. al., 1996, 1997). These processes extract ^{12}C from the seawater thus making it more enriched in ^{13}C. A negative excursion, by contrast, may result from large-scale oxidation of organic matter or a decrease in biomass.

The plot of $\delta^{13}C$ values in Figure 4.40, shows carbon-isotope variations observed in the five formations of the Sauk strata that were examined for this study. The data are arranged in a vertical sequence such that the Upper

Cambrian formations, namely Little Falls, Galway and Hoyt are followed upwards by the Gailor and finally the stratigraphically youngest Tribes Hill Formation (refer to Table 1 for the stratigraphic succession).

In general , the $\delta^{13}C$ compositions display some oscillations, but are however, mostly negative in value. The $\delta^{13}C$ values reported from the Upper Cambrian sections range from -0.3 to -3.2 $^{0}/_{00}$. In comparison, the values in the Lower Ordovician rocks range from +0.1 to - 2.9 $^{0}/_{00}$. Thus, there appears to be a shift towards more positive $\delta^{13}C$ values in the Early Ordovician. This positive shift is however small compared to the major excursions reported in other studies (Friedman, et. al., 1996; Friedman and Chakraborty, 1997; Bowring et. al., 1998; Brasier and Sukhov, 1998; Saltzman et.al, 1998) and is therefore difficult to interpret.

In addition, the positive excursion in $\delta^{13}C$ (-0.5 to 4.5 $^{0}/_{00}$) that was globally correlated in the Late Cambrian, known as the SPICE excursion (Saltzman et.al, 1998) was found in rocks that are perhaps correlatable with the Galway Formation of this study. However, no such dramatic shifts in the $\delta^{13}C$ values are observed in the Galway or any of the Upper Cambrian formations that were examined for this study.

4.4.1.2 Oxygen-isotopic compositions:

The oxygen-isotopic composition of the carbonate minerals depends on the composition of the precipitating water and on the temperature of precipitation

(Allan and Wiggins, 1993; Friedman and Chakraborty, 1997). According to Montanez and Read (1992), dolomite precipitated from evaporatively concentrated Early Ordovician seawater at or near gypsum saturation, at slightly elevated temperatures of sabkha porewaters (30 to 40 ^{0}C) would display $\delta^{18}O$ values from -3.5 to 2.0 $^{0}/_{00}$ PDB. This is because the ocean water will be enriched in ^{18}O, under highly evaporative conditions. As a result there is a positive correlation between salinity and oxygen isotopic composition (Friedman et. al., 1996; Friedman and Chakraborty, 1997). In contrast, there is an inverse correlation between the temperature of precipitation and the degree of enrichment of ^{18}O in the carbonate mineral. Therefore at high temperatures of precipitation carbonate minerals display more depleted values of $\delta^{18}O$.

The Upper Cambrian dolomites of this study show a range of values from -5.1 to -10.73 $^{0}/_{00}$. These values are depleted compared to the value of nonaltered marine invertebrates and cements for that period (-5.0 $^{0}/_{00}$). The Lower Ordovician dolomites of this study exhibit $\delta^{18}O$ values between -5.00 and -8.88 $^{0}/_{00}$, whereas the unaltered marine cements and micrites from other studies have values between -6.6 and -4.5 $^{0}/_{00}$ PDB (Figure 4.39). These depleted $\delta^{18}O$ values reflect recrystallization during burial by waters depleted in ^{18}O relative to seawater and or diagenetic fluids at elevated temperatures. The early diagenetic dolomites display more enriched $\delta^{18}O$ compositions, while the late-diagenetic saddle dolomites and stylolite-related dolomites are extremely depleted. The $\delta^{18}O$ values of the main-stage, replacement dolomites of intermediate burial are

more depleted than the early dolomites, but more enriched compared to the deep-burial dolomites (Figure 4.3).

4.4.2 Paleotemperatures:

Figure 4.41 shows the isotopic compositions of the different dolomite types in this study and their distribution compared to the accepted range of high-temperature (burial) and low-temperature (near-surface) dolomites (Allan and Wiggins,1993). The distribution of isotopic values within the zone of overlap between the low- and high-temperature dolomites and mostly within the zone of high-temperature dolomites, reflect the long diagenetic history of these Sauk carbonates, spanning the entire spectrum of near-surface, shallow-, and deep-burial environments.

The isotopic values of early formed, fine-textured dolomites (1 and 2) plot mostly within the zone of overlap between high- and low-temperature dolomites. The pervasive, replacement dolomites (3a) and (4), that range in size from medium- to coarse-textured mosaics, display isotopic values that lie in the zone of high-temperature dolomites as well as within the zone of overlap. The late-stage, deep-burial dolomite cements (6 and 7) show values that are consistent with high-temperature dolomites. The distribution of isotopic values of the partially replaced limestones of the Hoyt and Tribes Hill formations indicate that dolomitization may have occurred at high temperatures. Dolomitization in the

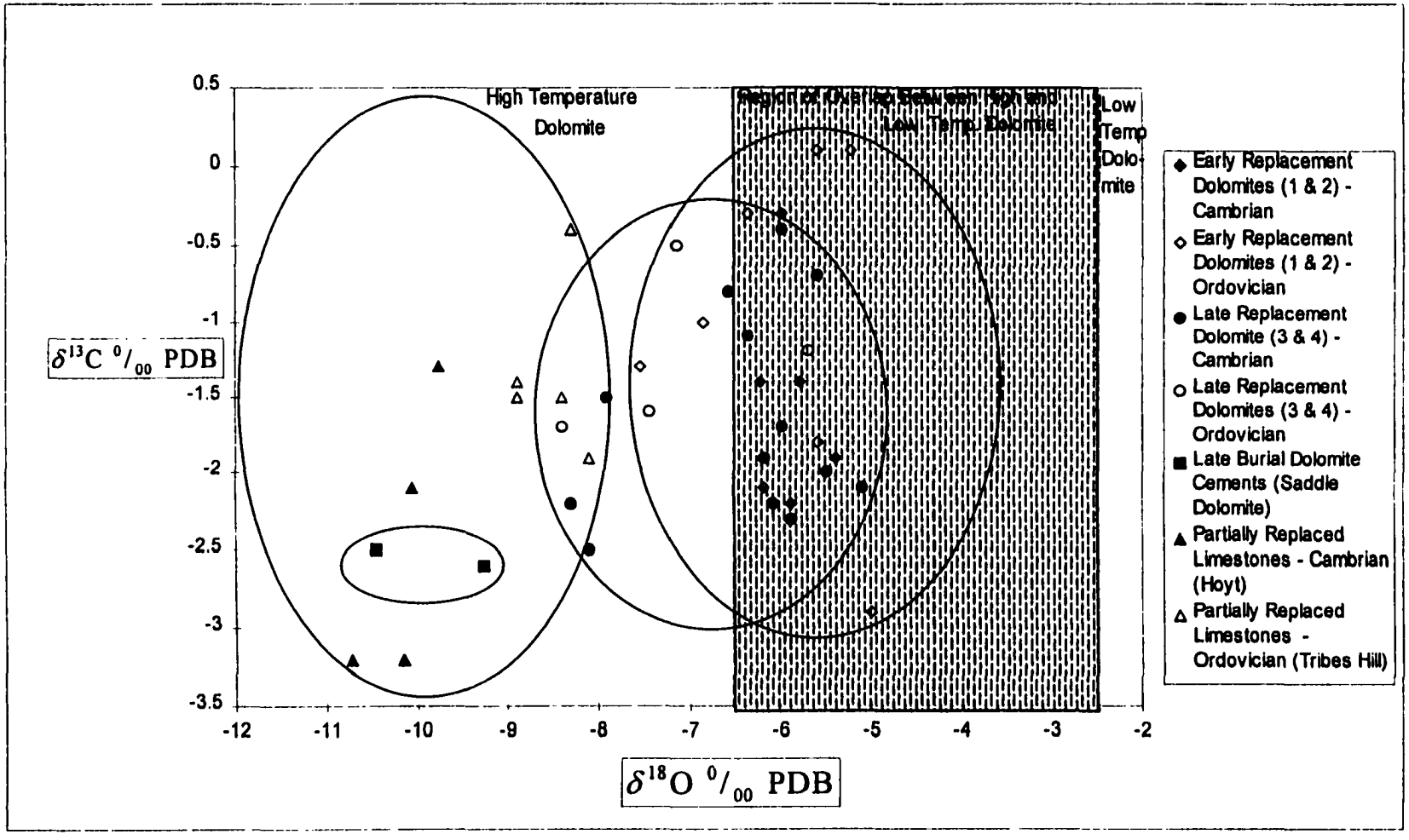

Figure 4.41: Carbon and oxygen isotopic compositions of the Sauk Sequence carbonates of this study are compared with isotopic ranges of most "high temperature" and "low temperature" dolomites of a variety of ages that span most of the Phanerozoic. The shaded area represents the region of overlap between high and low temperature dolomite (that lies between $\delta^{18}O$ values of -6.5 $^0/_{00}$ and -2.5 $^0/_{00}$ PDB). Most Phanerozoic low temperature dolomites (represented by the unshaded area to the right) have $\delta^{18}O$ values that range from -6.5 to +9.0 $^0/_{00}$ PDB, whereas high temperature burial dolomite and dolomite cements of various ages (represented by the unshaded area to the left) have $\delta^{18}O$ values that range from - 16 to -2.5 $^0/_{00}$ PDB. The temperature data for Phanerozoic dolomites from other studies was taken from Allan and Wiggins, 1993 p. 27.

Hoyt and Tribes Hill strata, which are only partly dolomitized, was relatively late in their diagenetic history. The common dolomite types in the Hoyt and Tribes Hill formations are Dolomite (3a), Dolomite (3b), and Dolomite (4), which were all formed during late replacement in the burial environment at elevated temperatures. The dolomites in the Tribes Hill units (especially Dolomite 3b) are intimately related to stylolite formation, which implies a post-compaction, burial origin. Thus dolomitization by burial waters at elevated temperatures was possibly responsible for the depleted oxygen-isotopic compositions of the Hoyt and Tribes Hill formations.

The temperature of dolomitization can be calculated from the oxygen-isotopic compositions using Friedman and O' Neil's (1977) equation:

$$[3.2 * 10^6 T (^0 K)^{-2}] - 1.5 = \delta^{18}O_{dol} - \delta^{18}O_{water} \quad ------ (1)$$

In this equation, 'T' is the temperature of dolomitization, $\delta^{18}O_{dol}$ is the measured value of the oxygen-isotopic composition of the dolomite and $\delta^{18}O_{water}$ is the estimated value of the oxygen-isotopic composition of water.

The problem with this approach is that the oxygen-isotopic composition of the dolomitizing fluid ($\delta^{18}O_{water}$) is not known. However, the $\delta^{18}O_{water}$ can be estimated using the approach suggested by Allan and Wiggins (1993 p.19). In their method, the fluid-inclusion homogenization temperature (Th, which gives an estimate of the minimum temperature of crystallization of the host mineral), from a sample, for which both fluid-inclusion and isotope data are known, is used. Substituting the Th for T in equation (1), the $\delta^{18}O$ of the dolomitizing fluid can be

calculated. This calculated value of $\delta^{18}O_{water}$ can then be used to calculate the dolomitizing temperature of other dolomites for which $\delta^{18}O_{water}$ is not known.

Fluid-inclusion analysis was not carried out in this study. However, fluid-inclusion studies on the Sauk carbonates of the Saratoga platform have been carried out by other workers (Urschel and Friedman, 1984; Sarwar, 1992; Sarwar and Friedman, 1994). Data from one sample of a dolomite vein from the Tribes Hill Formation that was analyzed by Urschel and Friedman (1984) was used to calculate the value of $\delta^{18}O_{water}$ by substituting the fluid inclusion homogenization temperature (112.9 ^{0} C) for 'T' and the $\delta^{18}O$ value (-9.91 $^0/_{00}$ PDB) for $\delta^{18}O_{dol}$ in equation (1). Thus, the value of $\delta^{18}O_{water}$ for the Tribes Hill sample (from Urschel and Friedman, 1984) was determined to be 0.6560 $^0/_{00}$ SMOW. This value was then substituted for $\delta^{18}O_{water}$ in equation (1) and used to calculate the temperature of dolomitization of the different dolomite samples in this study for which the oxygen-isotope values were measured.

Table 5 contains the measured isotopic and calculated temperature data for the Sauk carbonates of this study. The temperature of dolomitization ranges from 74.21 ^{0}C to 120.71 ^{0}C. These values are not as high as those from vug- and fracture-filling dolomite and calcites of the Galway, Hoyt and Gailor formations, noted by Sarwar and Friedman (1994) (Table 6). Their measured values of maximum homogenization temperature (Th_{max}) range from 224 to 245 ^{0} C. High-salinity values ranging from 4.78 to 29.2 wt% NaCl were also reported

Table 5: STABLE ISOTOPIC COMPOSITIONS AND CALCULATED TEMPERATURES OF THE SAUK CARBONATES IN THIS STUDY

Description		Sample	$\delta^{18}O$ PDB	$\delta^{13}C$ PDB	Temp (°C)
GALWAY FORMATION					
Replacement Dolomite-1		GB-1	-5.39 ‰	-1.9 ‰	76.9
Replacement Dolomite-4		GB-1	-5.49 ‰	-2.0 ‰	77.5
Replacement Dolomite-4		GB-2	-5.97 ‰	-1.7 ‰	80.9
Replacement Dolomite-3a		GB-6	-5.59 ‰	-0.7 ‰	78.2
Replacement Dolomite-2		GB-8	-5.88 ‰	-2.2 ‰	80.3
Replacement Dolomite-1		GB-10	-6.17 ‰	-2.1 ‰	82.3
Replacement Dolomite-4		GB-13	-6.17 ‰	-1.9 ‰	82.3
Replacement Dolomite-3a		GA-2	-6.36 ‰	-1.1 ‰	83.7
Saddle Dolomite-6		GA-3	-9.27 ‰	-2.6 ‰	107.1
Replacement Dolomite-4		GA-3	-6.07 ‰	-2.2 ‰	81.6
Replacement Dolomite-1		B-3	-5.78 ‰	-1.4 ‰	79.6
Replacement Dolomite-4		R-5	-7.91 ‰	-1.5 ‰	95.7
HOYT FORMATION					
Partially Dolomitized Limestone with Calcite-1 & Dolomite-4		SQ-1	-10.05 ‰	-2.1 ‰	114.2
Replacement Dolomite-4		PG-1	-8.11 ‰	-2.5 ‰	97.2
Stromatolite with Calcite-1 & Dolomite-3a		PG-6	-10.73 ‰	-3.2 ‰	120.7
Replacement Dolomite-4		PG-8	-8.30 ‰	-2.2 ‰	98.8
Dolomitized Ooids with Replacement Dolomite-4		PG-10	-10.15 ‰	-3.2 ‰	115.1
Dolomitized Ooids with Replacement Dolomite-4		LP-1	-9.76 ‰	-1.3 ‰	111.5
Replacement Dolomite-2		LP-4	-6.21 ‰	-1.4 ‰	86.6
GAILOR FORMATION					
Replacement Dolomite-2		BS-1	-7.53 ‰	-1.3 ‰	92.6
Replacement Dolomite-2		BS-6	-5.59 ‰	-1.8 ‰	77.5
Cement Dolomite-5		BS-9	-7.14 ‰	-0.5 ‰	89.6
Replacement Dolomite-2		GL-4	-5.59 ‰	+0.1 ‰	78.2
Replacement Dolomite-4		GL-5	-7.43 ‰	-1.6 ‰	91.8
Replacement Dolomite-2		GL-9	-5.20 ‰	+0.1 ‰	75.5
Replacement Dolomite-3a		FJ-6	-5.68 ‰	-1.2 ‰	78.9
Cement Dolomite-5		FJ-11	-8.40 ‰	-1.7 ‰	99.6
LITTLE FALLS FORMATION					
Replacement Dolomite-3a		H/1	-6.56 ‰	-0.8 ‰	85.2
Saddle Dolomite-6		H/3	-5.68 ‰	-1.5 ‰	78.9
Replacement Dolomite-3a		H/6	-5.97 ‰	-0.4 ‰	80.9
Replacement Dolomite-3a		H/8	-5.10 ‰	-2.1 ‰	74.9
Saddle Dolomite-6		H/8	-10.44 ‰	-2.5 ‰	117.9
Replacement Dolomite-2		H/11	-5.97 ‰	-0.3 ‰	80.9
Replacement Dolomite-3a		H/13	-5.88 ‰	-2.3 ‰	80.3
TRIBES HILL FORMATION					
Replacement Dolomite-3a	(Pal. Bridge mem.)	16/2	-8.88 ‰	-1.4 ‰	103.8
Replacement Dolomite-3a	(Wolf Hollow mem.)	16/7	-6.36 ‰	-0.3 ‰	83.7
Replacement Dolomite-3b	(Pal. Bridge mem.)	V-1	-8.40 ‰	-1.5 ‰	99.6
Calcite-1	(Pal. Bridge mem.)	V-2	-8.88 ‰	-1.5 ‰	103.8
Replacement Dolomite-3b	(Wolf Hollow mem.)	V-5	-8.11 ‰	-1.9 ‰	97.2
Replacement Dolomite-2	(Fonda mem.)	V-10	-6.85 ‰	-1.0 ‰	87.3
Replacement Dolomite-3a	(Fonda mem.)	TB-2	-5.00 ‰	-2.9 ‰	74.2
Peloidal Limestone with Calcite-1	(Black Rr. Grp)	TB-5	-8.30 ‰	-0.4 ‰	98.8

for the Galway, Hoyt and Gailor samples from their measured fluid inclusion melting temperatures (Tm) (Table 6).

The temperature and salinity data reported by Sarwar and Friedman's study, indicate the maximum temperatures and salinities, that were probably reached during the formation of the fracture- and void-filling cements, when the Sauk strata underwent deep burial. Maximum burial depths ranging from 6.8 to 7.5 km have been calculated for these rocks (Table 6). In comparison, the temperature values calculated for the dolomites in this study (Table 5) are estimates of minimum dolomitization temperatures.

Assuming a paleogeothermal gradient of 30 ^{0}C/km and a mean annual surface temperature of 20 ^{0}C (Sarwar and Friedman, 1994), the temperature data in Table 5, suggests that dolomitization took place in a range of burial depths, from approximately 1.8 to 3.36 km. These depth values differ from the maximum depths reported by Sarwar and Friedman's study, largely because these values are calculated for replacement dolomites and some burial cements whereas their values are only for void-filling and fracture-filling cements. Another reason for the disparity between the results is perhaps due to the fact that the depths calculated in this study are based on estimates of minimum temperatures of dolomitization.

Table 6: Fluid Inclusion data and calculations of salinity and maximum burial depth for Sauk Carbonates on the Saratoga Platform (Data from Tables 1 and 4 of Sarwar and Friedman, 1994)

LOCATION #. (Sarwar & Friedman, 1994)	LOCATION (This study)	ROCK UNIT (Fmn.)	TYPE OF CEMENT	HOMOGENI-ZATION TEMP. (Th_{max}) °C	MELTING TEMP. (Tm) °C	FLUID SALINITY (equiv. Wt% NaCl)	MAXIMUM DEPTH OF BURIAL (Km)
73	Outcrop #4 (Route 9N)	Galway	Vug-fill. Dol. Vug-fill. Qtz.	224 189	-24 -30	25.34 29.2	6.8
74	Route 29	Hoyt	Vug-fill. Cal.	239	N.A.	—	7.3
75	Outcrop #2 (Route 29)	Galway	Vug-fill. Dol.	236.6	-20.6	23.08	7.2
76	Outcrop #10 (Route 67)	Gailor	Fract.-fill. Cal.	225	-10, -15, 10.4	13.98, 18.78, 14.40	6.8
77	Outcrop #11 (Route 67)	Gailor	Vug-fill. Cal.	245	-22, -12, -2.9	24, 16, 4.78	7.5

4.4.3 Trace-Element Distribution:

The Sr contents in these dolomites vary from 0 to as high as 1434 ppm. Most of the high values ranging from 120 to 800 ppm occur in early dolomites or zoned late dolomites where they are perhaps remnants of early-formed dolomites. In general Sr is absent in the late-diagenetic dolomites. The high Sr values that are consistently above 155 ppm may be inferred to indicate early dolomites to have formed from supersaturated evaporitic / hypersaline brines in a syndepositional peritidal setting (Machel and Anderson,1989). The otherwise low or absent Sr may reflect diagenetic modification of unstable precursor dolomites. The dissolution and precipitation during recrystallization causes Sr to be depleted in the recrystallized dolomites (Land,1980). Thus, neomorphism or

recrystallization during or after dolomitization could be partly responsible for the low Sr contents in the late-diagenetic dolomites.

The Fe and Mn concentrations are generally high in the Sauk dolomites and lower in the nondolomitized limestone matrix. Distribution coefficients of Fe and Mn in carbonates are greater than one and thus they are incorporated in the dolomites during diagenesis (Veizer and Demovic, 1974; Land, 1985). Fe contents increase with burial and are especially high in stylolite-related dolomites (Dolomite 3b) and in saddle dolomites (Dolomite 6) indicating highly reducing burial environments. The dolomites inferred to have resulted from meteoric fluids (Dolomite 5) are lower in Fe reflecting less reducing conditions.

4.4.4 Geochemical Trends:

The following differences are seen between late-diagenetic dolomites which have stabilized more with progressive diagenesis compared to early-diagenetic dolomites. The late-diagenetic dolomites are :

(1) more stoichiometric than early formed dolomites;

(2) coarser than early dolomite;

(3) more depleted in $\delta^{18}O$ and Sr^{2+};

(4) more enriched in Fe^{2+} and Mn^{2+};

These geochemical differences imply that early dolomite formed from modified seawater in the depositional environment and soon after, whereas late dolomite formed by:

(1) recrystallization or neomorphism of early formed dolomite;

(2) replacement of limestone at elevated temperatures;

(3) cementation in fractures and secondary pore spaces;

Similar textural and geochemical patterns have been recognized by several authors in other dolomitized sequences (Banner and others, 1988; Cander and others, 1988; Qing and Mountjoy, 1989; Amthor and Friedman, 1991, 1992; Montanez and Read, 1992; Farr, 1992; Qing, 1998; Wendte and others, 1998).

CHAPTER 5 - SILICIFICATION

5.1 Types of Silicification:

In the Sauk carbonates of this study, the products of silicification are observed in the form of chert, authigenic quartz, and authigenic feldspar. Chert is observed in the Galway, Little Falls and Gailor formations and is virtually absent in the Hoyt and Tribes Hill formations. Authigenic quartz and feldspar occur throughout the sequence in minor amounts.

5.2 Chert:

Chert in these strata occurs as massive beds, as intergranular cement in sandstones, as laminated layers in dolostone, as interstitial cements in dolomites, as fracture filling cement or as pods in dolostones. The main fabrics observed are:

- microcrystalline granular quartz (<20μm)
- megaquartz (>20μm)
- spherulitic chalcedony
- chalcedonic overlays

5.2.1 Microcrystalline Quartz:

Microcrystalline quartz consists of tiny crystals of quartz that are less than 20μm in diameter. They display an equigranular texture with pin-point extinction.

Folk and Pittman (1971) term this microquartz. This type of texture is noted only in outcrops of the Little Falls and Gailor formations.

In the Little Falls Formation, microcrystalline quartz occurs as matrix around detrital sand-sized quartz grains, which show signs of dissolution (Figure 5.1). Very fine crystals of calcite and dolomite also occur in the matrix. This indicates that dolomitization of the precursor carbonate, possibly a micrite was arrested by silicification.

Silicified ooids are observed in elongate pods of chert, which form a discontinuous layer within a dolostone bed in the Little Falls section (outcrop #14). The ooids display concentric and radial structures and are completely replaced by microcrystalline quartz. In addition, the interparticle submarine, acicular cements, between the ooids, appear to have been replaced by fibrous quartz (Figure 5.2). In these oolitic grainstones, silicification is pervasive. It can therefore be deduced that silicification took place subsequent to complete cementation of the oolitic limestone. However, as the ooids do not appear to have been subjected to any physical distortion, silicification may have occurred fairly early in the diagenetic history, prior to any physical compaction of the host rock. Late fractures filled with calcite crosscut these chert pods.

The textural relations indicate that replacement of micritic matrix in sandy carbonates was perhaps an early-diagenetic event. Early dolomitization of the micrite was interrupted by silicification. The high microporosity and high surface

Figure 5.1: Partially dolomitized, sandy chert from the Little Falls Formation (sample # H/2, outcrop # 14). Dolomite appears pale brown with patches of red where stained by Alizarin Red 'S'. The matrix is composed of microcrystalline quartz with pinpoint extinction. Dolomitization was interrupted by silicification that formed microcrystalline quartz. Some detrital quartz grains show dissolution (arrow). The red stained patches within the dolomites, indicate later dedolomitization of the early-formed dolomite. Thin section is viewed under crossed nicols.

Figure 5.2: Thin-section photomicrograph of completely silicified oolitic grainstone from the Little Falls Formation (sample # H/7, outcrop # 14). The ooids are replaced by microquartz (M) and the early marine, fibrous cements by fibrous chalcedony (C). Thin section is viewed under crossed nicols.

area of the fine-textured lime muds may have facilitated replacement, provided chemical conditions were favorable.

The silicification of the oolitic grainstones is also inferred to be an early diagenetic phenomenon. This silicification may have been related to emergence of oolite shoals above sea level when they were invaded by meteoric water. For silicification to occur the pore solution must be acidic, supersaturated with respect to silica and undersaturated with respect to the carbonate minerals dissolved. According to Knauth's (1979) model for chert in shallow-water carbonates, meteoric water circulating through shallow-water carbonates may be mixed with marine pore fluids forming a geochemical environment conducive to calcite dissolution and simultaneous silica precipitation.

In some of the chert beds of the Gailor Formation that are interbedded with dolostones, finely laminated chert (Figure 5.3) is common. This texture is observed in the Pallette Quarry (outcrop #13). In the same rocks are seen pods of spherulitic chalcedony surrounded by dolomite (Figure 5.4). The extremely fine texture of the microcrystalline quartz in these finely laminated cherts, indicates that silicification is likely to have occurred by the replacement of the fine lime muds on the tidal flats.

In other examples of chert in the Gailor Formation, in particular at outcrop #12, it is evident that dolomitization was interrupted by silicification. Scattered clusters of dolomite occur surrounded by microcrystalline quartz (Figures 4.15, 5.5). The etched or corroded borders of the dolomite rhombs indicate that

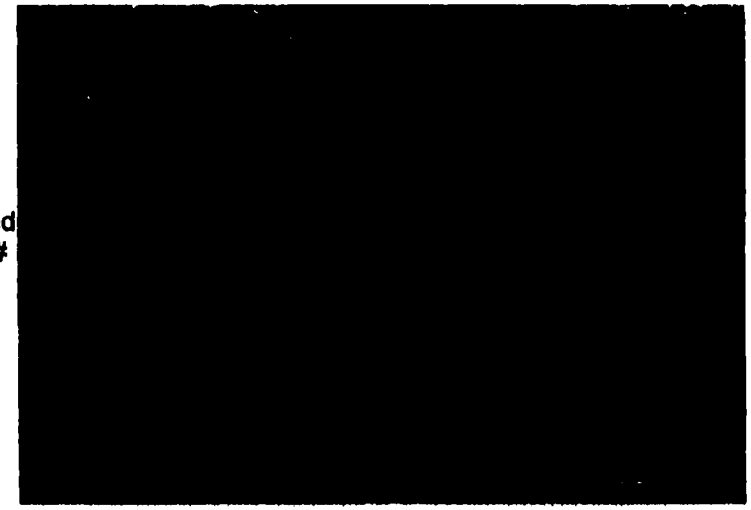

Figure 5.3: Thin-section photomicrograph of finely-laminated chert from the Gailor Formation (sample # GL-29, outcrop # 13). Thin section is viewed under crossed nicols.

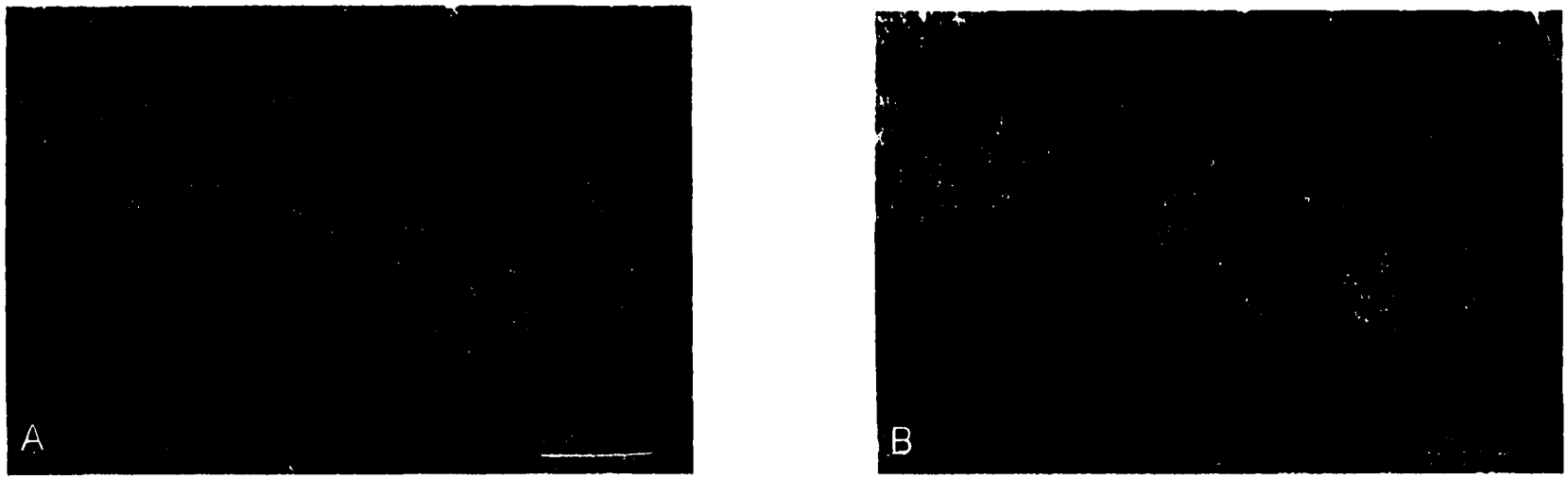

Figure 5.4: Thin-section photomicrograph of chert associated with dolomite in the Gailor Formation (sample # GL-29, outcrop # 13). Pods of spherulitic chalcedony (Chal.) occur within replacement mosaic of dolomite. Corroded rhombs of dolomite are seen within the pods of chalcedony, indicating that in this example, silicification postdated dolomitization. (A) is viewed in plane-polarized light and (B) under crossed nicols.

Figure 5.5: Thin-section photomicrograph of dolomitic chert from the Gailor Formation (sample # GL-22, outcrop #12). Euhedral rhombs of dolomite are seen floating in microcrystalline quartz. The rhombs are etched in places indicating that they predate the silicification and were subjected to slight dissolution and replacement by silica. Thin section is viewed under crossed nicols.

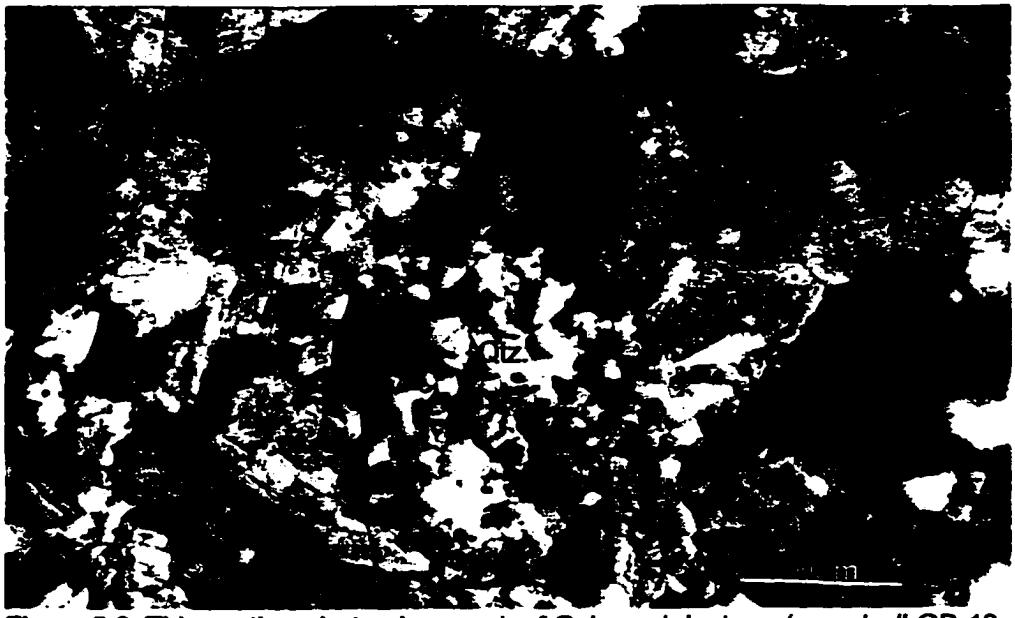

Figure 5.6: Thin-section photomicrograph of Galway dolostone (sample # GB-13, outcrop #1), containing clusters of megaquartz that has replaced the Dolomite (4) mosaic in places. The etched crystals of Dolomite (4) show that silicification postdated dolomitization. Thin section is viewed under crossed nicols.

dolomitization antedated silicification. In places, dolomite has been replaced by dedolomite as well (Figure 4.15).

5.2.2 Megaquartz:

Megaquartz occurs as replacive mosaics or as cement in voids with a progressive increase in size towards the center of the void. This type is generally 20μm or greater in size.

In the Galway Formation (Figure 5.6) megaquartz is seen to replace Dolomite (4) mosaics. In this example, the corroded margins of dolomite rhombs, where associated with the megaquartz clusters, indicate that silicification postdated dolomitization. The megaquartz patches are also associated with detrital grains of quartz and feldspar which sometimes have corroded margins (Figure 5.7). Isolated euhedral, doubly terminated, quartz crystals are also seen poikilotopically within the dolomite. In comparison with the megaquartz clusters, the authigenic quartz euhedra appear to antedate dolomitization. In figure 5.7, it can be seen that the euhedral quartz crystal has been corroded at the rim and occurs surrounded by coarse dolomite. The presence of doubly terminated quartz crystals, within these Galway dolostones may point to the presence of former evaporites (Friedman and Shukla, 1980). The authigenic quartz is likely to have filled voids created where sulfates, that were possibly present in the lime muds of the peritidal environment, were dissolved. In places, fitted particle to particle contacts are observed between

Figure 5.7:Thin-section photomicrograph of Galway dolostone (sample # GB-13, outcrop #1), where detrital and authigenic quartz occurs scattered within the dolomite mosaic. Fitted margins between detrital quartz and saddle dolomite indicate chemical compaction. Arrow points to crystal of doubly-terminated, authigenic quartz, that displays corroded margins. Thin section is viewed under crossed nicols.

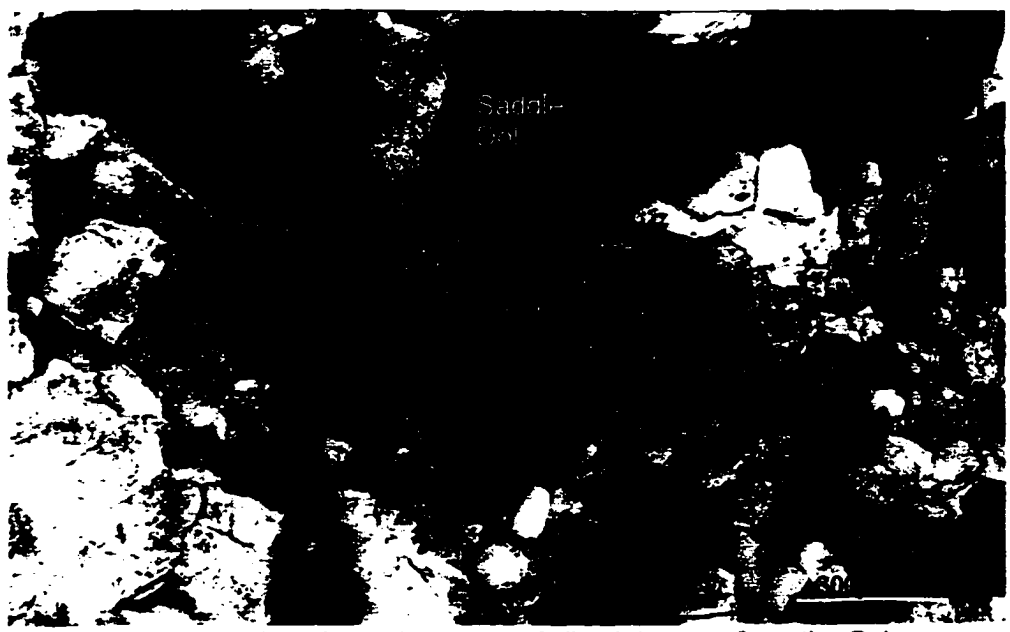

Figure 5.8:Thin-section photomicrograph of silty dolostone from the Galway Formation (sample # GB-13, outcrop #1). Fitted fabric of saddle dolomite and detrital quartz shows effects of chemical compaction. This may have been a source of Mg and silica for later dolomitization and silicification. Thin section is viewed under crossed nicols.

the detrital quartz and saddle dolomites (Figure 5.8), which is an artefact of late-diagenetic pressure dissolution.

These textural relations indicate that silicification occurred in two phases, first during early diagenesis, antedating dolomitization and next during late diagenesis, postdating Dolomite (4) and saddle dolomite. The late-diagenetic phase of silicification, may also postdate burial compaction and related pressure dissolution. The silica for the formation of megaquartz may have been derived locally from the pressure dissolution of detrital quartz and feldspar.

In chert beds of the upper Gailor Formation, associated with karst breccia, pervasive silicification of precursor carbonate has resulted in a microcrystalline quartz matrix with scattered allochems replaced by megaquartz clusters and spherulitic chalcedony (length-slow) (Figures 5.9, 5.4). Scattered rhombs of dolomite in the microcrystalline quartz matrix suggest that dolomitization was interrupted by silicification which proceeded to completion. The dolomite rhombs, however, resisted silicification. Wendte et. al. (1998) also report similar isolated rhombs of dolomite within chert in the Devonian Swan Hills platform carbonates. Fractures filled with chalcedonic overlays (Figure 5.10) and megaquartz cements crosscut the matrix. The chalcedonic overlays are also length-slow. Late fractures filled with Dolomite (7) and dedolomite postdate the chert. The dolomite within the chert also has been dedolomitized.

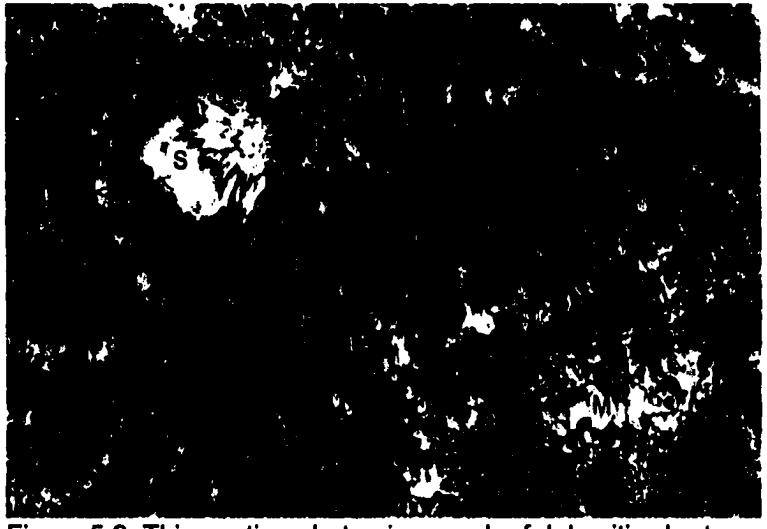

Figure 5.9: Thin-section photomicrograph of dolomitic chert from the Gailor Formation (sample # GL-22, outcrop #12). Pockets of spherulitic clacedony (S) and megaquartz (M) occur in a matrix composed of microcrystalline quartz. Thin section is viewed under crossed nicols.

Figure 5.10: Thin-section photomicrograph of dolomitic chert from the Gailor Formation (sample # GL-22, outcrop #12). Fibrous length-slow chalcedony fills fractures in a microcrystalline quartz mosaic. A patch of very fine-crystalline dolomite occurs adjacent to fracture. Center of void is filled with megaquartz. Thin section is viewed under crossed nicols.

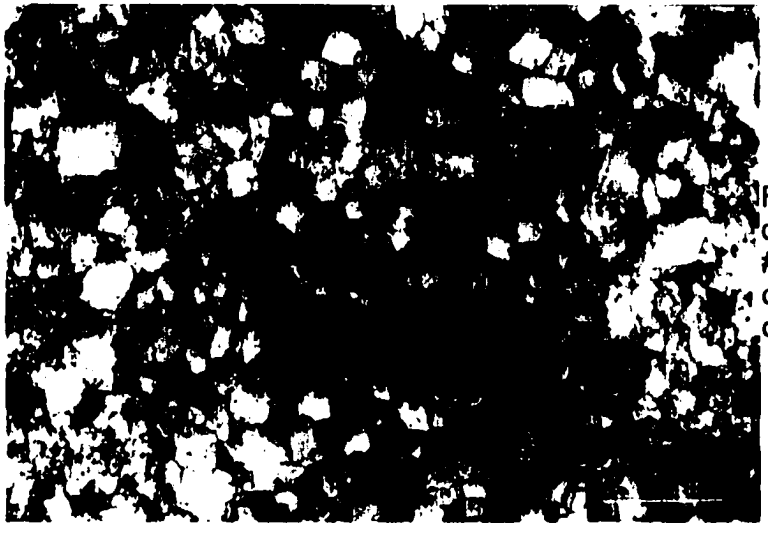

Figure 5.11:Thin-section photomicrograph of fenestral dolostone from the Gailor Formation (sample # GL-4, outcrop #10), shows a fracture filled with fibrous chalcedony that crosscuts mosaic dolomite. Thin section is viewed under crossed nicols.

The length-slow chalcedony and clusters of spherulitic chalcedony may be indicative of the former presence of evaporites (Folk and Pittman,1971; Milliken, 1979).

5.2.3 Fracture- and Pore-filling Cements:

Fibrous chalcedony occurs as void-filling cements in healed fractures related to stylolites that traverse Dolomite (3a) mosaics (Figure 5.11). Intercrystalline vugs in Dolomite (4) mosaics in the Gailor are seen to have megaquartz cements (Figure 5.12).

These cements appear to have postdated late-dolomite mosaics and tectonic stresses, and therefore are interpreted to be late diagenetic in origin.

In the chert beds of the Gailor formation, vugs filled with spherulitic chalcedony occur in the microcrystalline quartz matrix (Figure 5.9). It is not clear if they are void- filling cements or replacements of allochems. The vugs may have been evaporitic molds prior to silicification (Folk and Pittman, 1971; Friedman,1980; Milliken, 1978). In Figure 5.13, a vug lined with megaquartz and subsequently filled with calcite is observed, which may be a remnant evaporite nodule.

5.3 Detrital Quartz and Feldspar:

Quartz occurs as detrital particles in the sandstones and sandy dolostones of the Galway and Little Falls formations. The quartz particles are

Figure 5.12:Thin-section photomicrograph of coarse-textured dolostone from the Gailor Formation (sample # GL-5, outcrop #10), where intercrystalline voids in Dolomite (4) mosaic are filled with late-diagenetic quartz cement (arrow). Thin section is viewed under crossed nicols.

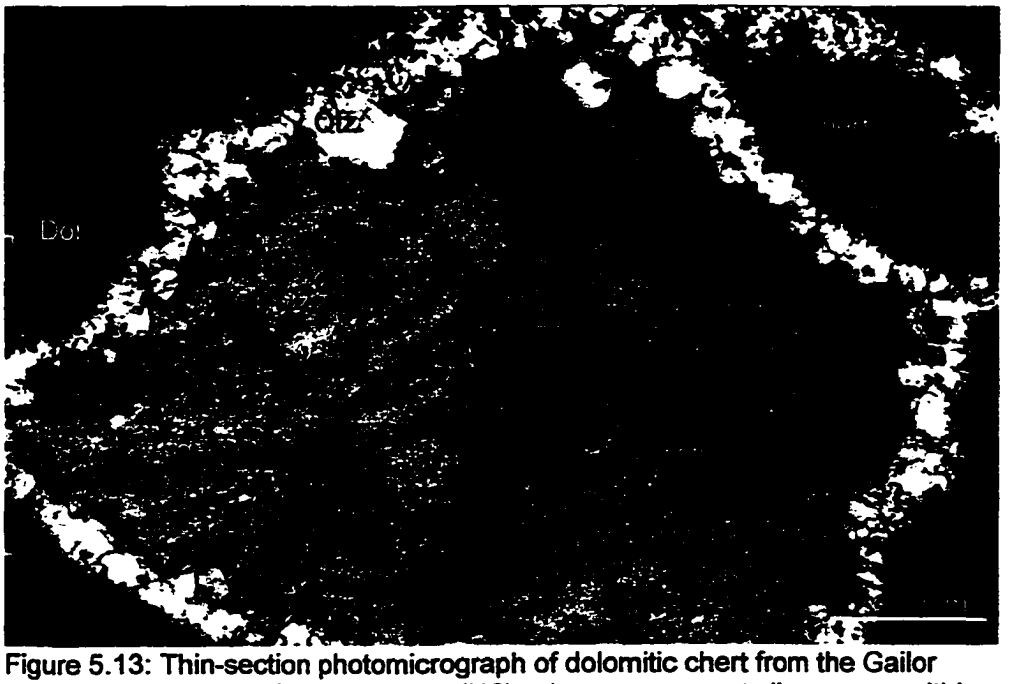

Figure 5.13: Thin-section photomicrograph of dolomitic chert from the Gailor Formation (sample # GL-20, outcrop #12), where megaquartz lines a vug within a matrix of microcrystalline quartz. The vug has been occluded by late-diagenetic calcite. Thin section is viewed under crossed nicols.

generally well sorted and well rounded. The roundness of these particles seems to correspond to their size. The fine, medium and coarse sands are well-rounded whereas the silt-sized particles are sub-angular. Scattered silt-sized quartz and feldspar particles occur in the dolostones of the entire Sauk sequence. The quartz and feldspars display authigenic overgrowths that have developed in optical continuity on the parent particles and appear dark under the luminoscope (Figure 3.2). The boundary between the detrital particles and the secondary overgrowths are usually marked by a thin zone of microinclusions (Figure 5.14). The textural relationships between the mosaic dolomite and the quartz particles show that the authigenic overgrowths postdated the main stage of dolomitization. Some quartz particles do not possess any authigenic overgrowths (Figure 5.15). When viewed under cathode light, the detrital feldspars luminesce blue and the quartz is non-luminescent.

5.4 Authigenic Feldspar:

In addition to the authigenic feldspar overgrowths on detrital feldspar grains, patches of authigenic feldspar occur in the feldspathic dolostones of the Gailor and Tribes Hill formations (Figures 3.27, 3.28, 3.38 and 3.39). As discussed in sections 3.41 and 3.61, the presence of alkali feldspar in these Lower Ordovician strata can be explained as having resulted from precipitation from highly alkaline, saline pore waters that may have been derived from the

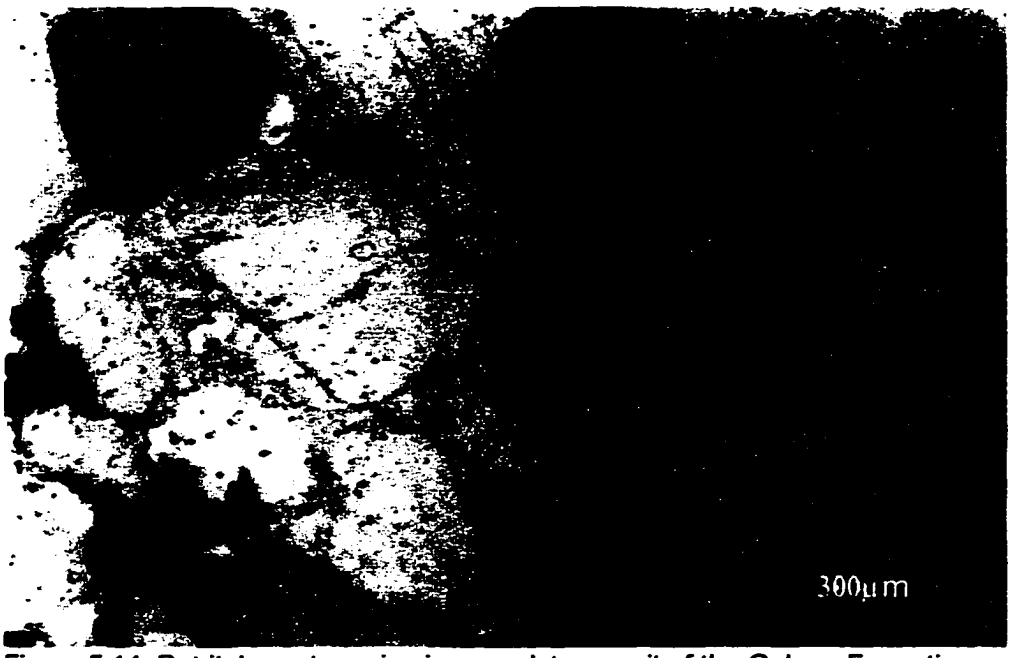

Figure 5.14: Detrital quartz grains in a sandstone unit of the Galway Formation (sample # GA-1, outcrop # 4), with authigenic overgrowths (O). Thin section is viewed in plane-polarized light.

Figure 5.15: Rounded quartz grains with no authigenic overgrowths in a sandstone from the Little Falls Formation (sample # H/6, outcrop # 14). Thin section is viewed in plane-polarized light.

dissolution of detrital feldspars. Another explanation that has been proposed is that the alkali feldspars are products of the diagenetic alteration of zeolites that formed from wind-blown tephra that was deposited among the intertidal-flat sediments (Friedman and Braun, 1975; Buyce and Friedman, 1975; Friedman, 1990; Friedman, Sanders and Kopaska-Merkel, 1992, p.276).

5.5 Sources of Silica:

Some sources of non-detrital silica in sediments suggested by other studies are as follows:

-(1) siliceous tests and skeletal elements of organisms (Hesse, 1990 a)

-(2) weathering solutions in semi-arid climates (Hesse, 1990 a)

-(3) dissolution of quartz and other detrital silicates in a hypersaline marginal marine environment of high but fluctuating pH (Banks, 1970)

-(4) pressure-dissolution of quartz in sediments (Banks, 1970).

In the Sauk carbonates of this study, no siliceous skeletal elements or sponge spicules have been observed, hence such a source for the silica is not likely. Weathering of the nonvegetated, Precambrian metamorphics of the Adirondacks region, which were adjacent to the depositional area, may have generated silica-rich meteoric fluids that circulated through the early-formed carbonates of the Sauk sequence.

In the Gailor, Little Falls and Galway formations, facies analysis indicates that peritidal deposition occurred in a hypersaline, marginal-marine setting. In

hypersaline environments of generally high pH, where carbonate and evaporite precipitation is favored, the pore fluids may get enriched in silica. In addition, the presence of leached detrital quartz and fitted pressure-dissolution fabrics in the quartz grains indicate that pressure dissolution at depth may have been a source of silica for late-diagenetic silicification.

5.6 Geochemical Conditions for Silicification:

Fluctuating pH in pore solutions may be responsible for silicification in the near-surface depositional environment of carbonate deposition (Friedman et. al., 1992, p106). The lowering of the pH which is a function of the availability of carbonic acid or the partial pressure of CO_2, has been observed to dissolve calcite and precipitate silica (Knauth, 1979; Lovering and Patten, 1962). These authors postulate that silica precipitation is favored at low temperatures and pressures, if the pore fluids are acidic and supersaturated with silica. Thus, the formation of chert would be a near-surface phenomenon. In their study of the silicified oolitic grainstones of the Jurassic Camarena Formation, Bustillo and others (1998), inferred that silicification involved meteoric waters and took place during phases of emergence. The presence of bedded chert has been cited as an indicator of intermittent emergence in carbonates (Friedman, 1994 a, b; Friedman and Radke, 1979; Guo, 1994; Guo et. al., 1996.) and is considered a former silcrete. Silcrete forms at or near the surface from the precipitation of silica from evaporation of upwardly moving silica-rich solutions in an arid climate.

By contrast, the late-diagenetic replacement of dolomites (3) and (4) by megaquartz may have resulted from silica enrichment in acidic, continental-derived, circulating porewaters, that migrated regionally along fractures and faults into the burial realm or due to pressure dissolution of the abundant detrital quartz in the carbonates. The low pH and high silica content would dissolve carbonate and precipitate quartz.

5.7 Timing of Silicification in the Sauk Carbonates:

The products of two stages of silicification are observed in the Sauk strata under investigation. The microcrystalline-quartz-cemented sandstones and the pervasively silicified oolitic grainstones in the Little Falls Formation indicate early replacement perhaps related to fluctuating pH in the near-surface pore waters or due to meteoric waters mixing with marine pore waters, when oolite shoals are temporarily emergent in the depositional environment. The scattered occurrences of authigenic quartz euhedra within the Galway dolostones are also inferred to be early diagenetic. In addition, the chert beds observed in the Gailor Formation are also interpreted as having formed early in the diagenetic history of these carbonates. Textural relationships of detrital quartz and feldspar particles with associated dolomite indicate that the silica overgrowths formed early in the course of diagenesis (see figures 3.2, 4.10), prior to the main stage of dolomitization.

The second stage of silicification, as noted in the Galway Formation (Figure 5.6), where megaquartz replaces Dolomite (4) mosaics and in the Gailor Formation (Figure 5.11), where fibrous chalcedony fills healed fractures, is definitely late diagenetic and postdates the main stage of dolomitization and stylolitization. The late silicification may be either locally due to concentration of silica in pore fluids derived from pressure dissolution of detrital quartz or may have occurred in conjunction with uplift of the strata causing the flushing of porous horizons with silica-rich, continental-derived meteoric fluids.

CHAPTER 6 - CALCITE AND DEDOLOMITE

6.1 Introduction:

Four types of calcite are recognized in the Sauk carbonate strata and they have been named calcites (1), (2), (3) and (4). Calcites (1) and (2) represent precursor carbonate material. Calcite (3) is a burial calcite cement and Calcite (4) is dedolomite.

6.2 Precursor calcite:

Both calcites (1) and (2) occur in the limestones of the Hoyt and Tribes Hill formations. They are considered to have formed in the depositional or near-surface environment, prior to dolomitization.

6.2.1 Calcite (1) :

This calcite shows a microcrystalline texture and is found as a micrite matrix in the skeletal packstones and wackestones (Figure 6.1). It also occurs in micritized ooids (Figure 3.13), micritic intraclasts (Figure 6.2), pellets, and peloids (Figure 6.3). The paragenetic relations show that Calcite (1) predates replacement mosaics of Dolomite (3) and Dolomite (4).

Under the luminoscope this calcite appears dull to non-luminescent. The geochemical properties indicate that Calcite (1) is generally low in Fe and Mn and sometimes high in Sr (Figure 4.2).

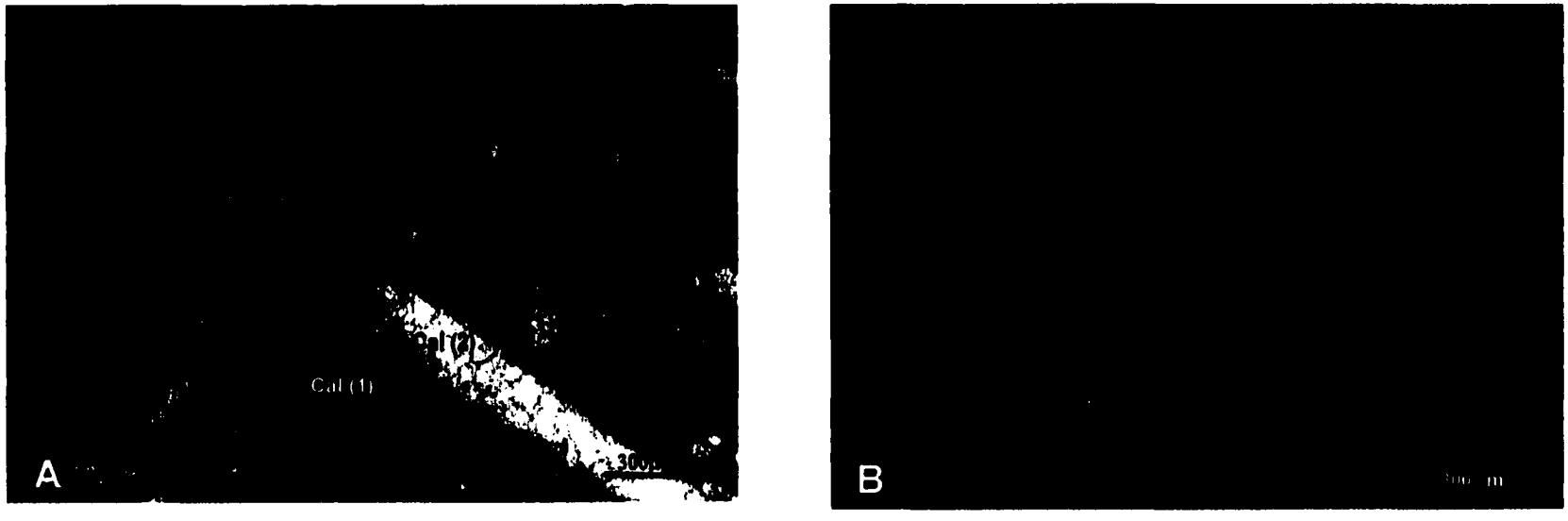

Figure 6.1: Non-luminescent Calcite (1) forms the matrix in skeletal wackestones of Tribes Hill Formation (outcrop #16, sample # V-11).Calcite (2) occurs as cement, filling skeletal molds. (A) is viewed under plane-polarized light and (B) under cathodoluminescence.

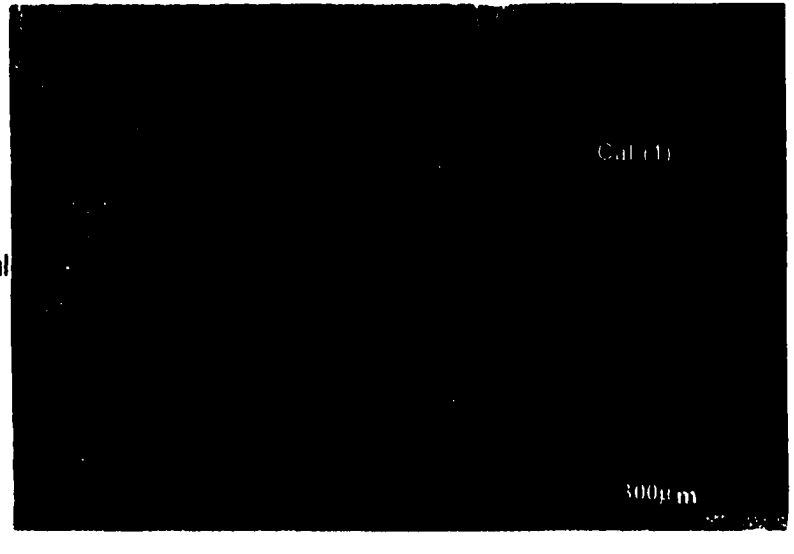

Figure 6.2:Photomicrograph of skeletal grainstone from the Tribes Hill Formation (Sample # 16/4 from outcrop # 15). Intraclasts of Calcite (2) occur in a matrix composed of skeletal fragments where the matrix has been selectively dolomitized. Thin section is viewed under plane-polarized light.

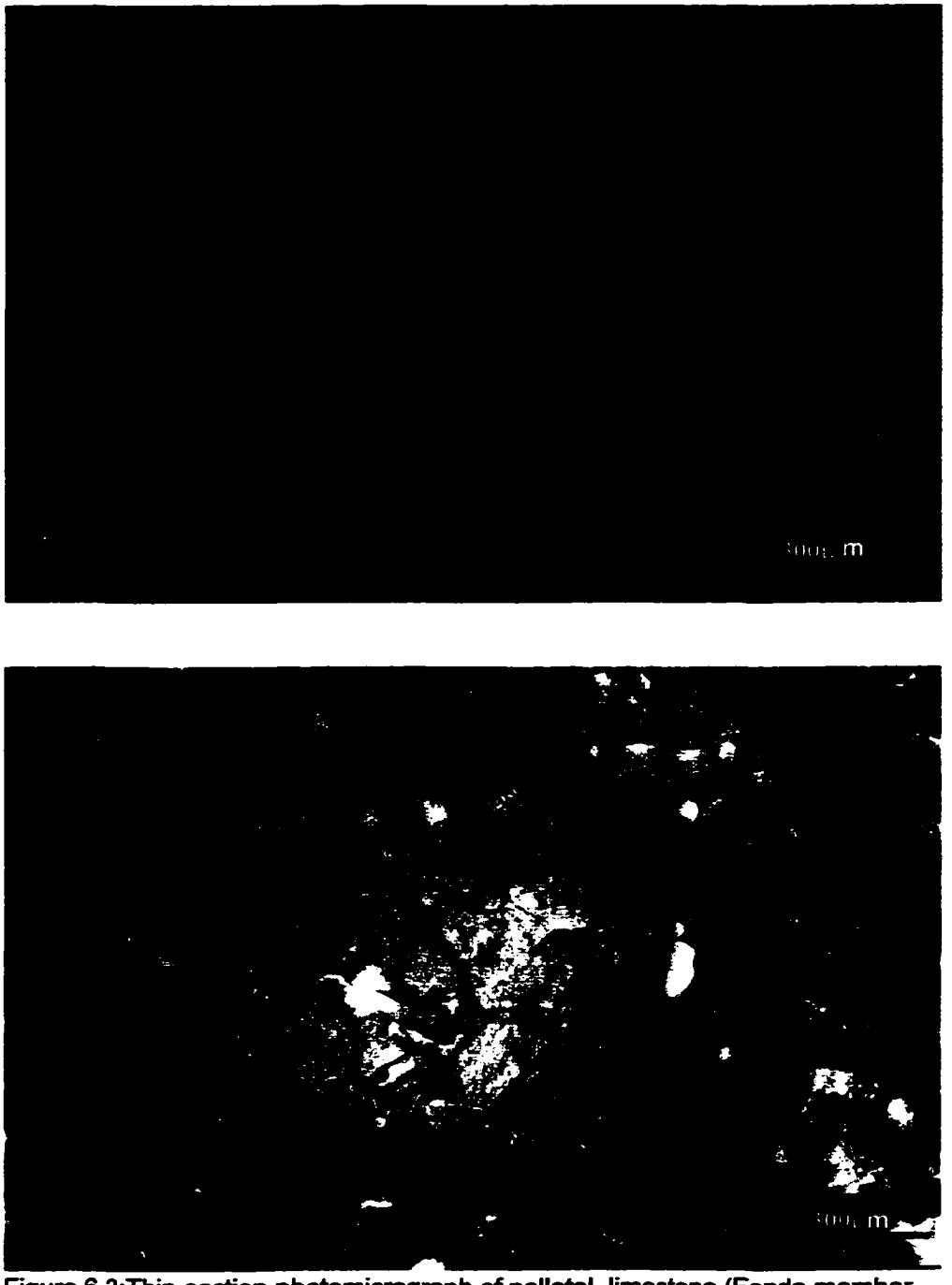

Figure 6.3:Thin-section photomicrograph of pelletal limestone (Fonda member of Tribes Hill), where the pellets are composed of non-luminescent, microcrystalline Calcite-1. Spherical vug is filled with non-luminescent Calcite (3). (A) is viewed under cathodoluminescence and (B) in plane-polarized light.

The low trace-element content and variable Sr contents indicate that Calcite (1) formed in the marine depositional environment in oxic surface conditions, where Fe^{2+} and Mn^{2+} were not available for incorporation into the crystals.

6.2.2 Calcite (2):

Calcite (2) occurs as sparry fibrous or equant cements around ooids (Figure 4.22), skeletal particles (Figure 6.4) and skeletal molds (Figure 6.1). Under cathodoluminescence, this calcite also appears dull to non-luminescent. Microprobe spot analysis indicates that this calcite type is generally low in Mn and its content of Fe ranges up to 3900 ppm. Sr is usually absent in these calcites.

The low Mn and higher Fe contents of these Calcite (2) cements imply that they precipitated in the near-surface environment, from oxygenated waters that were low in divalent Fe and Mn. Paragenetic relationships (Figure 6.4) show that Calcite (2) predates dolomitization and is therefore considered a precursor carbonate.

6.3 Burial Calcite (3):

This calcite occurs predominantly as poikilotopic void-filling cement (Figures 4.24, 4.36, 6.5) and less commonly as outer rims of Dolomite (4). Rarely it may irregularly replace mosaic dolomite (Figure 6.6). Under the luminoscope,

Figure 6.4: Photomicrograph of skeletal grainstone (Sample # 16/2 from outcrop # 15) from the Tribes Hill Formation, as viewed under cathodoluminescence. Calcite (2) occurs as dull-luminescent cement attached to selected surfaces of skeletal particles. Some zoned crystals of Calcite (2) are present in the matrix between the skeletal particles. Dolomitization is confined to the micritic matrix and rarely transects the skeletal fragments. Results of microprobe spot analysis of points numbered (1) through (4) are shown in histogram below. Point (1) is in Calcite (1); point (2) is in Calcite (2); points (3) and (4) are in zoned Dolomite (3a).

Major- and Trace-Element Compositions
(For points in Figure 6.4)

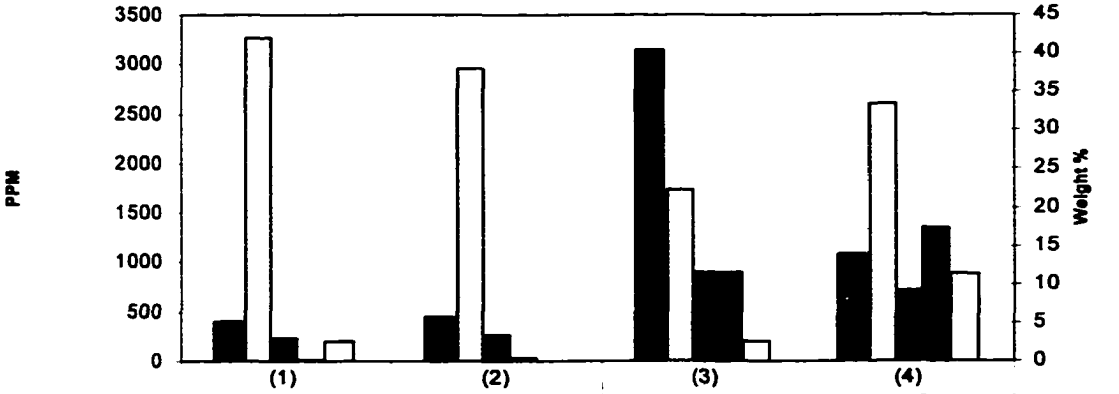

	(1)	(2)	(3)	(4)
■Fe (ppm)	409	455	3140	1085
■Mn (ppm)	237	264	893	705
□Sr (ppm)	205	0	200	889
□Ca (Wt%)	41.92	38.01	22.3	33.54
■Mg (Wt%)	0.255	0.378	11.5	17.24

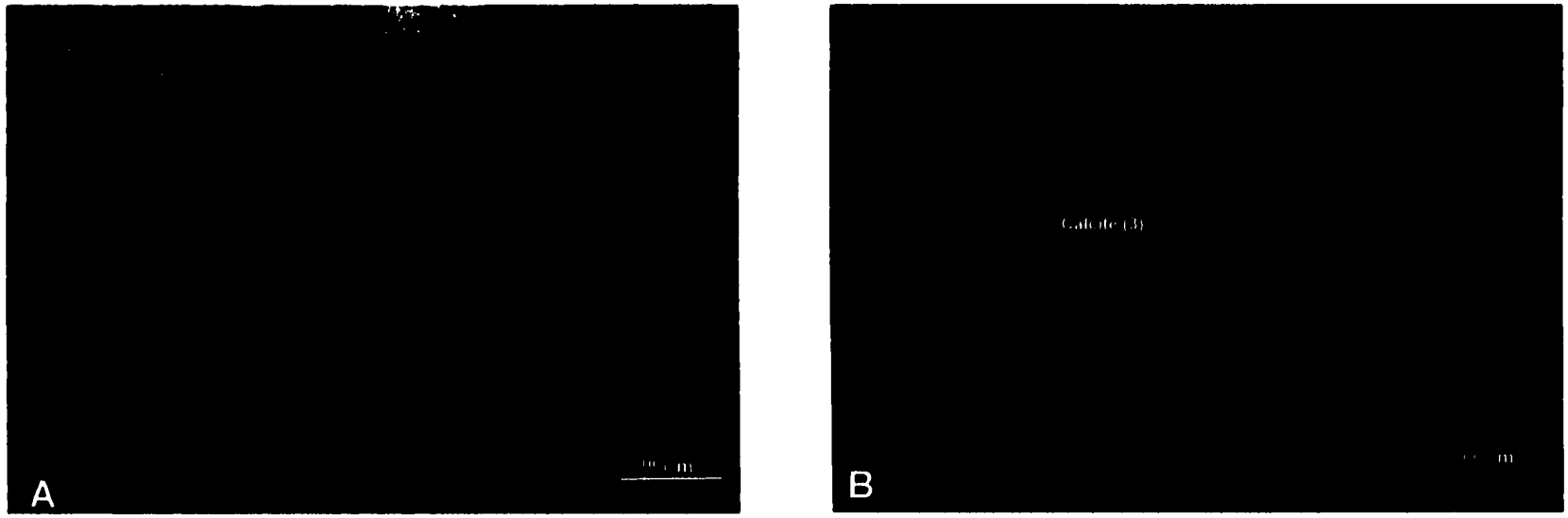

Figure 6.5: Photomicrograph of a thin section of Little Falls dolostone (sample # H/10 from outcrop # 14). Calcite (3) occurs as poikilotopic void-filling cement containing zoned dolomite crystals. Photo (A) is viewed in plane-polarized light and (B) under cathodoluminescence.

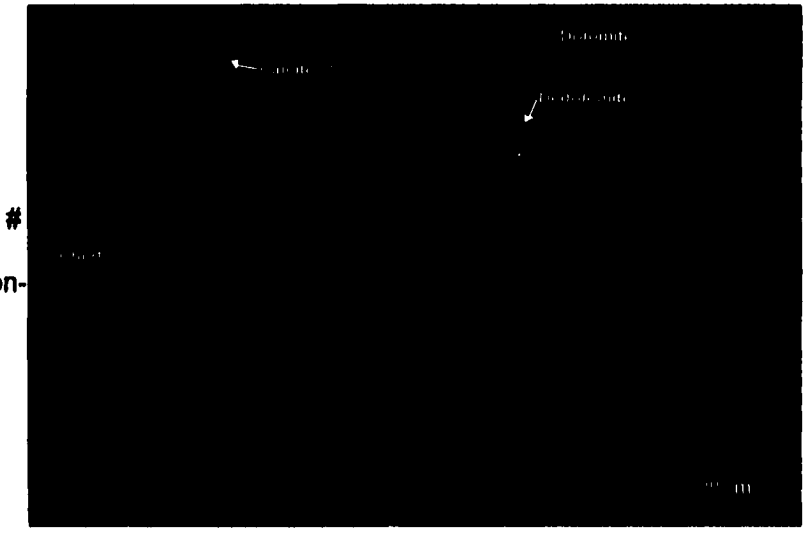

Figure 6.6: Photomicrograph of a thin section dolomitic chert sampled from the Gailor Formation (sample # GL-20, outcrop # 12). Dull-luminescent Calcite (3)occurs as patches partially replacing red-luminescent mosaic dolomite. Chert appears non-luminescent or black. Thin section is viewed under cathodoluminescence.

Calcite (3) is dull-luminescent appearing dull yellow in color. Fractures that postdate the dolomites (3) and (4) are commonly filled with Calcite (3) (Figure 6.7). Calcite (3) is common in vugs (Figure. 6.3). When the void-filling calcite is zoned, the final zone is usually dull-luminescent Calcite (3) following earlier formed bright-luminescent calcite (Figure 6.8).

Microprobe analysis shows that Calcite (3) is high in Fe, Mn, and Sr (Figures 4.2, 4.36, 6.7). The geochemical data and the textural relationships point to a late, deep-burial origin for Calcite (3), where negative-Eh formation waters, with high concentrations of reduced Fe (Fe^{2+}), precipitated calcite, occluding all residual porosity.

6.4 Calcite (4) / Dedolomite:

The products of dedolomitization or the replacement of dolomite by calcite are observed, to variable extent, in all the formations that were studied. Dedolomite is represented by bright yellow-luminescent calcite filling fractures, vugs (Figures 4.9, 5.13), veinlets (Figure 4.7) and irregularly replacing dolomite mosaics 1, 2, 3 and 4 (Figures 4.11, 4.27). In most examples, dedolomite randomly transects zoning in the host dolomite (Figure 6.9), but it one example dedolomitization appears to have been zone-selective (Figure 6.10). The paragenetic relationships show that dedolomite postdates saddle dolomite and in places replaces it (Figure 4.35). In Figure 6.11 dedolomite can be seen to have

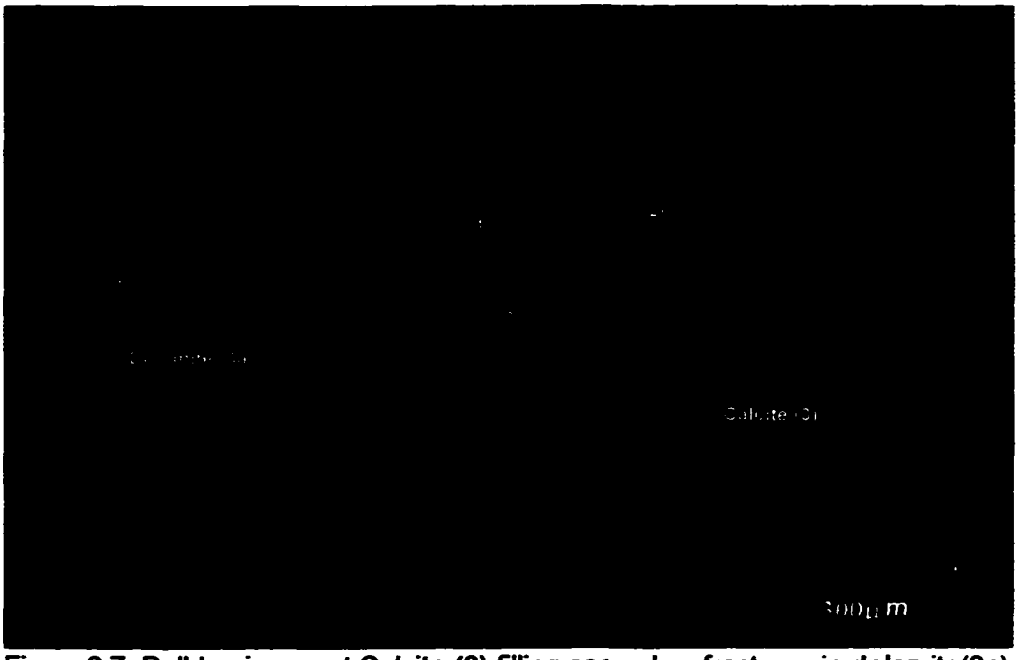

Figure 6.7: Dull-luminescent Calcite (3) filling secondary fractures in dolomite(3a) mosaic in sample from the Gailor Formation (sample # GL-12, outcrop # 12). Thin section is viewed under cathodoluminescence. The results of microprobe spot analysis of points numbered (1) through (3) are shown in histogram below. Point (1) is in red luminescent Dolomite (3a); point (2) is in dull-luminescent Calcite (3); point (3)is in iron-rich outer zone of Dolomite (3a).

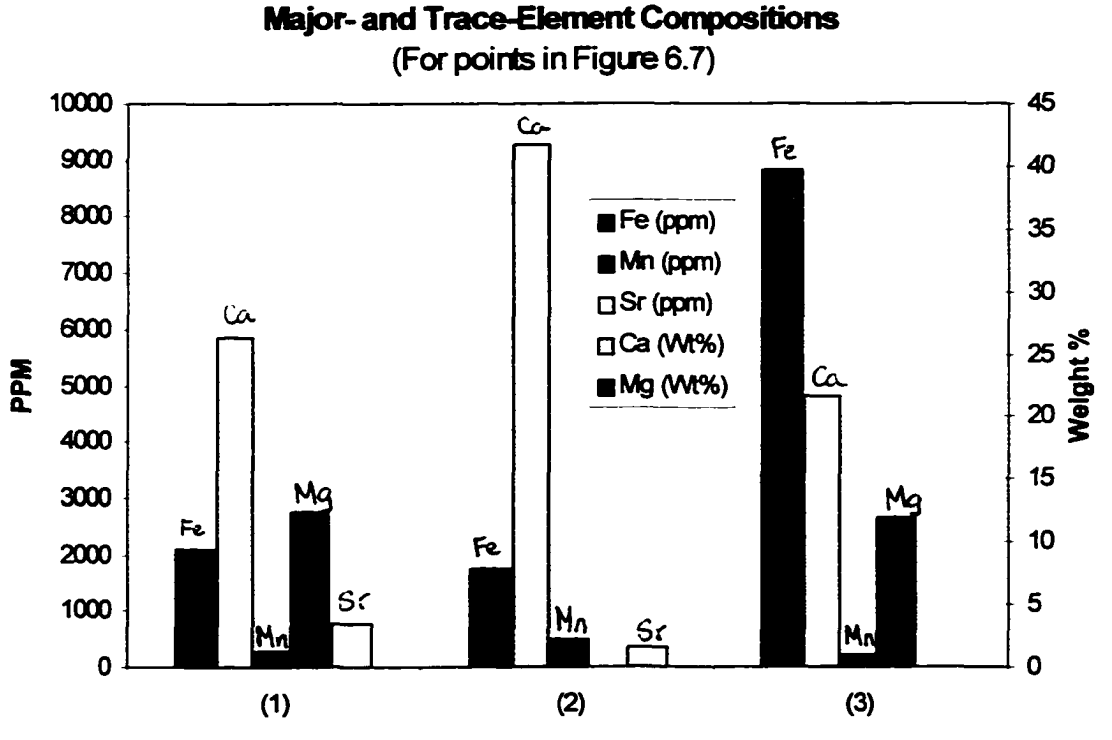

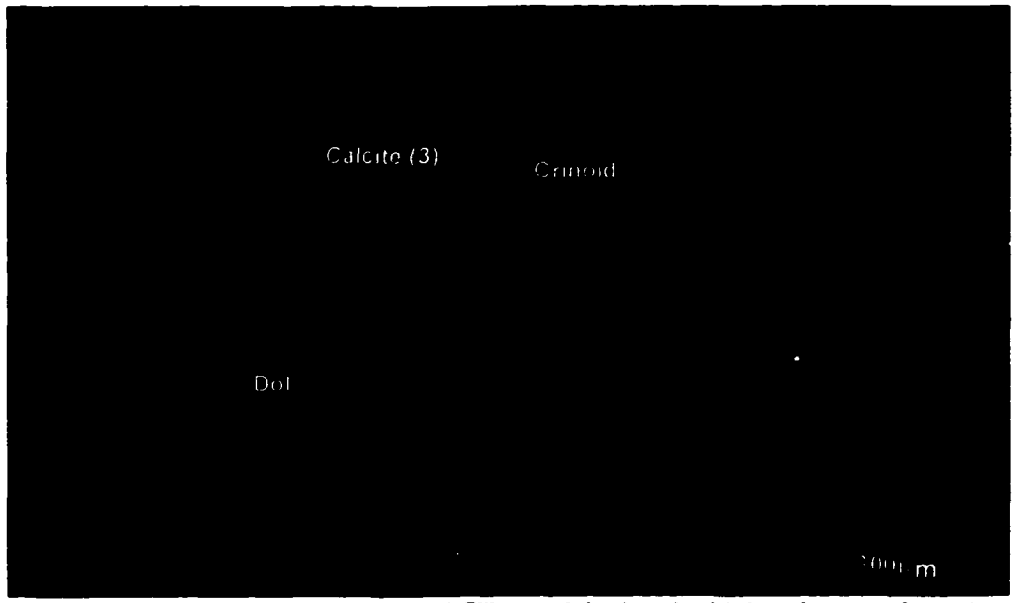

Figure 6.8: Photomicrograph of void-filling calcite in crinoidal grainstone from the Gailor Formation (sample # GL-16, outcrop # 12). The nonluminescent zone to the right side of the photograph is a crinoidal fragment composed of precurser Calcite (2). Zoned, void-filling calcite with bright to dull-luminescent Calcite (3) appears to have grown syntaxially from the crinoidal particle. The final zone is dull-luminescent indicating progressive enrichment of Fe and relative depletion of Mn with time and or burial. Thin section is viewed under cathodoluminescence.

Figure 6.9: Photomicrograph of karst breccia (Gailor Formation, Sample # GL-11, outcrop # 9). Zoned Dolomite (3a) is partially replaced by Dolomite (4) and then has been later irregularly replaced by dedolomite (bright yellow).Thin section is viewed under cathodoluminescence.

Figure 6.10: Photomicrograph of fenestral dolostone (Little Falls Formation, Sample # H/13, outcrop # 14), shows dedolomites (bright yellow), confined to a selected zone in Dolomite (3a). Thin section is viewed under cathodoluminescence. The results of microprobe spot analysis of points numbered (1) through (4) are shown in histogram below. Point (1) is in red luminescent Dolomite (3a); point (2) is in non-luminescent zone of Dolomite (3a); point (3) is in iron-rich outer zone of Dolomite (3a) and point (4) is in bright yellow luminescent dedolomite.

Major- and Trace-Element Compositions
(For points in Figure 6.10)

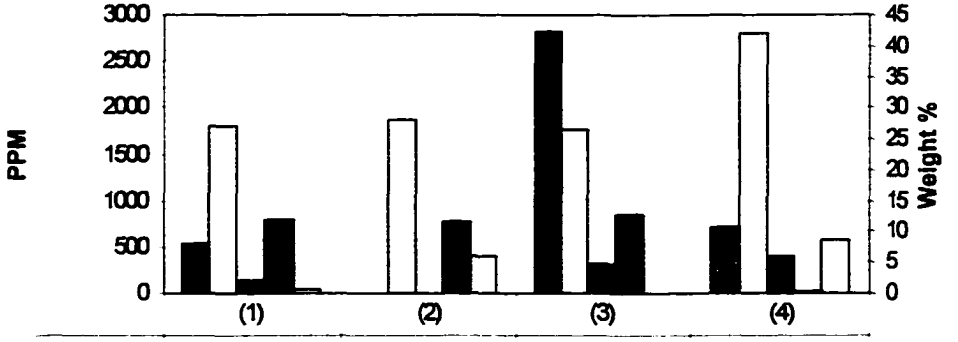

	(1)	(2)	(3)	(4)
■ Fe (ppm)	534	0	2826	711
■ Mn (ppm)	136	0	325	400
□ Sr (ppm)	47	388	0	581
□ Ca (Wt%)	27.11	28.11	26.59	42.16
■ Mg (Wt%)	11.99	11.48	12.72	0.195

postdated Dolomite (7). The relationship between dedolomite and Calcite (3) is not always clear, but traces of dedolomite are seen bordering Calcite (3), indicating that burial-calcite cements replaced earlier formed dedolomite (Figure 4.26).

Microprobe analysis indicates that Calcite (4) is low in Fe and rich in Mn (Figures 4.3, 6.10, 6.11). The lower Fe^{2+} and higher Mn^{2+} in the dedolomite than in the replacive dolomites suggest that the dedolomitization fluids were meteoric in origin as the Mn^{2+} content is higher than Fe^{2+} content in fresh water. Exposure of carbonate strata to fresh water with a low $[Mg^{2+}] / [Ca^{2+}]$ ratio, low CO_2 partial pressure and a temperature below 50^0 C is considered to promote dedolomitization (DeGroot, 1967, Evamy, 1967). This would indicate that during dedolomitization, the strata may have been uplifted or emergent (Friedman, 1994a,b; Guo, 1994; Guo et.al., 1996).

The association of dedolomite with the karst facies in the Gailor (Figures 6.9, 6.11), supports a meteoric origin. The dedolomite in the Sauk carbonates of this study may have formed during emergence related to the following :

- exposure at parasequence boundaries;
- exposure or uplift related to the post-Sauk pre-Tippecanoe surface of unconformity;
- exposure at surface outcrops related to modern weathering;

The selective dedolomitization of zones in Dolomite (4), the occurrence of dedolomite in the karst breccia, and the possibility that burial calcite postdates

Figure 6.11: Photomicrograph of sample of karst breccia from the Gailor Formation (Sample # GL-11, outcrop # 9). Dedolomite (bright yellow luminescence) has replaced the red-luminescent dolomite mosaic. Here dedolomite appears to postdate non-luminescent Dolomite (7) cement lining the fracture. Thin section is viewed under cathodoluminescence. Results of microprobe spot analysis of points numbered (1), (2) and (3) are in the histogram. Point (1) is in Mn-rich dedolomite; point (2) is in red-luminescent replacement mosaic dolomite and point (3) is in late-diagenetic, Fe-rich cement Dolomite (7).

Major- and Trace-Element Compositions
(For points in Figure 6.11)

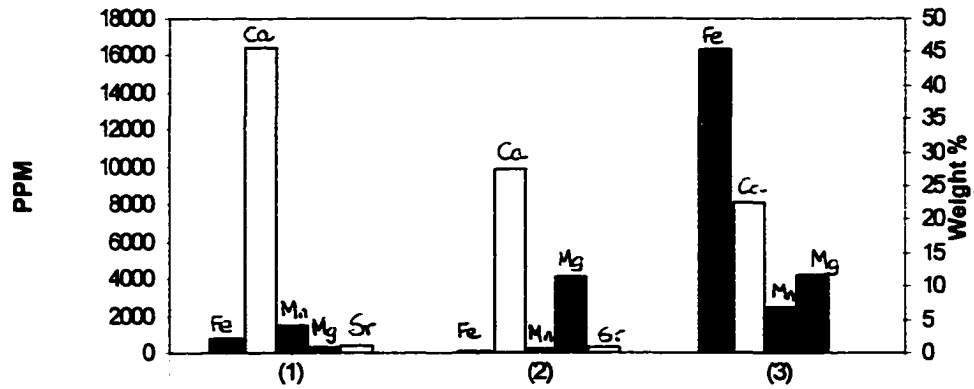

	(1)	(2)	(3)
Fe (ppm)	823	145	16289
Mn (ppm)	1516	236	2408
Sr (ppm)	381	283	0
Ca (Wt%)	45.76	27.39	22.62
Mg (Wt%)	0.827	11.35	11.62

dedolomite is indicative of an unconformity-related origin. Where dedolomite appears to postdate all other diagenetic events, it is inferred to result from post-Paleozoic weathering and current exposure in surface outcrops.

CHAPTER 7- DIAGENETIC HISTORY AND EVOLUTION OF THE CARBONATE PLATFORM

7.1 Paragenesis:

The main diagenetic events that have been documented in the Sauk Sequence carbonates of this study are dolomitization, dissolution of unstable precursor carbonate, stylolitization, silicification, dedolomitization, and cementation of residual pore spaces. From the facies characteristics, textural relationships and geochemical attributes of the components of these rocks, the following paragenetic sequence is recognized:

EARLY STAGE

-Initial carbonate sediments (lime mud, peloids, ooids, skeletal particles, stromatolites, microbial filaments) and detrital quartzo-feldspathic sands.

-Syndepositional early dolomitization restricted to supratidal, intertidal, and subtidal muds generating microcrystalline and very fine-crystalline dolomite mosaics 1 and 2.

-Early marine cements in packstones and grainstones around ooids.

-Early marine micritization: micrite envelopes around allochems preserve their outlines.

-Dissolution of allochems in meteoric diagenetic realm leaving moldic porosity.

-Silicification during emergence of ooid shoals, emergence at tops of parasequences and/or by the formation of silcrete.

MAIN STAGE

-Massive dolomitization forming pervasive red-luminescent dolomites 3 and 4 during progressive burial.

-Mechanical and chemical compaction resulting in fitted fabrics, dissolution seams, anastomosing stylolites, and microstylolites.

-Dolomitization (Dolomite 3b) related to stylolites (Tribes Hill).

UPLIFT STAGE

-Late-diagenetic silicification (fractures and vugs).

-Replacive Dolomite (5) and cement Dolomite (5) related to uplift.

-Dedolomite related to uplift.

LATE STAGE

- Saddle dolomite, Dolomite (7) and ferroan calcite precipitated as void- and fracture-filling cements during burial.

- Dedolomite formed as void- and fracture-filling cement and as dolomite replacements during the final stage of uplift and erosion of the strata.

7.2 Evolution of the Carbonate Platform:

The facies study of the Cambro-Ordovician strata has shown that during this period of regional transgression, an aggrading pattern of multiple meter-scale, upward-shallowing, depositional sequences developed on the Saratoga Platform. Each upward-shallowing unit or parasequence represent products of subtidal, intertidal, and supratidal sub-environments. Oolite shoals were present bordering the marginal peritidal environment and separated from it by subtidal lagoons. The entire Sauk Sequence in the study area shows products of these environments interfingering with one another. Towards the top of the sequence, a gradual deepening to a more subtidal to shallow-marine setting is observed in the younger members of the Tribes Hill Formation.

From the diagenetic study of these strata it is evident that no one model can explain the massive, pervasive dolomitization of the entire sequence. These rocks display a long and complex diagenetic history. Dolomitization itself occurred in four stages as noted above and was associated with other diagenetic events such as silicification, calcitization, and stylolitization (Figure 7.1).

Dolomitization in the near-surface environment during and soon after deposition can be explained by the 'reflux model' and or the 'capillary concentration' of hypersaline interstitial pore water and the microbial decomposition of organic matter (Chapter 4). The depositional facies-associations and the geochemical characteristics of the dolomite types present in these strata indicate that an evaporitic setting may well have existed, where

modified seawater was responsible for syndepositional dolomitization on the intertidal flats. The carbon-isotope values, presence of pyrite, and abundance of microbial structures in the strata support the possibility of shallow subsurface dolomitization instigated by bacterial sulfate reduction that accompanied organic-matter degradation. Thus, both processes may have been responsible for the initiation of dolomitization very early in the diagenetic history.

FIGURE: 7.1 PARAGENESIS OF THE SAUK SEQUENCE IN CENTRAL NEW YORK

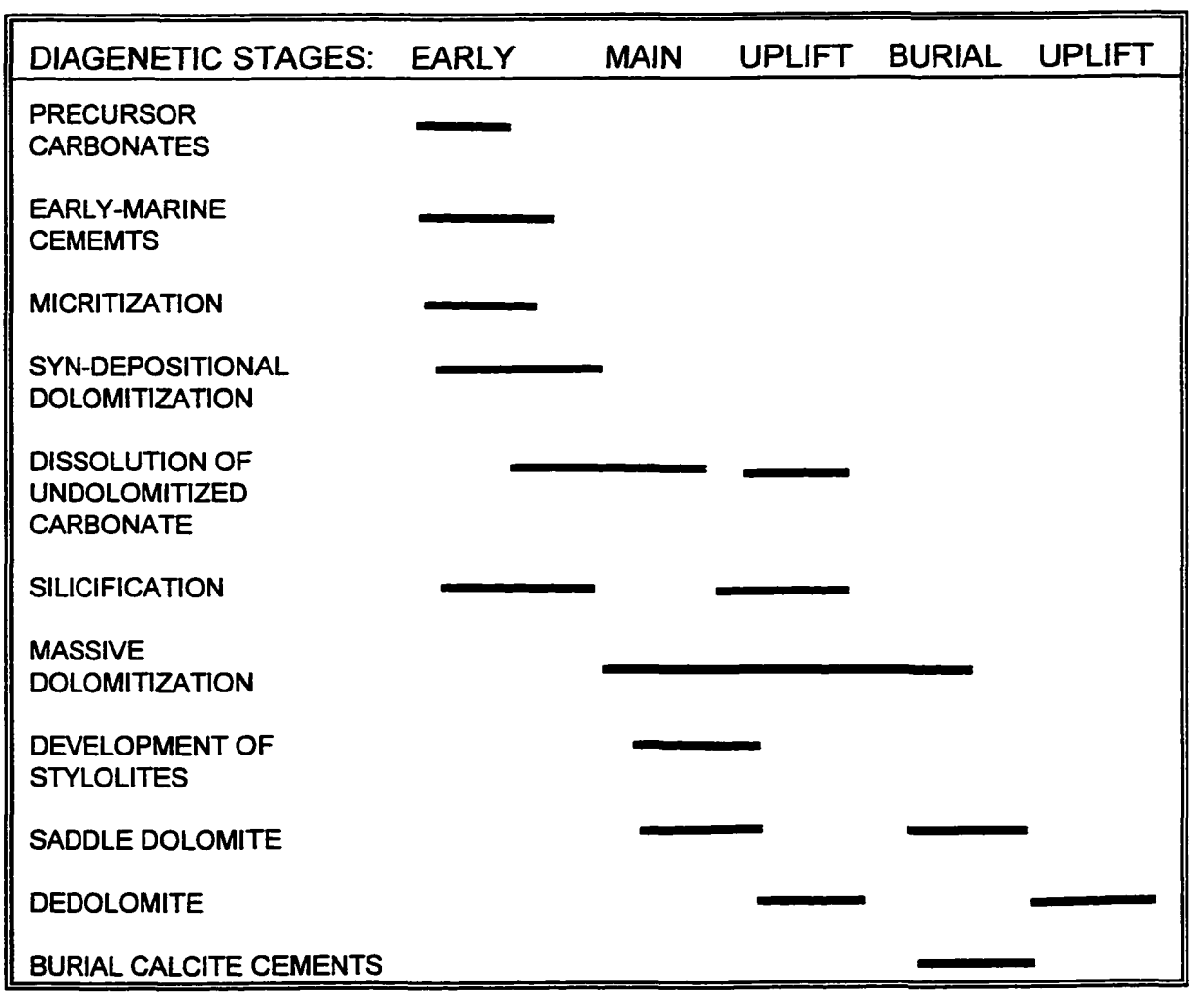

The main stage of massive dolomitization, however, occurred in the subsurface during progressive burial. Anoxic meteoric fluids, formation fluids, or modified seawater moved through the strata causing neomorphism, recrystallization, and replacement to produce Fe- and Mn-rich luminescent, dolomite mosaics. Progressive burial and changing composition of dolomitizing fluids precipitated more Fe-rich overgrowth zones at depth. "Topographic recharge", "tectonic compaction", and "thermal convection" are some of the mechanisms of subsurface fluid flow suggested by other workers for regional subsurface dolomitization on ancient platforms (Morrow, 1997). However, from the spatial distribution of fluid-inclusion homogenization temperatures recorded on the Saratoga Platform (Sarwar and Friedman, 1995, p.75, Fig.21), there appears to be no particular spatial trend in the paleotemperature data. Therefore, it is inferred that the subsurface dolomitization in the Sauk strata under investigation, occurred due to the burial of the strata, within a normal paleo-geothermal gradient of 30^0 C/km (Sarwar and Friedman, 1995).

The main stage of subsurface dolomitization was followed by a phase of uplift when the strata were infiltrated by less-reducing Mn-rich meteoric fluids that formed brightly luminescent replacive Dolomite 5, cement Dolomite 5, and dedolomite. Subsequently the strata were buried again to even-greater depths where ferroan cements of calcite and dolomite occluded all remaining pore spaces. Paleotemperature studies of the Sauk carbonates (Urschel and Friedman, 1984; Sarwar, 1992; Sarwar and Friedman, 1994, 1995), show that

maximum burial depths of 6.8 to 7.5 km may have been reached before the strata were uplifted to form the surface outcrops of today.

Thus a complex interplay of several diagenetic processes that occurred at different times and at different stages of burial were responsible for the pervasive dolomitization of the Sauk Sequence that developed into the Saratoga Platform.

7.3 Comparison with the Sauk Sequence in the Appalachian Fold-Thrust Belt:

In Guo's study (Guo, 1994), the Sauk carbonates of the Saratoga Platform (Beekmantown Group of Fisher, 1977) on the western shelf were examined in a core from the Finnegan boring (Guo, 1994; Guo, et. al., 1990) and compared with coeval rocks (Wappinger Group) that were part of the central shelf (confined to the Appalachian fold-thrust belt). The study demonstrates that deposition on the central shelf began early in the Cambrian whereas deposition in the western shelf on the Saratoga Platform began only by Late Cambrian time. Another difference between the subprovinces that was noted by Guo's work was that the Sauk strata on the Saratoga Platform were comparatively richer in terrigenous sediment as well as limestones. But, nevertheless, both subprovinces of the carbonate platform developed in a tropical coastal setting involving supratidal flats, intertidal flats, and adjacent subtidal zones. The facies characteristics inferred from the Sauk Sequence observed in the Finnegan boring are consistent with the results of this study.

The diagenetic history of the Wappinger Group (Guo, 1994) compares closely with that inferred for the Sauk strata in this study. Similar stages of dolomitization, namely (1) early syndepositional, (2) second shallow burial, and (3) late deep burial have been established in the Wappinger Group. In addition dedolomitization and chert related to post-Early Ordovician emergence also have been demonstrated in the upper strata of the Wappinger Group. This stage is described as the 'Uplift stage' in the diagenetic history documented in this study. The oxygen-isotope compositions of the dolomites in the Wappinger Group also show similar values and trends when compared with the values noted in this study. Thus, it can be inferred that the rocks of the Sauk Sequence on the Saratoga Platform have undergone a diagenetic history that is the same asthat in the rocks of the central shelf within the Appalachian fold-thrust belt.

The remarkable similarity in the inferred diagenetic sequence observed in the platform strata and the Appalachian fold-belt sequence is significant because it implies that the burial histories of the two provinces are similar as well. Figure 7.2 shows the burial curve that has been inferred for the rocks of the Wappinger Group (From Guo, 1994, p.92). This burial history curve shows that after the Sauk Sequence had been deposited, an initial subsidence of the top of the Wappinger Group occurred in the Early Cambrian, followed by an uplift during the Early Middle Ordovician where subaerial erosion developed the post-Sauk, pre-Tippecanoe surface of unconformity. A second, more-extensive subsidence is inferred to have occurred later in the Middle Ordovician when the Sauk

Sequence was buried under the Tippecanoe Sequence as well as one or more thrust sheets. This was followed in the Silurian by a third, prolonged period of subsidence where the strata were subjected to deep burial. As the diagenetic history of the Sauk strata on the Saratoga Platform (this study) is almost identical to that of the Sauk strata in the Appalachian fold belt (Wappinger Group of Guo, 1994), the burial history inferred for the Wappinger Group can be applied to the platform strata as well. When comparing the two subprovinces, one important difference that must be noted is that in the fold belt, the thickness and strata are still preserved to prove the extent of burial, whereas that is not so on the Saratoga Platform.

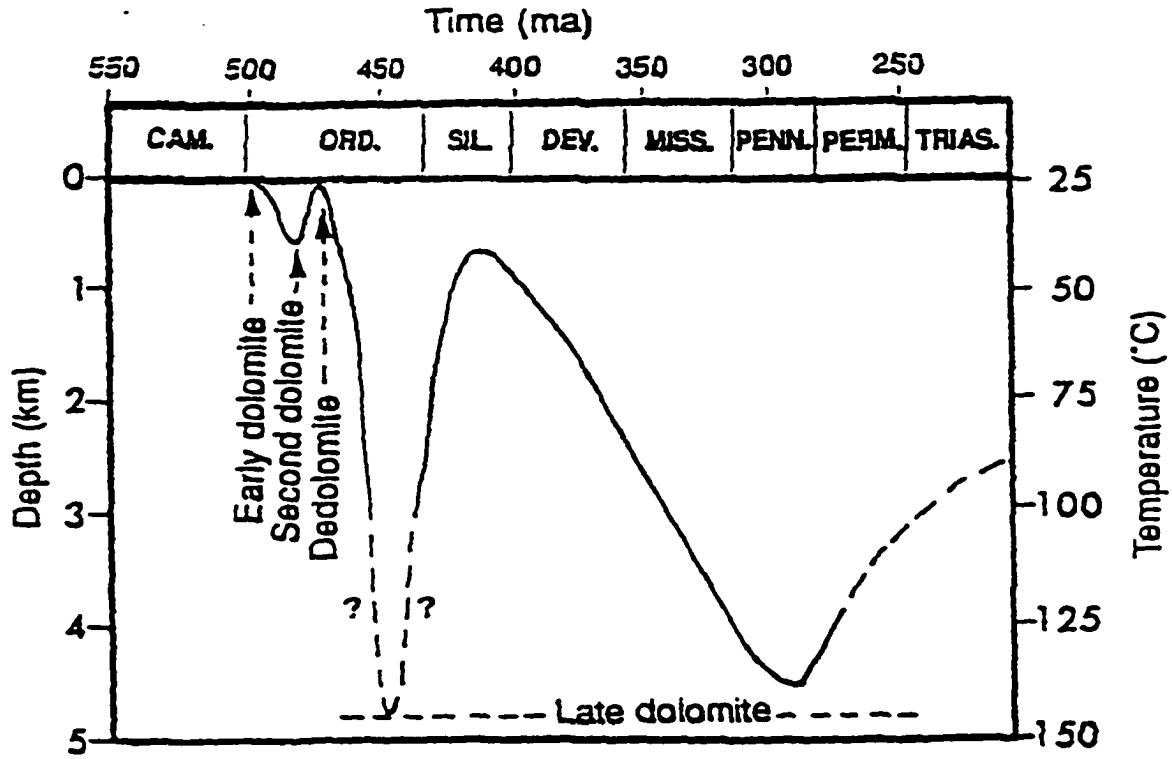

Figure 7.2. Schematic geohistory curve showing time history of burial of the top of the Halcyon Lake Formation (Wappinger Group). From Guo, 1994, p. 92.

CHAPTER 8 - CONCLUSIONS

This study discusses the origin of dolomite in the context of the diagenetic evolution of the carbonate sequence that developed on the Saratoga Platform during Cambro-Ordovician time. The entire succession is dominated by dolomite with subbordinate amounts of siliciclastics and limestones and is therefore considered an ideal setting for the study of massive dolostones. All of the previous work done on the rocks of this area have focused on the establishment of the paleoenvironmental setting in which this sequence developed, whereas this study focuses on the diagenetic events and stages of dolomite formation that took place after the deposition of the carbonate strata.

Deposition of the Sauk sequence carbonates on the Saratoga Platform took place in a shallow-marine, sea-marginal, peritidal setting in The Tropical belt of what was then the Southern Hemisphere.

Meter-scale, upward-shallowing, depositional sequences are common in the Little Falls, Galway, Hoyt, Gailor and Tribes Hill formations, that make up the Sauk strata in the study area. These parasequences are composed of vertically stacked lithofacies that represent shallow subtidal to intertidal to supratidal sub-environments of deposition.

The common lithofacies that imply subtidal deposition in these strata are *ooidal/peloidal/ skeletal dolostones and limestones; mottled dolostones and* limestones; stromatolitic boundstones; herring-bone cross-stratified sandstones

and sandy dolostones; and shale. Cryptmicrobial-laminated dolostones, intraclast dolostones and thin-bedded, mudcracked, fenestral dolomudstones are suggestive of intertidal to supratidal deposition. In addition features related to emergence, such as chert, dedolomite and dissolution-collapse breccias are also observed in these units.

Various combinations of these lithofacies are found present in all the formations in this study. The Little Falls, Galway and Gailor formations are dominated by dolomitized units and display characteristics of shallow subtidal to supratidal deposition. Dolomites in the mixed carbonate-siliciclastic units of the Galway Formation, formed initially by syndepositional replacement of precursor carbonate by evaporated seawater. This is suggested by the high Sr values, paucity of fauna and $^{87}Sr/^{86}Sr$ values that are similar to coeval seawater.

In comparison, the Hoyt and Tribes Hill formations are fossiliferous and limestone-rich, with lithofacies associations that imply predominantly subtidal to intertidal depositional conditions with normal salinities. Oolite shoals are common in the Hoyt deposits, separated from the shoreline tidal deposits by subtidal lagoonal sub-environments.

The Tribes Hill deposition began under intertidal to supratidal conditions and progressively deepened to more subtidal conditions. This is suggested by the thin-bedded, cryptmicrobial laminated and feldspathic dolostones of the lower Fort Johnson member that marks the onset of Tribes Hill deposition. The succeeding Palatine Bridge, Wolf Hollow and Fonda members of the Tribes Hill

Formation are comparatively more limestone-rich, fosssiliferous, and display characteristics of subtidal deposition.

Storm deposits are common particularly in the Little Falls, Galway, Gailor, and Tribes Hill formations, where beds of intraclasts were deposited by high-energy, storm-generated waves.

The Little Falls, Galway, Gailor and the Fort Johnson member of the Tribes Hill Formation have been completely dolomitized, whereas in the Hoyt and upper members of the Tribes Hill Formation, dolomitization was only partial. Petrographic and geochemical data suggest that dolomitization in the completely dolomitized units took place in multiple stages beginning early in the depositional environment. In the partially dolomitized units especially in the Tribes Hill Formation, dolomitization occurred late in the diagenetic history. This is suggested by the association of dolomite with stylolites in the skeletal wackestones and packstones of the Tribes Hill Formation, indicating a post-compaction origin.

I recognize seven dolomite types in the rocks studied. They are numbered 1 to 7 and are interpreted to represent four stages of dolomitization. Microcrystalline Dolomite (1) and fine-crystalline Dolomite (2) are considered to be products of early diagenesis of fine-crystalline lime mud and represent the first stage of dolomitization. The extremely fine crystal size, low trace-element content, high Sr content, and their presence in fenestral dolomudstones, intraclasts and cryptmicrobial laminated dolostones indicate dolomitization was

likely to have been initiated early in the diagenetic history of these dolostones, possibly in the depositional environment.

The second or main stage of dolomitization occurred in the shallow subsurface and is represented by medium-crystalline replacement mosaics of zoned, planar-e to planar-s Dolomite (3) and nonzoned planar-s to non-planar mosaics of Dolomite (4). The cathodoluminescence characteristics of these dolomites indicate they resulted from multiple episodes of dolomitization, and recrystallization. Brightly luminescent distinct zoning, blotchy irregular luminescence as well as a total lack of zoning are observed in these dolomites. Cathodoluminescence cement stratigraphy indicates that Dolomite (4) post-dates Dolomite (3).

The third stage of dolomitization took place during uplift of the strata, when Fe-poor, meteoric fluids circulated through the host rock precipitating bright-orange luminescent Dolomite (5) cements and replacement mosaics in porous parts.

Unlike the earlier stages, the fourth and final stage of dolomitization was not replacive in nature, but rather pore-filling dolomitization. This stage occurred in the deep subsurface where hot subsurface brines precipitated saddle dolomite (Dolomite 6) and Dolomite (7) in solution vugs, intercrystalline pore spaces, fractures and veinlets.

Compared with the early formed dolomites, the late-diagenetic dolomites are more stoichiometric , coarser in size, more depleted in $\delta^{18}O$ and Sr^{2+} and

more enriched in Fe^{2+} and Mn^{2+}. These geochemical differences imply that early dolomite formed from modified seawater in the depositional environment and soon after, whereas late dolomite formed by recrystallization or neomorphism of early formed dolomite, replacement of limestone at elevated temperatures, and by cementation in fractures and secondary pore spaces.

The seven different dolomite types recognized in the rocks of this study and the four stages of dolomitization that were inferred from their relationships among one another, indicate that the massive dolostones that form this Sauk Sequence did not develop in one widespread dolomitization event. In fact, the results of this study indicate that dolomitization may have been initiated in the depositional environment, in an evaporitic, peritidal setting, very early in the diagenetic history. However, the main stage of dolomitization occurred in the burial realm. Therefore, it is inferred that the massive dolostones of the Saratoga Platform, resulted in part from syndepositional dolomitization and in the most part from burial dolomitization.

Although the major diagenetic modification in these carbonates took place in the form of dolomitization, other events such as silicification, cementation by burial calcite in the deep subsurface, and dedolomitization in the near-surface environment are also significant events that were involved in their complex diagenetic evolution.

The diagenetic history of the Sauk Sequence on the Saratoga Platform is remarkably similar to that noted for the Sauk Sequence in the Appalachian fold-

thrust belt in eastern New York. This implies that the burial history of the two subprovinces are comparable as well. The diagenetic sequence and the burial-history curve of the Sauk Sequence indicate that the strata were subjected to an initial subsidence in Early Cambrian time, which was followed by an uplift that elevated the strata into the realm of meteoric diagenesis. This uplift of the strata in the Early Middle Ordovician developed the post-Sauk, pre-Tippecanoe surface of unconformity. A second subsidence to greater depths occurred subsequently in the Middle Ordovician, with the deposition of the younger Tippecanoe Sequence and development of overthrust sheets that are recorded in the Appalachian fold-thrust belt. A final episode of deep burial is inferred to have begun in the Silurian that continued to the end of the Paleozoic Era. The Sauk strata are inferred to have reached maximum burial depths of 6.8 to 7.5km.

APPENDICES

Appendix I - Sample Locations

OUTCROP SECTIONS	LOCATION	SAMPLE	LITHO-FACIES	FORMATION
#1	Route 29, West of 147 Jn at Green corners.	GB-8, GB-9, GB-11, GD-2, GD-3, GB-10, GB-3, GB-12, GB-13, GB-2, GD-4, GB-1	1, 2, 3, 4, 5, 6,7,8	GALWAY
#2	Route 29, East of 147 Jn.	GB-5, GB-4, GB, B-3, B-1, B-2, GB-7, GB-6,B-4,B-5, B-6	3,5,7,8, 9	GALWAY
#3	Route 29, Town of East Galway, 6 miles west from intersection with Petrified Gardens Road	GD-1, GC-2, GC-1, GC-3	3,4,5,8, 9	GALWAY
#4	Route 9N	GA-4, GA-3, GA-1, GA-2,GA-5	1,5,6,7, 9	GALWAY
#5	Railroad cut near Canty Road	R-1, R-2, R-3, R-4, R-5	1,3,5,7, 8	GALWAY
#6	Petrified Gardens	PG-1, PG-2, PG-3, PG-4, PG-13 PG-7, PG-8, PG-9, PG-10, PG-6, PG-11, PG-12	1,4,5,7, 8,9,10	HOYT
#7 & #8	Lester Park Quarry	LP-1, LP-2, LP-3, LP-4, LP-5	1,3,4,6, 8	HOYT
#8A	Skidmore Quarry	SQ-1,SQ-2, SQ-3	1	HOYT
#9	Route 67, 1.6 miles West of Jn 147.	GL-11, BS-1, BS-2, BS-3, BS-4, BS-5, BS-6, BS-7, BS-8, BS-9, BS-10, BS-11	3,7,8,10 ,11	GAILOR
#10	Route 67, 2.3 miles West of Jn 147	FJ-8,FJ-9,FJ-10, FJ-11,GL-1, GL-2, GL-3, GL-4, GL-5, GL-6, GL-7, GL-8, GL-9, GL-10	2,3,7,11	GAILOR

OUTCROP SECTIONS	LOCATION	SAMPLE	LITHO-FACIES	FORMATION
#11	Route 67,West of #10	FJ-1, FJ-7, FJ-2, FJ-3, FJ-4, FJ-5, FJ-6	2,3,7,8	GAILOR
#12	Route 67, West of #11	GL-12, GL-13, GL-14, GL-15, GL-16, GL-17, GL-18, GL-19, GL-20, GL-21, GL-22	1,3,4,7, 8,9,10, 11	GAILOR
#13	Pallette Quarry	GL-23, GL-24, GL-25, GL-26, GL-27, GL-28, GL-29, GL-30, GL-31	2,3,7,8, 10	GAILOR
#14	Route 5 E	H/6, H/1, H/2, H/5, H/3, H/4, H/7, H/8, H/13, H/9, H/10, H/11	1,2,3,5, 7,8,10, 11	LITTLE FALLS
#15	Route 5 West, East of Amsterdam, NY	16/4, 16/3, 16/5,16/1, 16/2, 16/6, 16/7	1,2,3,7	TRIBES HILL: Palatine Bridge member and Wolf Hollow member
#16	Van Wie Creek	V-1, V-2, V-3, V-4, V-5, V-6, V-7, V-8, V-9, V-10, V-11, V-12	1,3	TRIBES HILL: Palatine Bridge member and Wolf Hollow member
#17	Borden Road	TB-1, TB-2, TB-3, TB-4, TB-5, TB-6, TB-7, TB-8, TB-9	1,3,7,9	TRIBES HILL: Fonda member
#18	Fort Hunter Quarry	FJ-12, FJ-13, FJ-14	8,9	TRIBES HILL: Fort Johnson member

Appendix II – Outcrop Descriptions

OUTCROP #1 (Route 29, West of 147): Galway Formation

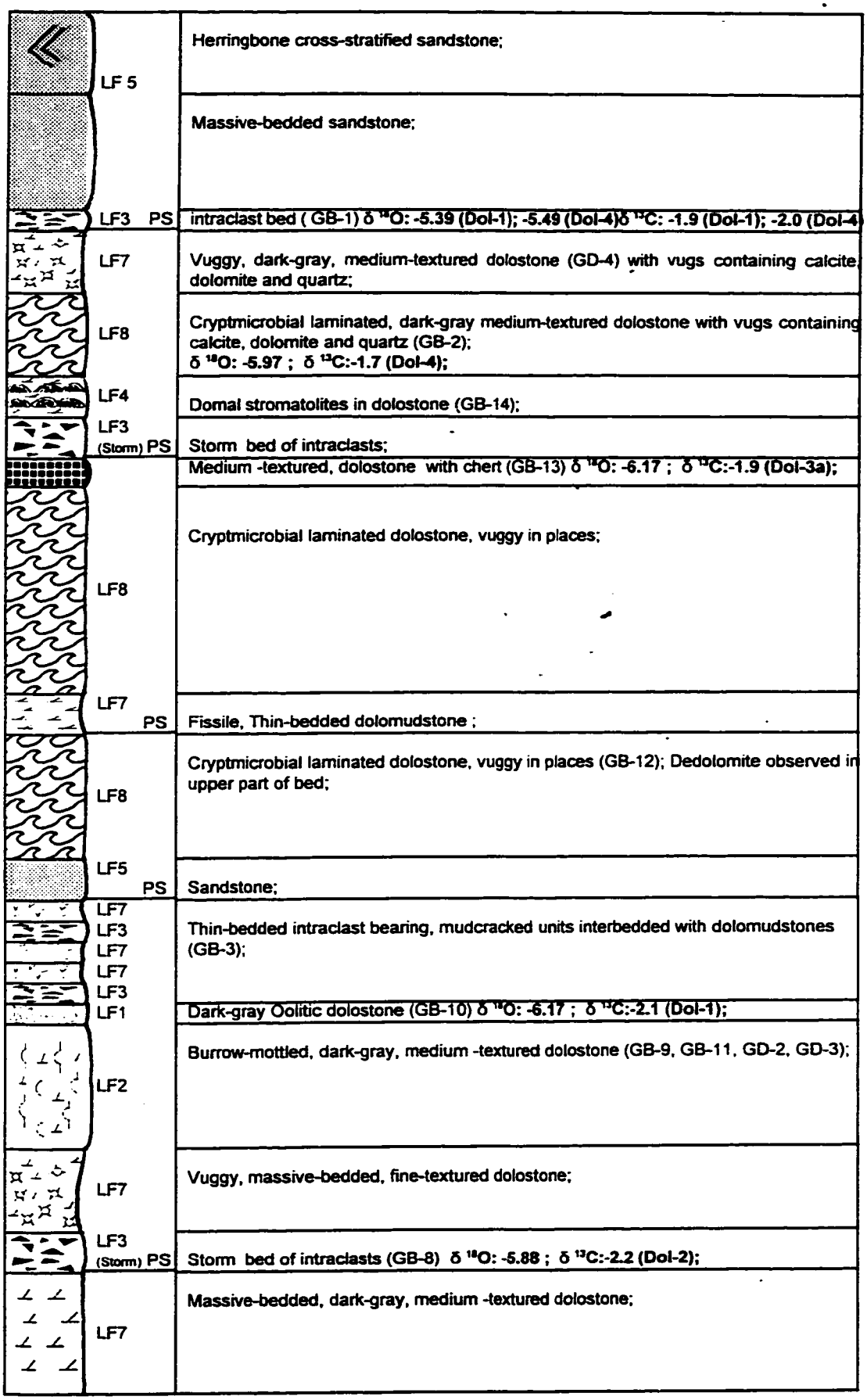

OUTCROP #2 (Route 29, East of 147): Galway Formation

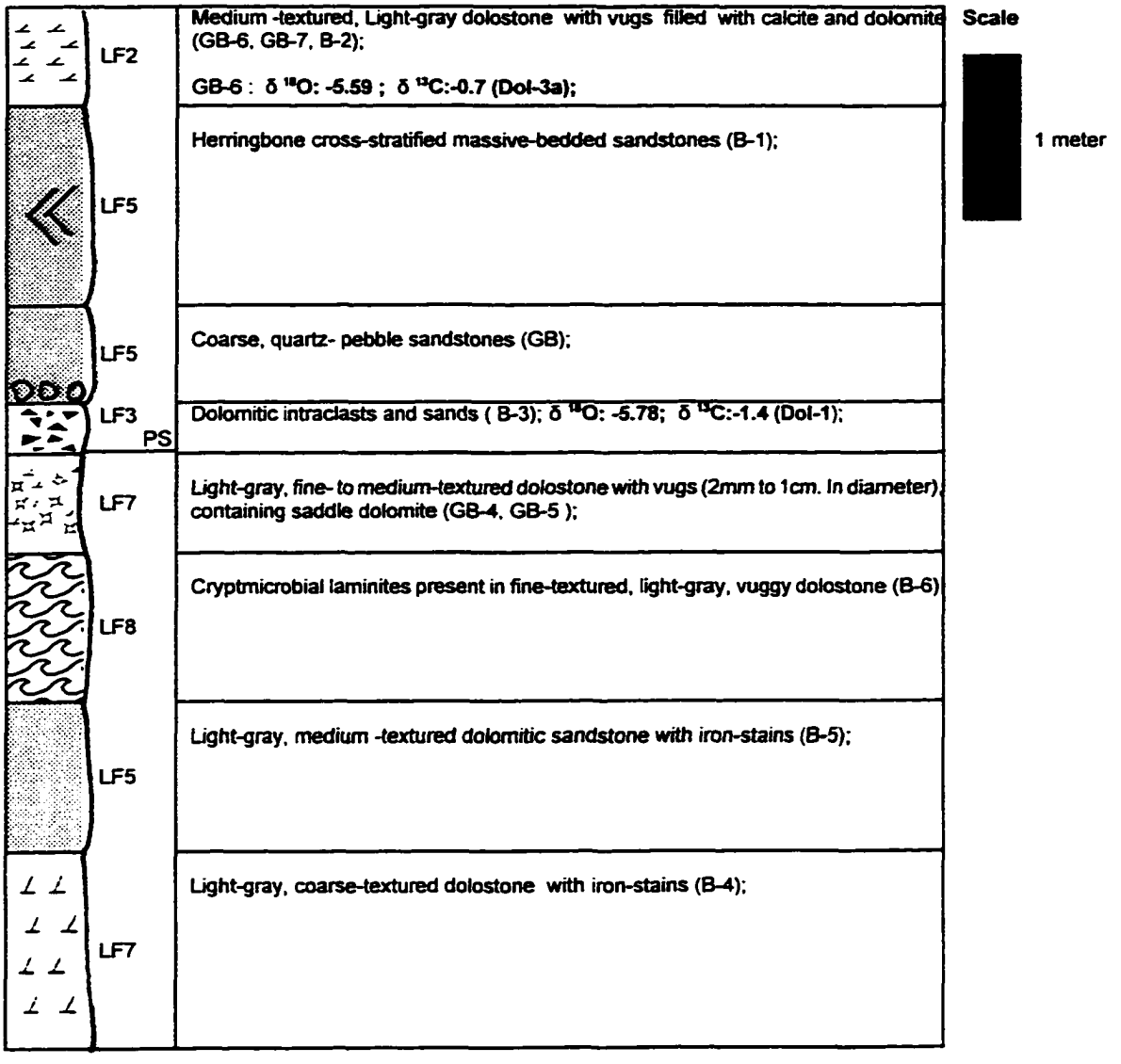

OUTCROP #3 (Route 29, East Galway): Galway Formation

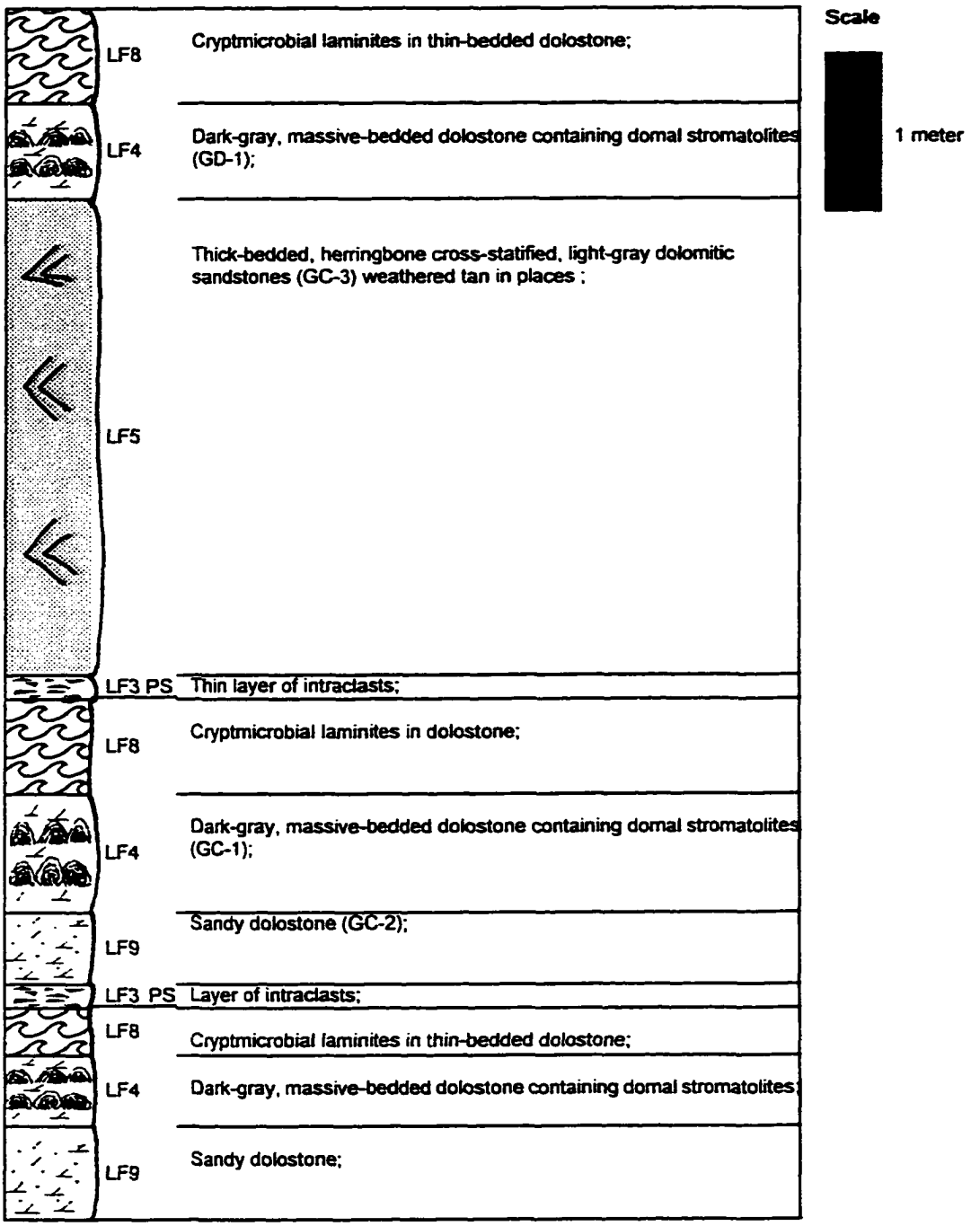

OUTCROP #4 (Route 9N):Galway Formation

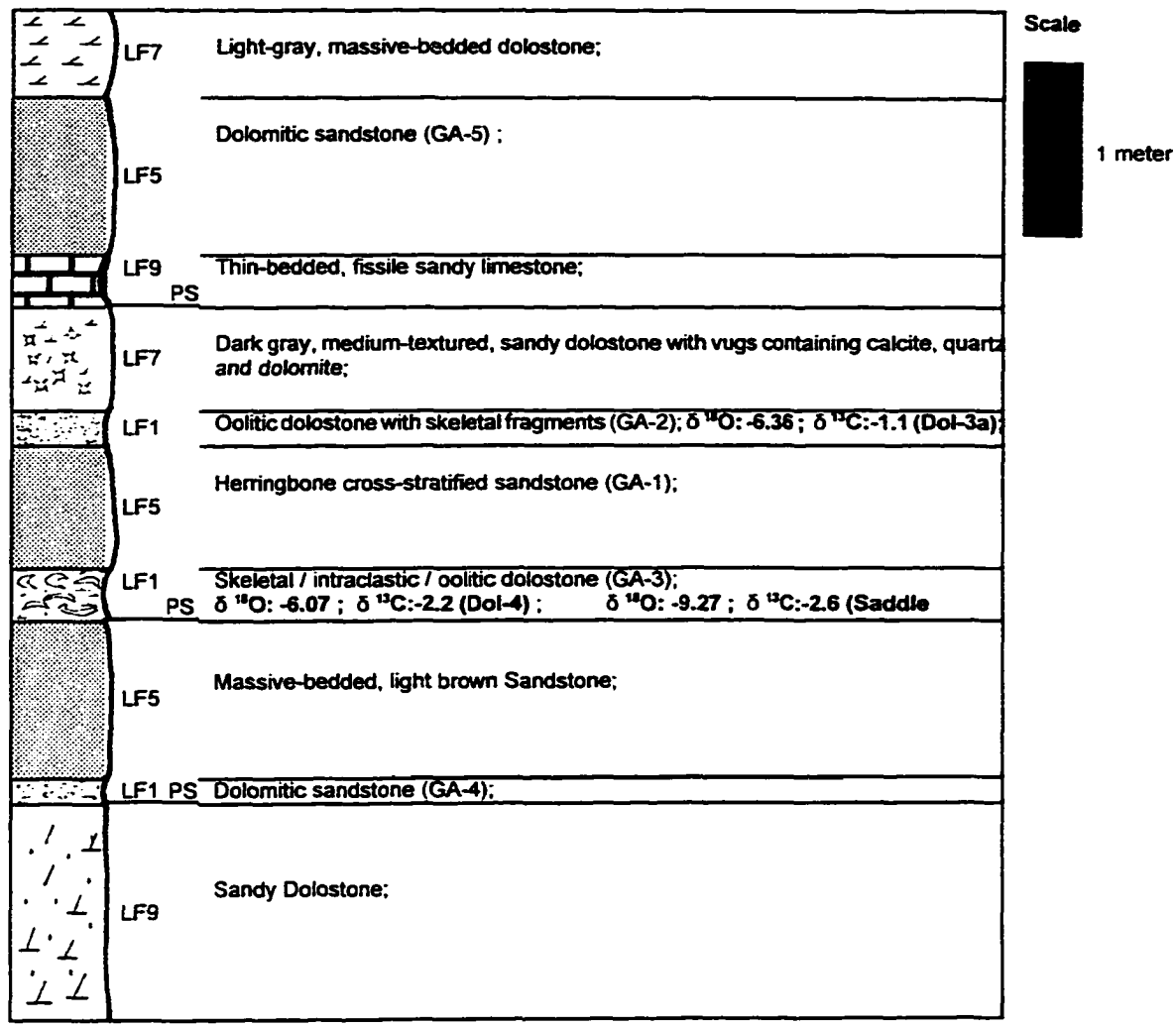

OUTCROP #5 (Railroad cut near Canty Road):Galway Formation

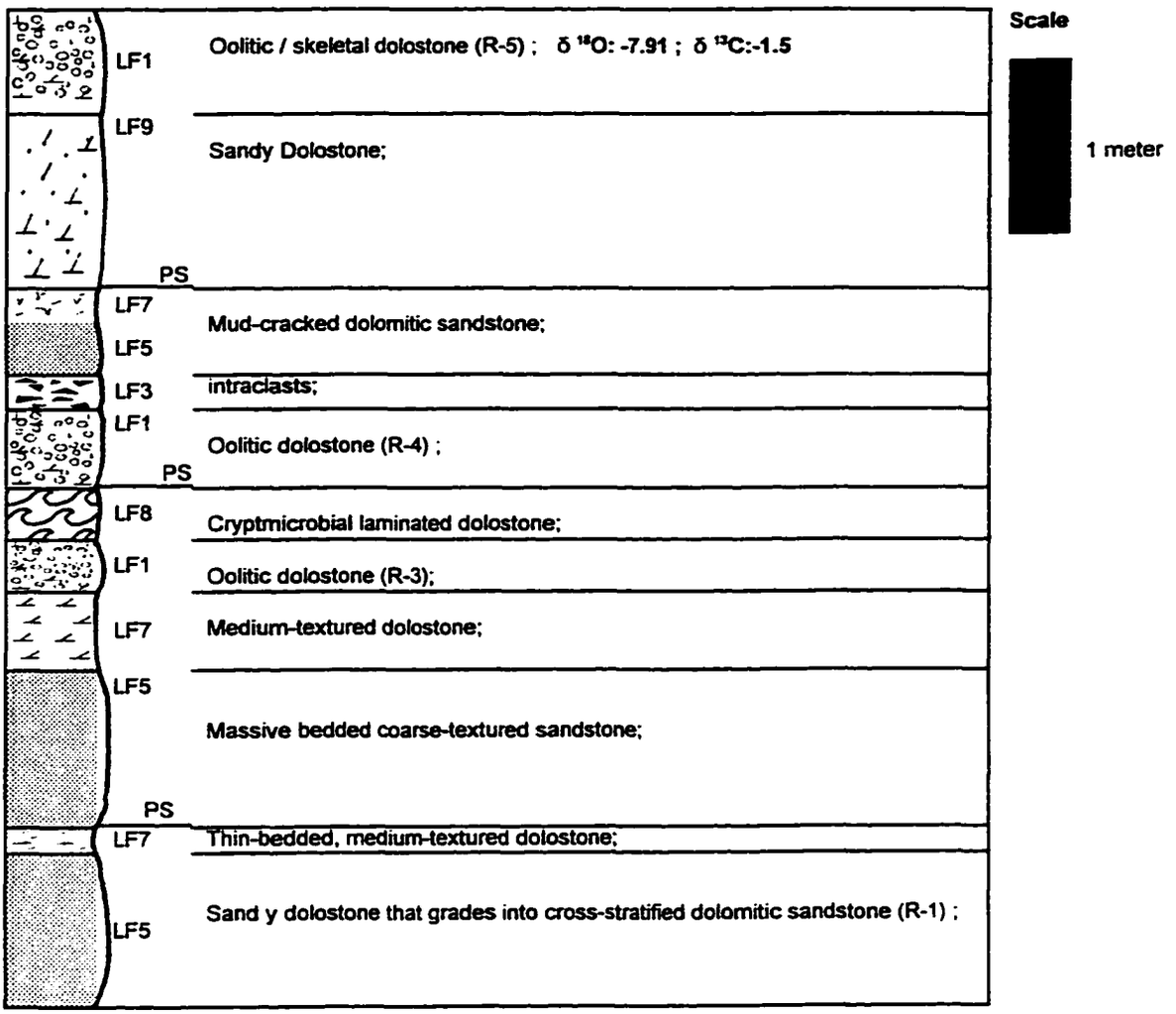

OUTCROP #6 (Petrified Gardens): Hoyt and Galway Formations

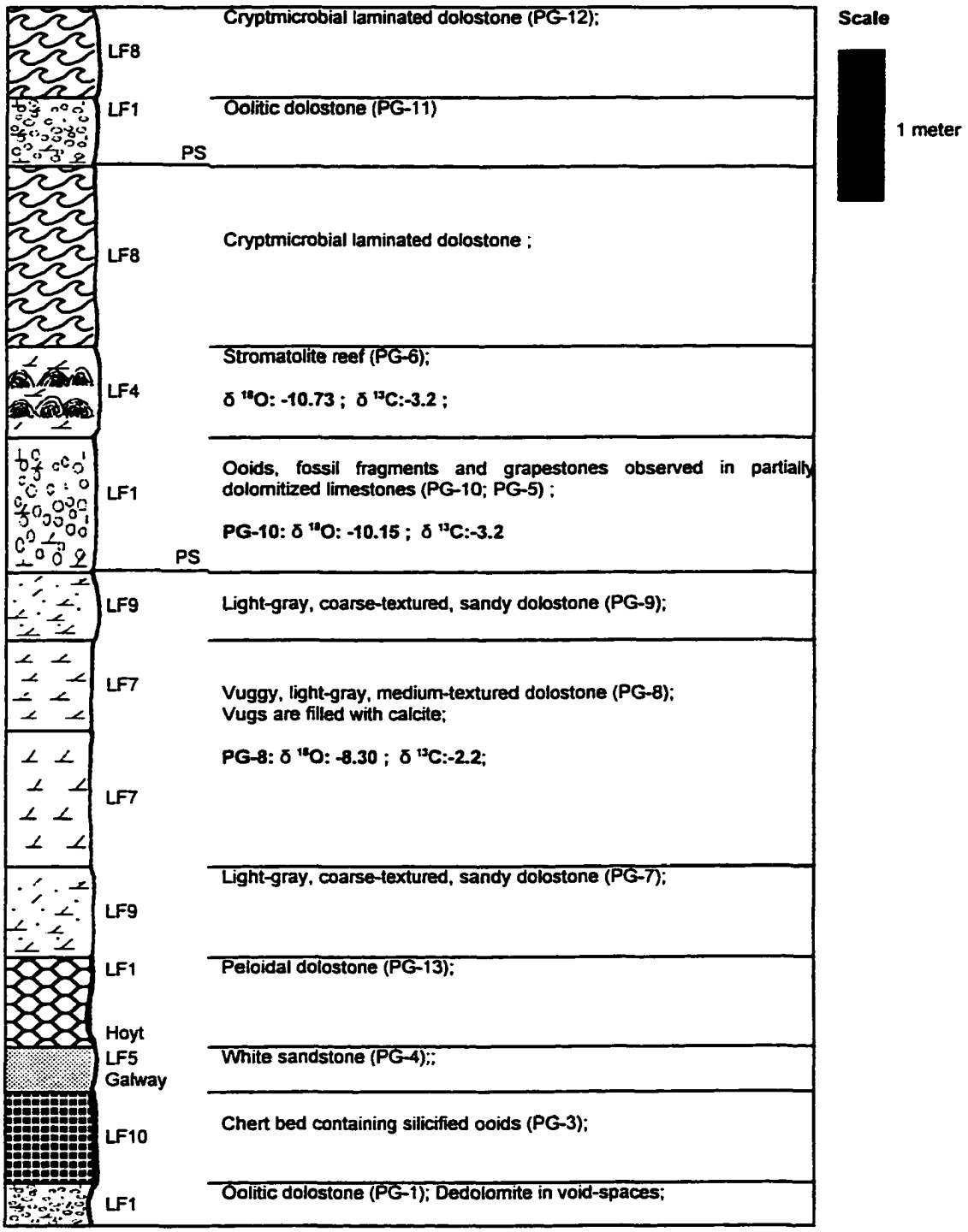

OUTCROP #7 (Lester Park Quarry): Hoyt Formation

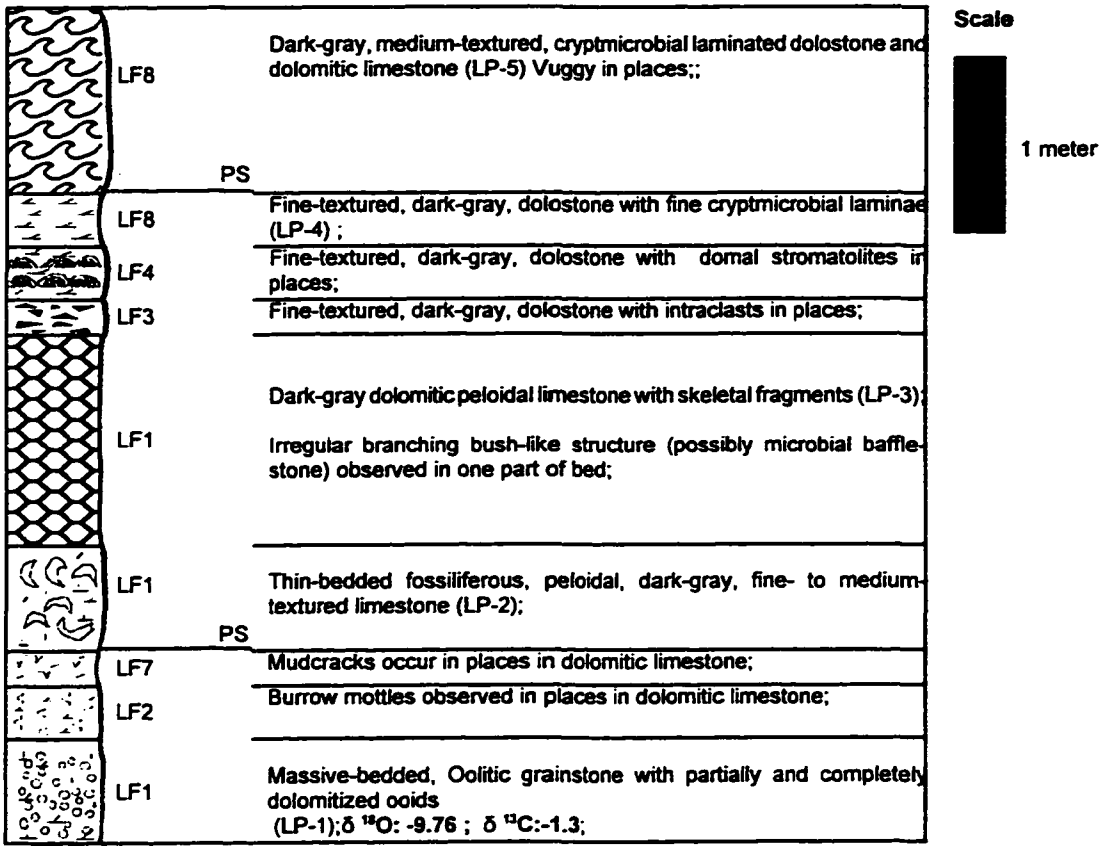

OUTCROP #8 (Roadcut on Petrified Gardens Road): Hoyt Formation

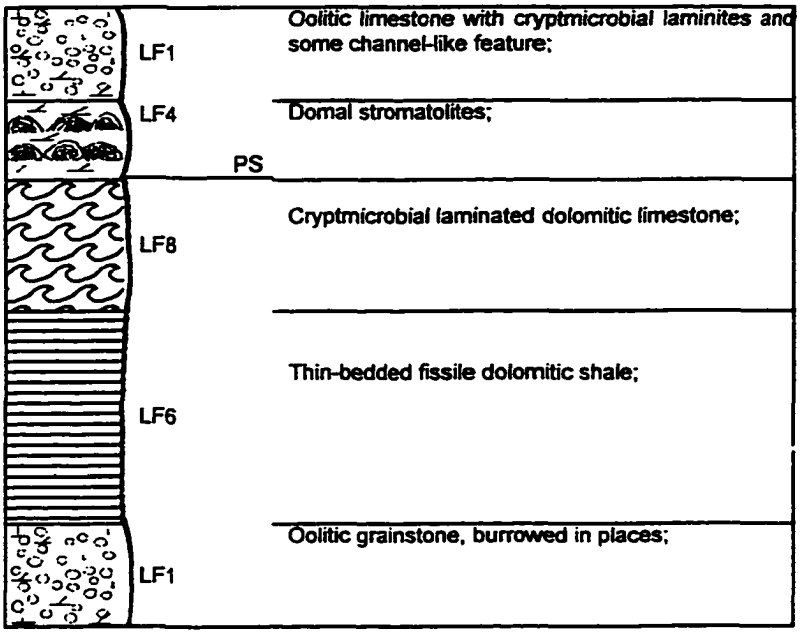

OUTCROP #9 (Route 67, 2.67km west of 147): Gailor Formation

LF8	Cryptmicrobial laminated dolostone;
LF3	Intraclast layer;
LF8	Cryptmicrobial laminated dolostone;
LF11	Karst breccia with clasts of vuggy or laminated dolomudstones, pods of cher surrounded by a coarse-textured sandy dolostone; (BS-1, BS-2, BS-3, BS-4, BS-5,BS-6, BS-7, BS-8, BS-9); BS-1:δ ^{18}O: -7.53 ; δ ^{13}C:-1.3; BS-6:δ ^{18}O: -5.59 ; δ ^{13}C:-1.8; BS-9: δ ^{18}O: -7.12 ; δ ^{13}C:-0.5;
LF8	Cryptmicrobial laminated dolostone; (GL-11); Dedolomite present;
LF7	Vuggy dolostone with some pyrite;

Scale

1 meter

OUTCROP #10 (Route 67, 3.83km west of 147): Gailor Formation

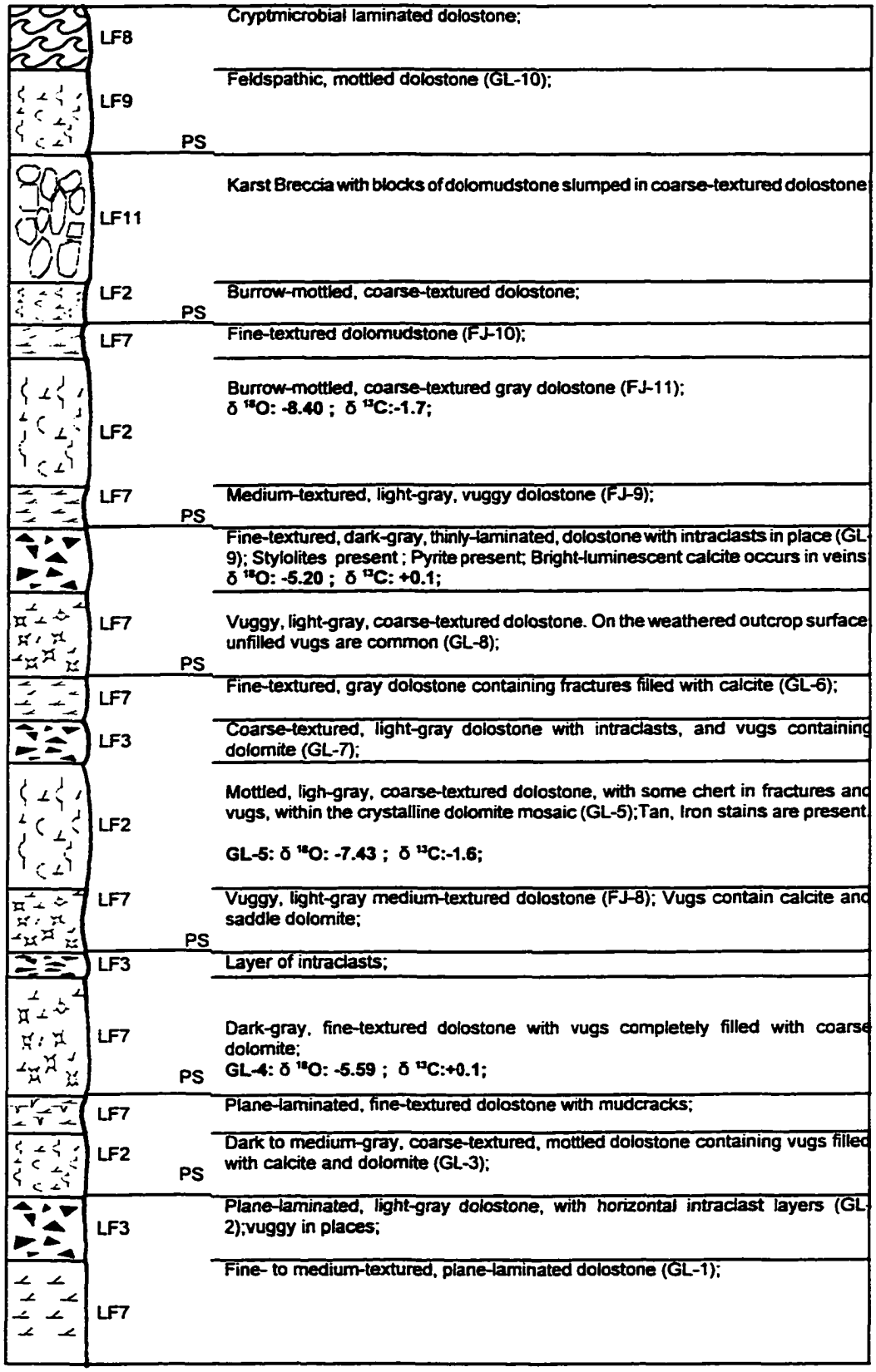

OUTCROP #11 (Route 67, West of #10): Gailor Formation

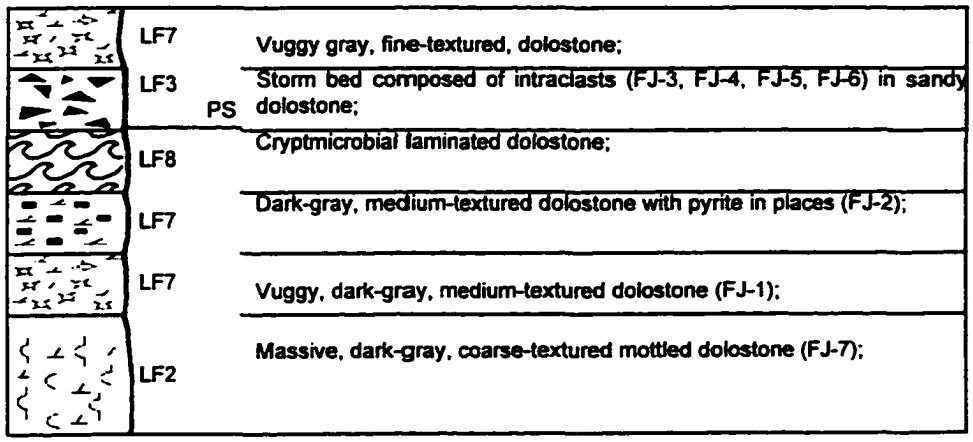

OUTCROP #12 (Route 67, West of #11 near Manny Corners): Gailor Formation

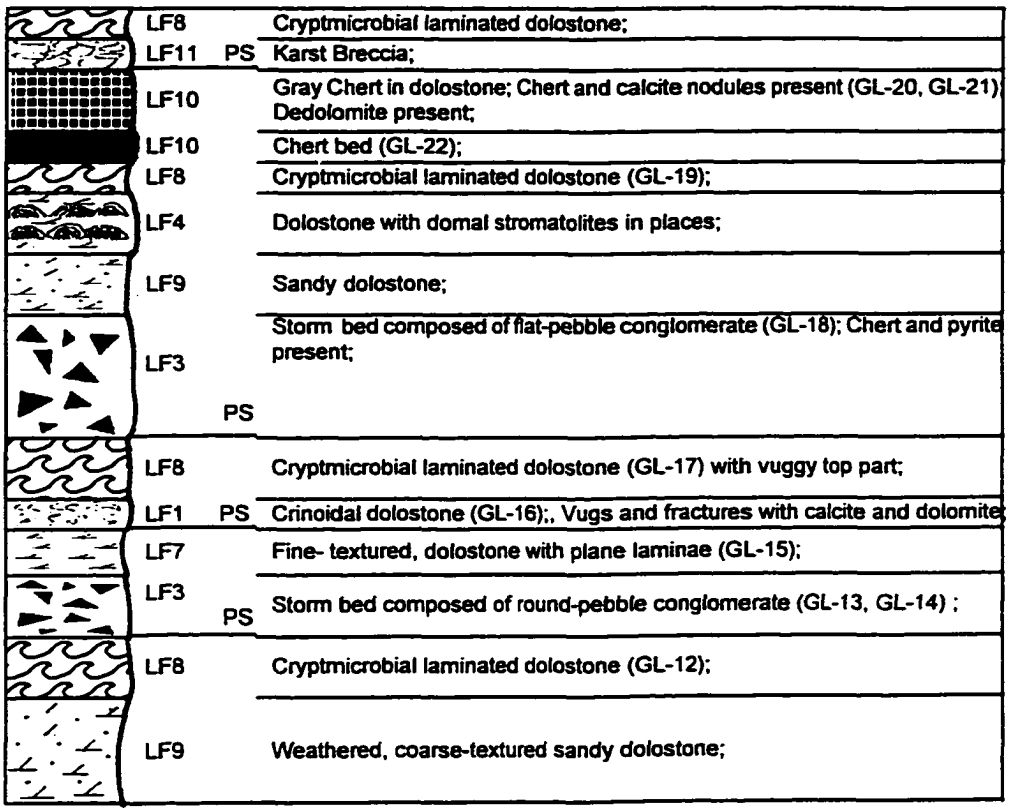

OUTCROP #13, Pallette Quarry (Route 29W, Saratoga Springs): Gailor Formation

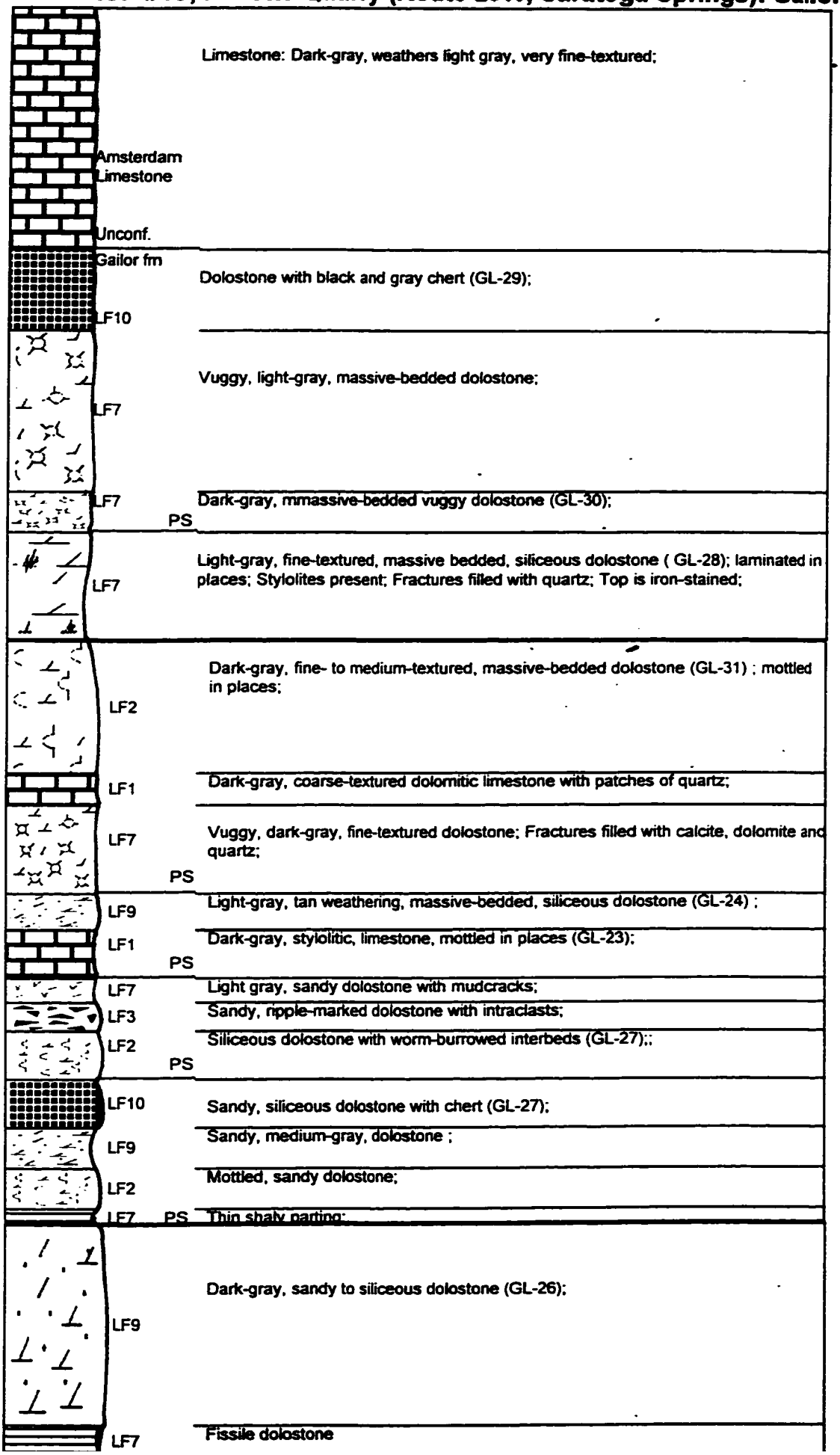

OUTCROP #14 (Route 5 East): Little Falls Formation

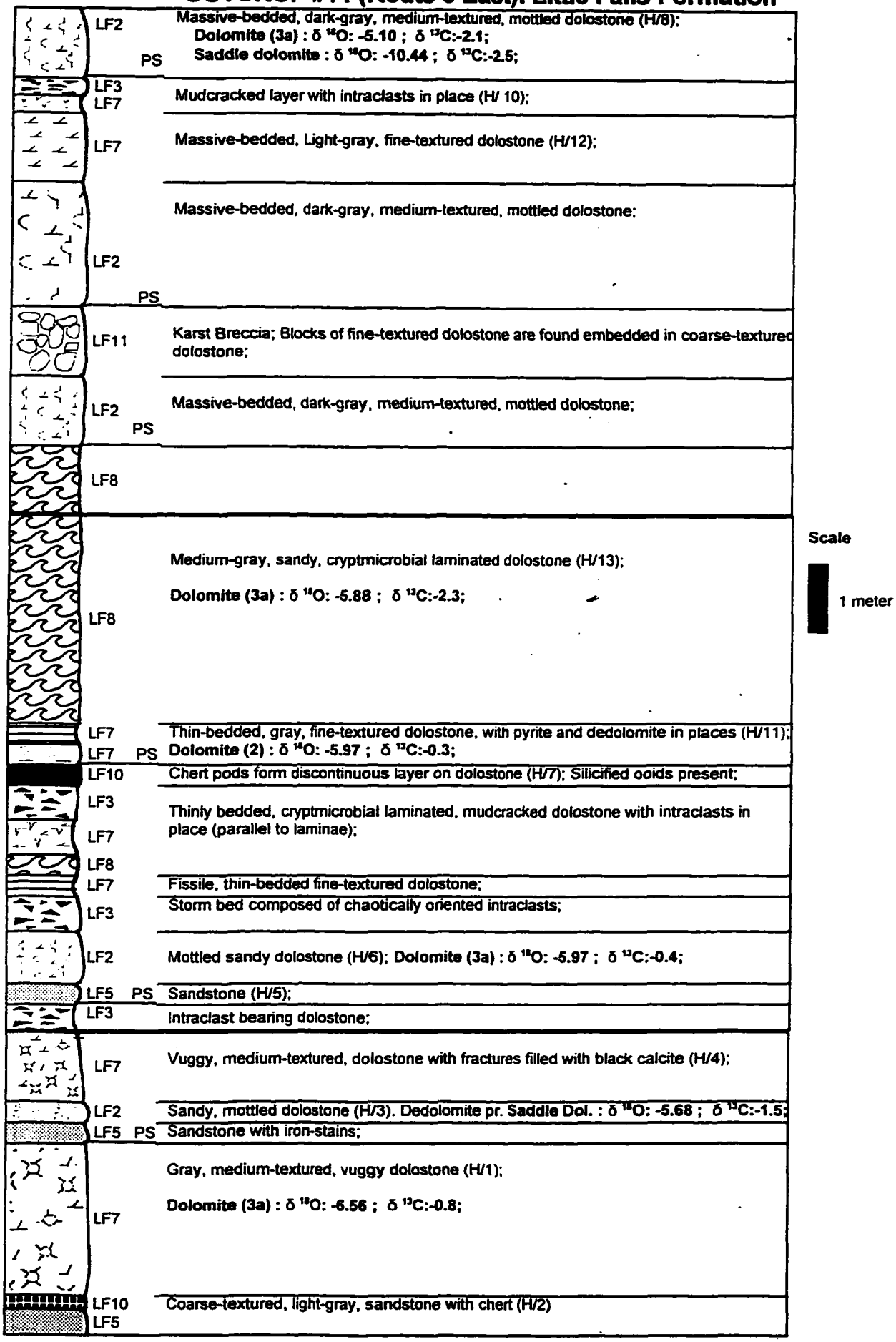

OUTCROP #15 (Route 5 West, East of Amsterdam): Tribes Hill Formation (Wolf Hollow and Palatine Bridge members)

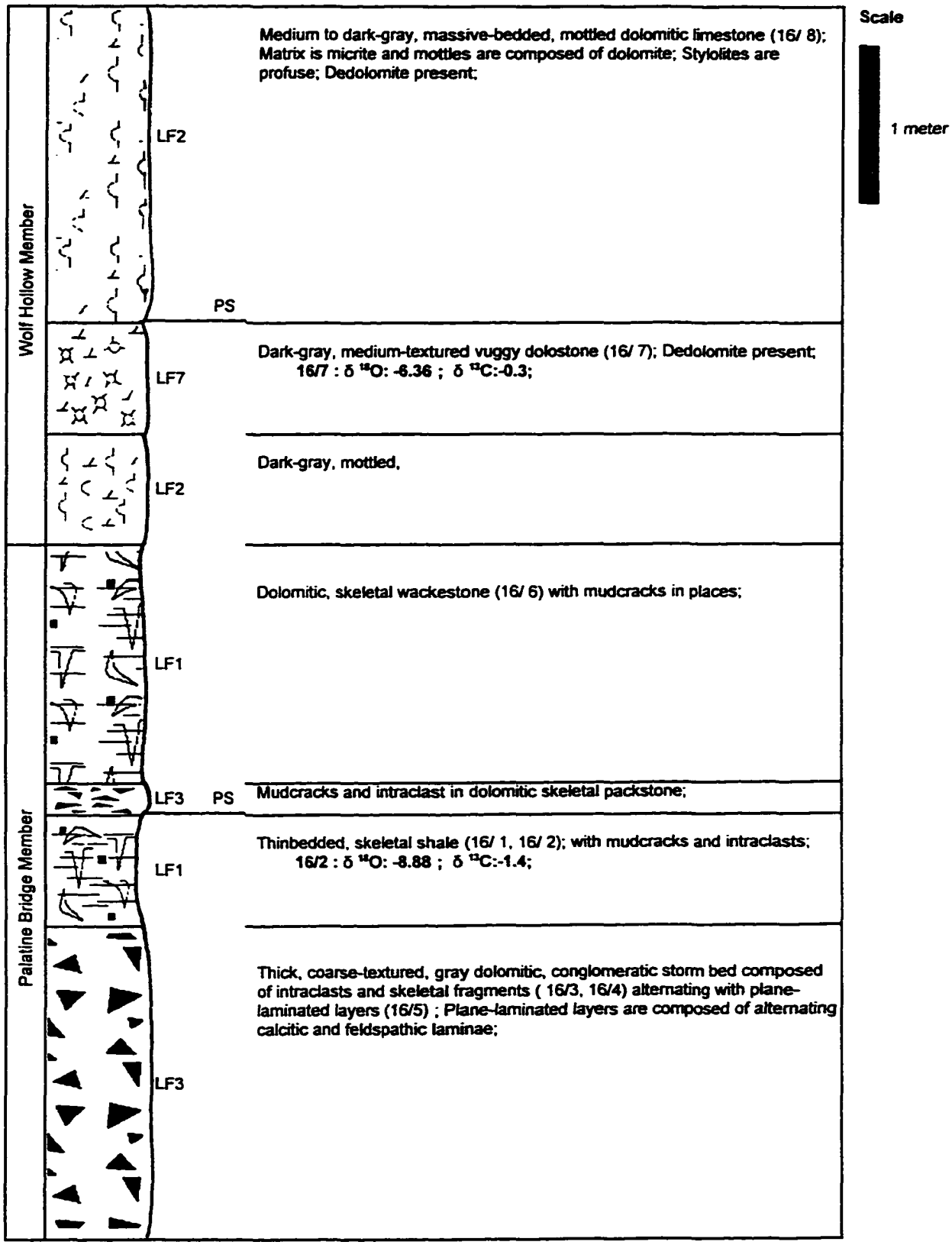

OUTCROP #16 (Van Wie Creek): Tribes Hill Formation (Fonda, Wolf Hollow and Palatine Bridge members)

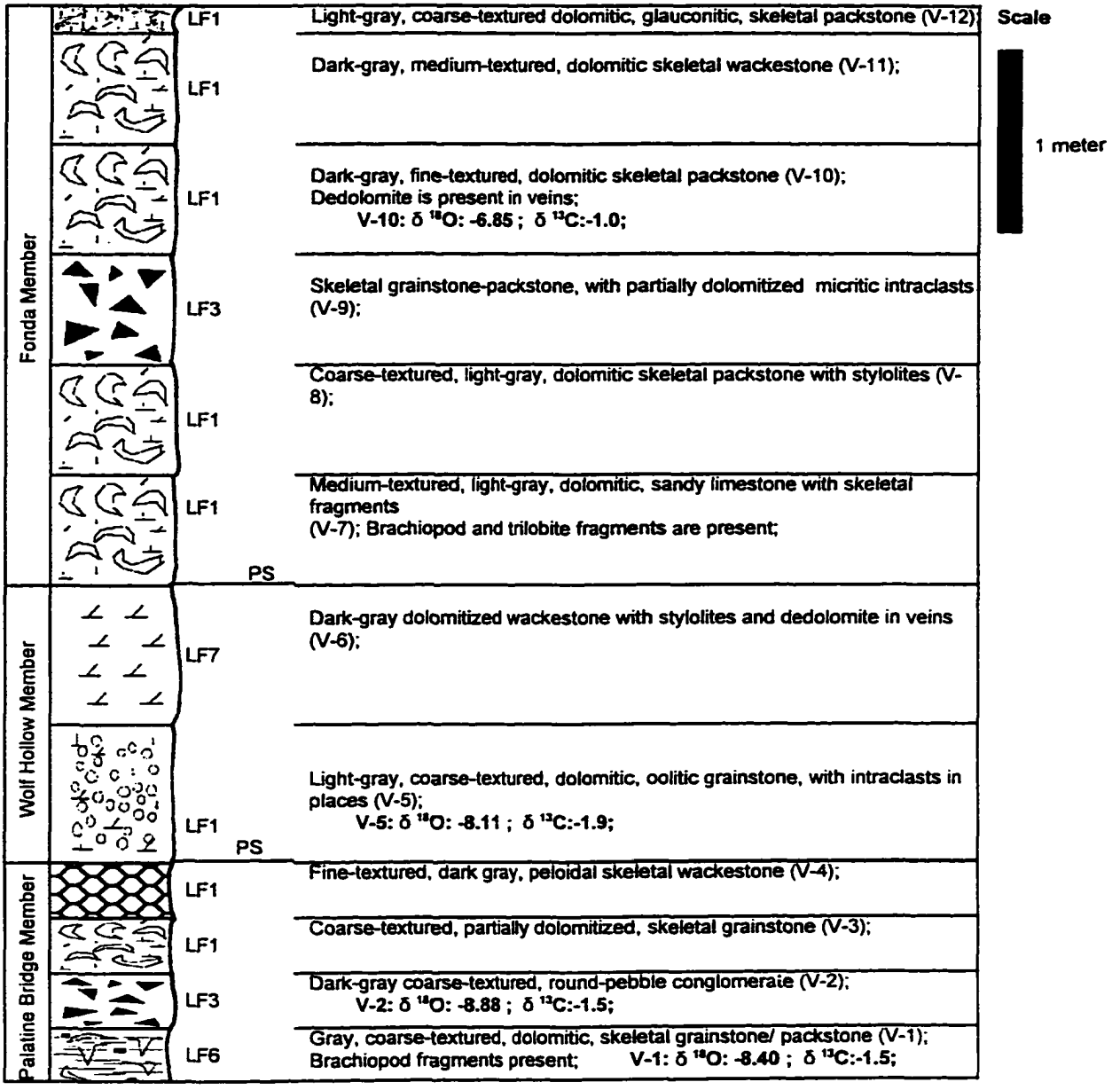

OUTCROP #17 (Roadcut on Borden Road): Tribes Hill Formation (Fonda member) and Black River Group

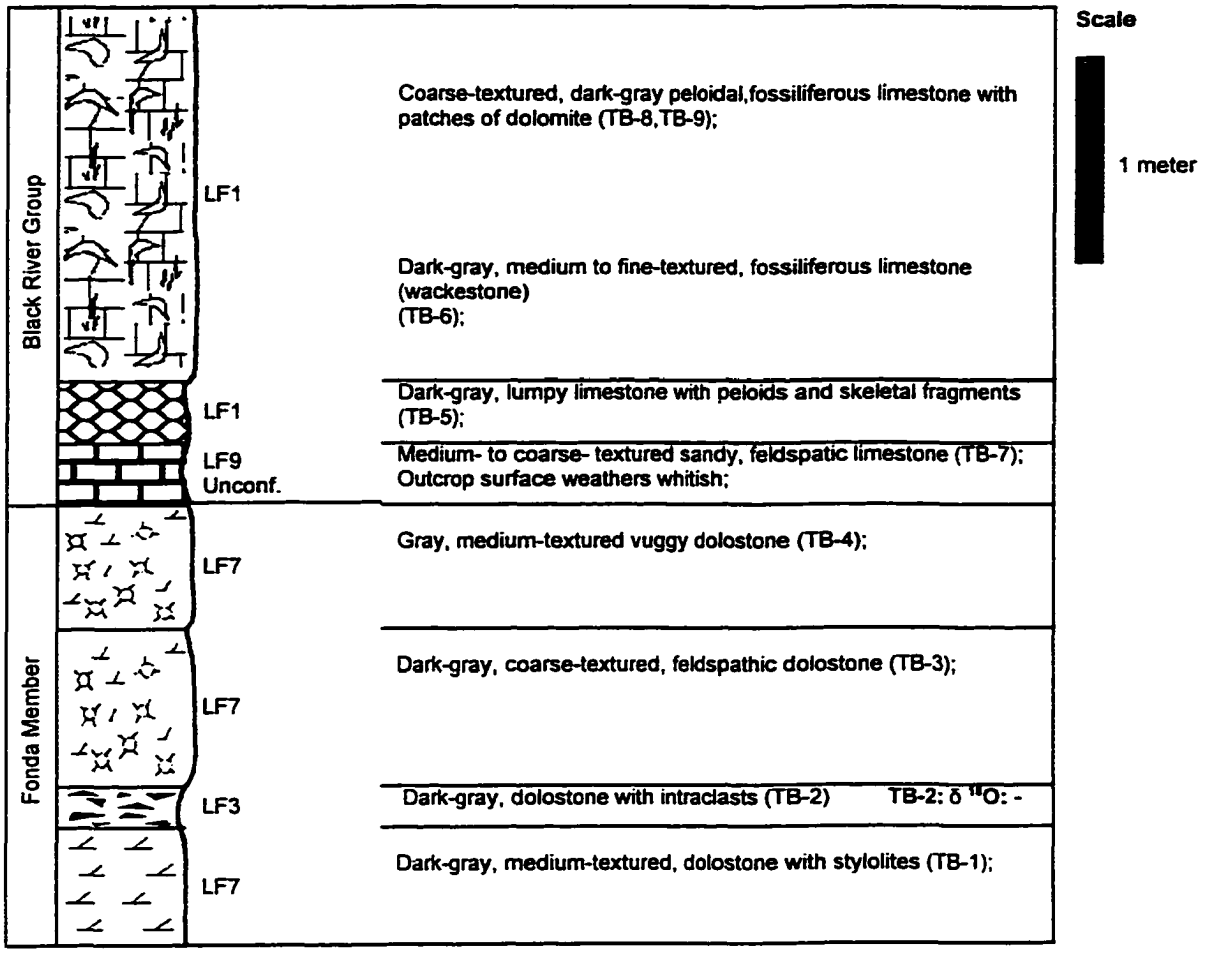

OUTCROP #18 (Fort Hunter Quarry): Tribes Hill Formation (Fort Johnson member)

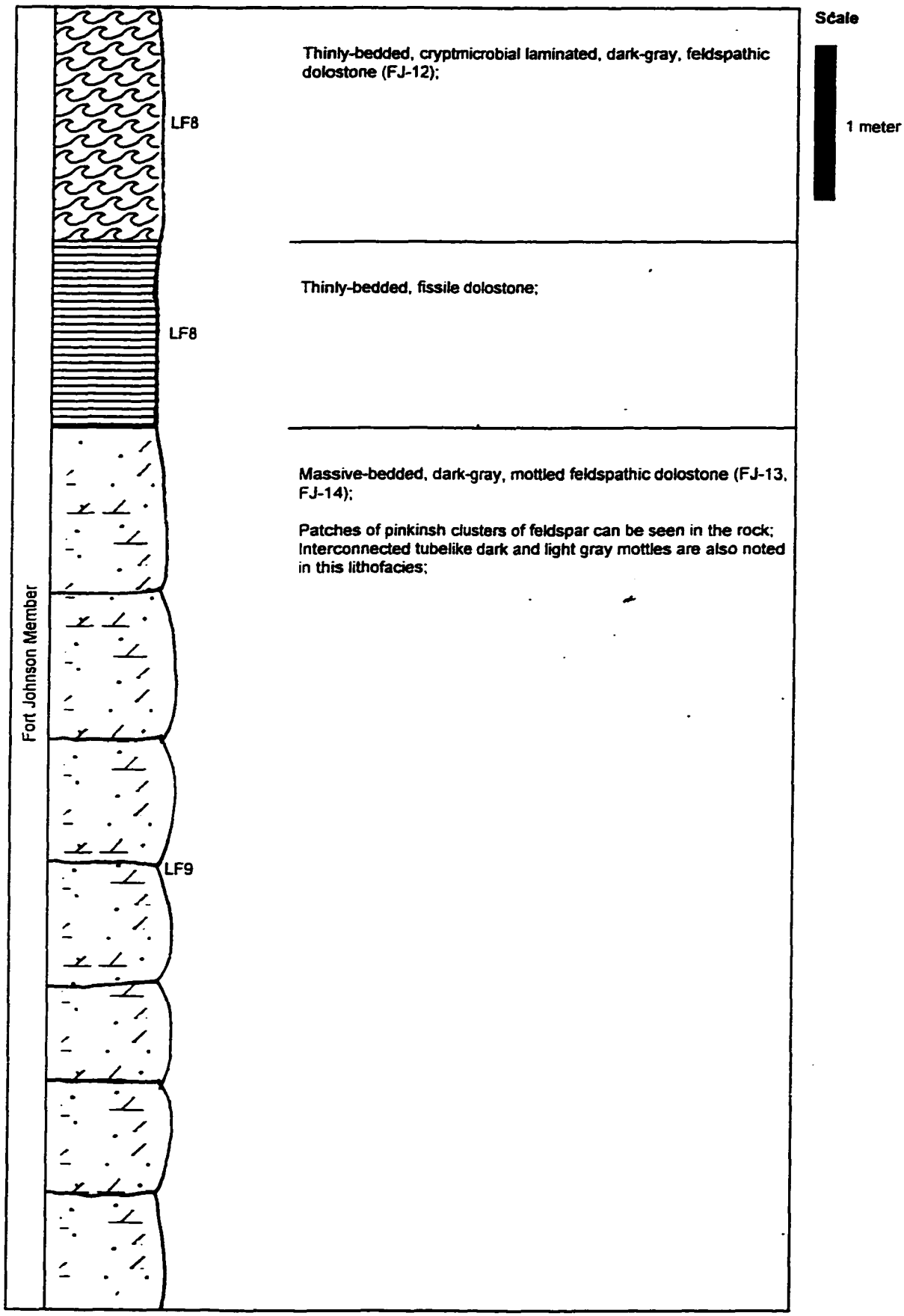

Appendix III – Geochemical Data

Major- and Trace-Element Chemistry of the Galway Dolostones

Description	out-crop #	Sam-ple	$CaCO_3$ Mol %	$MgCO_3$ Mol %	Crystal size (μm)	Ca wt%	Mg wt%	Fe ppm	Mn ppm	Sr ppm	$\delta^{18}O$ ‰	$\delta^{13}C$ ‰
Replacement Dolomite-1	1	GB-8	52.9	47.0	<10	24.43	13.14	1602	521	0		
Dolomite-5	1	GB-8	51.5	48.4	75	22.42	12.78	286	373	0		
Replacement Dolomite-2	1	GB-8	52.8	47.1	40	23.61	12.79	673	262	0	-5.88	-2.2
Replacement Dolomite-2	1	GB-8	50.4	49.5	40	22.23	13.23	619	377	0		
Replacement Dolomite-1	1	GB-8	53.0	46.9	<10	24.01	12.88	1624	374	0		
Saddle Dolomite-6	1	GB-8	50.0	49.9	400	21.57	13.04	5748	730	0		
Saddle Dolomite-6	1	GB-8	55.4	44.8	200	25.41	12.33	15341	3538	172		
Dolomite-5	1	GB-8	53.1	46.8	70	24.08	12.86	541	659	0		
Saddle Dolomite-6	1	GB-8	50.1	49.8	400	21.05	12.67	16064	2977	0		
Dolomite-5	1	GB-8	53.5	46.4	75	24.06	12.65	0	372	37		
Replacement Dolomite-2	1	GB-8	50.9	49.0	30	21.88	12.80	1521	259	0		
Replacement Dolomite-1	1	GB-8	53.1	46.8	<10	23.67	12.65	774	539	0		
Saddle Dolomite-6	1	GB-12	56.5	43.4	300	25.15	11.70	21000	5486	0		
Saddle Dolomite-6	1	GB-12	52.7	47.2	500	20.94	11.40	16015	3158	0		
Replacement Dolomite-2	1	GB-12	58.5	41.5	45	24.58	10.58	14343	3022	663		
Dolomite-5	1	GB-12	55.2	44.7	120	24.95	12.24	17854	3579	300		
Saddle Dolomite-6	1	GB-13	50.1	49.8	450	21.85	13.14	2186	383	0		
Replacement Dolomite-4	1	GB-13	51.3	48.6	120	22.72	13.05	604	812	192	-6.17	-1.9
Cement Calcite-3	1	GB-13	98.8	0.01		40.22	0.252	4076	5173	0		
Cement Calcite-3	1	GB-13	99.4	0.06		41.87	0.173	4050	6373	0		
Saddle Dolomite-6	1	GB-13	50.9	49.0	450	21.31	12.41	1867	814	0		
Replacement Dolomite-4	1	GB-13	52.6	47.3	150	25.07	13.72	429	627	438		
Replacement Dolomite-4	3	GC-1	51.4	48.5	150	23.69	13.55	0	719	160		
Replacement Dolomite-4	3	GC-1	49.7	50.2	180	21.37	13.10	0	476	0		
Replacement Dolomite-4	3	GC-2	52.3	47.6	150	23.41	12.93	1464	880	165		
Replacement Dolomite-4	3	GC-2	49.7	50.2	150	21.75	13.34	1523	882	0		
Replacement Dolomite-4	3	GC-2	51.1	48.8	150	22.68	13.16	395	1044	0		
Replacement Dolomite-4	4	GA-3	51.6	48.3	120	22.13	12.57	10550	3257	0	-6.07	-2.2
Replacement Dolomite-4	4	GA-3	52.2	47.8	120	22.05	12.25	19706	4505	652		
Cement Calcite-3	1	GB-3	99.7			41.61	0.125	2132	5750	242		
Replacement Dolomite-4	1	GB-3	50.3	49.6	150	21.27	12.71	257	794	0		
Replacement Dolomite-1	1	GB-3	52.2	47.7	6	22.92	12.71	71	397	0		
Saddle Dolomite-6	2	GB-6	53.0	46.9	450	19.98	10.72	14577	4543	0		
Saddle Dolomite-6	5	R-5	53.6	46.2	850	24.37	12.76	2328	1102	0	-7.91	-1.5
Replacement Dolomite-4	5	R-5	50.8	49.1	150	22.13	13.00	773	780	31		
Dolomite-5	1	GB-10	49.5	50.4	120	21.77	13.43	41	575	0		
Dolomite-5	1	GB-10	52.6	47.3	120	23.93	13.02	342	421	0		
Dolomite-1 in Ooids	1	GB-10	51.8	48.1	<10	22.7	12.96	0	719	0	-6.17	-2.1

Major- and Trace-Element Chemistry of the Gailor Dolostones

Description	Out-crop #	Sam-ple	$CaCO_3$ Mol %	$MgCO_3$ Mol %	Crystal Size (μm)	Ca wt%	Mg wt%	Fe ppm	Mn ppm	Sr ppm	$\delta^{18}O$ ‰	$\delta^{13}C$ ‰
Replacement Dolomite-3a	9	BS-2	55.5	44.4	320	23.72	11.49	3243	254	0		
Calcite Cement-4 (Dedolomite)	9	BS-2	99.4			44.89	0.157	1046	1833	748		
Calcite Cement-4 (Dedolomite)	9	BS-2	99.2			40.98	0.199	2121	3319	0		
Replacement Dolomite-3a	9	BS-2	50.7	49.2	300	22.07	12.99	616	0	215		
Replacement Dolomite-2	9	BS-6	56.2	44.0	40	24.84	11.72	1397	29	0	-5.59	-1.8
Replacement Dolomite-2	9	BS-6	53.02	46.9	45	22.97	12.33	55	0	0		
Replacement Dolomite-2	9	BS-6	55.8	44.2	45	24.12	11.60	1032	289	0		
Calcite Cement-3	9	BS-6	66.8	33.1		27.70	8.33	620	258	498		
Cement Dolomite-7	9	BS-6	55.0	44.9	80	24.88	12.28	9915	424	192		
Dolomite-5	9	BS-6	54.0	45.9	200	23.17	11.97	0	133	0		
Calcite Cement-4 (Dedol.)	9	GL-11	97.1	0.02		45.76	0.827	823	1516	381		
Cement Dolomite-7	9	GL-11	54.1	45.8	200	22.62	11.62	16289	2408	0		
Replacement Dolomite-3a	9	GL-11	59.4	40.5	300	27.39	11.35	145	236	283		
Replacement Dolomite-3a	9	GL-11	58.9	41.0	320	26.05	11.03	4380	893	270		
Replacement Dolomite-3a	10	GL-1	50.7	49.2	100	21.75	12.78	5811	168	140		
Saddle Dolomite-6	10	GL-1	53.2	46.7	250	23.11	12.29	7983	818	0		
Saddle Dolomite-6	10	GL-1	52.1	47.9	900	21.91	12.22	17911	2543	0		
Replacement Dolomite-3a	10	GL-1	53.1	46.8	150	23.59	12.60	3099	0	0		
Replacement Dolomite-4	10	GL-3	52.6	47.3	300	24.33	13.27	1566	345	131		
Calcite Cement-4 (Dedolomite)	10	GL-3	99.4			41.40	0.153	1220	1487	0		
Replacement Dolomite-4	10	GL-3	54.5	45.5	100	24.67	12.47	2976	102	541		
Replacement Dolomite-4	10	GL-3	51.3	48.6	300	22.26	12.79	5380	530	539		
Dolomite-5	10	GL-4	59.7	40.2	300	26.84	10.96	14902	103	116	-5.59	+0.1
Replacement Dolomite-3a	10	GL-4	56.5	43.4	150	24.72	11.52	449	298	589		
Replacement Dolomite-3a	10	GL-4	56.3	43.6	180	26.15	12.26	1510	194	1434		
Replacement Dolomite-3a	12	GL-12	56.2	43.7	100	26.36	12.43	2080	271	781		
Calcite Cement-3	12	GL-12	99.7			41.33	0.044	1152	361	1017		
Calcite Cement-3	12	GL-12	99.9			41.78	0.027	1740	482	332		
Cement Dolomite-7	12	GL-12	52.4	47.5	150	21.69	11.95	8803	197	0		
Calcite Cement-3	12	GL-12	75.9	24.0		35.19	6.78	442	0	212		
Replacement Dolomite-3a	12	GL-14	54.0	45.9	150	23.50	12.11	3749	247	0		
Replacement Dolomite-3a	12	GL-14	58.0	41.9	120	26.16	11.47	976	271	5		
Replacement Dolomite-4	12	GL-14	51.6	48.3	80	22.08	12.53	1692	79	0		
Replacement Dolomite-4	12	GL-14	51.2	48.7	100	20.89	12.01	2214	517	0		
Saddle Dolomite-6	12	GL-14	52.5	47.4	650	21.00	11.51	3924	33	0		
Replacement Dolomite-4	12	GL-14	51.0	48.9	100	21.86	12.71	2011	137	0		
Calcite Cement-3	12	GL-14	75.6	24.3		31.93	6.24	10372	1109	0		
Saddle Dolomite-6	12	GL-14	51.4	48.5	550	21.98	12.59	3706	0	0		
Replacement Dolomite-4	12	GL-14	52.5	47.4	120	22.65	12.43	2246	298	0		
Replacement Dolomite-4	12	GL-16	49.9	50.0	150	24.61	15.00	294	0	121		
Calcite Cement-3	12	GL-16	77.4	22.5		34.20	6.04	1154	0	253		
Replacement Dolomite-4	12	GL-16	52.7	47.2	155	22.85	12.39	522	0	0		
Cement Dolomite-7	12	GL-16	50.9	49.0	150	22.96	13.37	1717	32	0		
Replacement Dolomite-4	12	GL-16	50.9	49.0	160	21.72	12.67	906	0	0		
Replacement Dolomite-3a	12	GL-18	53.3	46.6	120	23.85	12.65	3848	16	0		
Dedolomite Calcite-4	12	GL-18	68.8	30.1		29.05	7.59	1748	222	129		
Cement Dolomite-7	12	GL-18	55.0	45.0	300	22.97	11.43	7052	170	0		
Saddle Dolomite-6	12	GL-19	54.3	45.6	900	24.45	12.46	827	0	0		
Saddle Dolomite-6	12	GL-19	57.0	42.9	750	24.87	11.32	446	47	598		
Saddle Dolomite-6	12	GL-19	56.7	43.2	470	25.66	11.88	6928	82	217		
Replacement Dolomite-3a	12	GL-19	54.9	45.0	130	21.17	10.55	3606	307	0		
Saddle Dolomite-6	12	GL-19	57.5	42.4	150	25.85	11.57	6410	0	309		
Replacement Dolomite-5	12	GL-19	54.5	45.4	150	24.35	12.33	658	304	191		
Replacement Dolomite-5	12	GL-19	56.9	43.0	170	27.79	12.73	82	69	82		
Replacement Dolomite-3a	12	GL-19	53.4	46.5	165	22.97	12.15	436	0	528		
Replacement Dolomite-3a	12	GL-20	51.3	48.6	250	21.95	12.60	1477	244	0		
Replacement Dolomite-3a	12	GL-20	51.8	48.1	220	23.41	13.18	2245	178	0		
Replacement Dolomite-3a	12	GL-20	54.0	45.9	200	23.42	12.08	436	17	226		
Calcite Cement-3	12	GL-21	98.8			42.24	0.417	2575	256	303		
Calcite Cement-3	12	GL-21	74.3	25.6		31.58	6.60	456	97	0		
Saddle Dolomite-6	12	GL-21	55.4	44.5	360	25.01	12.17	6301	85	0		
Cement Dolomite-7	12	GL-22	52.4	47.5	150	22.69	12.51	19816	786	0		
Dolomite-3a in Chert	12	GL-22	59.4	40.5	100	27.70	11.48	3058	231	0		
Dolomite-3a in Chert	12	GL-22	53.0	46.9	100	24.19	12.98	120	12	86		

Major- and Trace-Element Chemistry of the Hoyt Carbonates

Description	Out-crop #	Sam-ple	$CaCO_3$ Mol %	$MgCO_3$ Mol %	Crystal Size (μm)	Ca wt%	Mg wt%	Fe ppm	Mn ppm	Sr ppm	$\delta^{18}O$ ‰	$\delta^{13}C$ ‰
Calcite-1 in Stromatolite	6	PG-6	99.2		<15	38.44	0.193	458	520	134		
Dolomite-3a in Stromatolite	6	PG-6	53.9	46.0	300	22.84	11.82	3181	985	191	-10.73	-3.2
Replacement Dolomite-4	6	PG-8	58.7	41.2	400	24.96	10.62	1436	348	50	-8.30	-2.2
Calcite Cement-3	6	PG-8	82.3	17.6		35.37	4.61	471	641	62		
Replacement Dolomite-4	6	PG-8	58.8	41.1	350	24.80	10.52	4918	1241	151		
Replacement Dolomite-4	6	PG-10	51.2	48.7	300	22.08	12.76	3626	882	40	-10.15	-3.2
Replacement Dolomite-4	6	PG-10	49.4	50.5	320	21.12	13.12	2716	1090	0		
Calcite Cement-2 in Oolitic Limestone	6	PG-10	98.7			40.20	0.299	3916	669	0		
Replacement Dolomite-4	7	LP-1	50.0	50.0	150	21.11	12.81	2619	734	0	-9.76	-1.3
Calcite Cement-2	7	LP-1	99.9			38.73	0.109	108	264	0		
Replacement Dolomite-4	7	LP-1	50.6	49.3	150	21.92	12.95	1795	386	0		
Calcite Cement-3	7	LP-4	85.1	14.8		30.97	3.28	4192	995	0	-6.21	-1.4
Replacement Dolomite-1	7	LP-4	56.0	43.9	15	23.29	11.08	2425	383	214		
Cement Dolomite-5	7	LP-4	55.8	44.1	180	23.94	11.46	5586	798	0		

Major- and Trace-Element Chemistry of the Little Falls Carbonates (outcrop # 14)

Description	Sample	$CaCO_3$ Mol %	$MgCO_3$ Mol %	Crystal Size (μm)	Ca wt%	Mg wt%	Fe ppm	Mn ppm	Sr ppm	$\delta^{18}O$ ‰	$\delta^{13}C$ ‰
Replacement Dolomite-3a	H/1	54.9	45.0	150	24.42	12.13	1268	419	254	-6.56	-0.8
Replacement Dolomite-3a	H/1	53.4	46.5	100	22.71	12.00	1686	0	4		
Replacement Dolomite-3a	H/1	55.0	44.9	120	24.32	12.03	4485	145	0		
Replacement Dolomite-3a	H/3	52.3	47.6	180	24.25	13.40	236	0	268		
Saddle Dolomite-6	H/3	55.7	44.2	1000	25.89	12.47	4798	141	0	-5.68	-1.5
Replacement Dolomite-3a	H/3	55.3	44.6	120	25.22	12.35	0	122	0		
Replacement Dolomite-2	H/3	56.5	43.4	60	27.87	13.00	198	198	777		
Replacement Dolomite-3a	H/8	53.6	46.3	150	22.30	11.69	576	291	0	-5.10	-2.1
Calcite Cement-3	H/8	97.8			41.00	0.564	2115	822	0		
Calcite Cement-3	H/8	98.1			40.46	0.460	1503	105	333		
Replacement Dolomite-3a	H/8	58.1	41.8	150	27.44	11.99	0	269	521		
Replacement Dolomite-3a	H/9	56.7	43.2	150	27.04	12.50	158	67	167		
Replacement Dolomite-3a	H/9	53.9	46.0	160	24.20	12.54	408	145	489		
Zoned Saddle Dolomite-6	H/10	57.0	42.9	600	27.28	12.46	14497	214	172		
Replacement Dolomite-2	H/10	55.2	44.7	40	24.17	11.88	19724	63	426		
Replacement Dolomite-3a	H/10	55.6	44.3	200	26.37	12.73	159	60	0		
Replacement Dolomite-2	H/11	54.8	45.1	35	27.40	13.68	532	45	476	-5.97	-0.3
Replacement Dolomite-3a	H/13	57.8	42.1	350	27.11	11.99	534	136	47	-5.88	-2.3
Replacement Dolomite-3a	H/13	52.5	47.4	250	22.81	12.49	650	0	0		
Replacement Dolomite-3a	H/13	59.7	40.2	300	28.11	11.48	0	0	388		
Dedolomite Calcite-4	H/13	99.2			42.16	0.195	711	400	581		
Replacement Dolomite-3a	H/13	55.9	44.0	350	26.59	12.72	2826	325	0		

Major- and Trace-Element Chemistry of the Tribes Hill Carbonates

Description	out-crop #	Mem-ber	Sam-ple	$CaCO_3$ Mol %	$MgCO_3$ Mol %	Crystal Size (μm)	Ca wt%	Mg wt%	Fe ppm	Mn ppm	Sr ppm	$\delta^{18}O$ ‰	$\delta^{13}C$ ‰
Replacement Dolomite-3a	15	Pala-	16/2	54.0	45.9	250	22.30	11.50	3140	893	200	-8.88	-1.4
Dull luminescent Calcite-1	15	tine	16/2	99.0			41.92	0.255	409	237	205		
Replacement Dolomite-3a	15	Bridge	16/2	54.1	45.8	250	33.54	17.24	1085	705	889		
Dull luminescent Calcite-2	15		16/2	98.0			38.01	0.378	455	264	0		
Dolomite-5	15		16/7	55.5	44.4	180	23.62	11.47	289	254	106		
Replacement Dolomite-3a	15		16/7	55.7	44.2	70	25.64	12.33	571	0	431	-6.36	-0.3
Dolomite-7	15	Wolf	16/7	53.9	46.0	75	23.95	12.40	4572	185	0		
Replacement Dolomite-3a	15	Hollow	16/7	56.1	43.8	70	25.84	12.26	0	0	0		
Cement Calcite-3	15		16/8	98.1			42.56	0.492	259	0	0		
Non-luminescent Calcite-1	15		16/8	99.2			40.66	0.309	335	72	0		
Non-luminescent Calcite-1	15		16/8	98.8			39.07	0.274	961	223	0		
Stylolite Dolomite-3b	15		16/8	53.7	46.2	100	23.62	12.35	2582	287	0		
Calcite Cement-3	16		V-6	67.8	32.1		35.04	10.07	1040	0	0		
Stylolite Dolomite-3b	16	Wolf	V-6	57.5	42.4	150	24.50	10.95	5140	0	0		
Non-luminescent Calcite-3	16	Hollow	V-6	77.5	22.4		31.95	5.62	2478	0	368		
Non-luminescent Calcite-1	16		V-6	99.5			49.39	0.141	469	0	1292		
Dull luminescent Calcite-1	16		V-9	98.8			38.25	0.275	324	362	0		
Replacement Dolomite-3a	16		V-9	55.1	44.8	250	22.99	11.32	2513	453	0		
Zoned Calcite Cement-3	16		V-9	67.2	32.7		23.60	6.96	13861	858	0		
Stylolite Dolomite-3b	16	Fonda	V-10	55.6	44.3	72	23.62	11.41	1724	254	29	-6.85	-1.0
Stylolite Dolomite-3b	16		V-10	55.0	44.9	75	22.33	11.08	2255	68	260		
Stylolite Dolomite-3b	16		V-10	55.9	44.0	70	28.73	13.75	7394	356	209		
Calcite-1	16		V-10	99.3			82.47	0.333	283	434	1495		
Calcite-1	16		V-10	98.9			38.42	0.257	2100	265	348		
Calcite Cement-3	17		TB-1	63.3	36.6		27.32	9.59	2602	220	0		
Dolomite-5	17		TB-1	51.7	48.2	250	22.42	12.67	622	464	0		
Replacement Dolomite-3a	17		TB-1	56.1	43.8	70	23.84	11.29	735	0	0		
Dolomite-5	17		TB-2	53.1	46.8	250	22.85	12.23	345	198	39		
Replacement Dolomite-3a	17		TB-2	52.5	47.4	400	22.11	12.10	4194	0	0	-5.0	-2.9
Dolomite-5	17	Fonda	TB-2	52.9	47.0	180	23.88	12.86	393	360	327		
Replacement Dolomite-3a	17		TB-4	52.3	47.6	75	23.76	13.12	2045	184	579		
Replacement Dolomite-3a	17		TB-4	54.2	45.7	250	23.53	12.03	3360	331	358		
Replacement Dolomite-3a	17		TB-4	55.2	44.7	80	24.12	11.83	4061	0	0		
Dolomite-5	17		TB-4	53.3	46.6	250	22.87	12.15	628	107	53		

REFERENCES

Adams, J.E. and Rhodes, M.G., 1960, Dolomitization by seepage refluxion: AAPG Bulletin, v. 44, p.1912-1920.

Aigner, T., 1982, Calcareous tempestites: storm-dominated stratification in upper Muschelkalk limestones (middle Trias, SW Germany), p. 180-198, in G. Einsele and A. Seilacher (eds.), Cyclic and Event Stratification: Springer-Verlag, New York, 536 p.

Aigner, T., 1985, Storm depositional systems, in G.M. Friedman, H.J. Neugebauer, and Adolph Seilacher (eds.), Lecture Notes in Earth Sciences, v. 3: Springer-Verlag, 174p.

Allan, J.R., and Wiggins, W.D., 1993, Dolomite Reservoirs, geochemical techniques for evaluating origin and distribution, AAPG Continuing Education Course note Series #36.

Amthor, J.E., and Friedman, G.M., 1991, Dolomite-rock textures and secondary porosity development in Ellenburger Group Carbonates (Lower Ordovician), West Texas and Southeastern New Mexico: Sedimentology, v. 38, p.343-362.

Amthor, J.E., and Friedman, G.M., 1992, Early to late diagenetic dolomitization of platform carbonates: Lower Ordovician Ellenburger group, Permian basin, West Texas: Journal of Sedimentary Petrology, v. 62, no.1, p.131-144.

Badiozamani, K.,1973, The Dorag dolomitization model-application to Middle Ordovician of Wisconsin: Journal of Sedimentary Petrology, v.43, p.965-984.

Baker, P.A., and Kastner, M., 1981, Constraints on the formation of sedimentary dolomite: Science, v.213, p.214-216.

Bambach, R.K., Scotese, C.R., and Zieglert, A.M., 1980, Before Pangaea: The geographies of the Paleozoic World: American Scientist, v. 68, p.26-38.

Banks, N.G., 1970, Nature and origin of early and late cherts in the Leadville Limestone, Colorado: GS A Bulletin, v.81, p.3033-3048.

Banner, J.L., Hanson, G.N., and Meyers, W.J., 1988, Determination of initial Sr isotopic compositions of dolostones from the Burlington Keokuk Formation (Mississipian): constraints from cathodoluminescence, glauconite, paragenesis and analytical methods: Journal of Sedimentary Petrology, v. 58, p.673-687.

Banner, J.L., Hanson, G.N., and Meyers, W.J., 1988, Water-rock interaction history of regionally extensive dolomites of the Burlington-Keokuk Formation (Miss.) Isotopic evidence, in Shukla, V. and Baker, P.A., (eds.), Sedimentology and Geochemistry of Dolostones: SEPM Special Publication. No. 43, p. 97-113.

Barnaby, R.J., and Read, J.F., 1992, Dolomitization of a carbonate platform during late burial: Lower to Middle Cambrian Shady dolomite, Virginia Appalachians: Journal of Sedimentary Petrology, v. 62, no. 6, p.1023-1043.

Bathurst, R.G.C., 1983, Early diagenesis of carbonate sediments, in Parker, A., and Sellwood, B.W., (eds.), Sediment Diagenesis: p.379-417.

Bathurst, R.G.C., 1994, Carbonate sediments and their diagenesis, Developments in Sedimentology 12: Elsevier Scientific Publishing Company, 658p.

Berner, R.A., 1970, Sedimentary pyrite formation: Am. Jour., Sci. 268, p.1-23.

Bird, J.M., and Dewey, J.F., 1970, Lithosphere plate continental margin tectonics and the evolution of the Appalachian orogen: GSA Bulletin, V. 81, p.1031-1060.

Bowring, S.A., Erwin, D.H., Jin, Y.G., Martin, M.W., Davidek, K., and Wang, W., 1998, U/Pb Zircon geochronology and Tempo of the End-Permian mass extinction: Science, v.280, p.1039-1045.

Braithwaite, C.J.R., 1991, Dolomites, a review of origins, geometry and textures, Transactions of the Royal Society of Edinburgh: Earth Sciences, 82(2), p.99-112.

Brasier, M.D., and Sikhov, S.S., 1998, The falling amplitude of carbon isotopic oscillations through the lower to middle Cambrian: northern Siberia data: Canadian Journal of Earth Science, v. 35, p.353-373.

Braun, M., and Friedman, G.M., 1969, Carbonate lithofacies and environments of the Tribes Hill Formation (Lower Ordovician) of the Mohawk Valley, New York: Journal of Sedimentary Petrology v. 39, p.113-135.

Buchbinder, L.G., and Friedman, G.M.,1980, Vadose, phreatic and marine diagenesis of Pleistocene-Holocene carbonates in a bore-hole-Mediterranean coast of Israel: Journal of Sedimentary Petrology, 50, p.395-409.

Bustillo, M.A., Delgado, A., Rey, J., and Ruiz-Ortiz, P.A., 1998, Meteoric water participation in the genesis of Jurassic cherts in the Subbetic of southern Spain- a significant indicator of penecontemporaneous emergence: sedimentary Geology, 119, p.85-102.

Buyce, M.R., and Friedman, G.M., 1975, Significance of authigenic K-feldspar in Cambrian-Ordovician Carbonate rocks of the proto-Atlantic shelf in North America: Journal of Sedimentary Petrology, v. 45, p.808-821.

Cander, H.S., Kaufman, J., Daniels, L.D., and Meyers, W.J., 1988, Regional dolomitization of shelf carbonates in the Burlington-Keokuk Formation (Miss.), Illinois and Missouri: Constraints from cathodoluminescent zonal stratigraphy; in Shukla, V. and Baker, P.A., (eds.), Sedimentology and Geochemistry of Dolostones: SEPM Special Publication. No. 43, p.129-144.

Chuanmao, L., Friedman, G.M., and Zhaochang, Z., 1993, Carbonate storm deposits (Tempestites) of Middle to Upper Cambrian age in the Helan Mountains: Carbonates and Evaporites, v. 8, p. 181-190.

Clarke, J.M., and Schuchert, C., 1899, Nomenclature of N.Y. series of geological formations: Science, new ser., v. 10, p. 876.

Compton, J.S., 1988, Sediment composition and precipitation of dolomite and pyrite in the Neogene Monterey and Sisquoc Formations, Santa Maria Basin area, California, in Shukla, V. and Baker, P.A., (eds.), Sedimentology and Geochemistry of Dolostones: SEPM Special Publication. No. 43, p.53-64..

Conway, S.W., and Friedman, G.M., 1984, Depositional environments and diagenesis of the Lower Ordovician Gailor Formation, Schenectady county, New York: Northeastern Geology, v. 6, no. 3, p.135-150.

Curl, M.W., Zagorski, T.W., and Friedman, G.M., 1984, Depositional environments and diagenesis of subsurface Tribes Hill Formation (Lower Ordovician) Mohawk Valley, New York: The Compass of Sigma Gamma Epsilon, v. 61, no. 4, p.216-243.

Curtis, C.D., and Coleman, M.L., 1986, Controls on the precipitation of early diagenetic calcite, dolomite, and siderite concretions in complex depositional sequences, in D. L. Gautier (ed.), Roles of Organic Matter in Sediment Diagenesis: SEPM Special Publication No. 38. p.23-33.

Cushing and Ruedemann, R., 1914, Geology of Saratoga Springs and vicinity: New York State Museum Bulletin 169: 177p.

DeGroot, K., 1967, Experimental dedolomitization: Journal of Sedimentary Petrology, v. 37, p.1216-1220.

Demicco, R.V., and Hardie, L.A., 1994, Sedimentary structures and early diagenetic features of shallow marine carbonate deposits: SEPM Atlas Series No.1, 265p.

Dickson, J.A.D., 1966, Carbonate identification and genesis as revealed by staining, Journal of Sedimentary Petrology, v.36, 491-505.

Dix, G.R., Robinson, G.W., and McGregor, D.C., 1998, Paleokarst in the Lower Ordovician Beekmantown Group, Ottawa Embayment: structural control inboard of the Appalachian orogen: GSA Bulletin, v.110, no. 8, p.1046-1059.

Dockal, J.A. (1988), Thermodynamic and kinetic description of dolomitization of calcite and calcitization of dolomite (dedolomitization): Carbonates and Evaporites, v. 3, 125-141.

Dolfi, R.U., and Friedman, G.M., 1983, Regional lithofacies of Lower Ordovician (Canadian age) strata of New York and New England: Northeastern Geology, v. 4, no. 2, p. 44-53.

Dorobek, S.L., Smith, T.M., and Whitsitt, P.M., 1993, Microfabrics and geochemistry of meteorically altered dolomite in Devonian and Mississipian Carbonates, Montana and Idaho, in R. Rezak, and D.L. Lavoie, (eds.) Carbonate Microfabrics : Frontiers in Sedimentology, Springer-Verlag, New York.

Dunham, R.L., 1962, Classification of carbonate rocks according to their depositional texture, in W. E. Ham,(ed.), Classification of Carbonate Rocks: AAPG Memoir 1, p.108-121.

Dunn, J.R., and Fisher, D.W., 1954, Occurrence, properties and paragenesis of anthraxolite in the Mohawk Valley: American Journal of Science, v. 252, p.489-501.

Eaton, Amos, 1824, A geological and agricultural survey of the district adjoining the Erie Canal in the State of New York, Albany, 163p.

Ervilus, P.A., and Friedman, G.M., 1991, Notes on Cambro-Ordovician dolostones (The Pine Plains Formation) in southern New York: Northeastern Geology, vol. 13, no. 3, p.165-176.

Evamy, B.D., 1967, Dedolomitization and the development of rhombohedral pores in limestones: Journal of Sedimentary Petrology, v. 37, no. 4, p 1204-1215.

Farr, M.R., 1992, Geochemical variation of dolomite cement within the Cambrian Bonneterre Formation, Missouri: evidence for fluid mixing: Journal of Sedimentary Petrology, v. 62, no.4, p. 636-651.

Fisher, D.W., 1954, Lower Ordovician (Canadian) stratigraphy of the Mohawk Valley, New York: GSA Bulletin, v. 65, p. 71-96.

Fisher. D.W., 1965, Mohawk Valley strata and structure, in Guide Book, Field trips in the Schenectady area, New York State Geological Association 37th Annual Meeting, Union College.

Fisher, D.W., 1977, Correlation of the Hadrynian, Cambrian and Ordovician rocks in New York State: New York State Museum, Map and Chart Series no.25, 75p.

Fisher, D.W., 1980, Bedrock Geology of the Central Mohawk Valley, New York: New York State Museum Map and Chart, Series no.33.

Fisher, D. W., and Hanson, G.F., 1951, Revisions in the geology of Saratoga Springs, New York and vicinity: American Journal of Science, v. 249, p.795-814.

Fisher, D. W., Isachsen, Y. W., Rickard, L. V., Broughton, J.G., and Offield, T.W., 1961, *Geologic Map of New York: New York State Museum and Science Service, Map and Chart Series No. 5.*

Fisher, D. W., Isachsen, Y. W., and Rickard, L. V., 1970, Geologic map of New York State: New York State Museum And Science Service, Map and Chart Series No. 15.

Fisher, D.W., and Mazzullo, S.J., 1976, Lower Ordovician (Gascodian) Great Meadows Formation in eastern New York: GSA Bulletin, v. 87, p.1443-1448.

Folk, R. L., and Pittman, J.S., 1971, Length-slow chalcedony: a new testament for vanished evaporites: Journal of Sedimentary Petrology, v. 41, p.1045-1058.

Friedman, G.M., 1959, Identification of carbonate minerals by staining methods: Journal of Sedimentary Petrology,v. 29, no.1, p.87-97.

Friedman, G.M., 1964, Early diagenesis and lithification in carbonate sediments: Journal of Sedimentary Petrology, v.34, p.777-813.

Friedman, G.M., 1965, Terminology of crystallization textures and fabrics in sedimentary rocks: Journal of Sedimentary Petrology, v. 35, no. 3, p.643-655.

Friedman, G.M., 1977, Carbonate and terrigenous sedimentary facies of tidal origin, Eastern New York, in P.C Wilson (ed.), Guidebook to Field Excursions conducted at the 49th Annual Meeting of the New York State Geological Association, NY State Geological Association, United States, p.1-16.

Friedman, G.M., 1980, *Dolomite is an evaporite mineral: Evidence from the rock record and from sea-marginal ponds of the Red Sea*, in Zenger, D.H., Dunham, J.B., and Ethington, R.L., (eds.), Concepts and Models of Dolomitization: SEPM Special publication, 28, p 69-80.

Friedman, G.M., 1985, Cambro-Ordovician shoaling and tidal deposits marginal to Iapetus ocean and middle to upper Devonian peritidal deposits of the Catskill fan-delta complex, in R.H. Lindemann (ed.), The New York State Geological Association 57th Annual Meeting Field Trip Guidebook, NY State Geological Association, United States, p.5-28.

Friedman, G.M., 1988, Spectacular domed microbial mats (cabbage heads) and oolitic limestone at Lester Park, near Saratoga, New York: Northeastern Geology, v.10, no.1, p. 8-12.

Friedman, G.M., 1990, Anthracite and concentrations of alkali feldspar (microcline) in flat-lying undeformed Paleozoic strata: a key to large-scale vertical crustal uplift, p. 16-28, in Heling, D., Rothe, P., Forstner, U. and Stoffers, P., (eds.), Sedimemnts and sedimentary environments: Springer-Verlag, 317p.

Friedman, G.M., 1994 a, Stacking patterns of cyclic parasequences in Cambro-Ordovician carbonates of Eastern New York and Western Vermont: Northeastern Geology, v. 16, p.145-157.

Friedman, G.M., 1994 b, Upper Cambrian-Lower Ordovician (Sauk) platform carbonates of the Northern Appalachian (Gondwana) Passive Margin: Carbonates and Evaporites, v. 9, p.143-150.

Friedman, G.M., 1995, Cambro-Lower Ordovician (Sauk) facies and sequences: Case Histories from Eastern North America: in P.H. Pausé, and M.P. Candelaria, (eds.), Carbonate Facies and Sequence Stratigraphy: Practical Applications of Carbonate Models, Permian Basin Section: SEPM Publication 95-36 and Permian Basin Graduate Center Publication 5-95, p.1-9.

Friedman, G.M., 1996 a, Early Ordovician microbial reef mounds of the Tribes Hill Formation, Mohawk Valley, New York: Carbonates and Evaporites, v. 11, no. 2, p.226-240.

Friedman, G.M., 1996 b, Strontium-isotopic signatures reflect an origin of dolomite by fresh-water effluent: The Pine Plains Formation (Wappinger Group, Cambrian) of Southeastern New York: Carbonates and Evaporites, v. 11, no. 1, 1996, p.134-140.

Friedman, G.M., 1997, The Tribes Hill Formation (Lower Ordovician) East-Central New-York: Perspective and update: Northeastern Geology and Environmental Sciences, v. 19, no. 3, p.216-221.

Friedman, G.M., and Sanders, J.E., 1967, Origin and occurrence of dolostones, in Chillingar, G.V., Bissel, H.J., and Fairbridge, R.W., (eds.), Carbonate rocks, origin, occurrence and classification: Elsevier Publishing Company, Amsterdam, p.267-348.

Friedman, G.M., Amiel, A.J., Braun, M., and Miller, D.S.,1973, Generation of carbonate particles and laminites in algal mats-example from sea-marginal hypersaline pool, Gulf of Aqaba, Red Sea: AAPG Bulletin, v. 5, p.541-557.

Friedman, G.M. and Braun, M., 1975, Shoaling and tidal deposits that accumulated marginal to the proto-Atlantic ocean; the Tribes Hill Formation (Lower Ordovician) of the Mohawk Valley, New York, in Ginsburg, R.N., (ed.), Tidal Deposits: a casebook of recent examples and fossil counterparts: Springer-Verlag, New York, p.307-314.

Friedman, G.M., and Radke, B., 1979, Evidence for sabkha overprint and conditions of intermittent emergence in Cambro-Ordovician carbonates of northeastern North America and Queensland, Australia: Northeastern Geology, v. 1, p.18-42.

Friedman, G.M., and Shukla, V., 1980, Significance of authigenic quartz euhedra after sulfates: example from the Lockport Formation (Middle Silurian) of New York: Journal of Sedimentary Petrology, Vol. 5, No. 4, p.1299-1304.

Friedman, G.M., Sanders, J.E., and Martini, J.P., 1982 Excursion 17A: Sedimentary Facies: Products of sedimentary environments in a cross-section of the classic Appalachian mountains and adjoining Appalachian Basin in New York and Ontario: Eleventh International Congress on Sedimentology, Mc Master University, Hamilton, Ontario, Canada, variously paginated.

Friedman, G.M., Sanders, J.E., and Kopaska-Merkel, D.C., 1992, Principles of sedimentary deposits: stratigraphy and sedimentology, New York: Macmillan Publishing Co., 717p.

Friedman, G.M., Chakraborty, C., and Kolkas, M. M., 1996, $\delta^{13}C$ excursion in the End-Proterozoic strata of the Vindhyan basin (Central India): its chronostratigraphic significance: Carbonates and evaporites, v. 11, no.2, p.206-212.

Friedman, G.M., and Chakraborty, C., 1997, Stable isotopes in marine carbonates:Their implications for the paleoenvironment with special reference to the Proterozoic Vindhyan carbonates (Central India): Journal of the Geological Society of India, v.50, p.131-158.

Friedman, I., and O'Neil, J.R., 1977, Compilation of stable isotope fractionation factors of geochemical interest : USGS Professional Paper 440KK, 12p.

Gao, G. and Land, L.S., 1991, Early Ordovician Cool Creek Dolomite, Middle Arbuckle Group, Slick Hills, SW Oklahoma, U.S.A.: Origin and modification: Journal of Sedimentary Petrology, v. 61, no. 2, p.161-173.

Gao, G., Land, L.S., and Folk, R.L., 1992, Meteoric modification of early dolomite and late dolomitization by basinal fluids, Upper Arbuckle Group, Slick Hills, South Western Oklahoma: AAPG Bulletin, v. 76, no. 11, p.1649-1664.

Goldhammer, R.K., Dunn, P.A., Hardie, L.A., 1990, Depositional cycles, composite sea level changes, cycle stacking patterns, and the heirarchy of stratigraphic forcing: Examples from Alpine Triassic carbonates: GSA Bulletin, v. 102, p.535-562.

Gradstein, F.M., and Ogg, J., 1996, A Phanerozoic Time Scale: Episodes, Vol. 19, nos. 1&2, p.3-5.

Gregg, J.M., and Sibley, D.F., 1984, Epigenetic dolomitization and the origin of xenotopic texture: Journal of Sedimentary Petrology, v.54, p.908-931.

Gunatilaka, A., 1987, The dolomite problem in the light of recent studies: Modern Geology, v. 11, p.311-324.

Guo, B., 1994, Diagenesis: Cementation dolomitization and dedolomitization, including petrophysical characteristics of carbonate rocks: City University of New York Graduate School, Ph. D. Dissertation 285p.

Guo, B., Sanders, J.E., and Friedman, G.M., 1990, Columbia Gas Company No. 1 Finnegan Boring, Washington County, New York: Microlithofacies and petroleum prospects in Lower Paleozoic platform strata beneath Taconic Allochthon: Northeastern Geology, vol. 12, no. 4, p.238-265.

Guo, B., Sanders, J.E., and Friedman, G.M., 1996, Timing and origins of dedolomite in Upper Wappinger Group (Lower Ordovician) strata, Southeastern New York: Carbonates and Evaporites, v. 11, no. 1, 1996 p.113-133.

Hall, J., 1847, Descriptions of the organic remains of the lower division of the New York system, equivalent of the Lower Silurian rocks of Europe: Paleontology of New York, v. 1, 338p.

Harris, D.C., and Meyers, W.J, 1987, Regional dolomitization of subtidal shelf carbonates: Burlington and Keokuk Formations (Mississipian), Iowa and Illinois, in Marshall, J.D. (ed.), Diagenesis of Sedimentary Sequences: Geological Society Special Publication No. 36, p.237-258.

Harris, R.L., and Friedman, G.M., 1982, Depositional environments of the subsurface Ogdensburg Formation (Lower Ordovician) in Northern New York State: Northeastern Geology, v. 4, no. 3/4, p.151-166.

Hesse, R., 1990 a, Silica Diagenesis: Origin of inorganic and replacement cherts, in McIlreath, I.A., and Morrow, D.W., (eds) Diagenesis: Geoscience Canada Reprint Series 4, p.253-275.

Hesse, R., 1990 b, Early diagenetic pore water / sediment interaction: modern offshore basins, in McIlreath, I.A., and Morrow, D.W., (eds) Diagenesis: Geoscience Canada Reprint Series 4, p. 277-316.

Hardie, L. A., 1987, Dolomitization:a critical view of some current views: Journal of Sedimentary Petrology, v.57, p.166-183.

Isachsen, Y. W.,1985, Structural and tectonic studies in New York state: New York State Geol. Surv., Office of Nuclear Regulatory Research, Washington, 74p.

Isachsen, Y. W.,1992, Still rising after all these years: Natural History, May issue, p.31-33.

Isachsen, Y. W., Landing, E., Lauber, J. M., Rickard, L. V., and Rogers, W. B., 1991, Geology of New York, A simplified account: New York State Museum Educational leaflet No. 28.

Keith, B. D., and Friedman, G. M., 1977, A slope-fan-basin model, Taconic sequence, New York and Vermont:: Journal of Sedimentary Petrology, V. 47, p.1220-1241.

Knauth, L. P., 1979, A model for the origin of chert in limestone: Geology, v.7, p.274-277.

Kupecz, J.A., and Land, L.S., 1991, Late-stage dolomitization of the Lower Ordovician Ellenburger Group, West Texas: Journal of Sedimentary Petrology, v. 61, p.551-574.

Kupecz, J.A., and Land, L.S., 1994, Progressive recrystallization and stabilization of early-stage dolomite (Lower Ordovician Ellenburger Group, West Texas), in Purser, B.H., Tucker, M.E. and Zenger, D.H. (eds.) Dolomites - A volume in honour of Dolomieu: Spec. Pub. of Int. Assoc. of Sedimentology 21, p.255-279.

Kupecz, J.A., Montanez, I.P. and Gao, G. (1992), Recrystallization of dolomite with lime. In Rezak, R. and Lavoie, D. Carbonate microfabrics (eds.), Frontiers in sedimentology: Springer Verlag, New York.

Land, L.S., 1980, The isotopic and trace element geochemistry of dolomite: the state of the art, in Zenger, D.H., Dunham, J.B., and Ethington, R.L., (eds.), Concepts and models of dolomitization: SEPM Special publication, 28, p.87-110.

Land, L.S., 1985, The origin of massive dolomite: Journal of Geological Education, v. 33, p.112-125.

Landing, E., Westrop, S.R., and Knox, L.A., 1996, Conodonts, stratigraphy, and relative sea-level changes of the Tribes Hill Formation (Lower Ordovician, East-central New York): Journal of Paleontology, v.70, p.656-680.

Lange, J., 1995, Generalized geologic columnar section, Pallette stone corporation, Saratoga Springs, Quarry1-8 R: unpublished report.

Linn, E.H., 1998, A review of Cambro-Ordovician reservoir qualities in northwest Pennsylvania and southwest New York: Northeastern Geology and Environmental Sciences, v. 20, no. 2, p.157-170.

Logan, B.W., Rezak, R., and Gebelein, C.D., 1964, Classification and environmental significance of algal stromatolites: Journal of Geology, v.72, p.68-83.

Lovering, T.G., and Patten, L.E., 1962, The effect of CO_2 at low temperature and pressure on solutions supersaturated with silica in the presence of limestone and dolomite: Geochimica et Cosmochimica Acta, v. 26, p.253-284.

Lu, F.H., and Meyers, W.J., 1998, Massive dolomitization of a late Miocene carbonate platform: a case of mixed evaporative brines with meteoric water, Nijar, Spain: Sedimentology, v. 45, p.263-277.

Machel, H.G., 1987, Saddle dolomite as a by-product of chemical compaction and thermochemical sulfate reduction: Geology, v.15, p.936-940.

Machel, H.G., and Burton, E.A., 1991, Factors governing cathodoluminescence in calcite and dolomite and their implications for studies of carbonate diagenesis, in Charles E. Barker and Otto C. Kopp, (eds.) Luminescence microscopy: quantitative and qualitative aspects: SEPM Short Course 25, p.37-57.

Machel, H.G., and Anderson, J.H., 1989, Pervasive subsurface dolomitization of the Nisku Formation in Central Alberta: Journal of Sedimentary Petrology, v. 59, p.891-911.

Machel, H.G., Mason, R.A., Mariano, A.N., and Mucci, A., Causes and emission of luminescence in calcite and dolomite, in Charles E. Barker and Otto C. Kopp, (eds.) Luminescence microscopy: quantitative and qualitative aspects: SEPM Short Course 25, p. 9-25.

Mattes, B.W., and Mountjoy, E.W., 1980, Burial dolomitization of the Upper Devonian Miette buildup, Jasper National Park, Alberta, in Zenger,D.H., Dunham, J.B., and Ethington, R.L., (eds.), Concepts and Models of Dolomitization: SEPM Special Publication No.28, p.259-297.

Mazzullo, S.J., 1978, Early Ordovician tidal flat sedimentation: Western margin of proto-Atlantic ocean: Journal of Sedimentary Petrology v. 48, no.1, p.49-62.

Mazzullo, S.J., 1992, Geochemical and neomorphic alteration of dolomite: a review: Carbonates and Evaporites, v. 7, p.21-37.

Mazzullo, S.J., and Friedman, G.M., 1975, Conceptual model of tidally influenced deposition on margins of epeiric seas: Lower Ordovician (Canadian) of eastern New York and south-western Vermont: AAPG Bulletin, v. 59, p.2123-2141.

Mazzullo, S.J., and Friedman, G.M., 1977, Competitive algal colonization of peritidal flats in a scizohaline environment: The Lower Ordovician of New York: Journal of Sedimentary Petrology, v. 47, no. 1, p.398-410.

Mazzullo, S.J., Agostino, P., Seitz, J.N., and Fisher, D.W., 1978, Stratigraphy and depositional environments of the Upper Cambrian-Lower Ordovician sequence, Saratoga Springs, New York: Journal of Sedimentary Petrology, v. 48, no.1, p. 99-116.

Milliken, K. L., 1978, The silicified evaporite syndrome-Two aspects of silicification history of former evaporite nodules from southern Kentucky and northern Tennessee: Journal of Sedimentary Petrology, v. 49, p.245-256.

Montanez, I.P. and Read, J.F., 1992, Fluid-rock interaction history during stabilization of early dolomites, Upper Knox Group (Lower Ordovician), U.S. Appalachians: Journal of Sedimentary Petrology, v. 62, no. 5, p.753-778.

Morrow, D.W., 1990 a, Dolomite- Part 1: The chemistry of dolomitization and dolomite precipitation, in I.A. McIlreath and D.W, Morrow (eds.), Diagenesis: Geoscience Canada Reprint Series 4, p.113-123.

Morrow, D.W., 1990 b, Dolomite- Part 2: Dolomitization models and ancient dolostones, in I.A. McIlreath and D.W, Morrow (eds.) Diagenesis: Geoscience Canada Reprint Series 4, p.125-139.

Morrow, D.W., 1997, Regional subsurface dolomitization: models and constraints: Geoscience Canada, v. 25, no. 2, p. 57-70.

Owen, R.W., and Friedman, G.M., 1984, Late Cambrian algal deposition in the Hoyt Limestone, eastern New York state: Northeastern Geology, v. 6, no. 4, p.222-237.

Philips, S. S., and Friedman, G.M., 1995, Carbonate diagenesis and dolomitization of Cambro-Ordovician (Sauk sequence) platform strata in central New York (abstract): AAPG Bulletin, v.79, no.9, p.1417.

Purser, B., Tucker, M., and Zenger, D. eds., 1994, Dolomites, A volume in honour of Dolomieu: Special Publication No. 21, International Association of Sedimentologists, Blackwell Scientific, 451 p.

Qing, H., 1998, Petrography and geochemistry of early-stage, fine- and medium-crystalline dolomites in the Middle Devonian Presqu'ile Barrier at Pine Point, Canada: Sedimentology, v. 45, p. 433-446.

Qing, Qing, H., and Mountjoy, E.W., 1989, Multistage dolomitization in Rainbow Buildups, Middle Devonian Keg River Formation, Alberta, Canada: Journal of Sedimentary Petrology, v. 59, no.1, p.114-126.

Qinjun, Y., and Demicco, R.V., 1997, Dolomitization of the Cambrian carbonate platform, Southern Canadian Rocky Mountains: Dolomite front geometry, fluid inclusion geochemistry, isotopic signature, and hydrologic modelling studies: American Journal of Science, v. 297, p.892-938.

Radke, B.M., and Mathis, R.L., 1980, On the formation of saddle dolomite: Journal of Sedimentary Petrology, v 50, p.1149-1168.

Read, J.F., and Horbury, A.D.,1993, Eustatic and tectonic controls on porosity evolution beneath sequence-bounding unconformities and parasequence disconformities on carbonate platforms, in A.D. Horbury and A.G. Robinson (eds.) Diagenesis and Basin Development: AAPG Studies in Geology #36, p.155-197.

Rickard, L.V., 1973, Stratigraphy and structure of the subsurface Cambrian and Ordovician carbonates of New York: New York State Museum and Scientific Survey, Map and Chart Series 18.

Rogers, W.B., Isachsen, Y.W., Mock, T.D., and Nyahay, R.E., 1990, New York State Geological Highway Map: New York State Museum Educational Leaflet No. 33.

Rubin, D.M., and Friedman, G.M., 1977, Intermittently emergent shelf carbonates: an example from the Cambro-Ordovician of Eastern New York State: Sedimentary Geology, v. 19, p.81-106.

Rubin, D.M., and Friedman, G.M., 1981, Origin of chert grains and a halite-silcrete bed in the Cambrian and Ordovician Whitehall Formation of Eastern New York State: Journal of Sedimentary Petrology, v. 51, no.1, p.69-72.

Saller, A.H., 1984, Petrologic and geochemical constraints on the origin of subsurface dolomite, Enewetak Atoll: and example of dolomitization by normal seawater: Geology, v.12, p. 217-220.

Saltzman, M.R., Runnegar, B., and Lohmann, K.C., 1998, Carbon isotope stratigraphy of Upper Cambrian (Steptoean Stage) sequences of the eastern Great Basin: Record of a global oceanographic event: GSA Bulletin, v.110, no.3, p.285-297.

Sanders, J.E., 1995, Lower Paleozoic carbonate-clast diamictites: Relationship to thrust sheets that advanced across the floor of the Northern Appalachian Ordovician foreland basin: Northeastern Geology and Environmental Sciences, v.17, no.1, p.23-45.

Sarwar, G., 1992, Geology of missing strata: The Post-Devonian of New York State: City University of New York Graduate School, Ph. D. Dissertation.

Sarwar, G., and Friedman, G.M., 1994, Late Paleozoic sediment cover of the Adirondacks, New York: evidence from fluid inclusions and clay diagenesis: Northeastern Geology, v.16, no.1, p.18-36.

Sarwar, G., and Friedman, G.M., 1995, Post-Devonian sediment cover over New York state: evidence from fluid-inclusion, organic maturation, clay diagenesis and stable isotope studies, in S. Bhattacharji, G.M. Friedman, H.J. Neugebauer, and A. Seilacher (eds.), Lecture Notes in Earth Sciences, v.58: Springer-Verlag,109p.

Scotese, C.R., Bambach, R.K., Barton, C., VanderVoo, R., and Ziegler, A.M., 1979, Paleozoic base maps: Jour. Geology, V87, p.217-277.

Scotese, C.R.,and McKerrow, W.S.,1990, Revised world maps and introduction, in McKerrow, W.S.& Scotese, C.R. (eds.), Paleozoic Paleogeography and Biogeography: Geological Society Memoir No.12, p.1-21.

Searl, A., 1989, Saddle dolomite - a new view of its nature and origin: Mineral Mag. 53, p.547-555.

Selleck, B.W., 1987, Origin of voids in the peritidal facies of the Theresa Formation and Ogdensburg dolostone (Lower Ordovician), New York and Ontario: Northeastern Geology, V.9, No.2, p.76-88.

Sepkoski, Jr. J. J., 1982, Flat-pebble conglomerates, storm deposits and the Cambrian bottom fauna, p.371-385, in G. Einsele and A. Seilacher (eds), Cyclic and Event Stratification: Springer-Verlag, New York, 536 p.

Shinn, E. A., 1968, Practical significance of bird's eye structures in carbonate rocks: Journal of Sedimentary Petrology, v.38, p.215-223.

Shukla, V., and Baker, P. A. eds., 1988, Sedimentology and geochemistry of dolostones: SEPM Special Publication No. 43, 266p.

Sibley, D.F., 1982, The origin of common dolomite fabrics: Clues from the Pliocene: Journal of Sedimentary Petrology, v.52, no.4, p.1087-1100.

Sibley, D.F., and Gregg, J. M., 1987, Classification of dolomite rock textures: Journal of Sedimentary Petrology, v.57, no. 6, p.967-975.

Sloss, L.L., 1953, The significance of evaporites: Journal of Sedimentary Petrology, v. 23, no. 3, p.143-161.

Sloss, L.L., 1963, Sequences in the cratonic interior of North America: GSA. Bull., v. 74, p.93-113.

Tucker, M.E., and Wright, V.P., 1992, Carbonate Sedimentology: Oxford, Blackwell, 482p.

Ulrich, E.O., and Cushing, R.N., 1910, Age relationship of the Little Falls Dolomite of the Mohawk Valley: N.Y. State Mus. Bull. 149, p.97-140.

Urschel, S.F., and Friedman, G.M., 1984, Paleodepth of burial of Lower Ordovician Beekmantown Group carbonates in New York State: The Compass of Sigma Gamma Epsilon, v. 61, no. 4.

Vail, P.R., Mitchum, R.M., and Thompson, S. (1977), Seismic stratigraphy and global changes of seal-level, part 4: global cycles of relative changes in sea-level: AAPG Memoir, v.26, p.83-97.

Vanuxem, L., 1842, Survey of the third geological district, in Geology of New York, Pt. 3: Albany, 306p.

Van Wagoner, J.C., Posamentier, H.W.,Mitchum, R.M., Vail, P.R., Sarg, J.F., Loutit, T.S., Hardenbol, J., 1988, An overview of the fundamentals of sequence stratigraphy and key definitions; in Wilgus, C.K., Hastings, B.S., Kendall, C.G. St. C., Posamentier, H.W., Ross, C.A., and Van Wagoner, J.C., (eds.), Sea-Level Changes- An Integrated Approach: SEPM Special Publication 42, p.39-46.

Veizer, J., and Demovic, R., 1974, Strontium as a tool in facies analysis: Journal of Sedimentary Petrology, v.44, p.93-115.

Walter, M.R., 1976, Stromatolites: New York: Developments in Sedimentology, v.20, Elsevier, 790p.

Wanless, H.R.,1983, Burial diagenesis, in limestones, Parker Sellwood, B.W., (eds.), Sediment Diagenesis: p.379-417.

Wendte, J., Qing, H., Dravis, J.J., Moore, S.L.O., Stasiuk, L.D., and Ward, G., 1998, High-temperature saline (thermoflux) dolomitization of Devonian Swan hills platform and bank carbonates, Wild River area, west-central Alberta: Bulletin of Canadian Petroleum Geology, Vol. 46, no. 2, p.210-265.

Wicander, R., and Monroe, J.S., 1989, Historical Geology: West Publishing Co., New York, 578p.

Wright, D.T., 1997, An organogenic origin for widespread dolomite in the Cambrian Eilean Dubh Formation, north-western Scotland: Journal of Sedimentary Research, v. 67, p.54-64.

Wright, V. P., 1992, Speculations on the controls on cyclic peritidal carbonates: ice-house versus green-house eustatic controls: Sedimentary Geology, v.147, p.1-5.

Zenger, D.H., 1972, Significance of supratidal dolomitization in the geological record: GSA Bull., v. 83, p.1-12.

Zenger, D.H., 1976, Definition of type Little Falls Dolostone (Late Cambrian), east-central New York: AAPG Bulletin 60: p.1570-1575.

Zenger, D.H., 1981, Stratigraphy and petrology of Little Falls Dolostone (Upper Cambrian), East-Central New York: New York State Museum Map and Chart Series 34, 138p.

Zenger, D.H., 1983, Burial dolomitization of the Lost Burro Formation (Devonian), east-central California, and the significance of late-diagenetic dolomitization: Geology v.11, p.519-522.

Zenger, D.H., and Dunham, J.B., 1988, Dolomitization of Siluro-Devonian limestones in a deep core (5350m), Southeastern New Mexico, in Shukla, U. and Baker, P.A.(eds.) Sedimentology and Geochemistry of Dolostones : SEPM Spec. Publ. 43, p.161-173.

Zenger, D.H., Dunham, J.B. and Ethington, R.L., eds., 1980, Concepts and Models of Dolomitization: SEPM Special Publication No. 28, 320p.

IMAGE EVALUATION
TEST TARGET (QA-3)

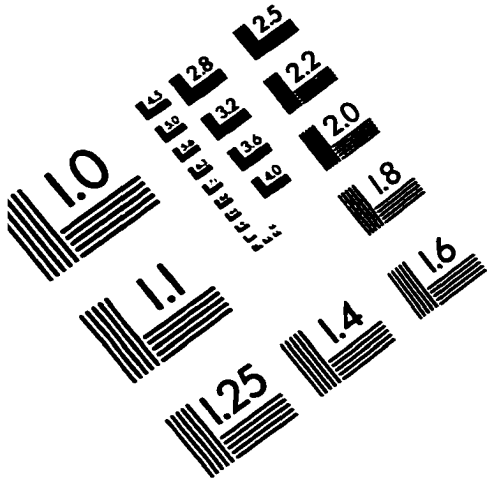

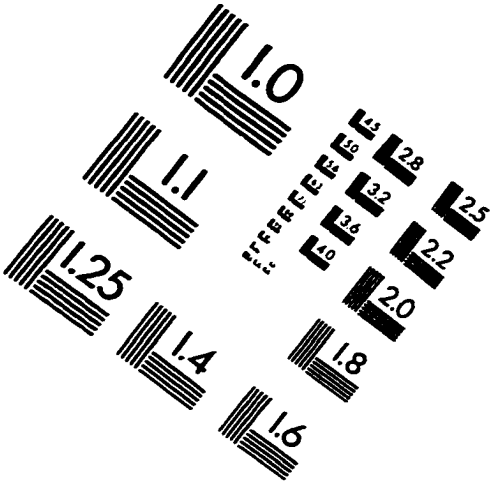

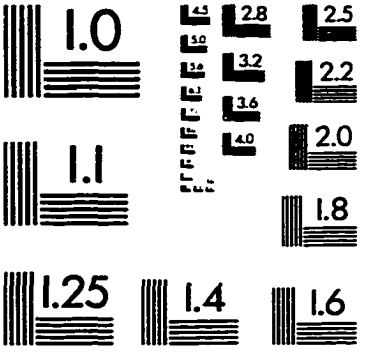

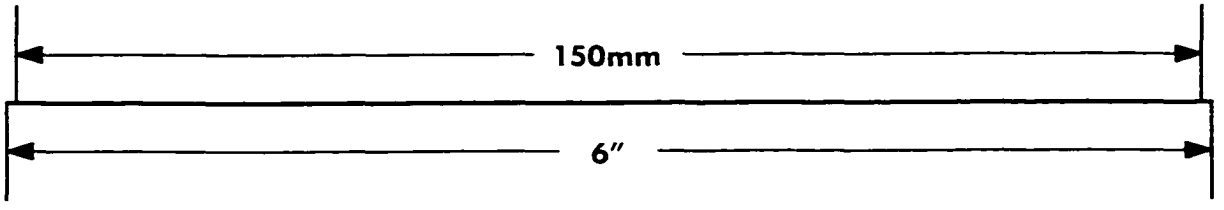

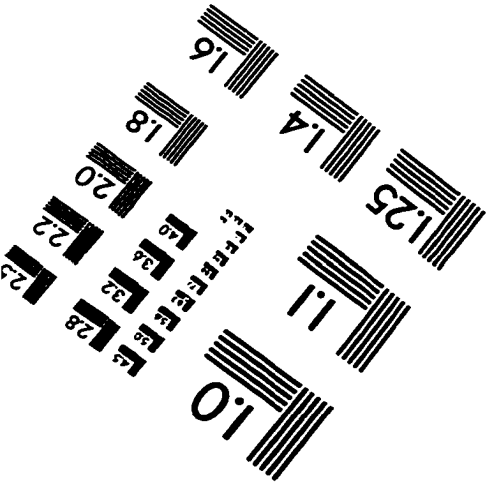

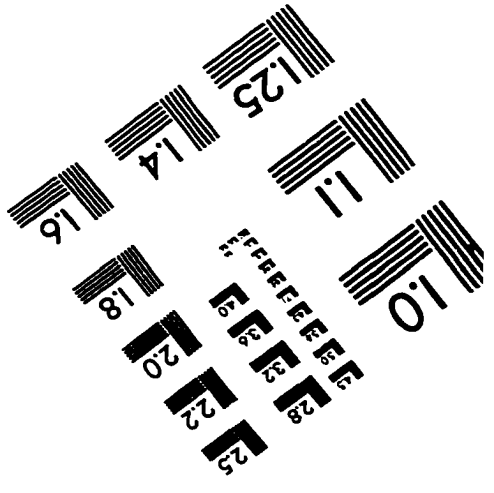

APPLIED IMAGE . Inc
1653 East Main Street
Rochester, NY 14609 USA
Phone: 716/482-0300
Fax: 716/288-5989